

Alma Mater Studiorum - Università di Bologna

DOTTORATO DI RICERCA IN
SCIENZE BIOMEDICHE E NEUROMOTORIE

Ciclo 36

Settore Concorsuale: 06/F1 - MALATTIE ODONTOSTOMATOLOGICHE

Settore Scientifico Disciplinare: MED/28 - MALATTIE ODONTOSTOMATOLOGICHE

NOVEL BIOMATERIALS FOR REGENERATION OF PERIAPICAL BONE
DEFECTS IN ENDODONTIC AND IMPLANT THERAPY

Presentata da: Andrea Spinelli

Coordinatore Dottorato

Matilde Yung Follo

Supervisore

Carlo Prati

Co-supervisore

Maria Giovanna Gandolfi

Esame finale anno 2024

1. Abstract

2. Microbiology of the root canal system

2.1 *Endodontic Microbial Communities in Apical Periodontitis. J Endod. 2023 Feb;49:178-189.*

3. Novel biomaterials in endodontics: premixed calcium-silicate based sealers

3.1 *Chemical-Physical Properties and Bioactivity of New Premixed Calcium Silicate-Bioceramic Root Canal Sealers. Int J Mol Sci. 2022;23:13914.*

4. Clinical Outcome and Biocompatibility of Innovative CaSi-based Obturation Techniques.

4.1 *The Use of Premixed Calcium Silicate Bioceramic Sealer with Warm Carrier-Based Technique: A 2-Year Study for Patients Treated in a Master Program. J Funct Biomater. 2023;14:164.*

4.2 *Clinical Evaluation of a Novel Premixed Tricalcium Silicate Containing Bioceramic Sealer Used with Warm Carrier-Based Technique: A 12-Month Prospective Pilot Study. Appl. Sci. 2023, 13, 11835.*

4.3 *Root canal treatment of compromised teeth as alternative treatment for patients receiving bisphosphonates: 60-month results of a prospective clinical study. Int Endod J 2021;54:156-71.*

5. Novel Endodontic Biomaterials and Advanced Implant Surface Technologies: Their Impact on the Decision Between Endodontic Retreatment and Implant Rehabilitation.

5.1 *Tissue-Level Laser-Lok Implants Placed with a Flapless Technique: A 4-Year Clinical Study. Materials 2023, 16, 1293.*

5.2 *10-year Historical Prospective Cohort Study of Calcium Phosphate-Blasted Acid-Etched Titanium Implants Placed in Different Ridges. Int J Oral Maxillofac Implants. 2023;38:697-708.*

5.3 *Micro-Nano Surface Characterization and Bioactivity of a Calcium Phosphate-Incorporated Titanium Implant Surface. J Funct Biomater. 2021 Jan 7;12:3.*

6. Conclusions

1. Abstract

Endodontic-related periapical bone defects are a common occurrence in the global populations. Considering the number of root canal treatments performed annually, new strategies and new biomaterials for the management of these bone defects will be important and highlight the need for continued research and development in endodontic field.

The present PhD thesis have several objectives and is divided into two main sections: one focused on in vitro and laboratory research and the other on clinical in vivo investigations.

The first part, focused on laboratory and in vitro research, investigated 2 main topics:

- the microbial communities of apical periodontitis to evaluate the predominant bacterial genera using 16sr DNA-targeted Nanopore sequencing;
- the physical-chemical properties of innovative premixed calcium-silicate based bioceramic sealers for endodontic therapy;

The second part, focused on in vivo clinical studies, investigated 2 main topics:

- the clinical application of premixed calcium-silicate-based sealers. Ethical committee approval was obtained for the use of these biomaterials in 2 separate in vivo studies. The first one is a prospective cohort study with a two-year follow-up where the test group was compared with a control group (considered the gold standard). The second is a pilot prospective cohort study with a 12-month follow-up which set the foundation for a subsequent randomized investigation. Thanks to these investigations, we validated a new technique that innovatively associates a warm obturation technique with calcium-silicate-based sealers. Historically, these sealers were only used with cold techniques. This investigation highlights the possibility for wider utilization and improvements in endodontic techniques.
- The outcome of 2 different types of implants characterized by different surface treatments and placed with different techniques. The marginal bone level and periodontal parameters were evaluated with a follow-up of 4 and 10 years.

This Ph.D thesis is based on a compilation of published papers I have done during my three-year PhD program.

2. Microbiology of the root canal system

The bacterial environment of the root canal can be very different depending on whether the tooth has a vital pulp (pulpitis-affected), a pulp necrosis, or has already been endodontically treated.

The bacterial microflora of a pulpitis-affected root canal is mainly composed by aerobes and facultative anaerobes (Winkler & Van Amerongen 1959). During the develop of pulpal disease process we can see a swift of the bacterial microflora. We can distinguish two different types of endodontic infections (Siqueira et al. 2014):

A primary endodontic infection is characterized by untreated inflamed / necrotic root canal. Bacteria are now predominantly anaerobic, and this is directly proportional to the time of infection (Fabricius et al. 1982). In this situation the most detected bacteria are: *Bacteroides*, *Prophyromonas*, *Prevotella*, *Fusobacterium*, *Treponema*, *Peptostreptococcus*, *Eubacterium*, and *Camphylobacter* (Neelakantan et al. 2017).

A secondary endodontic infection occurs after a root canal treatment and we can have two different scenarios: a persistent endodontic infection when we cannot observe a healing after the treatment, or a recurrent infection when we have a new infection even after years from the initial healing. The bacteria in these infections are different with a bacterial load typically lower, a limited variety of bacteria, but with a higher pathogenic activity. The most prevalent are *Enterococci*, *Streptococci*, *Lactobacilli*, *Actinomyces* and *fungi* (Neelakantan et al. 2017). High percentage of *Enterococcus faecalis* was observed in cases of a persistent apical periodontitis suggesting that these bacteria play an important role during the healing process (Pirani et al. 2008; Buonavoglia et al. 2013). Due to its resistance *Enterococcus faecalis* can survive inside the dentinal tubules (Love & Jenkinson 2002; Vieira et al. 2012), lateral canals and it is also resistant to the action of irritants such as sodium hypochlorite (Stuart et al. 2006). These characteristics have clinical implications, making it challenging to eradicate using standard irrigation and instrumentation protocols. However, it is important to note that a lot of studies highlight its relatively low pathogenicity suggesting that other pathogens are present in the complex biofilm of the recurrent infections.

The root canal system, specifically its apical third, is often referred as a critical territory (Siqueira et al. 2004). In infected root canals, bacteria tend to colonize this region. Consequently, they are in close contact with the periradicular tissues through the apical and accessory foramina

and can inflict damage on the tissues. The success of treatment depends on how well this infection is treated and eliminated. Apical anatomy plays an important role in the prognosis of root canal treatment. Anatomical complexities such as accessory or lateral canals, isthmuses, and apical deltas are often present hiding bacteria difficult to remove (Ordinola-Zapata et al. 2019). This may lead to post-treatment apical periodontitis. Therefore, treatment strategies should aim to reach these areas during the irrigation and instrumentation process. However, it's important to note that these lateral canals and ramifications are associated with endodontic treatment failure only in presence of necrosis or periapical lesion (not during an acute pulpitis in which the apical third is still safe from bacteria) when they are large enough to create a habitat for a significant bacterial population and allow them a direct access to the periradicular tissues (Ricucci et al. 2010). Bacteria persisting in the apical third are the primary etiologic agents of primary and post-treatment apical periodontitis (Provenzano et al. 2016).

In an animal model, it was demonstrated that the bacteria of the Red Complex (*Porphyromonas gingivalis*, *Tannerella forsythia*, *Treponema denticola*) could, once they infected the endodontic canal, spread to organs such as the heart, spleen, and brain (Foschi et al. 2006). Interestingly, *Treponema Denticola* has also been detected in remote organs like esophageal cancer sites (Narikiyo et al. 2004), and in the brains of patients with Alzheimer's disease (Riviere et al. 2002).

A lot of studies have been conducted using a bacterial DNA amplifications technique such as the polymerase chain reaction (PCR) and the Real-time PCR (Siqueira et al. 2003; Rôças et al. 2003; Foschi et al. 2005). In addition, the recent introduction of the Next Generation Sequencing can provide a more detailed mapping of the oral microbiome (de Brito et al. 2020; Buonavoglia et al. 2023).

Even with all these technological advancements, understanding the causes of endodontic failures that lead to endodontic infections is not always easy. If we consider that 52% of the people worldwide have at least one endodontic disease (Tibúrcio-Machado et al. 2021), understanding the microbial diversity of the root canal system by identifying which bacteria (or an association of bacteria) are more prevalent in these infections can be important for improving endodontic treatments and develop new clinical protocols.

The following study evaluate the microbial communities associated with root canals affected by apical periodontitis using nanopore sequencing.

REFERENCES

1. Buonavoglia A, Latronico F, Pirani C, Greco MF, Corrente M, Prati C. Symptomatic and asymptomatic apical periodontitis associated with red complex bacteria: clinical and microbiological evaluation. *Odontology* 2013 Jan;101:84-8.
2. Buonavoglia A, Zamparini F, Lanave G, Pellegrini F, Diakoudi G, Spinelli A, Lucente MS, Camero M, Vasinioti VI, Gandolfi MG, Martella V, Prati C. Endodontic Microbial Communities in Apical Periodontitis. *J Endod.* 2023 Feb;49:178-189.
3. de Brito LCN, Doolittle-Hall J, Lee CT, Moss K, Bambilra Júnior W. The apical root canal system microbial communities determined by next-generation sequencing. *Sci Rep* 2020 Jul 2;10:10932.
4. Fabricius L, Dahlén G, Ohman AE, Möller AJR. Predominant indigenous oral bacteria isolated from infected root canals after varied times of closure. *Scand J Dent Res* 1982;90:134 – 44.
5. Foschi F, Izard J, Sasaki H, Sambri V, Prati C et al. *Treponema denticola* in disseminating endodontic infections. *J Dent Res* 2006 Aug;85:761-5.
6. Foschi F, Cavrini F, Montebugnoli L, Stashenko P, Sambri V, Prati C. Detection of bacteria in endodontic samples by polymerase chain reaction assays and association with defined clinical signs in Italian patients. *Oral Microbiol Immunol* 2005 Oct;20(5):289-95.
7. Love RM, Jenkinson HF. Invasion of dentinal tubules by oral bacteria. *Crit Rev Oral Biol Med* 2002;13:171-83.
8. Narikiyo M, Tanabe C, Yamada Y, Igaki H, Tachimori Y, Kato H, Muto M, Montesano R, Sakamoto H, Nakajima Y, Sasaki H. Frequent and preferential infection of *Treponema denticola*, *Streptococcus mitis*, and *Streptococcus anginosus* in esophageal cancers. *Cancer Sci.* 2004;95:569-74.
9. Neelakantan P, Romero M, Vera J, Daood U, Khan AU et al. Biofilms in endodontics-current status and future directions. *Int J Mol Sci* 2017 Aug 11;18:1748.
10. Ordinola-Zapata R, Martins JNR, Niemczyk S, Bramante CM. Apical root canal anatomy in the mesiobuccal root of maxillary first molars: influence of root apical shape and prevalence of apical foramina - a micro-CT study. *Int Endod J.* 2019 Aug;52:1218-1227.
11. Pirani C, Bertacci A, Cavrini F, Foschi F, Acquaviva GL et al. Recovery of *Enterococcus faecalis* in root canal lumen of patients with primary and secondary endodontic lesions. *New Microbiol* 2008 Apr;31:235-40.

12. Provenzano JC, Antunes HS, Alves FR, Rôças IN, Alves WS, Silva MR, Siqueira JF Jr. Host-Bacterial Interactions in Post-treatment Apical Periodontitis: A Metaproteome Analysis. *J Endod.* 2016 Jun;42:880-5.
13. Ricucci D, Siqueira JF Jr. Fate of the tissue in lateral canals and apical ramifications in response to pathologic conditions and treatment procedures. *J Endod.* 2010 Jan;36:1-15
14. Riviere GR, Riviere KH, Smith KS. Molecular and immunological evidence of oral *Treponema* in the human brain and their association with Alzheimer's disease. *Oral Microbiol Immunol.* 2002;17:113-8.
15. Rôças IN, Siqueira JF Jr, Andrade AF, Uzeda M. Oral treponemes in primary root canal infections as detected by nested PCR. *Int Endod J.* 2003 Jan;36:20-6.
16. Siqueira JF Jr, Rôças IN. PCR methodology as a valuable tool for identification of endodontic pathogens. *J Dent.* 2003 Jul;31:333-9.
17. Siqueira JF Jr, Rôças IN, Alves FR, Santos KR. Selected endodontic pathogens in the apical third of infected root canals: a molecular investigation. *J Endod.* 2004 Sep;30:638-43.
18. Siqueira JF Jr, Rôças IN, Ricucci D, Hülsmann M. Causes and management of post-treatment apical periodontitis. *Br Dent J* 2014 Mar;216:305-12.
19. Stuart CH, Schwartz SA, Beeson TJ, Owatz CB. *Enterococcus faecalis*: its role in root canal treatment failure and current concepts in retreatment. *J Endod* 2006 Feb;32:93-8.
20. Tibúrcio-Machado CS, Michelin C, Zanatta FB, Gomes MS, Marin JA, Bier CA. The global prevalence of apical periodontitis: a systematic review and meta-analysis. *Int Endod J.* 2021 May;54:712-735.
21. Vieira AR, Siqueira JF Jr, Ricucci D, Lopes WS. Dentinal tubule infection as the cause of recurrent disease and late endodontic treatment failure: a case report. *J Endod* 2012 Feb;38:250-4.
22. Winkler KC, Van Amerongen J. Bacteriologic results from 4,000 root canal cultures. *Oral Surg Oral Med Oral Pathol.* 1959 Jul;12:857-75.

Alessio Buonavoglia, PhD,*
Fausto Zamparini, PhD,*
Gianvito Lanave, PhD,†
Francesco Pellegrini, MD,†
Georgia Diakoudi, PhD,†
Andrea Spinelli, MD,*
Maria Stella Lucente, PhD,†
Michele Camero, PhD,†
Violetta Iris Vasinioti, MD,†
Maria Giovanna Gandolfi, PhD,*
Vito Martella, PhD,† and
Carlo Prati, PhD*

BASIC RESEARCH – BIOLOGY

Endodontic Microbial Communities in Apical Periodontitis



SIGNIFICANCE

Generation of a profile of the most abundant and/or frequent bacterial genera in association to the presence/absence of ap -associated clinical signs, primary ap (pap)/secondary ap (sap), and periapical index (pai)
Statement of Clinical Relevance

To investigate the microbial communities of apical periodontitis and to assess the most abundant and frequent bacterial genera associated with root canals of patients with apical periodontitis-associated clinical signs, primary or secondary apical periodontitis, and periapical index using 16S DNA-targeted Nanopore sequencing.

From the *Department of Biomedical and Neuromotor Sciences, Dental School, University of Bologna, Bologna, Italy; †Department of Veterinary Medicine, University of Bari, Valenzano, Italy

Ethical approval: The Ethics Committee of Azienda Unità Sanitaria Locale of Bologna approved this study with authorization nr. 844-2021-OSS-AUSLBO-21160-ID 3118-Parere CE-AVEC-ENDO-MICROBIOTA 09/2021.

Address requests for reprints to Prof Gianvito Lanave, Department of Veterinary Medicine, University of Bari, 70010, Valenzano, Italy.
E-mail address: gianvito.lanave@uniba.it
0099-2399/\$ - see front matter

Copyright © 2022 American Association of Endodontists.
<https://doi.org/10.1016/j.joen.2022.11.015>

ABSTRACT

Introduction: Apical periodontitis (AP) represents an inflammatory condition of peri-radicular tissues due to invasion and colonization of bacteria in the root canals. Primary apical periodontitis (PAP) is associated with untreated necrotic root canal and can be efficiently treated with endodontic treatment to remove bacteria. Persistent/secondary apical periodontitis (SAP) is a perpetual periapical lesion due to unsuccessfully treated root canals after an initial apparent healing of the tooth. The aim of the study was evaluating the microbial communities associated with root canals using Nanopore sequencing. **Methods:** Seventeen samples from the root canals of 15 patients with AP were Polymerase Chain Reaction-amplified for 16S ribosomal DNA gene and sequenced. Information regarding the presence or absence of AP symptoms, PAP and SAP, and periapical index of patients were recorded. **Results:** Firmicutes, Bacteroidetes, and Actinobacteria were the most abundant phyla detected and *Phocaeicola*, *Pseudomonas*, *Rothia*, and *Prevotella* were the most prominent genera. In samples of patients with AP symptoms, the most frequent detected genera were *Cutibacterium*, *Lactobacillus*, *Pseudomonas*, *Dialister*, *Prevotella*, and *Staphylococcus*. In PAP samples, the most represented genera were *Cutibacterium*, *Lactobacillus*, *Pseudomonas*, and *Prevotella*, whilst in SAP cases were *Cutibacterium*, *Prevotella*, *Atopobium*, *Capnocytophaga*, *Fusobacterium*, *Pseudomonas*, *Solobacterium*, and *Streptococcus*. **Conclusions:** The results provide additional information on the microbiota of root-canals. These data evidence the complexity of the microbiota and the relationship with many clinical and endodontic conditions. Future studies must evaluate these conditions and identify their role in inducing bone damage and local and systemic disease, aiming to better elucidate the relationship between microbes and endodontic pathologies. (*J Endod* 2023;49:178–189.)

KEY WORDS

Apical periodontitis; microbiota; nanopore sequencing; root canals

Apical periodontitis (AP) is an inflammatory condition of peri-radicular tissues principally caused by bacteria and bacterial products^{1,2}. This endodontic disease can have different clinical presentations such as symptomatic/asymptomatic AP with presence/absence of apical radiolucent area³. Moreover, AP can be distinguished in primary apical periodontitis (PAP) or secondary/persistent apical periodontitis (SAP). PAP is associated with untreated inflamed/necrotic root canals whilst SAP is associated to previously root canals treated unsuccessfully^{4,5}.

Bacteria play a major role in the development of AP. For this reason, the determination of bacterial species in endodontic disease is important for the development of methods for effective treatment of these infections⁶.

To date, bacterial culture and Polymerase Chain Reaction (PCR) approaches have been adopted to assess the microbial composition of infected root canals. Although culturing may allow for the study of phenotypic characteristics of bacteria such as susceptibility to antimicrobials, this has various intrinsic limitations in terms of evaluation of multispecies in biofilms. In addition, endodontic biofilms can encompass non-cultivable microorganisms due to the absence of suitable culture media or to low-abundance of bacterial cells⁷.

Significant advances in the identification of bacteria have been made with the introduction of PCR-based amplification methods, thus overcoming the limitations of traditional, culture-based approaches^{8,9}. Nevertheless, PCR techniques exhibit constraints in the identification of multispecies in biofilms, as the use of specific primers able to amplify particular microorganisms is required¹⁰. The results obtained with PCR techniques have contributed to unveil the abundance of bacterial genera and species present in the entire endodontic microbiome¹¹. Moreover, the introduction of pyrosequencing and of next generation sequencing (NGS), bypassing the intrinsic limits of PCR techniques linked to the preliminary “blind” selection of specific primers, has largely improved the diagnostic performance allowing the identification of a much higher bacterial diversity in root canals^{1,12,13}. This has allowed gathering information on the composition of the entire microbial communities in PAP and SAP^{5,14}, assessing the effects of root canal treatment on endodontic microbiome^{6,15} and individuating bacteria potentially active in endodontic infections¹⁶.

As PAP and SAP, it is still unclear if other different aspects (ie, presence of clinical signs of AP, periapical index [PAI]) of endodontic disease can be associated with different core microbiome contributing, to various extent, in the pathogenesis of the disease, resistance to treatment and systemic implications¹⁷. In addition, geographical differences in terms of prevalence of some bacterial species or taxa¹⁸ could increase the complexity of this scenario. Finally, in recent years it has been realized that the oral microbiome is not a homogeneous collection of life forms, but rather an assortment of mini microbiomes at different sites in the mouth¹⁹. However, in contrast to the oral cavity, root canal environment should be unique in that it is a secluded space²⁰ and this could influence its microbiome composition. A metanalysis review of the literature¹ has revealed that Firmicutes, Actinobacteria, Bacteroidetes, Proteobacteria, and Fusobacteria are most prevalent in the intracanal samples. More specifically, members of the genera *Prevotella*, *Fusobacterium*, *Parvimonas*, *Lactobacillus*, *Streptococcus*, and *Porphyromonas* were highly associated with intracanal samples.

The aim of the study was to analyze the root canal microbiome using 16S ribosomal DNA (rDNA) NGS to understand whether there could be a correlation with the presence of AP-derived symptoms and with the severity of lesions, as measured by the PAI. Another aim of the study was to understand possible

differences in the microbiome composition between PAP and SAP cases.

MATERIALS AND METHODS

Study Population

A total of 15 patients were enrolled in the study. The patients were referred to the Endodontic Clinical Section, Dental School, Department of Biomedical and NeuroMotor Sciences, University of Bologna, Italy, to receive endodontic care. The exclusion criteria for this study were having received antibiotic therapy up to 3 months before starting endodontic therapy, systemic diseases, and pregnancy. The patients involved in the research signed a formal written informed consent form.

The study was performed in agreement with the ethical guidelines of the Declaration of Helsinki laid down in the 1964 and its later amendments or comparable ethical standards. The Ethics Committee of Azienda Unità Sanitaria Locale di Bologna approved this study with authorization nr. 844-2021-OSS-AUSLBO-21160-ID 3118-Parere CE-AVEC-ENDOMICROBIOTA 09/2021.

Study participants were healthy patients categorized under American society of Anesthesiologists ($n = 12$ as ASA 1 and $n = 3$ as ASA 2), with a mean age of 58 years old (range: 30–84, standard deviation = 20.1) and equally distributed in male ($n = 7$) and female ($n = 8$) gender. A total of 17 teeth affected by AP diagnosed by clinical and radiological evaluation were included. Thirteen teeth presented coronal leakage and/or coronal decay (PAP = 7; SAP = 6), whilst four teeth showed an apparent intact coronal seal (PAP = 1; SAP = 3). AP signs were considered presence of tissue swelling ($n = 2$), percussion/palpation sensitivity ($n = 7$), spontaneous pain ($n = 4$), sinus tracts ($n = 3$). Three teeth presented only clinical signs and symptoms without any radiological change in periapical bone structure (acute AP) whilst seven teeth presented periapical radiolucency in the absence of clinical symptomatology (chronic AP). Seven teeth were associated to symptomatology and presence of apical radiolucent area (exacerbated chronic AP)⁵.

PAP subgroup included necrotic teeth with untreated root canal system whilst SAP subgroup encompassed teeth with a previous endodontic treatment (SAP).

Pulpal necrosis was diagnosed by thermal and electric pulp sensibility tests. Periodontal probing was also performed to exclude severe periodontal disease (stage III and stage IV)¹⁸ and vertical root fractures. PAI score was used to categorize samples into a 5-point scale: PAI 1 and 2 were considered as

healthy status whilst PAI 3–5 as unhealthy periapical status^{21–23} (Table 1). Radiographic analyses were performed with evaluation of PAI score on periapical bidimensional projections using paralleling technique²¹. Teeth with PAI ≥ 3 presented a mean measurement of periapical radiolucency of 6.9 millimeters (range: 1 mm–18 mm, standard deviation = 6.4 mm).

A total of 17 samples were collected from the 15 patients enrolled in the study. Samples Z3 and Z4 and samples #18 and #19 were collected from 2 different patients, respectively.

The collected samples were classified on the basis of 3 different recorded parameters: (1) presence ($n = 10$) or absence of AP symptoms ($n = 7$); (2) presence of PAP ($n = 8$) or SAP ($n = 9$); (3) PAI ≤ 2 ($n = 5$) or PAI ≥ 3 ($n = 12$) (Table 1).

Root Canal Samples

After local anesthesia, the teeth were cleaned with ultrasonic tips to remove biofilms and subsequently isolated with a rubber dam. Surface disinfection of enamel and rubber dam were carried out using a small cotton swab soaked with 5% sodium hypochlorite solution (Nicolor 5, Ogna, Maggiò, Italy) for 30 seconds and dried with a sterile cotton pellet. No rubber dam leakage was observed during the sampling procedures. Removal of caries and old restorative materials was performed before gaining entrance to the root canal system. Before removal of the pulp chamber roof, cleaning of the tooth, access cavity and rubber dam was repeated as previously described. The working length was estimated by the preoperative Rx and 3 mm were subtracted to avoid an over-instrumentation of the tooth. For teeth with previous endodontic treatment, Gates–Glidden burs #2 and #3 (Dentsply Sirona, Charlotte, NC) were used to create a pathway through the gutta-percha. Reciprocating nickel–titanium instrument Reciproc Blue R25™ (diameter #25, regressive taper 08%) (VDW, Munich, Germany) was gently inserted into the pathway and pushed into the canal to remove the coronal part of gutta-percha. The instrument was then removed, cleaned and re-inserted in apical direction repeating the procedure until the working length was reached. No irrigants were used in order to leave unchanged as much as possible bacterial biofilm.

After gentle irrigation with sterile saline solution, a sterile #10 K-type stainless hand file (Dentsply Sirona, Charlotte, NC) was introduced into the root canal at the tooth apex level and the final working length was defined using an apex locator (Root ZX®; J. Morita

TABLE 1 - Clinical Parameters of Patients with Apical Periodontitis (AP) and Relative Root Canal Samples

Patients	Samples																
	*1	3	4	5	9	10	11	12	13	16	17	18 [†]	19 [†]	Z1	Z2	Z3 [‡]	Z4 [‡]
Age (y)	82	63	83	83	38	56	52	67	46	70	50	30	30	62	84	30	30
Gender	M	M	F	F	F	M	F	F	F	F	M	M	M	M	F	M	M
[§] SYM/ ASY	SYM	ASY	SYM	SYM	SYM	ASY	SYM	ASY	SYM	ASY	SYM	ASY	ASY	SYM	ASY	SYM	SYM
[¶] PAP/ SAP [#]	SAP	PAP	PAP	PAP	PAP	SAP	SAP	SAP	SAP	PAP	SAP	SAP	PAP	PAP	PAP	SAP	SAP
**PAI	3	1	3	3	1	1	3	4	5	4	3	5	5	2	2	4	4

ASY, asymptomatic; PAP, primary apical periodontitis; SAP, secondary/persistent apical periodontitis; SYM, symptomatic.

*Identification code of the root canal samples.

[†]Same patient.

[‡]Same patient.

[§]SYM: symptomatic AP.

^{||}ASY: asymptomatic.

[¶]PAP: Primary AP.

[#]SAP: Secondary/persistent AP.

**PAI: Periapical Index from 1 (healthy) to 5 (severe) periodontitis.

Corp., Kyoto, Japan) and performing a periapical x-Ray. In multirrooted teeth, samples were collected from the largest root canal.

After gently scraping with instrumentation along the root canal walls to disperse bacteria in the medium, paper points #15 (Dentsply Sirona, Charlotte, NC) were positioned as deep as possible in the canals for 60 seconds to soak up the fluid in the canal. Also, the hand file was carefully wiped with another paper point to collect residual material. The samples were collected in sterile tubes (Eppendorf AG, Hamburg, Germany) and subsequently stored at -20°C until use.

DNA Extraction

Paper points were homogenized by a Tissue Lyser (Qiagen GmbH, Hilden, Germany) in

2 mL Eppendorf safe-lock tubes containing Dulbecco Minimal Essential medium (30 Hz for 5 minutes). Subsequently, homogenates were centrifuged at 10.00 × g for 3 minutes. A total of 200 µL of the supernatants were then used for the subsequent DNA extraction using DNeasy PowerSoil PRO kit (Qiagen S.p.A., Milan, Italy) according to the manufacturer's protocol. The kit recovers inhibitor-free high yield DNA for direct use in NGS applications and integrates a patented Inhibitor Removal Technology (Qiagen S.p.A., Milan, Italy) that works particularly well for DNA isolation from challenging samples.

PCR amplification of 16s rDNA gene and Nanopore sequencing DNA extract were subjected to PCR reaction using the TaKaRa LA TaqTM (Takara Bio Europe S.A.S., Saint-Germain-en-Laye, France) mix and the

universal primers 27F (5'-GAGTTTGATCCTGGCTCAG-3') and 1492R (5'-GGTTACCTTGTTACGACTT-3') to amplify the complete sequence (1500 bp) of 16S rDNA gene²⁴. DNA library was prepared using the 16S barcoding kit SQK-RAB204 (ONT, Oxford, United Kingdom) and PCR products were pooled after measuring the DNA concentration and loaded on MinION Flow cell flongle on a MinION- Mk1C device (ONT, Oxford, United Kingdom). Sequencing was set for at least 24 hours.

Data Analysis

The data were produced using the MiniKNOW software (ONT). Basecalling was carried out with Guppy version (3.5.5). Downstream analyses were carried out using EPI2ME, a cloud-based data analysis

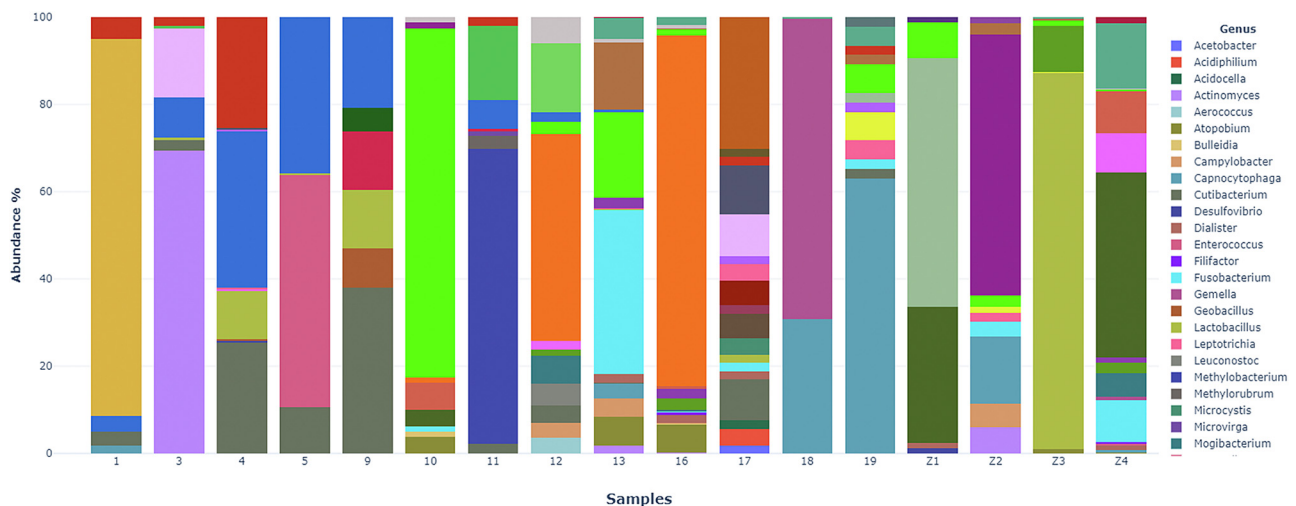


FIGURE 1 – Bacterial genera detected in the canal root samples of patients with apical periodontitis

TABLE 2 - Distribution of Sequence Dta, Expressed as Percentage, per Bacterial Genera in Samples from Patients with Symptomatic or Asymptomatic AP, Primary or Secondary/ Persistent Apical Periodontitis and Periapical Index ≤ 2 and ≥ 3

Bacterial genera	Total reads (%)	*SYM (%)	†ASY (%)	‡PAP (%)	§SAP (%)	 PAI≤ 2 (%)	PAI≥ 3 (%)
<i>Acetobacter</i>	0.1	100.0	0.0	0.0	100.0	0.0	100.0
<i>Acidiphilium</i>	0.2	100.0	0.0	0.0	100.0	0.0	100.0
<i>Acidocella</i>	0.1	100.0	0.0	0.0	100.0	0.0	100.0
<i>Actinomyces</i>	6.0	2.5	97.5	97.5	2.5	97.3	2.7
<i>Aerococcus</i>	0.2	0.0	100.0	0.0	100.0	0.0	100.0
<i>Atopobium</i>	1.3	48.0	52.0	37.9	62.1	14.1	85.9
<i>Bulleidia</i>	0.1	0.0	0.0	85.9	14.1	85.8	14.2
<i>Campylobacter</i>	0.8	32.8	67.2	34.2	65.8	32.8	67.2
<i>Capnocytophaga</i>	4.7	10.5	89.5	10.5	89.5	15.5	84.5
<i>Cutibacterium</i>	5.3	92.9	7.1	91.4	8.6	38.7	61.2
<i>Desulfovibrio</i>	0.1	100.0	0.0	100.0	0.0	77.3	22.7
<i>Dialister</i>	0.5	72.6	27.4	44.0	56.0	11.0	89.9
<i>Enterococcus</i>	5.1	100.0	0.0	99.4	0.6	0.0	100.0
<i>Filifactor</i>	0.1	42.1	57.9	57.9	42.1	0.0	100.0
<i>Fusobacterium</i>	4.4	92.7	7.3	5.8	94.2	5.1	94.9
<i>Gemella</i>	2.7	1.6	98.4	0.0	100.0	0.0	100.0
<i>Geobacillus</i>	0.5	100.0	0.0	100.0	0.0	96.4	3.6
<i>Lactobacillus</i>	5.5	99.0	1.0	23.1	76.9	12.9	87.1
<i>Leptotrichia</i>	0.3	6.0	94.0	94.0	6.0	35.3	64.7
<i>Leuconostoc</i>	0.2	0.0	100.0	0.0	100.0	0.0	100.0
<i>Methylobacterium</i>	3.6	100.0	0.0	0.0	100.0	0.0	100.0
<i>Methylobacterium</i>	0.2	100.0	0.0	0.0	100.0	0.0	100.0
<i>Microcystis</i>	0.2	100.0	0.0	0.0	100.0	0.0	100.0
<i>Microvirga</i>	0.1	100.0	0.0	0.0	100.0	0.0	100.0
<i>Mogibacterium</i>	0.7	52.1	47.9	4.6	95.4	0.0	100.0
<i>Moraxella</i>	0.7	100.0	0.0	96.1	3.9	96.1	3.9
<i>Neisseria</i>	0.3	3.1	96.9	96.9	3.1	20.4	79.6
<i>Nitrosococcus</i>	0.2	100.0	0.0	0.0	100.0	0.0	100.0
<i>Okeania</i>	0.1	100.0	0.0	0.0	100.0	0.0	100.0
<i>Olsenella</i>	0.9	71.8	28.2	21.2	78.8	0.0	100.0
<i>Oribacterium</i>	0.5	62.0	38.0	38.0	62.0	0.0	100.0
<i>Oscillatoria</i>	0.2	100.0	0.0	0.0	100.0	0.0	100.0
<i>Parvimonas</i>	4.4	95.7	4.3	33.8	66.2	38.0	62.0
<i>Pedobacter</i>	0.1	0.0	100.0	100.0	0.0	0.0	100.0
<i>Pelomonas</i>	0.3	100.0	0.0	100.0	0.0	100.0	0.0
<i>Peptoniphilus</i>	0.7	86.4	13.6	2.5	97.5	0.0	100.0
<i>Peptostreptococcus</i>	1.0	63.2	36.8	32.2	67.8	32.2	67.8
<i>Phocaeicola</i>	8.6	0.0	100.0	73.2	26.8	0.7	99.3
<i>Planktothrix</i>	0.2	100.0	0.0	9.6	90.4	0.0	100.0
<i>Porphyromonas</i>	2.8	97.2	2.8	100	0.0	97.2	2.8
<i>Prevotella</i>	6.8	31.9	68.1	12.6	87.4	67.1	32.9
<i>Propionibacterium</i>	2.9	0.0	100.0	97.8	2.2	100.0	0.0
<i>Pseudomonas</i>	7.7	84.7	15.3	89.0	11.0	23.1	76.9
<i>Psychrobacillus</i>	0.1	100.0	0.0	16.7	83.3	0.0	100.0
<i>Pyramidobacter</i>	0.7	0.0	100.0	0.0	100.0	0.0	100.0
<i>Roseomonas</i>	1.7	23.8	76.2	76.2	23.8	76.2	23.8
<i>Rothia</i>	7.5	100.0	0.0	0.0	100.0	0.0	100.0
<i>Selenomonas</i>	1.6	86.0	14.0	14.0	86.0	8.0	92.0
<i>Solobacterium</i>	0.5	20.0	80.0	11.8	88.2	12.4	87.6
<i>Sphingomonas</i>	0.9	96.2	3.8	3.8	96.2	3.8	96.2
<i>Stanieria</i>	0.5	100.0	0.0	3.4	96.6	0.0	100.0
<i>Staphylococcus</i>	2.1	88.4	11.6	67.1	32.9	7.9	92.1
<i>Streptococcus</i>	1.7	81.6	18.4	17.5	82.5	0.0	100.0
<i>Tannerella</i>	0.1	90.9	9.1	100.0	0.0	91.0	9.0
<i>Thermus</i>	0.1	0.0	100.0	100.0	0.0	0.0	100.0
<i>Treponema</i>	0.1	14.5	85.5	85.4	14.6	84.5	15.5
<i>Trichococcus</i>	0.1	100.0	0.0	0.0	100.0	0.0	100.0

(continued on next page)

TABLE 2 - Continued

Bacterial genera	Total reads (%)	*SYM (%)	†ASY (%)	‡PAP (%)	§SAP (%)	PAI≤2 (%)	PAI≥3 (%)
<i>Trichocoleus</i>	1.3	100.0	0.0	0.0	100.0	0.0	100.0
<i>Veillonella</i>	0.1	100.0	0.0	0.0	100.0	0.0	100.0
Total	100.0	55.5	44.5	46.4	53.6	27.4	72.6

ASY, asymptomatic; PAI, periapical index; PAP, primary apical periodontitis; SAP, secondary/persistent apical periodontitis; SYM, symptomatic.

*SYM: symptomatic AP.

†asymptomatic AP.

‡PAP: Primary AP.

§SAP: Secondary/persistent AP.

||PAI: Periapical Index from 1 (healthy) to 5 (severe) periodontitis.

platform (<https://epi2me.nanoporetech.com/>), using Fastq 16S 2021.09.09 (Metrichor Agent, ONT, Oxford, United Kingdom) workflow for analysis of sequences with quality score 10, minimum length filter of 1500 bases and BLAST Expected value of 0.01. Taxonomy was assigned using BLAST to the National Center for Biotechnology Information 16S + 18S ribosomal RNA database, with a minimum horizontal coverage of 30% and a minimum accuracy of 77% as default parameters. Reads obtained for each bacterial genus and species were collected, organized in Microsoft Office Excel xls sheets and then graphically represented as BarPlot charts. Taxa detected at $\geq 0.1\%$ relative abundance in samples were included for the analysis of the microbial communities, using “Plotly.py” open-source library for Python 3.7.9²⁵. Moreover, multi-layered pie charts at species level were generated by the “Krona” visualization tool²⁶.

Diversity Indexes

Statistical analyses were performed with R v.4.1.3 using the library “vegan” (<https://vegandevs.github.io/vegan/>). In order to evaluate the community’s composition, alpha diversity for each sample was assessed using Shannon index and measure of biodiversity was evaluated using Richness Menhinick’s index. Shapiro–Wilk test was performed to evaluate the normality of distribution of data. Two-sided Student’s *t* test for independent samples or Mann–Whitney U test were performed on the calculated alpha diversity and biodiversity values on the basis of categories: presence/absence of AP symptoms, presence of PAP/SAP and PAI ≤ 2 /PAI ≥ 3 . To identify possible sample stratification, beta diversity was assessed using (Bray–Curtis index and Principal Coordinate Analysis) was performed for each pair of categories. ANOVA test and Tukey Honestly Significant Difference as *post hoc* test were carried out on the calculated beta diversity values. The statistical significance was set at 0.05.

RESULTS

All 17 analyzed samples were positive for the presence of bacterial DNA. Nanopore sequencing on MinION MK1c revealed a total number of 632,794 16S rDNA gene sequences after quality control (median: 31,300 reads, range 23,000–59,976). A total of 308 Operational Taxonomic Units (OTUs) were identified and assigned to 9 phyla, 59 genera, and 240 species using Fastq 16S 2021.09.09 workflow. A total of 92,486 sequences (14.6%) could not be classified below the genus level.

The most abundant phyla detected were *Firmicutes* (27.9%) and *Bacteroidetes* (25.8%), followed by *Actinobacteria* (17.7%). The most prominent genera were *Phocaeicola* (8.6%), *Pseudomonas* (7.7%), *Rothia* (7.5%), and *Prevotella* (6.8%) (Fig. 1), whilst *Phocaeicola abscessus* (8.5%), *Rothia Dentocariosa* (7.4%), *Actinomyces israelii* (5.6%), and *Parvimonas micra* (4.4%) were the most abundant species. Despite being a close-ended analysis, the most representative taxa in the samples were detected, covering, on average, 78.9% of the post QC MinION-MK1C reads (range: 51%–87%).

Table 2 describes sequence data obtained for each sample in this study and subdivided for presence or absence of AP symptoms, evidence of PAP or SAP and PAI < 2 or PAI > 3 .

The presence of bacterial genera in the analyzed samples is reported in Table 3 whilst Table 4 reports the distribution of bacterial genera, expressed as percentage, in samples classified according to the recorded criteria. In Figure 2 bacterial genera detected in at least 40% of the samples for each category are reported.

Diversity Indexes

Alpha diversity among samples calculated by using Shannon index ranged between 0.51 and 2.51 (mean = 1.27; median = 1.083)

whilst the biodiversity value using Richness Menhinick’s index ranged between 0.006 and 0.10 (mean = 0.052; median = 0.043). Comparisons of alpha diversity and biodiversity values did not reach the thresholds of statistical significance ($P > .05$) for any of the considered categories (symptomatic vs asymptomatic cases, status of PAP/SAP and scores of PAI ≤ 2 /PAI ≥ 3).

Beta diversity for each pair of categories were assessed by using Bray–Curtis index and Principal Coordinate Analysis plot graphs were produced (Fig. 3). Comparisons of beta diversity of samples did not reveal statistical significance ($P > .05$) for the categories “symptomatic versus asymptomatic” and status of PAP/SAP. The beta diversity values differed significantly ($P < .05$) when considering the PAI scores (PAI ≤ 2 vs PAI ≥ 3).

DISCUSSION

NGS has improved the knowledge about the microbiota thriving in several districts of human body either in physiological and pathological conditions. In the present study, the microbiome composition was investigated in samples obtained from root canals of teeth with periapical lesions due to AP using 16S rDNA analysis on the MinION platform of ONT. Overall, in our study 308 Operational Taxonomic Units were identified and assigned to 9 phyla, 59 genera and 240 species using Fastq 16S 2021.09.09 workflow.

The rationale for the study was based on the hypothesis that local microbial insult can have relevant clinical implications, since bacteria located in these sites are in a strategic position to inflict damage to the host and to induce and maintain periapical inflammation. Therefore, the aims of the study were to understand whether there could be a correlation between the apical root canal microbiome and the presence of AP-derived symptoms. Moreover, assuming that the severity of AP lesions, scored with

TABLE 3 - Presence of Bacterial Genera in the Root Canal Samples of Patients with AP

Patients	Samples																
	*1	3	4	5	9	10	11	12	13	16	17	18 [†]	19 [†]	Z1	Z2	Z3 [‡]	Z4 [‡]
§SYM/ASY	SYM	ASY	SYM	SYM	SYM	ASY	SYM	ASY	SYM	ASY	SYM	ASY	ASY	SYM	ASY	SYM	SYM
¶PAP/SAP [#]	SAP	PAP	PAP	PAP	PAP	SAP	SAP	SAP	SAP	PAP	SAP	SAP	PAP	PAP	PAP	SAP	SAP
**PAI	3	1	3	3	1	1	3	4	5	4	3	5	5	2	2	4	4
Bacterial genera																	
<i>Acetobacter</i>	—	—	—	—	—	—	—	—	—	—	+	—	—	—	—	—	—
<i>Acidiphilium</i>	—	—	—	—	—	—	—	—	—	—	—	+	—	—	—	—	—
<i>Acidocella</i>	—	—	—	—	—	—	—	—	—	—	+	—	—	—	—	—	—
<i>Actinomyces</i>	—	+	—	—	—	—	—	—	+	+	—	—	—	—	+	—	—
<i>Aerococcus</i>	—	—	—	—	—	—	—	+	—	—	—	—	—	—	—	—	—
<i>Atopobium</i>	—	—	—	—	—	+	—	—	+	+	—	—	—	—	—	+	+
<i>Bulleidia</i>	—	—	—	—	—	+	—	—	—	+	—	—	—	—	—	—	—
<i>Campylobacter</i>	—	—	—	—	—	—	—	+	+	+	—	—	—	—	+	—	—
<i>Capnocytophaga</i>	+	—	—	—	—	—	—	—	+	—	—	+	+	—	+	—	+
<i>Cutibacterium</i>	+	+	+	+	+	—	+	+	+	+	+	—	+	—	—	—	—
<i>Desulfovibrio</i>	—	—	+	+	—	—	—	—	—	—	—	—	—	+	—	—	—
<i>Dialister</i>	—	—	—	—	—	—	—	—	+	+	+	—	—	+	—	—	+
<i>Enterococcus</i>	—	—	—	+	—	—	—	—	—	—	—	—	—	—	—	—	+
<i>Filifactor</i>	—	—	—	—	—	—	—	—	—	+	—	—	—	—	—	—	+
<i>Fusobacterium</i>	—	—	—	—	—	+	—	—	+	+	+	—	+	—	+	—	+
<i>Gemella</i>	—	—	—	—	—	—	—	—	—	—	—	+	—	—	—	—	+
<i>Geobacillus</i>	—	—	+	+	+	—	—	—	—	—	—	—	—	—	—	—	—
<i>Lactobacillus</i>	—	+	+	+	+	—	—	+	+	+	+	—	—	—	—	+	—
<i>Leptotrichia</i>	—	—	—	—	—	—	—	—	+	—	—	—	+	—	+	—	—
<i>Leuconostoc</i>	—	—	—	—	—	—	—	+	—	—	—	—	—	—	—	—	—
<i>Methylobacterium</i>	—	—	—	—	—	—	+	—	—	—	—	—	—	—	—	—	—
<i>Methylorubrum</i>	—	—	—	—	—	—	+	—	—	—	—	—	—	—	—	—	—
<i>Microcystis</i>	—	—	—	—	—	—	—	—	—	—	+	—	—	—	—	—	—
<i>Microvirga</i>	—	—	—	—	—	—	+	—	—	—	—	—	—	—	—	—	—
<i>Mogibacterium</i>	—	—	—	—	—	—	—	+	+	+	—	—	—	—	—	—	+
<i>Moraxella</i>	—	—	—	—	+	—	+	—	—	—	—	—	—	—	—	—	—
<i>Neisseria</i>	—	—	—	—	—	—	—	—	—	—	—	—	+	—	+	+	—
<i>Nitrosococcus</i>	—	—	—	—	—	—	—	—	—	—	+	—	—	—	—	—	—
<i>Okeania</i>	—	—	—	—	—	—	—	—	—	—	+	—	—	—	—	—	—
<i>Olsenella</i>	—	—	—	—	—	—	—	+	—	+	—	—	—	—	—	+	+
<i>Oribacterium</i>	—	—	—	—	—	—	—	—	+	+	—	—	—	—	—	—	+
<i>Oscillatoria</i>	—	—	—	—	—	—	—	—	—	—	+	—	—	—	—	—	—
<i>Parvimonas</i>	—	—	—	—	—	+	—	—	—	—	—	—	—	+	—	—	+
<i>Pedobacter</i>	—	—	—	—	—	—	—	—	—	—	—	—	+	—	—	—	—
<i>Pelomonas</i>	—	—	—	—	+	—	—	—	—	—	—	—	—	—	—	—	—
<i>Peptoniphilus</i>	—	—	+	+	—	—	—	+	—	—	—	—	—	—	—	—	+
<i>Peptostreptococcus</i>	—	—	—	—	—	+	—	—	—	+	—	—	—	—	—	—	+
<i>Phocaecicola</i>	—	—	—	—	—	+	—	+	—	+	—	—	—	—	—	—	—
<i>Plankothrix</i>	—	—	+	+	—	—	—	—	—	—	+	—	—	—	—	—	—
<i>Porphyromonas</i>	—	—	—	—	—	—	—	—	—	+	—	—	+	+	—	—	—
<i>Prevotella</i>	—	—	—	—	—	+	—	+	+	+	—	—	+	+	+	+	+
<i>Propionibacterium</i>	—	—	—	—	—	+	—	—	—	—	—	—	—	—	+	—	—
<i>Pseudomonas</i>	+	+	+	+	+	—	+	+	+	+	—	—	—	—	—	—	—
<i>Psychrobacillus</i>	—	—	+	+	—	—	—	—	—	—	+	—	—	—	—	—	—
<i>Pyramidobacter</i>	—	—	—	—	—	—	—	+	—	—	—	—	—	—	—	—	—
<i>Roseomonas</i>	—	+	—	—	—	—	—	—	—	—	+	—	—	—	—	—	—
<i>Rothia</i>	+	—	—	—	—	—	—	—	—	—	—	—	—	—	—	—	—
<i>Selenomonas</i>	—	—	—	—	—	—	—	—	+	+	—	—	+	—	+	+	—
<i>Solobacterium</i>	—	—	—	—	—	+	—	+	+	+	—	—	—	—	—	—	+
<i>Sphingomonas</i>	—	+	—	—	—	—	+	—	—	—	—	—	—	—	—	—	—
<i>Stanieria</i>	—	—	+	+	—	—	—	—	—	—	+	—	—	—	—	—	—
<i>Staphylococcus</i>	+	+	+	—	—	—	+	—	—	—	+	—	+	—	—	—	—
<i>Streptococcus</i>	—	—	—	—	—	—	—	—	+	+	—	+	+	—	—	+	+
<i>Tannerella</i>	—	—	—	—	—	—	—	—	—	+	—	—	—	+	—	—	—
<i>Thermus</i>	—	—	—	—	—	—	—	—	—	—	—	—	+	—	—	—	—

(continued on next page)

TABLE 3 - Continued

Patients	Samples																
	*1	3	4	5	9	10	11	12	13	16	17	18 [†]	19 [†]	Z1	Z2	Z3 [‡]	Z4 [‡]
<i>Treponema</i>	—	—	—	—	—	—	—	—	+	—	—	—	—	—	+	—	—
<i>Trichococcus</i>	—	—	—	—	—	—	—	—	—	—	+	—	—	—	—	—	—
<i>Trichocoleus</i>	—	—	—	—	—	—	—	—	—	—	+	—	—	—	—	—	—
<i>Veillonella</i>	—	—	—	—	—	—	—	—	+	—	—	—	—	—	—	—	+

ASY, asymptomatic; PAP, primary apical periodontitis; SAP, secondary/persistent apical periodontitis; SYM, symptomatic.

+ : Presence; - : Absence.

*Identification code of the root canal samples.

[†]Same patient.

[‡]Same patient.

[§]SYM symptomatic AP.

^{||}ASY: asymptomatic AP.

[¶]PAP: Primary AP.

[‡]SAP: Secondary/persistent AP.

**Periapical Index: from 1 (healthy) to 5 (severe) periodontitis.

PAI, could correlate with the microbial insult, it was interesting to explore the diversity of the root canal microbiome. Finally, since treatment of the root canal in PAP could determine contamination of a secluded environment with bacteria, it was interesting to understand whether there could differences between PAP and SAP cases. Alpha and beta diversity analyses were applied to explore possible trends in the 16S rDNA data generated from the patients enrolled in this study. In these analyses, there was no significant difference of the root canal microbiome in terms of presence of symptoms in patients. Attempts to establish a correlation of the clinical symptoms with root canal microbiome has been done in other studies²⁷ and the authors noted that bacterial genera *Fusobacterium*, *Porphyromonas*, *Phocaeicola*, *Olsenella*, *Campylobacter*, *Tannerella*, and *Fretibacterium* were significantly more abundant in the symptomatic patients, whereas *Sphingomonas* was more common in asymptomatic patients.

By converse, beta diversity reached the threshold of statistical significance ($P < .05$) when comparing the PAI categories (PAI ≤ 2 vs PAI ≥ 3), that is, the severity of the PA lesions. Significant changes in microbiome diversity in relation to PAI have been reported elsewhere¹⁶.

In our data, in cases with PAI ≥ 3 , facultative anaerobic Gram-positive bacteria predominated in root canals. *Cutibacterium*, *Lactobacillus*, and *Pseudomonas* were the most frequent genera. Interestingly, *Streptococcus* was identified in 50% of patients with PAI ≥ 3 , whilst it was not present in patients with PAI ≤ 2 . Likewise, *Cutibacterium* prevalence in patients with PAI ≥ 3 was higher than in cases with PAI ≤ 2 .

Also, on alpha and beta diversity analyses, the differences did not reach the threshold of statistical significance when comparing PAP and SAP cases. Primary infected root canals are untreated canals where microorganisms are able to access and colonize the pulpal tissue and impair its function whilst secondary/persistent infected root canals can be the result of either resilient bacteria thriving after initial treatment or contamination during the treatment procedure. This aspect has been investigated elsewhere but the results are controversial. Some Authors²⁸ noted a significant decrease in bacterial diversity in SAP samples compared with PAP cases, whilst others reported an increased microbiome diversity^{17,29} or no significant difference between PAP and SAP cases^{30,31}. This could indicate the presence of confounding elements in the various steps of the experiment, starting from the collection of samples, to the sequencing platform and the pipeline for data analysis of 16S rDNA.

Although the trends in our data were not supported statistically, *Cutibacterium*, *Lactobacillus*, and *Pseudomonas* appeared more common (>50%) in PAP whilst *Cutibacterium* and *Prevotella* were more common in SAP (Table 4). In particular, there was an increased prevalence of *Lactobacillus* in PAP cases (62.5% vs 33.3% of SAP cases). Likewise, *Cutibacterium* prevalence was higher in PAP (75%) than in SAP (55.6%) cases.

Microbiome studies based on 16Sr DNA sequencing have some limits, as the results are relatively rather than absolutely quantitative. Also, the results can be biased due to varying efficiency of PCR amplification and sequencing and of reference databases used for sequence analysis. Also, only some 15% of bacterial genomes contain a single 16s rDNA gene copy, whilst most bacterial phyla may contain species

with 1 or more copies³². In the present study, bacteriome analysis was based on the full-length 16S rDNA gene (V1–V9 regions), rather than on smaller portions. Due to constraints of some massive sequencing chemistry/platforms, reads covering the full length of the 16S rDNA gene cannot be generated³³, and several variable regions have been targeted for sequencing, limiting the resolution at the species level and causing ambiguity in taxonomic classification³⁴. The MinION sequencer from ONT is capable of producing long sequences with no theoretical read length limit and MinION sequencing targets the entire 16S rDNA gene, allowing the identification of bacteria with more accuracy^{35,36}. Also, whilst the costs for consumables can vary based on the multiplexing and chemistry among different NSG platforms, ONT platform can be used starting with a negligible investment in terms of hardware (eg, MinION).

Yet, variability between studies using complex NGS workflows is unavoidable and may stem from DNA extraction, from the 16S rDNA gene variable regions targeted by PCR, or from the sequencing bioinformatic analysis pipeline. For instance, our analysis relied on cloud-based data analysis platform Epi2me, using Fastq 16S 2021.09.09 workflow and taxonomy was assigned using the National Center for Biotechnology Information 16S + 18S ribosomal RNA database, rather than the more specific expanded Human Oral Microbiome Database (eHOMD) (<https://www.homd.org/>). eHOMD is a curated database containing information on bacteria in the human mouth and aerodigestive tract. Out of 774 bacterial species, 58% are officially named, 16% unnamed but cultivated, and 26% are known only as uncultivated phylotypes. In our study, there were only 14.6% of 16S rDNA sequences not classified

TABLE 4 - Distribution of Bacterial Genera, Expressed as Percentage, in the Root Canal Samples from Patients with Symptomatic or Asymptomatic AP, Primary or Secondary/ Persistent Apical Periodontitis and Periapical Index ≤ 2 and ≥ 3

Bacterial genera	Sample						
	Total (%)	*SYM (%)	†ASY (%)	‡PAP (%)	§SAP (%)	PAI ≤ 2 (%)	PAI ≥ 3 (%)
<i>Acetobacter</i>	5.9	10.0	0.0	0.0	11.1	0.0	8.3
<i>Acidiphilium</i>	5.9	10.0	0.0	0.0	11.1	0.0	8.3
<i>Acidocella</i>	5.9	10.0	0.0	0.0	11.1	0.0	8.3
<i>Actinomyces</i>	23.5	10.0	42.9	37.5	11.1	40.0	16.7
<i>Aerococcus</i>	5.9	0.0	14.3	0.0	11.1	0.0	8.3
<i>Atopobium</i>	29.4	30.0	28.6	12.5	44.4	20.0	33.3
<i>Bulleidia</i>	11.8	0.0	28.6	12.5	11.1	20.0	8.3
<i>Campylobacter</i>	23.5	10.0	42.9	25.0	22.2	20.0	25.0
<i>Capnocytophaga</i>	35.3	30.0	42.9	25.0	44.4	20.0	41.7
<i>Cutibacterium</i>	64.7	70.0	57.1	75.0	55.6	40.0	75.0
<i>Desulfovibrio</i>	17.6	30.0	0.0	37.5	0.0	20.0	16.7
<i>Dialister</i>	29.4	40.0	14.3	25.0	33.3	20.0	33.3
<i>Enterococcus</i>	11.8	20.0	0.0	12.5	11.1	0.0	16.7
<i>Fillifactor</i>	11.8	10.0	14.3	12.5	11.1	0.0	16.7
<i>Fusobacterium</i>	41.2	30.0	57.1	37.5	44.4	40.0	41.7
<i>Gemella</i>	11.8	10.0	14.3	0.0	22.2	0.0	16.7
<i>Geobacillus</i>	17.6	30.0	0.0	37.5	0.0	20.0	16.7
<i>Lactobacillus</i>	47.1	60.0	28.6	62.5	33.3	40.0	50.0
<i>Leptotrichia</i>	17.6	10.0	28.6	25.0	11.1	20.0	16.7
<i>Leuconostoc</i>	5.9	0.0	14.3	0.0	11.1	0.0	8.3
<i>Methylobacterium</i>	5.9	10.0	0.0	0.0	11.1	0.0	8.3
<i>Methylorubrum</i>	5.9	10.0	0.0	0.0	11.1	0.0	8.3
<i>Microcystis</i>	5.9	10.0	0.0	0.0	11.1	0.0	8.3
<i>Microvirga</i>	5.9	10.0	0.0	0.0	11.1	0.0	8.3
<i>Mogibacterium</i>	23.5	20.0	28.6	12.5	33.3	0.0	33.3
<i>Moraxella</i>	11.8	20.0	0.0	12.5	11.1	20.0	8.3
<i>Neisseria</i>	17.6	10.0	28.6	25.0	11.1	20.0	16.7
<i>Nitrosococcus</i>	5.9	10.0	0.0	0.0	11.1	0.0	8.3
<i>Okeania</i>	5.9	10.0	0.0	0.0	11.1	0.0	8.3
<i>Olsenella</i>	23.5	20.0	28.6	12.5	33.3	0.0	33.3
<i>Oribacterium</i>	17.6	20.0	14.3	12.5	22.2	0.0	25.0
<i>Oscillatoria</i>	5.9	10.0	0.0	0.0	11.1	0.0	8.3
<i>Parvimonas</i>	17.6	20.0	14.3	12.5	22.2	40.0	8.3
<i>Pedobacter</i>	5.9	0.0	14.3	12.5	0.0	0.0	8.3
<i>Pelomonas</i>	5.9	10.0	0.0	12.5	0.0	20.0	0.0
<i>Peptoniphilus</i>	23.5	30.0	14.3	25.0	22.2	0.0	33.3
<i>Peptostreptococcus</i>	17.6	10.0	28.6	12.5	22.2	20.0	16.7
<i>Phocaeicola</i>	17.6	0.0	42.9	12.5	22.2	20.0	16.7
<i>Planktothrix</i>	17.6	30.0	0.0	25.0	11.1	0.0	25.0
<i>Porphyromonas</i>	17.6	10.0	28.6	37.5	0.0	20.0	16.7
<i>Prevotella</i>	52.9	40.0	71.4	50.0	55.6	60.0	50.0
<i>Propionibacterium</i>	11.8	0.0	28.6	12.5	11.1	40.0	0.0
<i>Pseudomonas</i>	52.9	60.0	42.9	62.5	44.4	40.0	58.3
<i>Psychrobacillus</i>	17.6	30.0	0.0	25.0	11.1	0.0	25.0
<i>Pyramidobacter</i>	5.9	0.0	14.3	0.0	11.1	0.0	8.3
<i>Roseomonas</i>	11.8	10.0	14.3	12.5	11.1	20.0	8.3
<i>Rothia</i>	5.9	10.0	0.0	0.0	11.1	0.0	8.3
<i>Selenomonas</i>	29.4	20.0	42.9	37.5	22.2	20.0	33.3
<i>Solobacterium</i>	29.4	20.0	42.9	12.5	44.4	20.0	33.3
<i>Sphingomonas</i>	11.8	10.0	14.3	12.5	11.1	20.0	8.3
<i>Stanieria</i>	17.6	30.0	0.0	25.0	11.1	0.0	25.0
<i>Staphylococcus</i>	35.3	40.0	28.6	37.5	33.3	20.0	41.7
<i>Streptococcus</i>	35.3	30.0	42.9	25.0	44.4	0.0	50.0
<i>Tannerella</i>	11.8	10.0	14.3	25.0	0.0	20.0	8.3
<i>Thermus</i>	5.9	0.0	14.3	12.5	0.0	0.0	8.3
<i>Treponema</i>	11.8	10.0	14.3	12.5	11.1	20.0	8.3
<i>Trichococcus</i>	5.9	10.0	0.0	0.0	11.1	0.0	8.3

(continued on next page)

TABLE 4 - Continued

Bacterial genera	Sample						
	Total (%)	*SYM (%)	†ASY (%)	‡PAP (%)	§SAP (%)	PAI ≤2 (%)	PAI ≥3 (%)
<i>Trichocoleus</i>	5.9	10.0	0.0	0.0	11.1	0.0	8.3
<i>Veillonella</i>	11.8	20.0	0.0	0.0	22.2	0.0	16.7

ASY, asymptomatic; PAI, periapical index; PAP, primary apical periodontitis; SAP, secondary/persistent apical periodontitis; SYM, symptomatic.

*SYM: symptomatic AP.

†ASY: asymptomatic AP.

‡PAP: Primary AP.

§SAP: Secondary/persistent AP.

||PAI: Periapical Index from 1 (healthy) to 5 (severe) periodontitis.

below the genus level but our pipeline did not allow us to compare with the curated data of eHOMD, at least for the unclassified phylotypes.

Another limit of our study was the relatively small size of the samples, although there are several studies from the literature with similar sampling size. Shin et al (2018) critically reviewed 12 peer-reviewed articles that specifically used different NGS technologies to assess the intracanal polymicrobial communities from 2010 to 2017. The total sample size ranged from 7 to 48 samples, with a mean of 19 samples, that is, around our sampling size. Likely, larger or differently structured studies could be more useful to identify trends in root canal microbiome in dental pathologies.

CONCLUSIONS

The present study confirms the complexity of the root canal microbiome, organized in multispecies communities. A correlation was identified in the microbiome diversity only for

severe cases of AP, as measured with a standardized index (PAI), but not for AP symptoms. In addition, we were not able to find trends related to the nature of PAP and SAP cases. A possible interpretation of the data is that endodontic biofilms are constituted by a constant population (more abundant and frequent) forming a sort of “scaffold” in which minor bacterial sub-populations contribute to different aspects of apical periodontitis. However, it is possible that other layers of analysis could be necessary to pinpoint relevant information, such as prediction of functional attributes of microbiome population.

CREDIT AUTHORSHIP CONTRIBUTION STATEMENT

Alessio Buonavoglia: Conceptualization, Writing – original draft, Supervision, Validation.

Fausto Zamparini: Investigation, Writing – original draft. **Gianvito Lanave:** Data curation, Writing – original draft, Formal analysis, Software. **Francesco Pellegrini:** Investigation,

Software, Formal analysis. **Georgia Diakoudi:** Investigation, Software, Methodology. **Andrea Spinelli:** Investigation, Writing – review & editing. **Maria Stella Lucente:** Methodology. **Michele Camero:** Formal analysis, Writing – review & editing. **Violetta Iris Vasinioti:** Investigation, Software. **Maria Giovanna Gandolfi:** Investigation, Project administration. **Vito Martella:** Project administration, Writing – review & editing. **Carlo Prati:** Conceptualization, Project administration, Writing – review & editing, Supervision, Validation.

DATA AVAILABILITY STATEMENT

The data that support the findings of this study are available from the corresponding author upon reasonable request.

ACKNOWLEDGMENT

The authors deny any conflicts of interest related to this study.

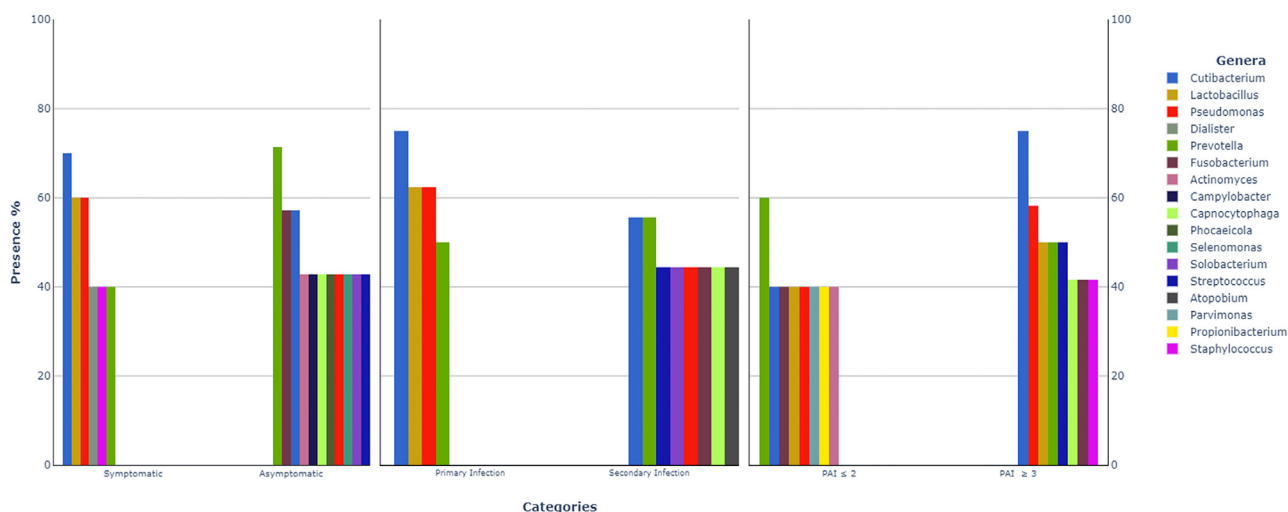


FIGURE 2 – Most represented bacterial genera (≥40%) in each category of samples from patients with apical periodontitis.

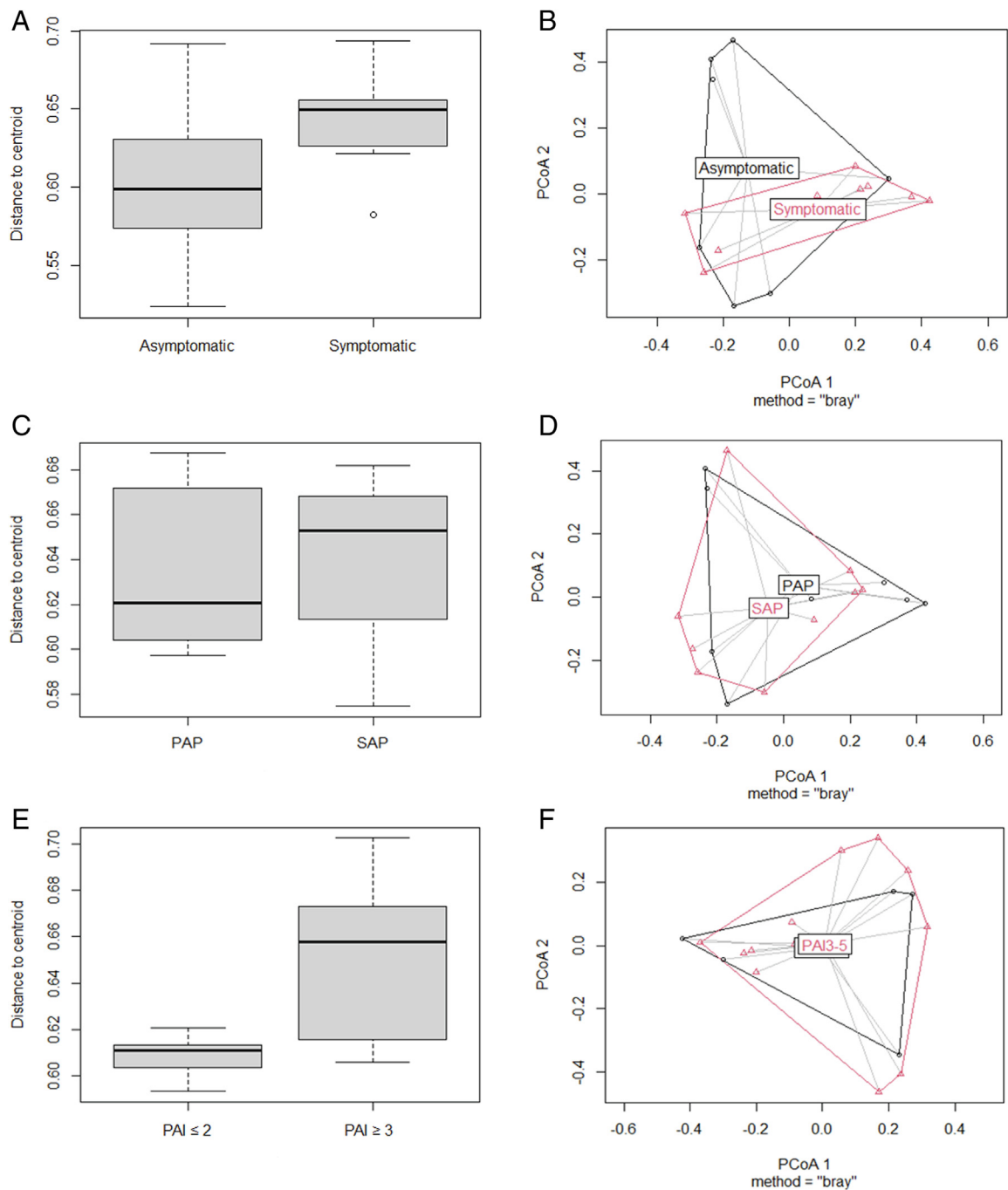


FIGURE 3 – Box and PCoA plots representing beta diversity according to Bray–Curtis index. Categories symptomatic versus asymptomatic, of primary apical periodontitis versus secondary/persistent apical periodontitis status and periapical index scores ≤ 2 vs ≥ 3 were assessed (panel A–F). PCoA, Principal Coordinate Analysis.

REFERENCES

1. Shin JM, Luo T, Lee KH, et al. Deciphering endodontic microbial communities by next-generation sequencing. *J Endod* 2018;44:1080–7.
2. Ricucci D, Siqueira José F. Biofilms and apical periodontitis: study of prevalence and association with clinical and histopathologic findings. *J Endod* 2010;36:1277–88.
3. Manoil D, Al-Manei K, Belibasakis GN. A systematic review of the root canal microbiota associated with apical periodontitis: lessons from next-generation sequencing. *Proteomics Clin Appl* 2020;14:1900060.

4. Gutmann James L, Baumgartner Craig J, Gluskin Alan H, et al. Identify and define all diagnostic terms for periapical/periradicular health and disease states. *J Endod* 2009;35:1658–74.
5. Alessio B, Francesca L, Chiara P, et al. Symptomatic and asymptomatic apical periodontitis associated with red complex bacteria: clinical and microbiological evaluation. *Odontology* 2013;101:84–8.
6. Lin LM, Domenico R, Lin J, Rosenberg PA. Nonsurgical root canal therapy of large cyst-like inflammatory periapical lesions and inflammatory apical cysts. *J Endod* 2009;35:607–15.
7. Foschi F, Izard J, Sasaki H, et al. *Treponema Denticola* in disseminating endodontic infections. *J Dent Res* 2006;85:761–5.
8. Fouad Ashraf F. Endodontic microbiology and pathobiology. *Dent Clin North Am* 2017;61:1–15.
9. Siqueira JF, Ras IN. Uncultivated phylotypes and newly named species associated with primary and persistent endodontic infections. *J Clin Microbiol* 2005;43:3314–9.
10. Paster Bruce J, Boches Susan K, Galvin Jamie L, et al. Bacterial diversity in human subgingival plaque. *J Bacteriol* 2001;183:3770–83.
11. Krishnan K, Chen T, Paster BJ. A practical guide to the oral microbiome and its relation to health and disease. *Oral Dis* 2017;23:276–86.
12. Siqueira JF, Rôças IN. Diversity of endodontic microbiota revisited. *J Dent Res* 2009;88:969–81.
13. Krallik P, Ricchi M. A basic guide to real time PCR in microbial diagnostics: definitions, parameters, and everything. *Front Microbiol* 2017;8. <https://doi.org/10.3389/fmicb.2017.00108>.
14. de Brito Luciana CN, Doolittle-Hall J, Lee C-T, et al. The apical root canal system microbial communities determined by next-generation sequencing. *Sci Rep* 2020;10:10932.
15. Buonavoglia A, Lanave G, Camero M, et al. Next-Generation Sequencing Analysis of Root Canal Microbiota Associated with a Severe Endodontic-Periodontal Lesion. *Diagnostics* 2021;11:1461.
16. Sánchez-Sanhueza G, Bello-Toledo H, González-Rocha G, et al. Metagenomic study of bacterial microbiota in persistent endodontic infections using next-generation sequencing. *Int Endod J* 2018;51:1336–48.
17. Korona-Glowniak I, Piatek D, Fornal E, et al. Patterns of oral microbiota in patients with apical periodontitis. *J Clin Med* 2021;10:2707.
18. Papapanou PN, Sanz M, Buduneli N, et al. Periodontitis: consensus report of workgroup 2 of the 2017 world workshop on the classification of periodontal and peri-implant diseases and conditions. *J Clin Periodontol* 2018;45:S162–70.
19. Campbell K. Oral microbiome findings challenge dentistry dogma. *Nature* 2021. <https://doi.org/10.1038/d41586-021-02920-w>.
20. Vertucci Frank J. Root canal anatomy of the human permanent teeth. *Oral Surg Oral Med Oral Pathol* 1984;58:589–99.
21. Orstavik D, Kerekes K, Eriksen HM. The periapical index: a scoring system for radiographic assessment of apical periodontitis. *Dental Traumatol* 1986;2:20–34.
22. Alghofaily M, Tordik P, Romberg E, et al. Healing of Apical Periodontitis after Nonsurgical Root Canal Treatment: The Role of Statin Intake. *J Endod* 2018;44:1355–60.
23. Zanini M, Decerle N, Hennequin M, Cousson P-Y. Revisiting Orstavik's PAI score to produce a reliable and reproducible assessment of the outcomes of endodontic treatments in routine practice. *Eur J Dental Education* 2021;25:291–8.
24. Lillo A, Ashley FP, Palmer RM, et al. Novel subgingival bacterial phylotypes detected using multiple universal polymerase chain reaction primer sets. *Oral Microbiol Immunol* 2006;21:61–8.
25. Sievert C. *Interactive Web-Based Data Visualization with R, plotly*. 1st ed, 9781138331457. Chapman & Hall; 2019.
26. Ondov Brian D, Bergman Nicholas H, Phillippy Adam M. Interactive metagenomic visualization in a Web browser. *BMC Bioinformatics* 2011;12:385.
27. Hou Y, Wang L, Zhang L, et al. Potential relationship between clinical symptoms and the root canal microbiomes of root filled teeth based on the next-generation sequencing. *Int Endod J* 2022;55:18–29.

28. Bouillaguet S, Manoil D, Girard M, et al. Root microbiota in primary and secondary apical periodontitis. *Front Microbiol* 2018;9:2374.
29. Tzanetakakis GN, Azcarate-Peril MA, Zachaki S, et al. Comparison of bacterial community composition of primary and persistent endodontic infections using pyrosequencing. *J Endod* 2015;41:1226–33.
30. Hong B-Y, Lee T-K, Lim S-M, et al. Microbial analysis in primary and persistent endodontic infections by using pyrosequencing. *J Endod* 2013;39:1136–40.
31. Keskin C, Demiryürek EÖ, Onuk EE. Pyrosequencing analysis of cryogenically ground samples from primary and secondary/persistent endodontic infections. *J Endod* 2017;43:1309–16.
32. Větrovský T, Baldrian P. The variability of the 16S rRNA gene in bacterial genomes and its consequences for bacterial community analyses. *PLoS One* 2013;8:e57923.
33. Ravi RK, Walton K, Khosroheidari M. MiSeq: a next generation sequencing platform for genomic analysis. *Methods Mol Biol* 2018;1706:223–32.
34. Kuczynski J, Lauber Christian L, Walters WA, et al. Experimental and analytical tools for studying the human microbiome. *Nat Rev Genet* 2012;13:47–58.
35. Leggett Richard M, Alcon-Giner C, Heavens D, et al. Rapid MinION profiling of preterm microbiota and antimicrobial-resistant pathogens. *Nat Microbiol* 2020;5:430–42.
36. Shin H, Lee E, Shin J, et al. Elucidation of the bacterial communities associated with the harmful microalgae *Alexandrium tamarense* and *Cochlodinium polykrikoides* using nanopore sequencing. *Sci Rep* 2018;8:5323.

3. Novel biomaterials in endodontics: premixed calcium-silicate-based sealers.

After the opening of the pulp chamber, the shaping and disinfection, the root canal must be obturated to obtain a proper three-dimensional seal and prevent a new bacterial contamination. Endodontic sealer aims to eliminate the marginal gap between the guttapercha and the dentin adapting to the dentinal wall.

Over the years, many sealers have been proposed on the market, each with different compositions and properties (**Table 1**).

Table 1 Formulation and composition of some of the most common traditional sealers			
Name	Manufacturer	Formulation	Composition
<i>Zinc Oxide-Eugenol Sealers</i>			
Pulp Canal Sealer	Kerr, Scafati, Italia	Powder	Zinc oxide, silver, resins, thymol iodide.
		Liquid	Eugenol, Canada balsam.
Roth's sealer	Roth International, Chicago, USA	Powder	Zinc oxide, resins, bismuth subcarbonate, barium sulfate, sodium borate.
		Liquid	Eugenol.
<i>Modified Zinc Oxide Sealers</i>			
N2	Hager Werken	Powder	Zinc oxide, barium sulfate, prednisolone, titanium dioxide, lead tetraoxide, bismuth subcarbonate, hydrocortisone, paraformaldehyde, phenylmercuric borate.
		Liquid	Eugenol, geraniol.
Endomethasone	Septodont, Saint Maur-des-Fosses, Francia	Powder	Zinc oxide, bismuth subcarbonate, desamethasone, hydrocortisone, thymol iodide, paraformaldehyde
		Liquid	Eugenol
Endometasone N	Septodont, Saint Maur-des-Fosses, Francia	Powder	Zinc oxide, bismuth subcarbonate, barium sulfate, sodium borate, iodoform.
		Liquid	Eugenol
<i>Calcium Hydroxide Sealers</i>			
CRCS	Hygenic/Whaledent Inc, Cuyahoga Falls, USA	Powder	Zinc oxide, hydrogenated rosin, esters, barium sulfate, calcium hydroxide, bismuth subcarbonate.
		Liquid	Eugenol, eucalyptol.
SealApex	Sybron Endo, Orange USA	Base	N-ethyl toluene sulfonamide resin, silicon dioxide, zinc oxide, calcium oxide.
		Catalyst	Isobutyl salicylate resin, silicon dioxide, barium sulfate, titanium dioxide.
Apexit Plus	Ivoclar Vivadent, Lichtenstein	Base	Hydrated rosin, calcium hydroxide, calcium oxide, silicon dioxide, alkyl ester of phosphoric acid.
		Catalyst	Disalicylate, bismuth hydroxide, bismuth carbonate, silicon dioxide, alkyl ester of phosphoric acid.
<i>Resin-Based Sealers</i>			
Diaket	3M/ESPE	Powder	Zinc oxide, bismuth phosphate.
		Liquid	2,2-dihydroxy-5,5-dichlorodiphenylmethane B-diketone, triethanolamine, caproic acid, vinyl chloride, vinyl acetate, and isobutyl vinyl ether.
Epiphany	Pentron Clinical Technologies	Sistema polimerizzante	Urethane dimethacrylate (UDMA), polyethylene glycol dimethacrylates (PEGDMA), bisphenol A ethoxylated dimethacrylate (EBPADMA), bisphenol A glycidyl dimethacrylate (BisGMA), polycaprolactone (PCL), barium borosilicate treated with silane, barium sulfate, silica, calcium hydroxide, bismuth oxychloride with amines, peroxides, photoinhibitors.
EndoREZ	Ultradent	Polymerization System	Polyurethane dimethacrylate (DUDMA), benzoyl peroxide.
AH 26	Dentsply DeTrey GmbH, Konstanz, Germania	Powder	Bismuth oxide, hexamethylenetetramine, silver powder, titanium oxide.
		Liquid	Bisphenol diglycidyl ether
AH-Plus	Dentsply DeTrey GmbH, Konstanz, Germania	Paste A	Epoxy resin, calcium tungstate, zirconium oxide, silica, iron oxide. .
		Paste B	Adamantanamine, N,N-dibenzyl-5-oxanonane-1,9-diamine, TCD-diamine, calcium tungstate, zirconium oxide, silica, silicone oil.
TopSeal	Dentsply DeTrey GmbH, Konstanz, Germania	Paste A	Bisphenol-A epoxy resin, bisphenol-F epoxy resin, calcium tungstate, zirconium oxide, silica, iron oxide pigments.
		Paste B	Dibenzylamine, aminoadamantane, tricycloendiamine, calcium tungstate, zirconium oxide, silica, silicone oil.
<i>Silicone-Based Sealers</i>			
Roekoseal-Automix	Coltène/Whaledent AG, Altstätten, Svizzera	Paste-Paste	Polydimethylsiloxane, silicone oil, paraffin oil, platinum catalyst, zirconium dioxide.
GuttaFlow	Coltène/Whaledent AG, Altstätten, Svizzera	Paste-Paste	Gutta-percha powders, polydimethylsiloxane, platinum catalyst, zirconium dioxide, silver powders.
GuttaFlow 2	Coltène/Whaledent AG, Altstätten, Svizzera	Paste-Paste	Gutta-percha powders, polydimethylsiloxane, platinum catalyst, zirconium dioxide, silver powders.
GuttaFlow bioseal	Coltène/Whaledent AG, Altstätten, Svizzera	Paste-Paste	Gutta-percha powders, polydimethylsiloxane, platinum catalyst, zirconium dioxide, silver powders, bioactive glass powders.

Bioceramic sealers is a vast category of endodontic biomaterials introduced for the first time approximately 30 years ago and proposed for root-end surgery thanks to their properties to set in a humid environment immediately after the contact with body fluids such as blood or saliva (Torabinejad M et al. 1993).

A lot of formulations were proposed, developed and modified to create a wide family of materials for different clinical applications such as repairing of root perforations (Sluyk SR et al. 1998; Mente J et al. 2010), creating an apical-plug in teeth with open apices (Pace R et al. 2010, Prati et al. 2014), pulp capping (Nair PN et al. 2008; Gandolfi MG et al. 2015), apexogenesis (Holden DT et al. 2008) and as a root canal filling material (Prati C & Gandolfi MG 2015) (Table 2).

Nome	Manufacturer	Formulation	Composition
MTA Fillapex	Angelus, Londrina, Brasile	Paste-Paste	Salicylate resin, diluent resin, natural resin, bismuth trioxide, nanoparticulate silica, calcium silicates.
BioRoot RCS	Septodont, Saint Maur-des-Fosses, Francia	Powder - Liquid	Tricalcium silicates, zirconium oxide, and excipients. Calcium chloride and excipients.
Tech Biosealer Endo	Isasan, Rovello, Italia	Powder - Liquid	White Portland cement, bismuth oxide, sodium fluoride.
Neo MTA Plus	Avalon Biomed, Houston, USA	Powder - Liquid	Tricalcium silicates, bismuth oxide, calcium silicates, calcium sulfates, silica, tantalum pentoxide.
Endoseal MTA	Maruchi, Corea del Sud	Premixed	Calcium silicates, calcium aluminates, calcium alumino-ferrites, calcium sulfates, radiopacifiers, thickening agent.
iRoot SP	Innovative BioCeramics, Vancouver Canada	Premixed	Calcium phosphates, calcium silicates, zirconium oxide, calcium hydroxide.
Endosequence	Brasseler, Savannah, USA	Premixed	Calcium silicates, monobasic calcium phosphate, zirconium oxide, tantalum pentoxide, and thickening agents.
TotalFill	FKG Dentaire, La Chaux-de-Fonds, Svizzera	Premixed	Calcium silicates, monobasic calcium phosphate, zirconium oxide, tantalum pentoxide, and thickening agents.
Ceraseal	Meta Biomed, Corea del Sud	Premixed	Zirconium dioxide (45–50%), tricalcium silicate (20–30%), dicalcium silicate (1–10%), tricalcium aluminate (1–10%), thickening agents, polyethylene glycol (PEG
NeoSealer Flo	Avalon Nusmile, USA	Premixed	Tantalite (50%), tricalcium silicate (25%), calcium aluminate (25%), dicalcium silicate (10%), tricalcium aluminate (5%), calcium sulfate (1%), PEG *, grossite
AH Plus Bioceramic	(Maruchi, South Korea)	Premixed	Zirconium dioxide (50–70%), tricalcium silicate (5–15%), dimethyl sulfoxide (10–30%), lithium carbonate (0.5%), thickening agents (<6%)

Their excellent biological properties were fully studied and discovered only later. During that time, a lot of studies demonstrated that calcium silicate sealers (CaSi) have bioactive properties. This means they have the ability to induce an active biological response, producing apatite and releasing biologically active ions (Gandolfi MG et al. 2011, 2013, 2015; Primus et al. 2019).

Bioactivity, therefore, is one of the main properties of these materials (Primus et al 2019). When placed in contact with bone tissue (for example, at the apex or beyond the apex), they quickly form a compact layer of calcium phosphate and apatite. This layer then leads to the activation of osteoblasts and mesenchymal cells, differentiating into osteoblast-like cells, which

will produce bone tissue ([Tatullo M et al 2019](#); [Gandolfi MG et al 2020](#)). In contrast, other non-bioactive materials will not promote the proliferation of osteoblastic and mesenchymal cells, remaining therefore bioinert.

Numerous animal studies have shown that CaSi based materials possess osteoconductive and osteoinductive capabilities, highlighting the biological properties of these materials. Many new experimental strategies for achieving bone defect regeneration involve scaffolds enriched with CaSi powders with a composition similar to the endodontic bioactive sealers ([Forni M et al. 2020](#); [Gandolfi MG et al. 2018, 2019, 2020](#)). Different formulations of polymer-based scaffolds (polylactic and polycaprolactone-based) have been enriched with different percentages of bioactive CaSi fillers. These highly porous scaffolds have shown the ability to interact with different populations of mesenchymal stem cells, inducing differentiation in an angiogenic ([Forni et al. 2020](#); [Gandolfi et al. 2022](#)), osteoblastic, and odontoblastic direction ([Tatullo et al. 2019](#)). These bioresorbable scaffolds could support new tissue ingrowth and the regeneration of critical sized defect.

It has been demonstrated that CaSi sealers, when immersed in solutions like blood, have the ability to nucleate on their surface a layer of amorphous calcium phosphate, a biological precursor of apatites ([Gandolfi et al 2010](#)). Another important property of these materials is their excellent biocompatibility ([Gandolfi MG et al. 2010, 2015](#)). These materials are claimed to stimulate periapical tissues towards bone and vascular regeneration. The chemical processes that lead to the nucleation of apatite have been described in different studies ([Primus et al. 2019](#); [Gandolfi et al. 2010, 2013](#)). During these processes, the materials release calcium ions (powerful signals for osteoblasts, osteoclasts, and odontoblasts) and OH ions (having a strong alkalizing effect) ([Ma S et al. 2005](#)). The release of Ca and OH ions lead to the rapid formation of calcium hydroxide after their preparation. The release of calcium ions, the alkalizing activity (that is, the ability to bring the pH to values close to 10), bioactivity, and their hydraulic properties have led to the use of these materials inside the root canal. Another important characteristic regards their ability to expand (other sealers contract a little bit after setting), improving the sealing of the root canal and eliminating porosity ([Iacono F et al. 2010](#)).

Bismuth oxide and other radiopacifiers such as Tantalum pentoxide and Zirconium dioxide provide adequate (but sometimes unsatisfactory) radiopacity, which the clinician must consider. The percentages of radiopacifiers among different sealers are also different and this led to a different radiopacity when used inside the root canal ([Zamparini et al. 2022](#)).

Bioceramic sealers can be divided into different generations, each distinguishable by their innovative properties and formulation.

The first generation of materials is widely used for retrograde fillings due to their excellent biological properties even if they have some drawback like their long setting time (several hours are needed to achieve complete hardening of the material), low radiopacity and difficulty to handle. This prolonged setting time produced a risk of material washout, compromising the post-surgical phases ([Prati C et al. 2014](#)). To overcome these limitations some modifications have been done and new formulations of powder-liquid or paste-to-paste have been proposed 15 years ago.

The second generation of materials allowed the use of sealer inside the endodontic canal as an endodontic sealer. These sealers have a high bioactivity but modest radiopacity. The powder must be mixed with the liquid, but the setting time is relatively short.

Recently, a new category of premixed, flowable, ready to use calcium-silicate-based sealers have been proposed and rapidly increased popularity among endodontic specialists and general practitioners thanks to their easy use. These biomaterials can be classified as the third generation of bioceramic sealers.

The term "bioceramic" is not specific but is widely used and include all ceramic materials that are bioactive or used in a biomedical context. All CaSi materials could indeed be defined as "bioceramics", that is, ceramic-derived materials used in a biological context. They are mainly composed by one or more bioactive agents (di/tri calcium silicate, tricalcium, aluminate), radiopacifier (zirconium, tantalum) and thickening agents. The percentages of these components can vary significantly from one sealer to another, and this confer different chemical-physical and biological properties that reflect a different technique of clinical use and application. They also require a humidity to set.

In vitro investigations have shown their biointeractive and biological capabilities of these innovative materials ([Zamparini et al. 2022](#); [Donnermeyer D et al. 2022](#); [Souza LC et al. 2023](#)).

The following paper investigate the chemical-physical properties and bioactivity of three different premixed calcium silicate-based sealers. The scientific rationale behind investigating the various properties of these new and innovative sealers is ultimately aimed at enhancing their clinical application. This investigation includes all clinically relevant parameters that may vary and influence the outcome of endodontic treatments. The comprehensive examination of these properties, including setting times, radiopacity, flowability, film thickness, open pore volume,

water absorption, solubility, calcium release, and alkalizing activity, is very important. It confirms that the sealers not only meet the technical requirements for a biomaterial but also can potentially contribute to the success of endodontic procedures by promoting healing and preventing reinfection. The study supports their clinical use for endodontic treatments.

REFERENCES

- 1) Donnermeyer D, Schemkämper P, Bürklein S, Schäfer E. Short and Long-Term Solubility, Alkalizing Effect, and Thermal Persistence of Premixed Calcium Silicate-Based Sealers: AH Plus Bioceramic Sealer vs. Total Fill BC Sealer. *Materials (Basel)* 2022;15:7320.
- 2) Forni M, Bernardini C, Zamparini F et al. Vascular wall-mesenchymal stem cells differentiation on 3D biodegradable highly porous CaSi-DCPD doped poly (α -hydroxy) acids scaffolds for bone regeneration. *Nanomaterials* 2020;10:243.
- 3) Gandolfi MG, Ciapetti G, Taddei P, Perut F, Tinti A et al. Apatite formation on bioactive calcium-silicate cements for dentistry affects surface topography and human marrow stromal cells proliferation. *Dent Mater* 2010;26:974-92.
- 4) Gandolfi MG, Taddei P, Tinti A, Dorigo ES, Rossi PL, Prati C. Kinetics of apatite formation on a calcium-silicate cement for root-end filling during ageing in physiological-like phosphate solutions. *Clin Oral Invest* 2010;14:659-68
- 5) Gandolfi MG, Shah SN, Feng R, Prati C, Akintoye SO. Biomimetic calcium-silicate cements support differentiation of human orofacial mesenchymal stem cells. *J Endod* 2011;37:1102-8.
- 6) Gandolfi MG, Taddei P, Modena E, Siboni F, Prati C. Biointeractivity-related *versus* chemi/physisorption-related apatite precursor-forming ability of current root end filling materials. *J Biomed Mater Res Part B Appl Biomater* 2013;101:1107-23.
- 7) Gandolfi MG, Siboni F, Botero T, Bossù M, Riccitiello F, Prati C. Calcium silicate and calcium hydroxide materials for pulp capping: biointeractivity, porosity, solubility and bioactivity of current formulations. *J Appl Biomater Funct Mater* 2015;13:1-18.
- 8) Gandolfi MG, Siboni F, Botero T, Bossù M, Riccitiello F, Prati C. Calcium silicate and calcium hydroxide materials for pulp capping: biointeractivity, porosity, solubility and bioactivity of current formulations. *J Appl Biomater Funct Mater* 2015;13:1-18.

- 9) Gandolfi MG, Spagnuolo G, Siboni F, Procino A, Riviuccio V et al. Calcium silicate/calcium phosphate biphasic cements for vital pulp therapy: chemical-physical properties and human pulp cells response. *Clin Oral Invest* 2015;19:2075-89.
- 10) Gandolfi MG, Zamparini F, Degli Esposti M, Chiellini F, Aparicio C et al. Polylactic acid-based porous scaffolds doped with calcium silicate and dicalcium phosphate dihydrate designed for biomedical application. *Mater Sci Eng C* 2018;82:163-81.
- 11) Gandolfi MG, Zamparini F, Degli Esposti M, Chiellini F, Fava F, Fabbri P, Taddei P, Prati C. Highly porous polycaprolactone scaffolds doped with calcium silicate and dicalcium phosphate dihydrate designed for bone regeneration. *Mater Sci Eng C Mater Biol Appl* 2019;102:341-61.
- 12) Gandolfi MG, Gardin C, Zamparini F, Ferroni L, Esposti MD et al. Mineral-doped poly(L-lactide) acid scaffolds enriched with exosomes improve osteogenic commitment of human adipose-derived mesenchymal stem cells. *Nanomaterials* 2020;10:432.
- 13) Holden DT, Schwartz SA, Kirkpatrick TC, Schindler WG. Clinical outcomes of artificial root-end barriers with mineral trioxide aggregate in teeth with immature apices. *J Endod.* 2008 Jul;34:812-7
- 14) Iacono F, Gandolfi MG, Huffman B, Sword J, Agee K et al. Push-out strength of modified Portland cements and resins. *Am J Dent* 2010;23:43-6.
- 15) Ma S, Yang Y, Carnes DL, Kim K, Park S, Oh SH, Ong JL. Effects of dissolved calcium and phosphorous on osteoblast responses. *J Oral Implantol* 2005;31:61-7.
- 16) Mente J, Hage N, Pfefferle T, Koch MJ, Geletneky B et al. Treatment outcome of mineral trioxide aggregate: repair of root perforations. *J Endod* 2010;36:208-13.
- 17) Nair PN, Duncan HF, Pitt Ford TR, Luder HU. Histological, ultrastructural and quantitative investigations on the response of healthy human pulps to experimental capping with mineral trioxide aggregate: a randomized controlled trial. *Int Endod J* 2008;41:128-50.
- 18) Pace R, Giuliani V, Nieri M, Di Nasso L, Pagavino G. Mineral trioxide aggregate as apical plug in teeth with necrotic pulp and immature apices: a 10-year case series. *J Endod* 2014;40:1250-4.
- 19) Primus CM, Tay FR, Niu LN. Bioactive tri/dicalcium silicate cements for treatment of pulpal and periapical tissues. *Acta Biomater* 2019;96:35-54.

- 20) Prati C, Siboni F, Polimeni A, Bossu M, Gandolfi MG. Use of calcium-containing endodontic sealers as apical barrier in fluid-contaminated wide-open apices. *J Appl Biomater Funct Mater* 2014;12:263-70.
- 21) Prati C, Siboni F, Polimeni A, Bossu M, Gandolfi MG. Use of calcium-containing endodontic sealers as apical barrier in fluid-contaminated wide-open apices. *J Appl Biomater Funct Mater* 2014;12:263-70.
- 22) Prati C, Gandolfi MG. Calcium silicate bioactive cements: biological perspectives and clinical applications. *Dent Mater* 2015;31:351-70.
- 23) Primus CM, Tay FR, Niu LN. Bioactive tri/dicalcium silicate cements for treatment of pulpal and periapical tissues. *Acta Biomater*. 2019 Sep 15;96:35-54.
- 24) Sluyk SR, Moon PC, Hartwell GR. Evaluation of setting properties and retention characteristics of mineral trioxide aggregate when used as a furcation perforation repair material. *J Endod*. 1998 Nov;24(11):768-71.
- 25) Souza LC, Neves GST, Kirkpatrick T, Letra A, Silva R. Physicochemical and Biological Properties of AH Plus Bioceramic. *J Endod*. 2023;49:69-76.
- 26) Tatullo M, Spagnuolo G, Codispoti B, Zamparini F, Zhang A et al. PLAbased mineral-doped scaffolds seeded with human periapical cyst-derived MSCs: a promising tool for regenerative healing in dentistry. *Mater* 2019;12:597.
- 27) Torabinejad M, Watson TF, Pitt Ford TR. Sealing ability of a mineral trioxide aggregate when used as a root end filling material. *J Endod*. 1993 Dec;19:591-5.
- 28) Zamparini F, Prati C, Taddei P, Spinelli A, Di Foggia M, Gandolfi MG. Chemical-Physical Properties and Bioactivity of New Premixed Calcium Silicate-Bioceramic Root Canal Sealers. *Int J Mol Sci*. 2022;23:13914.



Article

Chemical-Physical Properties and Bioactivity of New Premixed Calcium Silicate-Bioceramic Root Canal Sealers

Fausto Zamparini ^{1,2}, Carlo Prati ¹, Paola Taddei ³, Andrea Spinelli ¹, Michele Di Foggia ³
and Maria Giovanna Gandolfi ^{2,*}

¹ Endodontic Clinical Section, School of Dentistry, Department of Biomedical and Neuromotor Sciences, University of Bologna, 40125 Bologna, Italy

² Laboratory of Green Biomaterials and Oral Pathology, School of Dentistry, Department of Biomedical and Neuromotor Sciences, University of Bologna, 40125 Bologna, Italy

³ Biochemistry Unit, Department of Biomedical and Neuromotor Sciences, University of Bologna, 40126 Bologna, Italy

* Correspondence: mgiovanna.gandolfi@unibo.it

Abstract: The aim of the study was to analyze the chemical–physical properties and bioactivity (apatite-forming ability) of three recently introduced premixed bioceramic root canal sealers containing varied amounts of different calcium silicates (CaSi): a dicalcium and tricalcium silicate (1–10% and 20–30%)-containing sealer with zirconium dioxide and tricalcium aluminate (CERASEAL); a tricalcium silicate (5–15%)-containing sealer with zirconium dioxide, dimethyl sulfoxide and lithium carbonate (AH PLUS BIOCERAMIC) and a dicalcium and tricalcium silicate (10% and 25%)-containing sealer with calcium aluminate, tricalcium aluminate and tantalite (NEOSEALER FLO). An epoxy resin-based sealer (AH PLUS) was used as control. The initial and final setting times, radiopacity, flowability, film thickness, open pore volume, water absorption, solubility, calcium release and alkalinizing activity were tested. The nucleation of calcium phosphates and/or apatite after 28 days aging in Hanks balanced salt solution (HBSS) was evaluated by ESEM-EDX, vibrational IR and micro-Raman spectroscopy. The analyses showed for NeoSealer Flo and AH Plus the longest final setting times (1344 ± 60 and 1300 ± 60 min, respectively), while shorter times for AH Plus Bioceramic and Ceraseal (660 ± 60 and 720 ± 60 min, respectively). Radiopacity, flowability and film thickness complied with ISO 6876/12 for all tested materials. A significantly higher open pore volume was observed for NeoSealer Flo, AH Plus Bioceramic and Ceraseal when compared to AH Plus ($p < 0.05$), significantly higher values were observed for NeoSealer Flo and AH Plus Bioceramic ($p < 0.05$). Ceraseal and AH Plus revealed the lowest solubility. All CaSi-containing sealers released calcium and alkalinized the soaking water. After 28 days immersion in HBSS, ESEM-EDX analyses revealed the formation of a mineral layer that covered the surface of all bioceramic sealers, with a lower detection of radiopacifiers (Zirconium for Ceraseal and AH Plus Bioceramic, Tantalum for NeoSealer Flo) and an increase in calcium, phosphorous and carbon. The calcium phosphate (CaP) layer was more evident on NeoSealer Flo and AH Plus Bioceramic. IR and micro-Raman revealed the formation of calcium carbonate on the surface of all set materials. A thin layer of a CaP phase was detected only on AH Plus Bioceramic and NeoSealer Flo. Ceraseal did not show CaP deposit despite its highest calcium release among all the tested CaSi-containing sealers. In conclusion, CaSi-containing sealers met the required chemical and physical standards and released biologically relevant ions. Slight/limited apatite nucleation was observed in relation to the high carbonation processes.

Keywords: endodontic sealers; root canal sealers; calcium silicates; calcium silicates cements; bioceramics; bioactivity; calcium phosphate nucleation; apatite nucleation



Citation: Zamparini, F.; Prati, C.; Taddei, P.; Spinelli, A.; Di Foggia, M.; Gandolfi, M.G. Chemical-Physical Properties and Bioactivity of New Premixed Calcium Silicate-Bioceramic Root Canal Sealers. *Int. J. Mol. Sci.* **2022**, *23*, 13914. <https://doi.org/10.3390/ijms232213914>

Academic Editors:
Yoshiya Hashimoto and
Satoshi Komasa

Received: 21 October 2022
Accepted: 8 November 2022
Published: 11 November 2022

Publisher's Note: MDPI stays neutral with regard to jurisdictional claims in published maps and institutional affiliations.



Copyright: © 2022 by the authors. Licensee MDPI, Basel, Switzerland. This article is an open access article distributed under the terms and conditions of the Creative Commons Attribution (CC BY) license (<https://creativecommons.org/licenses/by/4.0/>).

1. Introduction

Since their first application as materials for root-end surgery, calcium silicate-based materials demonstrated excellent sealing ability and were able to set in the presence of moisture (such as blood or saliva) [1–5].

Calcium silicate-based materials (i.e., mainly containing CaSi particles) possess high biocompatibility and favorable biological properties, as demonstrated in a number of *in vitro* (cells studies) [6,7] and *ex vivo* (animal models) studies [8–10]. These positive interactions with biological tissues have been mostly attributed to their release of biologically interactive ions (such as calcium) [11–14] and the nucleation of an apatite layer on their surface [15–17], which starts immediately after the material hydration [18,19]. For these properties, calcium silicate-based materials have found a pivotal role in approaching complex endodontic cases, namely perforation repair and apical plugs for teeth with open apices [1–5]. The first generation of calcium silicate-based materials demonstrated some limitations, mostly attributable to their long setting time, low radiopacity, handling difficulties and grayish discoloration, which restricted the use of these materials as root canal sealers [20,21]. Modification of these endodontic materials to overcome most of these limitations have been done and root canal sealers based on calcium silicates have been proposed 10–15 years ago as powder–liquid or paste-to-paste formulations [3,5,22].

In recent times, premixed flowable sealers have been introduced for root canal treatment. Differently from the other formulations, these materials are ready to be used and do not require mixing as their setting reaction is achieved in the presence of moisture. Lately, CaSi-based materials have been generically named “bioceramics”. It must be pointed out that the definition of ceramic is generic and non-specific, referring to an inorganic material constituted by the combination of metallic and non-metallic elements. The term “bioceramics”, coined to highlight the positive biological behavior, refers to ceramic materials used for repairing or replacing damaged bone tissues. Bioceramics can directly interact with the surrounding tissue, either supporting tissue growth or inducing new tissue regeneration [23]. Therefore, the term “bioceramic” is vague and does not specifically refer to CaSi-containing materials. A positive interaction with surrounding periapical tissues without inducing inflammation or foreign body reactions has been reported for calcium silicate-based materials [8–10], while no studies exist regarding some recently introduced materials.

These new bioceramics have been developed by adding different percentages of CaSi and different radiopacifiers in their composition.

In this context, we want to highlight a distinction between calcium silicate-based (i.e., mainly containing CaSi particles) and calcium silicate-containing (i.e., containing minor amounts of CaSi) sealers.

Ceraseal is a premixed bioceramic sealer including tricalcium silicate (20–30%) and dicalcium silicate (1–10%) as bioactive components, and tricalcium aluminate (1–10%) and zirconium dioxide (45–50%) as radiopacifiers. Some traces of thickening agents are reported by the manufacturer.

NeoSealer Flo is a premixed bioceramic sealer constituted by tricalcium silicate (<25%) and dicalcium silicate (<10%) as bioactive components, and calcium aluminate (<25%), calcium aluminum oxide (grossite) (<6%), tricalcium aluminate (<5%) and tantalite (50%) as radiopacifier. Traces of calcium sulfate (<1%) are also reported by the manufacturer.

AH Plus Bioceramic is a premixed bioceramic sealer mostly composed of zirconium dioxide (50–70%) as a radiopacifier and tricalcium silicate (10–15%) as a bioactive component. Dimethyl sulfoxide and traces of lithium carbonate and thickening agents are also reported by the manufacturer.

To date, no literature is available regarding the chemical–physical properties and bioactivity of these recent bioceramic root canal sealers. Therefore, the aim of the study was to evaluate different clinically relevant chemical–physical properties such as ion release, setting times, radiopacity, open pore volume, water absorption, solubility, flow and film

thickness. The ability to nucleate apatite has also been assessed. The sealers were compared to a traditional epoxy resin-based sealer (AH Plus) used as control.

2. Results

2.1. Initial, Final Setting Times and Radiopacity

Setting times are reported in Table 1. Ceraseal showed the shortest initial setting times (60 ± 5 min), while NeoSealer Flo showed the longest setting time (480 ± 125 min). Ceraseal and AH Plus Bioceramic had similar final setting times (660 ± 60 and 720 ± 60 min), while NeoSealer Flo and AH Plus revealed significantly longer final setting time values (1300 ± 60 and 1344 ± 60 min) ($p < 0.05$). All sealers complied with ISO 6876/12: they showed different radiopacity values, but always higher than 3.0 mmAl. In particular, NeoSealer Flo showed the lowest value (5.0 ± 0.5 mmAl), and AH Plus the highest (11.5 ± 0.5 mmAl). AH Plus Bioceramic and Ceraseal showed intermediate values (8.0 ± 0.5 and 8.6 ± 0.5 mmAl, respectively).

Table 1. Initial and final setting times (min, mean \pm SD; n = 3) and radiopacity (mmAl, mean \pm SD; n = 3). Different superscript letters (vertical row) indicate statistically significant differences ($p < 0.05$) among materials.

	Initial Setting Time	Final Setting Time	Radiopacity
Ceraseal	60 ± 5^a	660 ± 60^a	8.0 ± 0.5^a
NeoSealer Flo	480 ± 125^b	1344 ± 60^b	5.5 ± 0.5^b
AH Plus Bioceramic	360 ± 60^c	720 ± 60^c	8.6 ± 0.5^b
AH Plus	470 ± 5^b	1300 ± 60^b	11.5 ± 0.5^c

2.2. Sealer Flowability and Film Thickness

Flowability and film thickness are reported in Table 2. Ceraseal showed the highest flowability and the lowest film thickness values, while NeoSealer Flo revealed the lowest flowability and highest film thickness values. AH Plus Bioceramic showed intermediate values. All sealers complied with ISO 6876/2012.

Table 2. Flowability (min, mean \pm SD; n = 3) and film thickness (μ m, mean \pm SD; n = 3) of just extruded sealers. Different superscript letters (vertical row) indicate statistically significant differences ($p < 0.05$) among materials.

	Flowability	Film Thickness
Ceraseal	2.94 ± 0.09^a	70.7 ± 4.0^a
NeoSealer Flo	1.88 ± 0.06^b	128.7 ± 8.1^b
AH Plus Bioceramic	2.38 ± 0.13^c	174.0 ± 5.3^c
AH Plus	2.96 ± 0.10^a	68.3 ± 2.9^a

2.3. Open Pore Volume, Water Absorption and Solubility

Table 3 reports the volume of open pores, water absorption and solubility of the tested materials. NeoSealer Flo and AH Plus Bioceramic showed higher volumes of open pores (0.048 ± 0.011 and 0.042 ± 0.011 , respectively) when compared to Ceraseal. AH Plus showed similar solubility when compared to Ceraseal ($p > 0.05$), but significantly lower porosity and water absorption ($p < 0.05$).

Table 3. Open pore volume (cm^3 , mean \pm SD; $n = 6$), water absorption and solubility (% , mean \pm SD; $n = 6$) of tested sealers. Analyses were performed on set materials (+100% of final setting time). Different superscript letters (vertical row) indicate statistically significant differences ($p < 0.05$) among materials.

	Open Pore Volume	Water Absorption	Solubility
Ceraseal	0.024 \pm 0.004 ^a	11.2 \pm 3.6 ^a	1.02 \pm 0.43 ^a
NeoSealer Flo	0.048 \pm 0.003 ^b	33.0 \pm 11.0 ^b	7.10 \pm 3.5 ^b
AH Plus Bioceramic	0.042 \pm 0.011 ^b	24.8 \pm 8.5 ^b	5.80 \pm 1.5 ^b
AH Plus	0.0030 \pm 0.0002 ^c	1.40 \pm 0.20 ^c	0.80 \pm 0.12 ^a

2.4. Alkalinizing Activity and Calcium Release

All the calcium silicate-based materials provided alkalinization of the soaking medium and released calcium (Tables 4 and 5).

Table 4. Alkalinizing activity (mean \pm SD; $n = 8$) of tested materials. The pH of soaking water was measured after immersion of set sealers (+100% of final setting time). Different superscript letters (vertical row) indicate statistically significant differences ($p < 0.05$) among sealers.

	3 h	1 Day	3 Days	7 Days	14 Days	28 Days
Ceraseal	9.51 \pm 0.10 ^a	10.01 \pm 0.28 ^a	9.64 \pm 0.34 ^a	9.01 \pm 0.13 ^a	8.75 \pm 0.15 ^a	8.13 \pm 0.16 ^a
NeoSealer Flo	8.73 \pm 0.10 ^b	8.40 \pm 0.04 ^b	8.23 \pm 0.12 ^b	8.43 \pm 0.03 ^b	8.38 \pm 0.06 ^b	8.17 \pm 0.11 ^a
AH Plus Bioceramic	8.6 \pm 0.6 ^b	9.5 \pm 0.5 ^{ab}	9.0 \pm 0.6 ^a	8.4 \pm 0.5 ^b	8.4 \pm 0.5 ^b	8.3 \pm 0.6 ^a
AH Plus	7.7 \pm 0.2 ^c	7.4 \pm 0.1 ^c	7.3 \pm 0.2 ^c	7.3 \pm 0.2 ^c	7.2 \pm 0.1 ^c	7.1 \pm 0.3 ^c
Deionized water	7.02 \pm 0.17 ^d	7.28 \pm 0.32 ^c	7.12 \pm 0.32 ^c	7.05 \pm 0.35 ^c	7.12 \pm 0.32 ^c	6.98 \pm 0.25 ^c

Table 5. Calcium release (ppm, mean \pm SD; $n = 8$) of tested sealers. Calcium release in soaking water was measured after immersion of set materials (+100% of final setting time). Different letters indicate statistically significant differences ($p < 0.05$) among materials.

	3 h	1 Day	3 Days	7 Days	14 Days	28 Days	Cumulative
Ceraseal	43.73 \pm 5.7 ^a	80.85 \pm 10.89 ^a	89.52 \pm 5.68 ^a	57.53 \pm 10.31 ^a	41.95 \pm 4.65 ^a	38.30 \pm 13.18 ^a	347.45 \pm 16.25 ^a
NeoSealer Flo	40.56 \pm 14.4 ^a	41.37 \pm 8.6 ^b	47.95 \pm 19.9 ^b	36.77 \pm 7.2 ^b	27.25 \pm 2.4 ^b	21.77 \pm 2.4 ^b	205.25 \pm 35.4 ^b
AH Plus Bioceramic	20.5 \pm 10.6 ^b	30.6 \pm 10.5 ^b	67.5 \pm 20.5 ^c	40.5 \pm 7.5 ^b	35.5 \pm 10.5 ^{ac}	20.58 \pm 8.6 ^b	200.5 \pm 80.5 ^b
AH Plus	1.8 \pm 0.8 ^c	1.9 \pm 0.5 ^c	1.3 \pm 0.4 ^d	2.1 \pm 0.2 ^c	2.5 \pm 1.2 ^d	0.5 \pm 0.2 ^c	1.4 \pm 0.5 ^c
Deionized water	1.6 \pm 0.5 ^c	1.5 \pm 0.3 ^c	1.2 \pm 0.1 ^d	1.1 \pm 0.1 ^c	1.5 \pm 0.6 ^d	0.5 \pm 0.2 ^c	0.7 \pm 0.5 ^c

Until 14 days, Ceraseal provided the highest pH values while NeoSealer Flo and AH Plus Bioceramic sealer provided lower alkalinizing activity; at 28 days, the three sealers show comparable pH values. AH Plus did not alkalinize the environment, a slight acidification of soaking water was observed from 1-day immersion.

The sealers that contained a higher amount of CaSi had higher cumulative Ca release. Ceraseal provided the highest values. NeoSealer Flo showed lower calcium release, with significant reduction for 14 days. AH Plus Bioceramic sealer proved high calcium release values after 3 and 7 days; the values reduced at the subsequent endpoints. AH Plus did not release calcium ions.

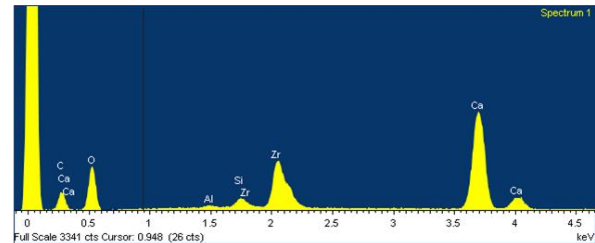
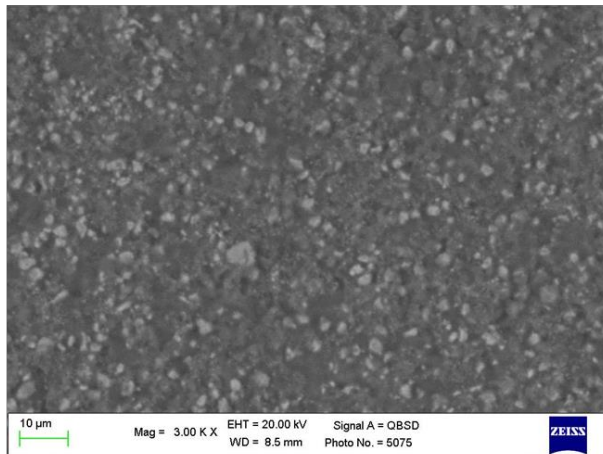
2.5. Surface Characterization and CaP Nucleation

2.5.1. Ceraseal

The set surface of Ceraseal was observed through ESEM at 3000 \times magnification. The surface was regular with small granules (range 2–5 μm) widely distributed. EDX

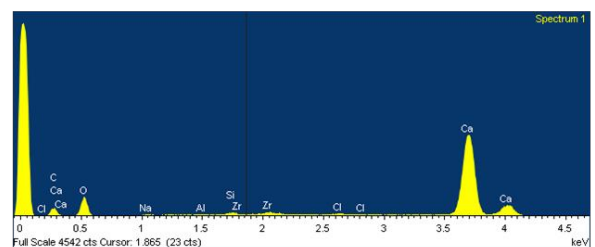
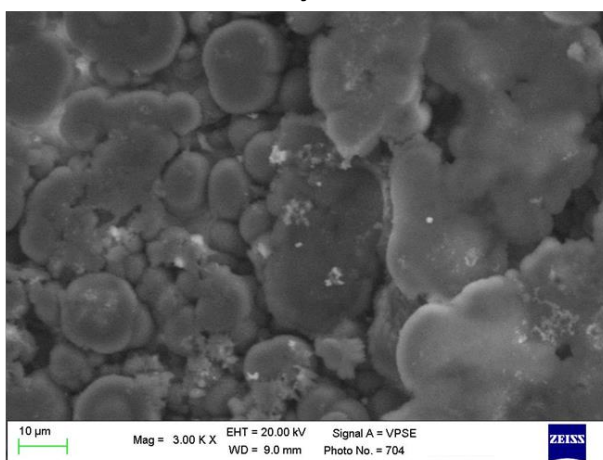
revealed the constitutional elements of the material, as declared by the manufacturer, namely zirconium (the radiopacifier used in this formulation), calcium and silicon (from calcium silicates). Al was detected as well (Figure 1). After 28 days immersion, ESEM images revealed an irregular surface with well-evident globular structures covering the sealer surface (ranging from 10 to 20 μm). EDX revealed an increase in Ca and a decrease in Zr and Si. Sodium (Na) and chlorine (Cl) were attributable to the HBSS solution. No P was detected.

Ceraseal set



Element	Weight%	Atomic%
C K	17.63	29.59
O K	43.88	55.29
Al K	0.28	0.21
Si K	0.89	0.64
Ca K	21.35	10.74
Zr L	15.98	3.53

Ceraseal after 28 days in HBSS



Element	Weight%	Atomic%
C K	11.31	19.03
O K	47.91	60.53
Na K	0.32	0.28
Al K	0.20	0.15
Si K	0.48	0.35
Cl K	0.37	0.21
Ca K	37.92	19.12
Zr L	1.50	0.33

Figure 1. ESEM images at 3000 \times of Ceraseal before and after immersion in HBSS. Set Ceraseal sample was characterized by a regular surface with small granules widely spread. EDX revealed the constitutional elements of the materials, namely Zr, Ca, Si and Al. After 28 days immersion, an irregular surface was observed. Numerous globular structures covering the sealer surface were detected. EDX revealed an increase in Ca and a decrease in Zr and Si. No P was detected.

Figures 2 and 3 show the average IR and micro-Raman spectra recorded on just extruded Ceraseal as well as on the surface of set disks before and after aging in HBSS for 28 days.

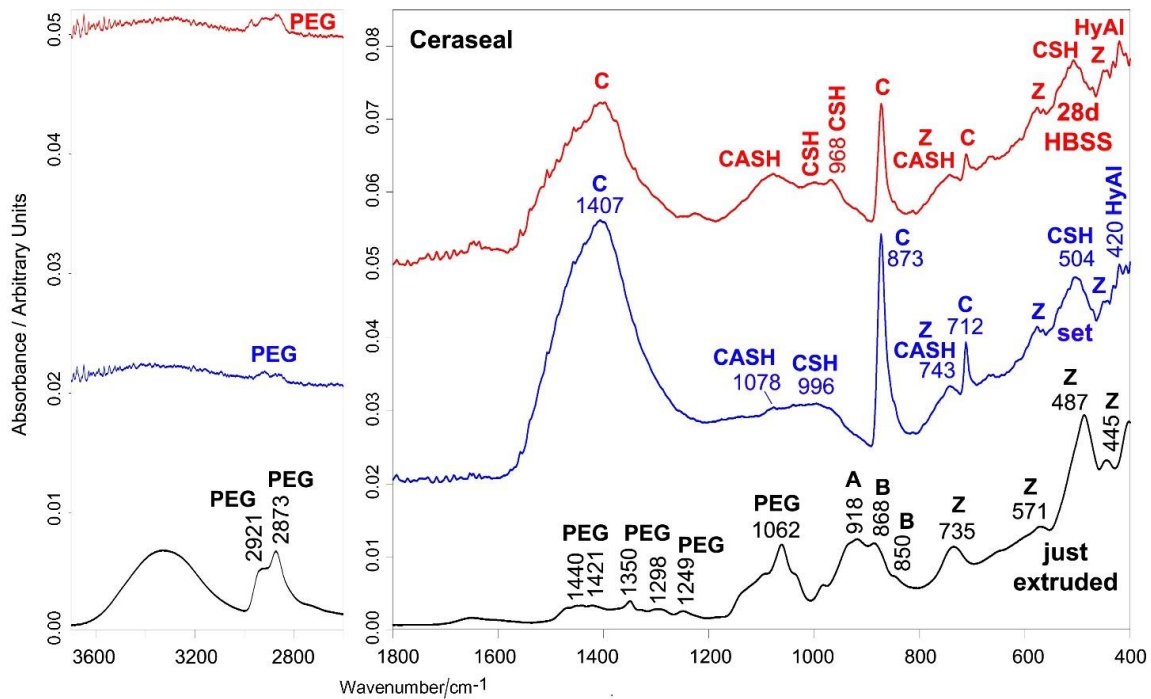


Figure 2. Average IR spectra recorded on just extruded Ceraseal (black) as well as on the surface of set disks before (blue) and after aging in HBSS for 28 days (red). The bands assignable to polyethylene glycol (PEG), alite (tricalcium silicate) (A), belite (dicalcium silicate) (B), monoclinic zirconia (Z), calcite (C), hydrated tricalcium aluminate (HyAl), CSH and CASH phases are indicated.

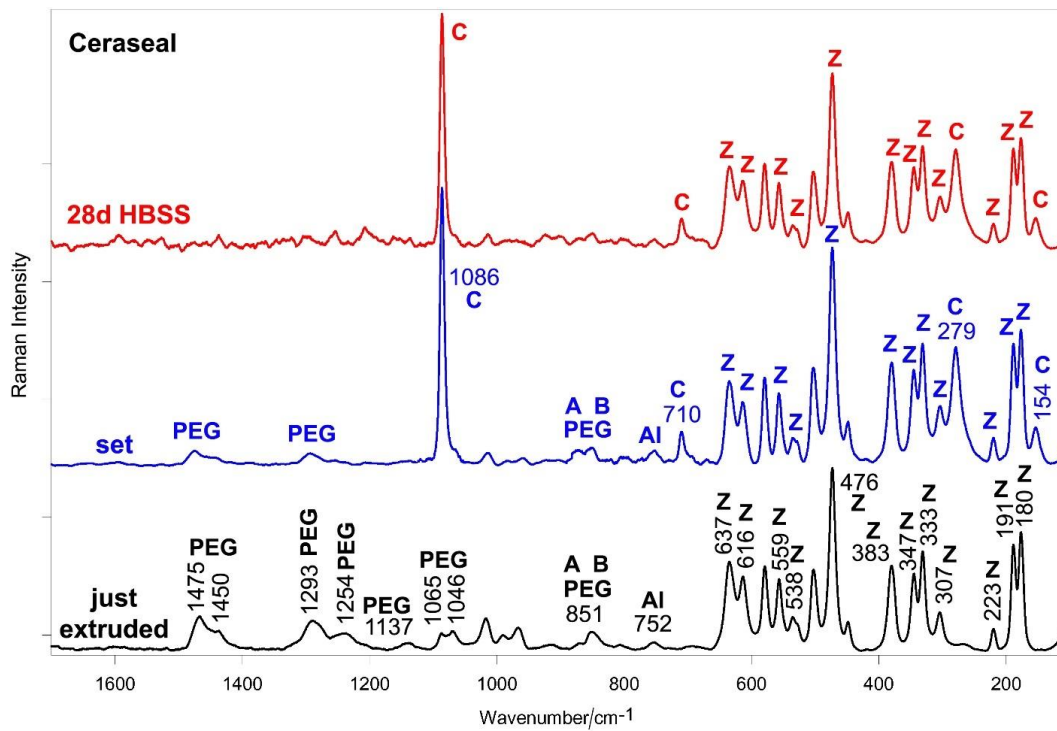


Figure 3. Average micro-Raman spectra recorded on just extruded Ceraseal (black) as well as on the surface of set disks before (blue) and after aging in HBSS for 28 days (red). The bands assignable to polyethylene glycol (PEG), tricalcium silicate (alite) (A), dicalcium silicate (belite) (B), tricalcium aluminate (Al), monoclinic zirconia (Z) and calcite (C) are indicated. PEG component was not indicated in the Material Safety Data Sheet.

The IR spectrum of just extruded Ceraseal (Figure 2) shows the bands of an organic component only generically declared by the manufacturer as a thickening agent. The IR spectrum would suggest that it could be polyethylene glycol (PEG) of high molecular weight (i.e., higher than 10,000 Da) [24]. The IR bands assignable to alite (tricalcium silicate), belite (dicalcium silicate) [25,26] and monoclinic zirconia [27] were observed as well, in agreement with the composition declared by the manufacturer. Tricalcium aluminate was not detected, since its (weak) marker band at about 750 cm^{-1} [28] is overlapped with the stronger spectral feature of zirconia at 736 cm^{-1} . The Raman spectrum of just extruded Ceraseal (Figure 3) confirms the presence of PEG [29], calcium silicates [30,31] and monoclinic zirconia [27,32]; tricalcium aluminate [33,34] was detected as well.

The IR spectrum of the set sample (Figure 2) is dominated by the bands of calcite [35–37]. Bands assignable to CaSi particles hydration are detected around 1000 cm^{-1} and at 504 cm^{-1} (calcium silicate hydrate (CSH) gel phase) [38], at 1078 cm^{-1} (calcium aluminosilicate hydrate (CASH) gel phase) [28], 743 cm^{-1} (symmetric stretching vibrations of Si-O-Si (Al) bridges in the Si-O-Si (Al) ring structure of highly polymerized silicates) [39] and 420 cm^{-1} (hydrated tricalcium aluminate) [38].

The micro-Raman spectrum (Figure 3) confirms the presence of calcite [40,41] as the prevailing phase. In both IR and Raman spectra, the PEG and zirconia components were still detected.

After 28 days of aging in HBSS, the main phase remained calcite; CaSi particles hydration proceeded and the IR bands at 1078 and 968 cm^{-1} (Figure 2) became the most prominent spectral features in the $1200\text{--}900\text{ cm}^{-1}$ range; the former band suggests the prosecution of CSH chain polymerization and replacement of Al by Si, the latter an increase in the Ca/Si ratio [28]. The bands of the PEG component were detected as weak spectral features (CH stretching at $2921\text{--}2873\text{ cm}^{-1}$). The micro-Raman spectrum (Figure 3) is dominated by the bands of calcite and zirconia.

2.5.2. NeoSealer Flo

ESEM images at $3000\times$ revealed a homogeneous surface with granules of different sizes and shapes (Figure 4). The smaller granules (less than $1\text{ }\mu\text{m}$) are spread on the whole surface. Larger quadrangular structures (sizes between 2 and $10\text{ }\mu\text{m}$) were not uniformly distributed. EDX analyses revealed the constitutional elements of the sealer, namely tantalum (Ta) (used as radiopacifier), Ca, Si and Al (from CaSi and calcium aluminates).

After 28 days immersion in HBSS, ESEM images at $3000\times$ revealed a less uniform surface with an irregular layer.

The layer was characterized by long needle-like structures (the length of these needles ranged from 10 to $30\text{ }\mu\text{m}$) and granules agglomerated in larger irregular structures (ranging from 2 to $5\text{ }\mu\text{m}$).

EDX microanalysis revealed an increase in Ca and Al, stability of Si and Ta (slight increase) and the appearance of P and Na, K, Cl (from HBSS).

Figures 5 and 6 show the average IR and micro-Raman spectra recorded on just extruded NeoSealer Flo as well as on the surface of set disks before and after aging in HBSS for 28 days.

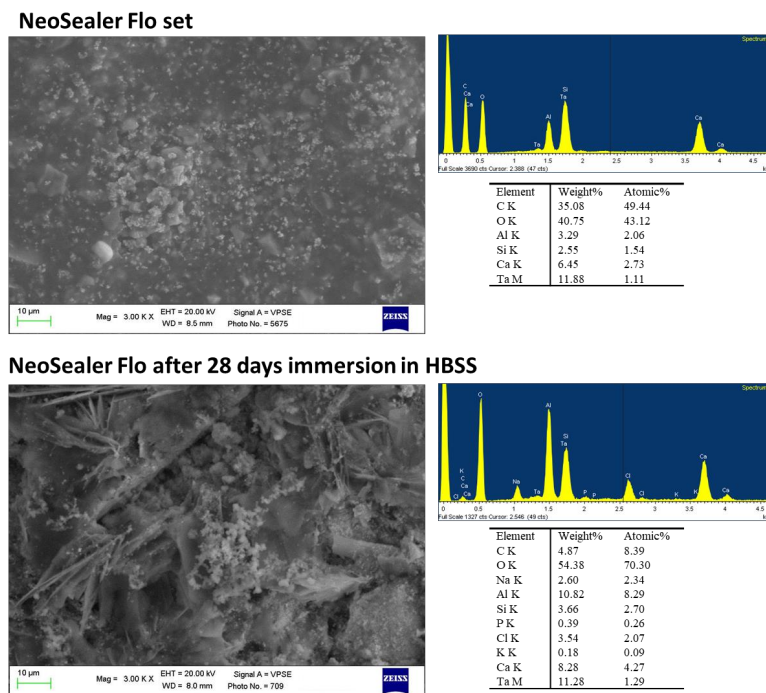


Figure 4. ESEM images at 3000× of NeoSealer Flo before and after immersion in HBSS. The set sample was characterized by a homogeneous surface with granules of different sizes and shapes. EDX analyses revealed the constitutional elements of the sealer, namely Ta, Ca, Si and Al. After 28 days immersion in HBSS, ESEM images revealed a less uniform surface with an irregular layer, characterized by needle-like structures and granules that were agglomerated in larger irregular structures. EDX microanalysis revealed an increase in Ca and Al, stability of Si and Ta and the appearance of P.

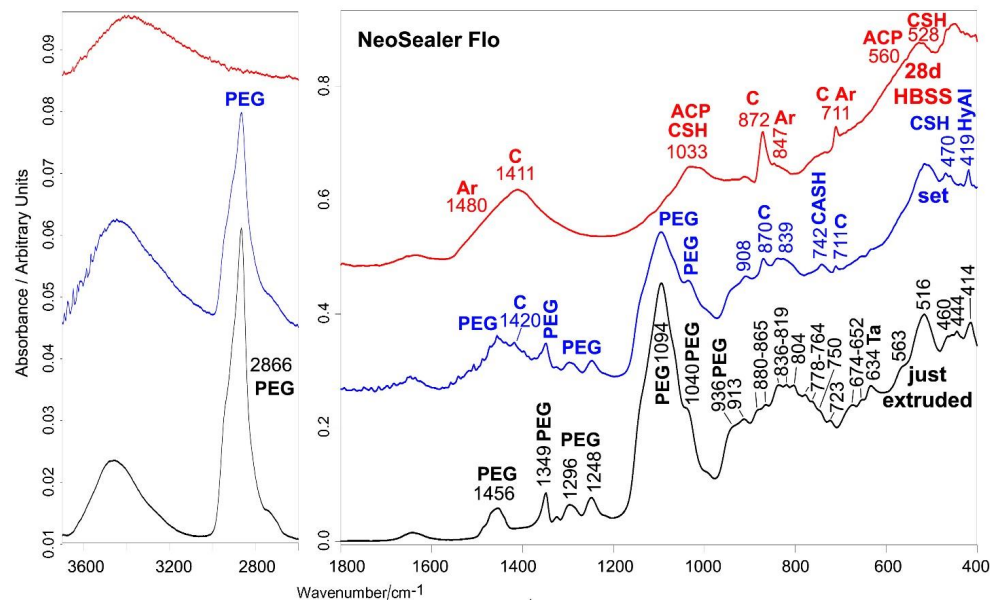


Figure 5. Average IR spectra recorded on just extruded NeoSealer Flo (black) as well as on the surface of set disks before (blue) and after aging in HBSS for 28 days (red). The bands assignable to polyethylene glycol (PEG), tantalite (Ta), calcite (C), aragonite (Ar), hydrated tricalcium aluminate (HyAl), amorphous calcium phosphate (ACP), CSH and CASH phases are indicated. With regard to the 950–400 cm^{-1} range, band assignments to calcium silicates and aluminates are reported in Table S1, Supplementary Material. PEG and grossite were not reported by the manufacturer in the Material Safety Data Sheet.

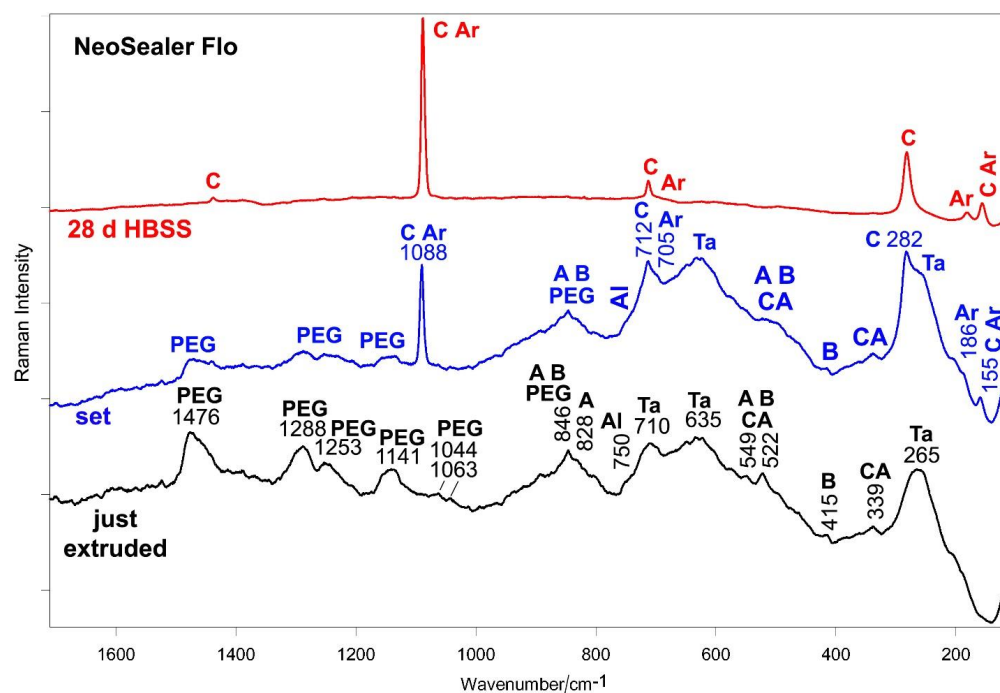


Figure 6. Average micro-Raman spectra recorded on just extruded NeoSealer Flo (black) as well as on the surface of set disks before (blue) and after aging in HBSS for 28 days (red). The bands assignable polyethylene glycol (PEG), tricalcium silicate (alite) (A), dicalcium silicate (belite) (B), tricalcium aluminate (Al), calcium monoaluminate (CA), calcite (C), aragonite (Ar) and tantalite (Ta) are indicated.

The IR spectrum of the just extruded sealer (Figure 5) showed the presence of an organic component not declared by the manufacturer in the Material Safety Data Sheet; on the basis of the IR spectrum, it is presumably PEG of low molecular weight (i.e., below 1000 Dalton) [24]. The IR spectral range below 1000 cm^{-1} is dominated by the bands assignable to silicate and aluminate phases (the latter prevalently as calcium monoaluminate and grossite) [25,26,42]. Grossite was not declared by the manufacturer in the Material Safety Data Sheet. Detailed assignments are given in Table S1, Supplementary Material. Tantalite is revealed by the IR band at 634 cm^{-1} [43], which also has a contribution from AlO_6 octahedra.

The micro-Raman spectrum of the just extruded sealer (Figure 6) confirmed the nature of the organic component [29], as well as the presence of tantalite [44], calcium silicates and aluminates; among aluminates, calcium monoaluminate and tricalcium aluminate were detected [30,31,33,34,42,45]. For this sealer, setting induced the formation of a calcium carbonate component; the bands of the organic phase weakened in both IR and micro-Raman spectra (Figures 5 and 6). Micro-Raman analysis (Figure 6) showed the presence of both calcite (prevailing phase, i.e., the most stable) and aragonite polymorphic forms [40].

Changes in the relative intensity and shifts of the silicate and aluminate bands in both IR and Raman spectra (Figures 5 and 6) may be ascribed to sealer hydration, according to previous studies [18,38,39]. In particular, the above assigned IR bands at 742 and 419 cm^{-1} (Figure 5) were detected.

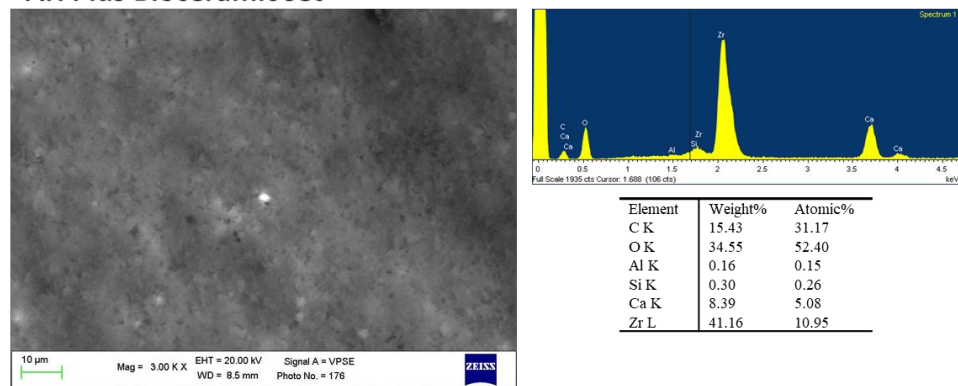
Upon aging in HBSS for 28 days, the IR bands of PEG were no longer detected (Figure 5); in particular, its strongest band at 1094 cm^{-1} disappeared, making visible the CSH band [28,39] at 1030 cm^{-1} , assignable to the Si-O stretching in aged set Portland cements [36]; the CSH phase was responsible for the increase in intensity of the 450 cm^{-1} band, as previously reported [18,38]. The IR spectrum of the sample immersed in HBSS for 28 days is dominated by the bands of calcite, which appeared even more prominent than in the set sample, suggesting that calcium carbonate deposition proceeded upon aging. The IR spectral feature that reveals signs of calcium phosphate deposition is the broadening

around 560 cm^{-1} , where the bending mode of amorphous calcium phosphates is reported to fall [46]. This phase could also contribute to the band at 1030 cm^{-1} since in this range PO_4^{3-} stretching modes are reported to fall. The calcium phosphate deposit is very thin, so that its Raman marker band at 960 cm^{-1} was never detected in the Raman spectra (Figure 6), which showed only the bands of calcium carbonate. This result confirms that the latter is the prevailing phase and suggests that the deposit was thick enough to mask the bands of the material underneath, which were no longer detected. Raman spectroscopy allowed us to clarify that a small amount of aragonite was also present.

2.5.3. AH Plus Bioceramic

ESEM images at $3000\times$ of the set sample revealed a uniform surface with few irregularities (Figure 7). EDX analyses revealed the constitutional elements of the sealer, namely Zr (the radiopacifier) Ca, Si and traces of Al. After 28 days in HBSS, the surface was completely covered by a uniform layer, composed of globular structures (range $5\text{--}10\ \mu\text{m}$) and some cubic-shaped structures (range $5\text{--}10\ \mu\text{m}$). EDX analysis revealed a marked increase in Ca, the decrease in Zr and the appearance of P, Na, Cl and Mg (from HBSS).

AH Plus Bioceramic set



AH Plus Bioceramic after 28 days in HBSS

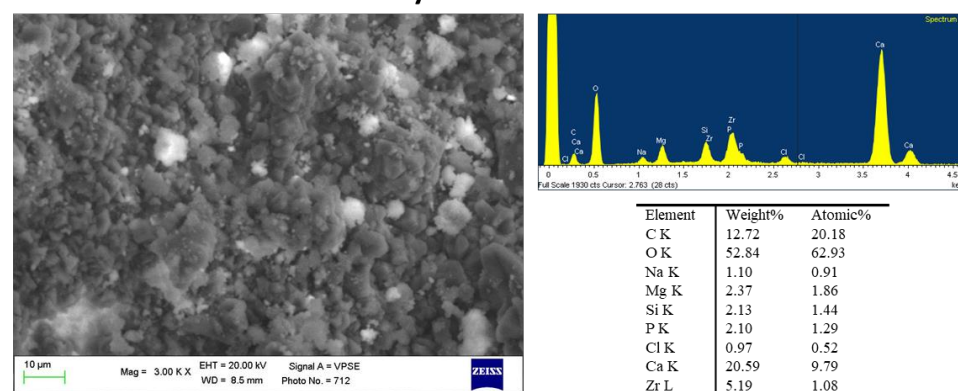


Figure 7. ESEM images at $3000\times$ of AH Plus Bioceramic before and after immersion in HBSS. ESEM on the set sample showed a uniform surface with few irregularities. EDX revealed constitutional elements of the sealer, namely Zr (the radiopacifier) Ca, Si and traces of Al. The surface was covered by a vast layer after 28 days in HBSS. The layer was composed of globular and cubic-shaped structures. EDX analysis revealed a slight increase in Si, a marked increase in Ca, the decrease in Zr, the appearance of P, Na, Cl and Mg.

Figures 8 and 9 show the average IR and micro-Raman spectra recorded on just extruded AH Plus Bioceramic as well as on the surface of set disks before and after aging in HBSS for 28 days. The IR spectrum of just extruded AH Plus Bioceramic (Figure 8) is dominated by the bands of dimethyl sulfoxide [47]; the bands of monoclinic zirconia dominate

the spectral range below 750 cm^{-1} [27]. No bands assignable to lithium carbonate [43] were detected, due to its low content ($<0.5\%$ w/w according to the MSDS). Tricalcium silicate (alite) is revealed by the shoulders at 937 and 903 cm^{-1} [25,28]. The band at 3643 cm^{-1} , assignable to $\text{Ca}(\text{OH})_2$ (portlandite), is due to a partial hydration of the silicate component.

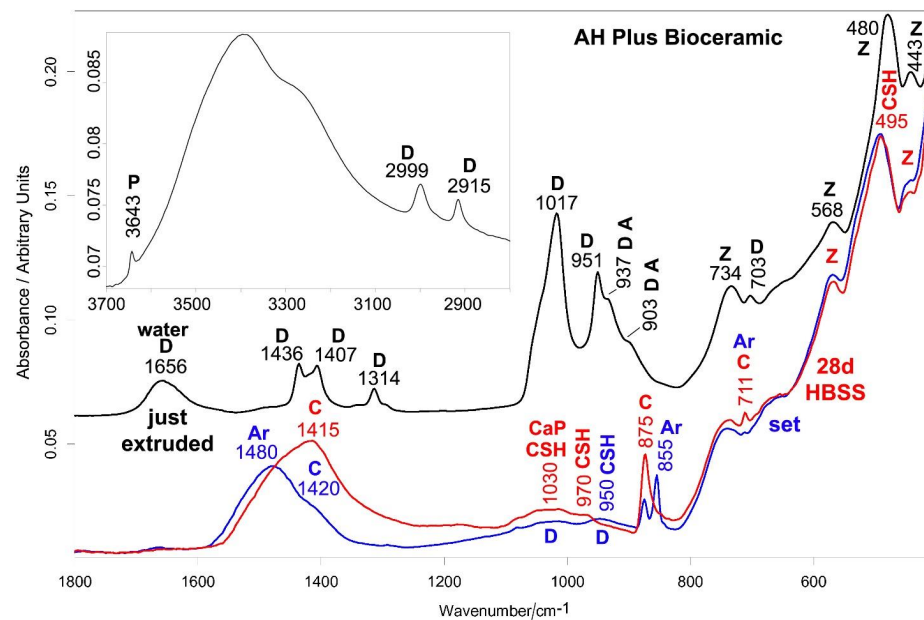


Figure 8. Average IR spectra recorded on just extruded AH Plus Bioceramic (black) as well as on the surface of set disks before (blue) and after aging in HBSS for 28 days (red). The inset shows the $3700\text{--}2800\text{ cm}^{-1}$ spectral range of the just extruded sealer. The bands assignable to portlandite (P), dimethyl sulfoxide (D), tricalcium silicate (alite) (A), monoclinic zirconia (Z), CSH phase, calcite (C), aragonite (Ar) and calcium phosphate (CaP) are indicated. Band assignable to water (1656 cm^{-1}) was also detected in the just extruded sealer.

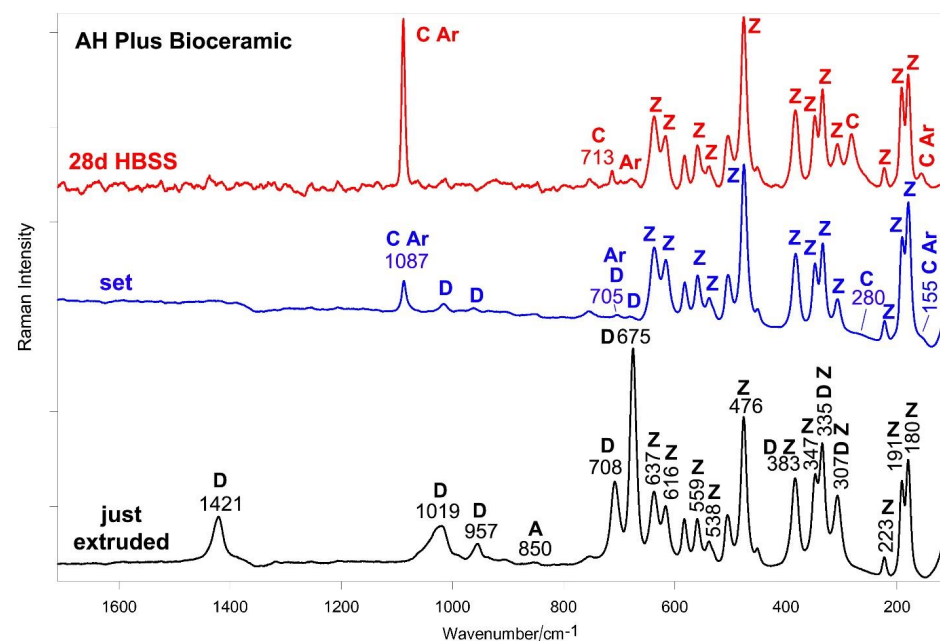


Figure 9. Average micro-Raman spectra recorded on just extruded AH Plus Bioceramic (black) as well as on the surface of set disks before (blue) and after aging in HBSS for 28 days (red). The bands assignable to dimethyl sulfoxide (D), tricalcium silicate (alite) (A), monoclinic zirconia (Z), calcite (C) and aragonite (Ar) are indicated.

The micro-Raman spectrum of just extruded AH Plus Bioceramic (Figure 9) shows the bands of dimethyl sulfoxide [48,49] and monoclinic zirconia [27,32]. Tricalcium silicate was revealed through the broad band at about 850 cm^{-1} [30,31,45]. No lithium carbonate [43] was detected.

In the Raman spectrum of the set sample (Figure 9), the bands of DMSO decreased in intensity, but did not disappear; the IR spectrum has to be interpreted accordingly (Figure 8). Therefore, the IR bands at about 1030 and 950 cm^{-1} have a contribution from DMSO, although they underwent a significant broadening upon sealer setting. Moreover, they may be assigned to the silicate component. Actually, the band at 950 cm^{-1} may be ascribed to the formation of the CSH phase [36,39] together with the component at about 1030 cm^{-1} as well as the shift and broadening of the band at 480 cm^{-1} due to the contribution of its Si-O-Si bending (reported at about 500 cm^{-1}) [39]. Both IR and Raman spectra (Figures 8 and 9) revealed that carbonation of the sealer occurred, with formation of calcite and aragonite polymorphs of calcium carbonate [29,35–37,40].

IR spectra (Figure 8) revealed that upon aging in HBSS the prevailing phase is calcite, with low amounts of aragonite; as expected, the most stable polymorph (i.e., calcite) becomes prevalent upon aging for 28 days and evidently aragonite transformed into calcite [40]. By normalizing the spectra to the intensity of the zirconia band at about 735 cm^{-1} , only a slight strengthening in the 1030 cm^{-1} spectral profile (where PO_4^{3-} stretching of calcium phosphates is reported to fall) was observed, whilst no significant increases in the $560\text{--}600\text{ cm}^{-1}$ bands (where PO_4^{3-} bending modes fall) were detected. These trends indicated minor amounts of calcium phosphate phases. The IR band at 950 cm^{-1} shifted to 970 cm^{-1} due to the release of DMSO (whose bands were no longer detected in Raman spectra, Figure 9) and cement maturation [36]. Raman spectra (Figure 9) confirm the presence of calcite and aragonite (the latter in lower amounts) and no detectable amounts of calcium phosphates; actually, the Raman marker band of this phase at about 960 cm^{-1} was not detected.

3. Discussion

The study investigated a series of chemical–physical properties of three recent pre-mixed bioceramic sealers. These materials can be used to deal with complex endodontic cases when a traditional sealer might not ensure a stable seal, such as in presence of wide and wet root apices.

Our data showed the setting times of all pre-mixed bioceramic sealers were longer than those reported by the manufacturers, while the setting times of AH Plus were similar to those reported in the literature [50,51].

We found that environmental moisture used to achieve the setting reaction of sealers induced longer setting times than those reported by manufacturers. A similar behavior is reported in a previous paper on IRoot, the first marketed pre-mixed bioceramic sealer, which showed longer sealer setting time with increasing content of humidity [52]. Clinicians should therefore consider waiting longer to ensure the complete material setting before tooth reconstruction. We must underline that it is difficult to clinically assess the suitable humidity of the root canal and no protocols are currently reported to provide a stable and reproducible setting of the sealers.

In order to penetrate into dentinal tubules and to seal complex anatomies, such as isthmuses, secondary canals and apical deltas, the sealer needs to possess high flowability and adequate thickness. In our study, all pre-mixed bioceramic sealers fulfilled the ISO specifications and the results were close to those reported by manufacturer declarations. Ceraseal, in particular, revealed a flowability comparable to AH Plus, which could provide a great advantage in cold obturation techniques, where highly flowable sealers are often recommended. AH Plus flow and film thickness were similar to those previously reported [53].

Concerning our results on radiopacity, all bioceramic sealers revealed lower values when compared to AH Plus. It should be noted that the radiopacity values of the bioceramic-

based materials (from 5.5 mm Al of NeoSealer Flo to 8.6 mmAl of AH Plus Bioceramic) were higher than those reported in previous studies where the same procedures were used for bioactive powder-liquid sealers, including Bioroot RCS (5.3 mmAl) [50], Tech Biosealer Endo [3] or paste-to-paste materials, such as MTA Fillapex (4.6 mmAl) [54]. NeoSealer Flo showed significantly lower values, most likely attributable to the presence of tantalite instead of zirconium oxide. No bismuth oxide was included, for the potential tooth discoloration issues and for the toxicity of bismuth when placed close to the periapical tissues [10,15,54]. According to the manufacturer, AH Plus Bioceramic sealer contains approx. 70% zirconium oxide, Ceraseal possesses approx. 50% zirconium oxide, while NeoSealer Flo approx. 40–50% tantalum pentoxide. The significantly higher radiopacity values (11.9 mmAl) of AH Plus may be related to the marked different composition of this sealer, showing higher percentages of calcium tungstate and zirconium oxide radiopacifying agents [50].

All the tested bioceramic sealers showed to be biointeractive materials able to leach calcium ions and to alkalize the soaking water. It is known that calcium ions are strong extracellular signals for mineralizing cells, such as osteoblasts [6,55]. This property is important for materials that should seal the periapical space in the presence of bone defects.

Interestingly, despite the low amount of CaSi (5–15%) in its composition, AH Plus Bioceramic showed a high cumulative calcium release.

Ceraseal provided the highest values of calcium release and alkalizing activity when compared to both NeoSealer Flo and AH Plus Bioceramic. These values were significantly lower than those reported for other materials that were tested under similar experimental conditions, such as Totalfill BC Sealer [56], BioRoot RCS [50] and Neo MTA Plus [57]. This behavior may be attributable to the different percentages of calcium silicates and calcium aluminates in the analyzed materials. Ceraseal and NeoSealer Flo included calcium aluminates in addition to tricalcium and dicalcium silicates, while lower percentages of tricalcium silicate are included in AH Plus Bioceramic sealer, as spectroscopically revealed by the lower relative intensity of the IR and Raman bands of the latter phase with respect to zirconia (Figure 2 versus Figures 3 and 8 versus Figure 9).

The percentage of bioactive CaSi particles in their composition influenced the biointeractive properties of the sealers. Indeed, numerous new biomaterials and scaffolds were developed by increasing the CaSi powder content to enhance the biointeractive and biological properties when applied in periapical bone defects [58,59], or to achieve pulpal revascularization procedures [60,61]. Similarly calcium aluminates (introduced in CaSi-based cement for endodontics to reduce the setting time [62]) showed high Ca^{2+} , OH^- and $\text{Al}(\text{OH})_4^-$ release [62].

Biointeractivity (release of biologically relevant ions) is related to the high open pore volume which forms an internal network of water-filled pores providing a large surface area involved in the leaching process [14,63]. The ion release depends on the nature of the network structure of the sealer responsible for water absorption and solubility as well as the permeability of the material to water diffusion [14,63].

Therefore, sealers with high open pore volume can absorb more water and consequently show higher solubility and potentially higher ion release (compatibly with their content of reactive CaSi particles). For this reason, NeoSealer Flo and AH Plus Bioceramic showed higher solubility, open pore volume and water absorption. However, a higher solubility of the material tested in water in vitro does not directly indicate a detrimental effect in vivo, as nucleation of apatite and carbonate may compensate and reduce the sealer behavior. It has been demonstrated that the solubility of MTA-like materials is lower when immersed in a medium containing serum protein [64].

Our ESEM-EDX analyses evidenced a layer rich in Ca and C with limited P peaks on the material surface after immersion in HBSS. Apatite nucleation ability was low. In some cases, such as in Ceraseal samples, P was not detected by EDX microanalysis. A possible explanation could be attributable to the Zr and P peaks overlapping, which could mask the presence of P on their surface [65]. This overlapping has also been found in AH Plus

Bioceramic, where the presence of P could be underestimated due to the presence of Zr in the material composition.

Previous studies have reported that calcium ions supplied by the rapid dissolution of portlandite ($\text{Ca}(\text{OH})_2$) and by the cement matrix may react with environmental carbonate ions to form a calcium carbonate superficial layer [19,38,66].

Apatite-like and calcite crystals were found on set Portland cement exposed to phosphate solution and CO_2 , and apatite-like phase formation on carbonated substrates [18,63,66]. In previous studies, the calcite crystalline form of calcium carbonate showed good biological activity [18,63,67,68]. Soluble $\text{Ca}(\text{OH})_2$ crystals allow the nucleation of calcium carbonate polymorphs and/or metastable calcium salt crystals that readily transform into the stable calcite phase in water [18,68]. Calcium carbonate may precipitate at the surface and in the sealer paste porosity, forming a protective layer of calcium carbonate [14,69,70], which can be useful in infected periapical areas. The protective calcium carbonate layer constrains or reduces the ionic diffusion from sealer bulk, reducing its degradation/solubility [14,69,70] and improving the endodontic seal.

In our study IR and micro-Raman spectroscopy allowed to detect the formation of calcium carbonate (as calcite and, in some cases, aragonite) on the surface of all set sealers. This phase strongly influenced the behavior of the materials in the aging tests, i.e., the nature of the phase nucleated upon immersion in HBSS.

The formation of a thin layer of a calcium phosphate phase was detected only on AH Plus Bioceramic and NeoSealer Flo. Ceraseal did not show any calcium phosphate deposits despite its highest calcium release among the tested sealers. This result may be explained by considering that upon setting, this sealer formed the highest relative amount of calcite, as suggested by the highest relative intensity of the Raman and IR bands of this phase (Figure 2 versus Figures 5 and 8, and Figure 3 versus Figures 6 and 9), further strengthening the idea that the material behavior in HBSS was strongly affected by the previous setting conditions.

Nevertheless, these data reveal low/no apatite nucleation on the sealers surface. Possible reasons for low apatite nucleation ability may be related to the low amount of CaSi in the composition of the tested sealers (15% in AH plus Bioceramic, 35% in Neosealer Flo, 20–40% in Ceraseal).

We highlight that a low amount of CaSi in the sealer formulation means lower silanol (Si-OH) functional groups, necessary for the apatite nucleation. It has been shown that the deprotonation of Si-OH at alkaline pH results in the formation of SiO⁻ groups [63,71,72], being able to induce a heterogeneous nucleation of calcium phosphates/apatite by bonding calcium ions from the silica-rich mineral particles [17,63,71,72].

As reported by Gandolfi et al. [17], the formation of CaP apatitic precursors is linked to both the ability to release mineralizing ions and the presence of functional groups able to bind ions and trigger the nucleation of apatite.

An additional reason for low apatite nucleation detected on the tested sealers can be attributable to the carbonation processes that may occur during the setting of the materials.

Interestingly, other premixed bioceramics such as Totalfill BC Sealer, revealed a markedly higher nucleation activity in a similar experimental set-up [58]. Indeed, Totalfill BC Sealer demonstrated higher calcium release, alkalization activity, in vitro solubility and apparent porosity [55,73]. The reason for such different behavior could be that Totalfill BC Sealer contained monobasic calcium phosphate in its formulation and a higher content of tricalcium and dicalcium silicates (approx. 50% of the formulation). It has been widely demonstrated that the association of calcium phosphate with hydraulic calcium silicates significantly improved apatite nucleation of the materials [13,19,63].

AH Plus demonstrated a thin CaP deposit despite the low/negligible amount of calcium ions released. This result agreed with previous studies [17,50], where sparse calcium phosphate deposits were detected on AH Plus after immersion in HBSS.

A limitation of this study may be the lack of ex vivo experiments regarding the osteoinductive and proangiogenic properties of the studied sealers.

Only a recent in vitro study on AH Plus Bioceramic sealer tested with human periodontal ligament stem cells [74] reported a similar cytocompatibility but lower mineralization potential when compared to another bioceramic premixed sealer (Endosequence BC Sealer) [74].

An animal model could validate the biointeractive properties found for the tested root canal sealers.

4. Materials and Methods

The control paste-to-paste sealer was prepared according to the manufacturer indications. The premixed sealers were ready to be used as specified by the manufacturers. The main components of the materials are listed in Table 6.

Table 6. Sealer formulation, lot and composition in accordance with manufacturer Safety Data Sheet. Asterisk (*) indicates the components detected by our investigation.

Sealer and Manufacturer	Formulation	Lot	Composition
Ceraseal (MetaBiomed, South Korea)	Premixed	CSL2108201	Zirconium dioxide (45–50%), tricalcium silicate (20–30%), dicalcium silicate (1–10%), tricalcium aluminate (1–10%), thickening agents, polyethylene glycol (PEG) *
NeoSealer Flo (Avalon Nusmile, USA)	Premixed	2020110502	Tantalite (50%), tricalcium silicate (25%), calcium aluminate (25%), dicalcium silicate (10%), tricalcium aluminate (5%), calcium sulfate (1%), PEG *, grossite *
AH Plus Bioceramic (Maruchi, South Korea)	Premixed	KI211103	Zirconium dioxide (50–70%), tricalcium silicate (5–15%), dimethyl sulfoxide (10–30%), lithium carbonate (0.5%), thickening agents (<6%)
AH Plus (Dentsply, Germany)	Paste– paste	2109000972	Paste A: diepoxide, calcium tungstate, zirconium oxide, aerosil, pigment (iron oxide) Paste B: 1-adamantane amine, N,N'-dibenzyl-5-oxa-nonandiamine-1,9, TCD-diamine, calcium tungstate, zirconium oxide, aerosil, silicone oil

Ceraseal is a premixed calcium silicate-based bioceramic sealer and includes, as bioactive components, tricalcium silicate (20–30%), dicalcium silicate (1–10%) and tricalcium aluminate (1–10%). The radiopacifier used is zirconium dioxide and constitutes approx. 45–50% of the composition. Some traces of thickening agents are reported by the manufacturer.

NeoSealer Flo is a premixed bioceramic sealer and includes, as bioactive components, tricalcium silicate (<25%), calcium aluminate (<25%), dicalcium silicate (<10%), grossite (<6%) and tricalcium aluminate (<5%). Tantalite is the radiopacifier and constitutes approx. 50% of the formulation. Traces of calcium sulfate are also reported (<1%).

AH Plus Bioceramic is a premixed bioceramic sealer mostly composed of zirconium dioxide as a radiopacifier (50–70%) and tricalcium silicate (10–15%) as a bioactive component. Dimethyl sulfoxide (DMSO) and traces of lithium carbonate and thickening agents are also reported by the manufacturer.

4.1. Initial, Final Setting Times and Radiopacity

Samples were compacted into a mold (10 mm diameter, 2 mm thickness; n = 3 per group) and stored at 37 °C and 99% relative humidity. The initial and final setting times were measured by evaluating the absence of indentation caused by Gillmore needles (ASTM C 226-07 Standard Specification for Air-Entraining Additions for Use in the Manufacture of Air Entraining Hydraulic Cement) with the following modifications performed in accordance with a previous investigation [63]. Ten grams of samples were used instead of 650 g and the physiological temperature of 37 °C instead of 25 °C. The initial Gillmore tip (113.4 g weight and 2.12 mm diameter) and the final Gillmore tip (453.6 g weight and 1.06 mm diameter) were used on the sealer paste.

Radiopacity was tested in accordance with ISO 6876/2012. The materials were compacted into molds (10.0 mm diameter, 1.0 mm height; $n = 3$ per group). The setting reaction was achieved in 99% relative humidity. Completely set samples were demolded and radiographed using a radiographic unit (Myray Cefla, Imola, Italy) with a reference aluminum step wedge (60 mm long, 10 mm wide thickness varying from 2 to 6 mm in 1 mm increments). The target–film distance was approx. 30 cm with the sample at 3 cm from the surface of the radiographic tube, 0.13 s exposure at 70 kV and 8 mA [56]. The film (Kodak dental film, Eastman Kodak Company, Carestream Health Inc., Rochester, New York, NY, USA) was processed (automatic developer, 4 min at 30 °C) and scanned (Epson Perfection V750 PRO, Jakarta, Indonesia). The radiographic density (colour intensity) data were converted (software ImageJ, Wayne Rasband, National Institutes of Health (NIH), Bethesda, MD, USA) into aluminum step wedge equivalent thickness (mm Al). A suitable sealer should possess radiopacity values equal to or higher than 3 mmAl.

4.2. Sealer Flow and Film Thickness

Sealers flow was measured according to ISO 6876/12. The material ($0.05 \text{ mL} \pm 0.005$) was dispensed onto one glass plate. After 3 min ($180 \text{ s} \pm 5$), a second glass plate was placed centrally on top of the material and an additional mass ($100 \text{ g} \pm 2$) was centrally located on the plate (total mass was $120 \text{ g} \pm 2$). Ten minutes after the mixing procedure, the weight was removed from the upper glass plate, and the major and minor diameters were measured with a calibrated ruler in mm. This test was replicated three times per material and repeated if discrepancies between minor and major diameters were present. As described in ISO 6876/12, the disk diameter should not be less than 1.7 mm for materials used with gutta-percha points.

Film thickness was measured as described in ISO 6876/12. Briefly, the thickness of 2 glass plates (25 mm length, area of approx. $625 \pm 50 \text{ mm}^2$) was measured using a micrometer. Sealers were placed between two glass plates. After 3 min ($180 \pm 5 \text{ s}$), a load of 150 N was vertically applied, and the sealer completely filled the area between the glass plates. Ten minutes after the sealer placement, the thickness of the two glass plates and the film of the sealer was measured using a micrometer. Sealer thickness was obtained by subtracting the total thickness and the thickness of the 2 plates previously recorded. The test was repeated 3 times for each material. As described in ISO 6876/12, film thickness should not be more than 50 μm for sealers used with other obturation materials.

4.3. Solubility, Water Absorption, Apparent Porosity

Materials compacted into molds (1.0 mm diameter, 1.6 mm height; $n = 6$ samples for each material) were placed at 37 °C and 99% relative humidity for a period of 100% longer than the final setting time [56]. Samples were demolded, weighed to determine the initial mass (I), immediately immersed vertically in 20 mL of distilled water and placed at 37 °C for 24 h [13,14,51,63]. The mass whilst suspended in water (S) was determined. The samples were then removed from water, the excess water from the surface of each sample was removed using a moistened filter paper and the saturated mass (M) was recorded. Finally, the samples were dried at 37 °C until the weight was stable, and the final dry mass (D) was recorded. Open pore volume ($\text{VOP} = M - D$, in cm^3), impervious portion volume ($\text{VIP} = D - S$, in cm^3) and apparent porosity ($P = [(M - D)/V] \times 100$, in percentage) were calculated following Archimedes principle. Water absorption ($A = [(M - D)/D] \times 100$) and solubility ($S = [(I - D)/D] \times 100$) were calculated as percentages of the original weight. Each weight measurement was repeated three times using an analytical balance (Bel Engineering series M, Monza, Italy) and determined to the nearest 0.001 g. Mean values of the measures were reported.

4.4. Alkalizing Activity and Calcium Release

Samples were compacted into a mold (8 mm diameter, 1.0 mm height; $n = 6$ per group) and placed at 37 °C and 99% relative humidity for a period of 100% longer than the final

setting time [56]. Then, the materials were demolded and immersed in 10 mL of deionized water (pH 6.8) in polypropylene sealed containers and stored at 37 °C. [13,14,50,57]. The soaking water was replaced at each endpoint (3 h and 1, 3, 7, 14, 28 days) and analyzed for pH and calcium content under magnetic stirring at room temperature (24 °C). A potentiometric method using a multiparameter laboratory meter (inoLab 750, WTW, Weilheim, Germany) was used. For pH measurements, a selective electrode (Sen Tix Sur; WTW) was used, while for calcium release, a calcium probe was used (calcium ion electrode, Eutech Instruments Pte Ltd., Singapore). An ionic strength adjuster was added (4 mol/L KCl; WTW) for calcium release measurements.

4.5. Surface Characterization and CaP Nucleation—ESEM-EDX, IR, Micro-Raman

Samples were compacted into a mold (1.0 mm diameter, 2.0 mm height) to reach the final setting time at 37 °C and 99% relative humidity. Then, the samples were demolded, immersed upright in 20 mL of Hanks balanced salt solution (HBSS, Lonza, Verviers, Belgium) and stored at 37 °C for 28 days (ISO 23317:2014), the medium was replaced weekly [15,17,56,57]. The surface of set and 28-day aged materials was examined by environmental scanning electron microscopy (ESEM; Zeiss EVO 50, Jena, Germany) with elemental dispersive X-ray microanalysis (EDX; Oxford Instruments, Abingdon, UK), and vibrational IR and micro-Raman spectroscopy.

Operative ESEM-EDX conditions are reported elsewhere [15,17,56,57]; reported images and elemental analyses are representative of each group. IR spectra were recorded in triplicate on a Bruker Alpha Fourier Transform FTIR spectrometer, equipped with a platinum attenuated total reflectance (ATR) single reflection diamond module (penetration depth 2 µm) and a deuterated lanthanum α -alanine-doped triglycine sulfate (DLaTGS) detector; the spectral resolution was 4 cm⁻¹.

Micro-Raman spectra were measured on the surface of the fresh samples as well as after aging in HBSS for 28 days. They were obtained using a Jasco NRS-2000C spectrometer with a microscope of 100× magnification. Five spectra at least were recorded on each sample and averaged. All the spectra were recorded in backscattering conditions with 5 cm⁻¹ spectral resolution using a 532 nm green diode-pumped solid-state laser (RgBLase LLC, Fremont, CA, USA) with a power of about 5 mW. A 160 K cooled digital charge-coupled device (Spec-10: 100B, Roper Scientific Inc., Sarasota, FL, USA) was used as a detector.

4.6. Statistical Analysis

Data were analyzed using Stata 17.1 (StataCorp, College Station, TX, USA). A two-way ANOVA with RM Student–Newman–Keuls post hoc test ($p < 0.05$) was performed for ion release and alkalizing activity. One-way ANOVA with Student–Newman–Keuls post hoc test ($p < 0.05$) was used for setting times, radiopacity, solubility, water absorption, apparent porosity, flow and film thickness.

5. Conclusions

The study results could be summarized as follows:

- The study supports the clinical use of the three bioceramic root canal sealers.
- The premixed bioceramic sealers met the required chemical and physical standards, but open pore volume, water absorption and solubility were higher when compared to conventional epoxy resin-based sealer.
- Clinicians should be aware that a longer setting time may occur with these materials.
- The premixed bioceramic sealers released biologically relevant ions (as Ca²⁺ and OH⁻) which could provide potential benefits when these materials are positioned close to periapical bone defects or extruded over the root apex.
- Apatite nucleation was slight due to carbonation processes that occurred during setting and after aging in HBSS.

Supplementary Materials: The following supporting information can be downloaded at: <https://www.mdpi.com/article/10.3390/ijms232213914/s1>.

Author Contributions: Author contribution: Conceptualization: C.P., M.G.G.; Investigation: F.Z., A.S., M.D.F., P.T.; Methodology: C.P., M.G.G., P.T.; Supervision: C.P., M.G.G., P.T.; Writing original draft: F.Z., A.S., M.D.F., P.T.; Final review and editing: C.P., M.G.G., P.T.; Visualization: F.Z., M.D.F.; Software: F.Z., A.S., M.D.F. All authors have read and agreed to the published version of the manuscript.

Funding: This research received no external funding.

Institutional Review Board Statement: Not applicable.

Informed Consent Statement: Not applicable.

Data Availability Statement: Not applicable.

Conflicts of Interest: The authors declare no conflict of interest.

References

1. Torabiinejad, M.; Chivian, N. Clinical applications of mineral trioxide aggregate. *J. Endod.* **1999**, *25*, 197–205. [[CrossRef](#)]
2. Niu, L.N.; Jiao, K.; Wang, T.D.; Zhang, W.; Camilleri, J.; Bergeron, B.E.; Feng, H.L.; Mao, J.; Chen, J.H.; Pashley, D.H.; et al. A review of the bioactivity of hydraulic calcium silicate cements. *J. Dent. Res.* **2014**, *42*, 517–533. [[CrossRef](#)] [[PubMed](#)]
3. Prati, C.; Gandolfi, M.G. Calcium silicate bioactive cements: Biological perspectives and clinical applications. *Dent. Mater.* **2015**, *31*, 351–370. [[CrossRef](#)] [[PubMed](#)]
4. Khalil, I.; Naaman, A.; Camilleri, J. Properties of Tricalcium Silicate Sealers. *J. Endod.* **2016**, *42*, 1529–1535. [[CrossRef](#)] [[PubMed](#)]
5. Primus, C.; Gutmann, J.L.; Tay, F.R.; Fuks, A.B. Calcium silicate and calcium aluminate cements for dentistry reviewed. *J. Am. Ceram. Soc.* **2022**, *105*, 1841–1863. [[CrossRef](#)]
6. Matsumoto, S.; Hayashi, M.; Suzuki, Y.; Suzuki, N.; Maeno, M.; Ogiso, B. Calcium ions released from mineral trioxide aggregate convert the differentiation pathway of C2C12 Cells into osteoblast lineage. *J. Endod.* **2013**, *39*, 68–75. [[CrossRef](#)]
7. Gandolfi, M.G.; Shah, S.N.; Feng, R.; Prati, C.; Akintoye, S.O. Biomimetic calcium-silicate cements support differentiation of human orofacial mesenchymal stem cells. *J. Endod.* **2011**, *37*, 1102–1108. [[CrossRef](#)]
8. Reyes-Carmona, J.F.; Felipe, M.S.; Felipe, W.T. The biomineralization ability of mineral trioxide aggregate and Portland cement on dentin enhances the push-out strength. *J. Endod.* **2010**, *36*, 286–291. [[CrossRef](#)]
9. Reyes-Carmona, J.F.; Santos, A.R.; Figueiredo, C.P.; Felipe, M.S.; Felipe, W.T.; Cordeiro, M.M. In vivo host interactions with mineral trioxide aggregate and calcium hydroxide: Inflammatory molecular signaling assessment. *J. Endod.* **2011**, *37*, 1225–1235. [[CrossRef](#)]
10. Gandolfi, M.G.; Iezzi, G.; Piattelli, A.; Prati, C.; Scarano, A. Osteoinductive potential and bone-bonding ability of ProRoot MTA, MTA Plus and Biodentine in rabbit intramedullary model: Microchemical characterization and histological analysis. *Dent. Mater.* **2017**, *33*, 221–238. [[CrossRef](#)]
11. Mizuno, M.; Banzai, Y. Calcium ion release from calcium hydroxide stimulated fibronectin gene expression in dental pulp cells and the differentiation of dental pulp cells to mineralized tissue forming cells by fibronectin. *Int. Endod. J.* **2008**, *41*, 933–988. [[CrossRef](#)]
12. Sun, J.; Wei, L.; Liu, X.; Li, J.B.; Wang, G.; Meng, F. Influences of ionic dissolution products of dicalcium silicate coating on osteoblastic proliferation, differentiation and gene expression. *Acta Biomater.* **2009**, *5*, 1284–1293. [[CrossRef](#)]
13. Gandolfi, M.G.; Spagnuolo, G.; Siboni, F.; Procino, A.; Riviello, V.; Pelliccioni, G.A.; Prati, C.; Rengo, S. Calcium silicate/calcium phosphate biphasic cements for vital pulp therapy: Chemical-physical properties and human pulp cells response. *Clin. Oral Investig.* **2015**, *19*, 2075–2089. [[CrossRef](#)]
14. Gandolfi, M.G.; Siboni, F.; Botero, T.; Bossù, M.; Riccitiello, F.; Prati, C. Calcium silicate and calcium hydroxide materials for pulp capping: Biointeractivity, porosity, solubility and bioactivity of current formulations. *J. Appl. Biomater. Funct. Mater.* **2015**, *13*, 43–60. [[CrossRef](#)] [[PubMed](#)]
15. Gandolfi, M.G.; Ciapetti, G.; Taddei, P.; Perut, F.; Tinti, A.; Cardoso, M.V.; Meerbeek, B.; Prati, C. Apatite formation on bioactive calcium-silicate cements for dentistry affects surface topography and human marrow stromal cells proliferation. *Dent. Mater.* **2010**, *26*, 974–992. [[CrossRef](#)]
16. Gandolfi, M.G.; Van Landuyt, K.; Taddei, P.; Modena, E.; Van Meerbeek, B.; Prati, C. Environmental Scanning Electron Microscopy Connected with Energy Dispersive X-ray Analysis and Raman Techniques to Study ProRoot Mineral Trioxide Aggregate and Calcium Silicate Cements in Wet Conditions and in Real Time. *J. Endod.* **2010**, *36*, 851–857. [[CrossRef](#)]
17. Gandolfi, M.G.; Taddei, P.; Modena, E.; Siboni, F.; Prati, C. Biointeractivity-related versus chemi/physisorption-related apatite precursor-forming ability of current root end filling materials. *J. Biomed. Mater. Res.* **2013**, *101*, 1107–1123. [[CrossRef](#)]
18. Taddei, P.; Tinti, A.; Gandolfi, M.G.; Rossi, P.L.; Prati, C. Vibrational study on the bioactivity of Portland cement-based materials for endodontic use. *J. Mol. Struct.* **2009**, *924–926*, 548–554. [[CrossRef](#)]

19. Gandolfi, M.G.; Taddei, P.; Tinti, A.; De Stefano Dorigo, E.; Prati, C. Alpha-TCP improves the apatite-formation ability of calcium-silicate hydraulic cement soaked in phosphate solutions. *Mater. Sci. Eng. C* **2011**, *31*, 1412–1422. [[CrossRef](#)]
20. Parirokh, M.; Torabinejad, M. Mineral trioxide aggregate: A comprehensive literature review—Part III: Clinical applications, drawbacks, and mechanism of action. *J. Endod.* **2010**, *36*, 400–413. [[CrossRef](#)] [[PubMed](#)]
21. Camilleri, J.; Gandolfi, M.G. Evaluation of the radiopacity of calcium silicate cements containing different radiopacifiers. *Int. Endod. J.* **2010**, *43*, 21–30. [[CrossRef](#)] [[PubMed](#)]
22. Sfeir, G.; Zogheib, C.; Patel, S.; Giraud, T.; Nagendrababu, V.; Bukiet, F. Calcium Silicate-Based Root Canal Sealers: A Narrative Review and Clinical Perspectives. *Materials* **2021**, *14*, 3965. [[CrossRef](#)] [[PubMed](#)]
23. Roy, M.; Bandyopadhyay, A.; Bose, S. Chapter 6—Ceramics in Bone Grafts and Coated Implants. In *Materials for Bone Disorders*; Bose, S., Bandyopadhyay, A., Eds.; Academic Press: Cambridge, MA, USA, 2017; pp. 265–314.
24. Keller, R.J. *The Sigma Library of FT-IR Spectra*; Sigma Chemical Company Inc.: St. Louis, MO, USA, 1986.
25. Hughes, T.L.; Methven, C.M.; Jones, T.G.J.; Pelham, S.E.; Fletcher, P.; Hall, C. Determining Cement Composition by Fourier Transform Infrared Spectroscopy. *Adv. Cem. Based Mater.* **1995**, *2*, 91–104. [[CrossRef](#)]
26. Ren, X.; Zhang, W.; Ye, J. FTIR study on the polymorphic structure of tricalcium silicate. *Cem. Concr. Res.* **2017**, *99*, 129–136. [[CrossRef](#)]
27. Phillippi, C.M.; Mazdiyasi, K.S. Infrared and Raman spectra of zirconia polymorphs. *J. Am. Ceram. Soc.* **1971**, *54*, 254–258. [[CrossRef](#)]
28. Hidalgo, A.; Petit, S.; Domingo, C.; Alonso, C.; Andrade, C. Microstructural characterization of leaching effects in cement pastes due to neutralisation of their alkaline nature Part I: Portland cement pastes. *Cem. Concr. Res.* **2007**, *37*, 63–70. [[CrossRef](#)]
29. Kuzmin, V.V.; Novikov, V.S.; Ustynyuk, Y.L.; Prokhorov, K.A.; Sagitova, E.A.; Nikolaeva, G.Y. Raman spectra of polyethylene glycols: Comparative experimental and DFT study. *J. Mol. Struct.* **2020**, *1217*, 128331. [[CrossRef](#)]
30. Potgieter-Vermaak, S.S.; Potgieter, J.H.; Van Grieken, R. The application of Raman spectrometry to investigate and characterize cement, Part I: A review. *Cem. Concr. Res.* **2006**, *36*, 656–662. [[CrossRef](#)]
31. Ibáñez, J.; Artús, L.; Cuscò, R.; Lòpez, A.; Menéndez, E.; Andrade, M.C. Hydration and carbonation of monoclinic C2S and C3S studied by Raman spectroscopy. *J. Raman Spectrosc.* **2007**, *38*, 61–67. [[CrossRef](#)]
32. Keramidas, V.G.; White, W.B. Raman Scattering Study of the Crystallization and Phase Transformations of ZrO₂. *J. Am. Ceram. Soc.* **1974**, *57*, 22–24. [[CrossRef](#)]
33. Torrén-Martín, D.; Fernández-Carrasco, L.; Martínez-Ramírez, S.; Ibáñez, J.; Artús, L.; Matschei, L. Raman Spectroscopy of anhydrous and Hydrated Calcium Aluminates and Sulfoaluminates. *J. Am. Ceram. Soc.* **2013**, *96*, 3589–3595. [[CrossRef](#)]
34. Black, L.; Breen, C.; Yarwood, J.; Deng, C.-S.; Phipps, J.; Maitland, G. Hydration of tricalcium aluminate (C3A) in the presence and absence of gypsum—studied by Raman spectroscopy and X-ray diffraction. *J. Mater. Chem.* **2006**, *16*, 1263–1272. [[CrossRef](#)]
35. Andersen, F.A.; Brecevic, L.; Beuter, G.; Dell’Amico, D.B.; Calderazzo, F.; Bjerrum, N.J.; Underhill, A.E. Infrared Spectra of Amorphous and Crystalline Calcium Carbonate. *Acta Chem. Scand.* **1991**, *45*, 1018–1024. [[CrossRef](#)]
36. Stepkowska, E.T.; Blanes, J.M.; Real, C.; Perez-Rodriguez, J.L. Hydration products in two aged cement pastes. *J. Therm. Anal. Calorim.* **2005**, *82*, 731–739. [[CrossRef](#)]
37. Chakrabarty, D.; Mahapatra, S. Aragonite crystals with unconventional morphologies. *J. Mater. Chem.* **1999**, *9*, 2953–2957. [[CrossRef](#)]
38. Taddei, P.; EModena, E.; ATinti, A.; FSiboni, F.; CPrati, C.; Gandolfi, M.G. Vibrational investigation of calcium silicate cements for endodontics in simulated body fluids. *J. Mol. Struct.* **2011**, *993*, 367–375. [[CrossRef](#)]
39. Lecomte, I.; Henrist, C.; Liégeois, M.; Maseri, F.; Rulmont, A.; Cloots, R. (Micro)-structural comparison between geopolymers, alkali-activated slag cement and Portland cement. *J. Eur. Ceram. Soc.* **2006**, *26*, 3789–3797. [[CrossRef](#)]
40. Carteret, E.T.C.; Dandeu, A.; Moussaoui, S.; Muhr, H.; Humbert, B.; Plasari, E. Polymorphism Studied by Lattice Phonon Raman Spectroscopy and Statistical Mixture Analysis Method. Application to Calcium Carbonate Polymorphs during Batch Crystallization. *Cryst. Growth Des.* **2009**, *9*, 807–812. [[CrossRef](#)]
41. Wehrmeister, U.; Jacob, D.E.; Soldati, A.L.; Loges, N.; Hägerb, T.; Hofmeister, W. Amorphous, nanocrystalline and crystalline calcium carbonates in biological materials. *J. Raman Spectrosc.* **2011**, *42*, 926–935. [[CrossRef](#)]
42. Hofmeister, A.M.; Wopenka, B.; Locock, A.J. Spectroscopy and structure of hibonite, grossite, and CaAl₂O₄: Implications for astronomical environments. *Geochim. Cosmochim. Acta* **2004**, *68*, 4485–4503. [[CrossRef](#)]
43. Nyquist, R.A.; Putzig, C.L.; Leugers, M.A. *The Handbook of Infrared and Raman Spectra of Inorganic Compounds and Organic Salts*; Academic Press: San Diego, CA, USA, 1997.
44. Dobal, B.S.; Katiyar, R.S.; Jiang, Y.; Guo, R.; Bhalla, A.S. Raman scattering study of a phase transition in tantalum pentoxide. *J. Raman Spectrosc.* **2000**, *31*, 1061–1065. [[CrossRef](#)]
45. Conjeaud, M.; Boyer, H. Some possibilities of Raman microprobe in cement chemistry. *Cem. Concr. Res.* **1980**, *10*, 61–70. [[CrossRef](#)]
46. Xu, G.; Aksay, I.A.; Grooves, J.T. Continuous crystalline carbonate apatite thin films. A biomimetic approach. *J. Am. Chem. Soc.* **2001**, *123*, 2196–2203. [[CrossRef](#)]
47. Wallace, V.M.; Dhupal, N.R.; Zehentbauer, F.M.; Kim, H.J.; Kiefer, J. Revisiting the Aqueous Solutions of Dimethyl Sulfoxide by Spectroscopy in the Mid- and Near-Infrared: Experiments and Car–Parrinello Simulations. *J. Phys. Chem. B* **2015**, *119*, 14780–14789. [[CrossRef](#)]

48. Martens, W.N.; Frost, R.L.; Kristof, J.; Klopogge, J.T. Raman spectroscopy of dimethyl sulphoxide and deuterated dimethyl sulphoxide at 298 and 77 K. *J. Raman Spectrosc.* **2002**, *33*, 84–91. [[CrossRef](#)]
49. Marble, C.B.; Xu, X.; Petrov, G.I.; Wang, D.; Yakovlev, V.V. New insights into a hydrogen bond: Hyper-Raman spectroscopy of DMSO-water solution. *Phys. Chem. Chem. Phys.* **2021**, *23*, 24047–24051. [[CrossRef](#)]
50. Siboni, F.; Taddei, P.; Zamparini, F.; Prati, C.; Gandolfi, M.G. Properties of BioRoot RCS, a tricalcium silicate endodontic sealer modified with povidone and polycarboxylate. *Int. Endod. J.* **2017**, *50*, 120–136. [[CrossRef](#)]
51. Baldi, J.V.; Bernardes, R.A.; Duarte MAOrdinola-Zapata, R.; Cavenago, B.C.; Moraes, J.C.; de Moraes, I.G. Variability of physicochemical properties of an epoxy resin sealer taken from different parts of the same tube. *Int. Endod. J.* **2012**, *45*, 915–920. [[CrossRef](#)]
52. Loushine, B.A.; Bryan, T.E.; Looney, S.W.; Gillen, B.M.; Loushine, R.J.; Weller, R.N.; Pashley, D.H.; Tay, F.R. Setting properties and cytotoxicity evaluation of a premixed bioceramic root canal sealer. *J. Endod.* **2011**, *37*, 673–677. [[CrossRef](#)]
53. Marciano, M.A.; Guimarães, B.M.; Ordinola-Zapata, R.; Bramante, C.M.; Cavenago, B.C.; Garcia, R.B.; Bernardineli, N.; Andrade, F.B.; Moraes, I.G.; Duarte, M.A. Physical properties and interfacial adaptation of three epoxy resin-based sealers. *J. Endod.* **2011**, *37*, 1417–1421. [[CrossRef](#)]
54. Demirci, G.K.; Kaval, M.E.; Kurt, S.M.; Serefoglu, B.; Güneri, P.; Hülsmann, M.; Caliskan, M.K. Energy-Dispersive X-Ray Spectrometry Analysis and Radiopacity of Five Different Root Canal Sealers. *Br. Dent. J.* **2021**, *32*, 1–11. [[CrossRef](#)] [[PubMed](#)]
55. Jung, G.Y.; Park, Y.J.; Han, J.S. Effects of HA released calcium ion on osteoblast differentiation. *J. Mater. Sci. Mater. Med.* **2010**, *21*, 1649–1654. [[CrossRef](#)] [[PubMed](#)]
56. Zamparini, F.; Siboni, F.; Prati, C.; Taddei, P.; Gandolfi, M.G. Properties of calcium silicate-monobasic calcium phosphate materials for endodontics containing tantalum pentoxide and zirconium oxide. *Clin. Oral Investig.* **2019**, *23*, 445–457. [[CrossRef](#)]
57. Siboni, F.; Taddei, P.; Prati, C.; Gandolfi, M.G. Properties of NeoMTA Plus and MTA Plus cements for endodontics. *Int. Endod. J.* **2017**, *50*, 83–94. [[CrossRef](#)]
58. Forni, M.; Bernardini, C.; Zamparini, F.; Zannoni, A.; Salaroli, R.; Ventrella, D.; Parchi, G.; Degli Esposti, M.; Polimeni, A.; Fabbri, P.; et al. Vascular Wall-Mesenchymal Stem Cells Differentiation on 3D Biodegradable Highly Porous CaSi-DCPD Doped Poly (α -hydroxy) Acids Scaffolds for Bone Regeneration. *Nanomaterials* **2020**, *29*, 243. [[CrossRef](#)]
59. Gandolfi, M.G.; Gardin, C.; Zamparini, F.; Ferroni, L.; Esposti, M.D.; Parchi, G.; Ercan, B.; Manzoli, L.; Fava, F.; Fabbri, P.; et al. Mineral-Doped Poly(L-lactide) Acid Scaffolds Enriched with Exosomes Improve Osteogenic Commitment of Human Adipose-Derived Mesenchymal Stem Cells. *Nanomaterials* **2020**, *29*, 432. [[CrossRef](#)]
60. Ho, C.C.; Fang, H.Y.; Wang, B.; Huang, T.H.; Shie, M.Y. The effects of Biodentine/polycaprolactone three-dimensional-scaffold with odontogenesis properties on human dental pulp cells. *Int. Endod. J.* **2018**, *51*, 291–300. [[CrossRef](#)]
61. Chiu, Y.C.; Fang, H.Y.; Hsu, T.T.; Lin, C.Y.; Shie, M.Y. The Characteristics of Mineral Trioxide Aggregate/Polycaprolactone 3-dimensional Scaffold with Osteogenesis Properties for Tissue Regeneration. *J. Endod.* **2017**, *43*, 923–929. [[CrossRef](#)]
62. Oliveira, I.R.; Andrade, T.L.; Jacobovitz, M.; Pandolfelli, V.C. Bioactivity of calcium aluminate endodontic cement. *J. Endod.* **2013**, *39*, 774–778. [[CrossRef](#)]
63. Gandolfi, M.G.; Taddei, P.; Siboni, F.; Modena, E.; Ciapetti, G.; Prati, C. Development of the foremost light-curable calcium-silicate MTA cement as root-end in oral surgery. Chemical-physical properties, bioactivity and biological behavior. *Dent. Mater.* **2011**, *27*, 134–157. [[CrossRef](#)]
64. Gandolfi, M.G.; Iacono, F.; Agee, K.; Siboni, F.; Tay, F.; Pashley, D.H.; Prati, C. Setting time and expansion in different soaking media of experimental accelerated calcium-silicate cements and ProRoot MTA. *Oral Surg. Oral Med. Oral Pathol. Oral Radiol. Endod.* **2009**, *108*, 39–45. [[CrossRef](#)] [[PubMed](#)]
65. Newbury, D.E. Mistakes encountered during automatic peak identification of minor and trace constituents in electron-excited energy dispersive X-ray microanalysis. *Scanning* **2009**, *31*, 91–101. [[CrossRef](#)] [[PubMed](#)]
66. Gallego, D.; Higuera, N.; Garcia, F.; Ferrel, N.; Hansford, D.J. Bioactive coatings on Portland cement substrates: Surface precipitation of apatite-like crystals. *Mater. Sci. Eng.* **2008**, *28*, 347–352. [[CrossRef](#)]
67. Zhao, W.; Wang, J.; Zhai, W.; Wang, Z.; Chang, J. The selfsetting properties and in vitro bioactivity of tricalcium silicate. *Biomaterials* **2005**, *26*, 6113–6121. [[CrossRef](#)]
68. Fujita, Y.; Yamamuro, T.; Nakamura, T.; Kotani, S.; Ohtsuki, C.; Kokubo, T. The bonding behavior of calcite to bone. *J. Biomed. Mater. Res.* **1991**, *25*, 991–1003. [[CrossRef](#)]
69. Coleman, N.J.; Nicholson, J.W.; Awosanya, K. A preliminary investigation of the in vitro bioactivity of white Portland cement. *Cem. Concr. Res.* **2007**, *37*, 1518–1523. [[CrossRef](#)]
70. Gandolfi, M.G.; Taddei, P.; Tinti, A.; De Stefano Dorigo, E.; Rossi, P.L.; Prati, C. Kinetics of apatite formation on a calcium-silicate cement for root-end filling during ageing in physiological-like phosphate solutions. *Clin. Oral Investig.* **2010**, *14*, 659–668. [[CrossRef](#)]
71. Sanchez, F.; Zhang, L. Molecular dynamics modeling of the interface between surface functionalized graphitic structures and calcium-silicate-hydrate: Interaction energies, structure, and dynamics. *J. Colloid Interface Sci.* **2008**, *323*, 349–358. [[CrossRef](#)]
72. Gandolfi, M.G.; Siboni, F.; Prati, C. Properties of a novel polysiloxane-guttapercha calcium silicate-bioglass-containing root canal sealer. *Dent. Mater.* **2016**, *32*, 113–126. [[CrossRef](#)]

-
73. Candeiro, G.T.; Correia, F.C.; Duarte, M.A.; Ribeiro-Siqueira, D.C.; Gavini, G. Evaluation of radiopacity, pH, release of calcium ions, and flow of a bioceramic root canal sealer. *J. Endod.* **2012**, *38*, 842–845. [[CrossRef](#)]
 74. Sanz, J.L.; López-García, S.; Rodríguez-Lozano, F.J.; Melo, M.; Lozano, A.; Llena, C.; Forner, L. Cytocompatibility and bioactive potential of AH Plus Bioceramic Sealer: An in vitro study. *Int. Endod. J.* **2022**, *55*, 1066–1080. [[CrossRef](#)]

4. *Clinical Outcome and Biocompatibility of Innovative CaSi-based Obturation Techniques.*

Several obturation techniques combining different types of gutta-percha and root canal sealers have been proposed over time. Regardless of the techniques used, the ideal obturation of the endodontic space is the one that ensures a perfect seal of the canal using biologically acceptable material for the periapical tissues. It should show no voids, have uniform radiopacity, and respect the anatomical morphologies of the root regarding its taper and curvature.

Among these techniques, one of the most used is the single cone technique because it is simple and intuitive to learn. However, it is partly criticized due to some limitations. It is not recommended for canals with an oval section, due to its inability to control the filling of the irregularities of the root canal and the consequent possibility of leaving many gaps between the sealer and the gutta-percha, especially in the vestibular and lingual areas.

To overcome the limitations of the single cone technique and ensure a better three-dimensional seal over time, warm techniques have been proposed ([Schilder et al. 1967](#)). One of the most used today is the carrier-based technique, which rapidly gained popularity due to its swift learning curve, ease of application (even by less experienced operators), and being less time-consuming ([Pirani et al. 2019](#)). *In vitro* studies have shown an almost complete absence of porosity, gaps, and voids in the root canal, compared to the continuous wave of condensation and warm lateral compaction. The primary application is in curved canals or difficult cases where it proves much easier to execute than other techniques.

Not all sealers are suitable to be used with this technique. Zinc oxide eugenol-based sealers and polymethyl siloxane sealers are not recommended for warm obturation techniques. Zinc oxide eugenol sealers have shown a reduced setting time due to the high temperature of the cone, leading to the presence of voids and irregularities in the obturation. Furthermore, once the sealer is set, it prevents the gutta-percha from reaching the apex, resulting in a short obturation.

One of the most used sealers associated with these techniques (both single cone and carrier-based technique) is the epoxy resin-based sealer such as AH Plus (AH Plus, Dentsply, Konstanz, Germany) thanks to its properties. This sealer is mainly composed of epoxy resins and contains calcium tungstate and zirconium oxide as radiopacifiers. It has shown moderate cytotoxicity, derived from the release of amines only during the initial phases of polymerization. After setting, the sealer exhibits excellent biocompatibility ([Jung S et al. 2018](#)). Moreover, it has optimal

marginal sealing capabilities and uniform fluidity. Furthermore, it also has high radiopacity, exceeding 11mmAl (almost exclusive to this sealer), that allows many details (such as the filling of the lateral canals, or the sealer extrusion) to be highlighted in X-rays. When used in a warm technique, it shows increased fluidity. In fact, heat application makes the sealer more fluid, allowing excellent flow of the gutta-percha/sealer system to the apex and into the lateral and accessory canals (Qu W et al. 2016; Donnermeyer D et al. 2020). Potential challenges include the possibility of sealer extrusion, especially if excessive pressure is applied or too much sealer is used. Another advantage is its ability to adhere to the canal walls (even in the presence of a smear layer) (Tagger M et al. 2002), the low solubility, and the low film thickness (Tyagi S et al. 2013).

The most remarkable limitation of this sealer is its hydrophobicity, with the impossibility of being used in the presence of fluids and blood inside the canal which must therefore be dry; otherwise, an irregular polymerization reaction occurs, leading to porosity, marginal gaps, and the absence of the desired endodontic seal. After setting, it shows a low shrinkage and has no bactericidal effect (Kooanantkul C et al 2023). For this reason, it does not fulfill Grossman's ideal root canal sealer properties (Grossman LI 1978).

CaSi-based sealers, as discussed in the previous chapter, have a broad spectrum of clinical applications thanks to their unique properties. These materials can set in the presence of moisture and blood and can expand (instead of shrinking) inside the canal after setting, sealing the discrepancies and filling voids between gutta-percha and the dentinal walls. Previous CaSi cements (such as MTA) proved to be osteoconductive and in some cases osteoinductive towards a great number of mineralizing cells (osteoblasts) and different populations of stem cells, including bone marrow stem cells (Gandolfi et al. 2011), human periodontal ligament stem cells (Giacomino et al. 2021) and human periapical cyst derived stem cells (Tatullo et al. 2019). This role of recently introduced premixed bioceramic based sealers has currently been investigated also towards vascular stem cells populations (unpublished data). The presence of vascular stem cells in the periapical area has been demonstrated in a large number clinical and histological studies (Leonardi et al. 2003; Virtej et al. 2013) and represent an interesting source of stem cells that could attach, proliferate on CaSi based sealers and finally, differentiate in mature osteoblasts. This property could result in a large number of patients where bone remodeling is slowed or compromised. For examples CaSi-based sealers can be used in difficult and medically compromised situations where the preservation of the tooth is strongly

recommended, such as in patients taking medication that affects bone remodeling mechanisms ([Zamparini et al. 2021](#)).

These characteristics make them suitable to be used as root canal sealers for cold obturation techniques, overcoming the limitations of the traditional single cone technique.

On the other hand, several issues were identified when used with warm techniques. A recent investigation demonstrated the rapid contraction of the CaSi-based sealer and an alteration of their mechanical properties when heat was applied ([Hadis & Camilleri 2020](#)). After heat application (100 °C for 60 seconds), the calcium silicate sealer showed a significant decrease in its flow and setting time ([Heran J et al. 2019](#)). That is the reason why, in the past, this class of sealers was never used with warm technique. However, the temperature inside the canal rarely reaches such high values for a long time. A recent study showed that the temperature in the endodontic canal during the execution of warm techniques reaches an average of 60°C for only a few seconds ([Donnermeyer D et al. 2018](#)).

When used with CaSi-based sealer, the single cone use and application are slightly different: in the traditional one, it was recommended to fill the root canal with a cone of gutta-percha that fit perfectly inside the canal and minimize the use of sealer thickness due to its shrinkage after setting. Now, this technique places more emphasis on the sealer that serves as a root canal filler due to its property to expand after setting.

To date, few clinical studies (and with a short follow-up) analyze the outcome of this technique. A recent retrospective study showed a success rate of about 90% at 3 years follow-up ([Chybowski et al. 2018](#)). In a prospective study, a traditional warm compaction technique with a resin sealer was compared to a single cone with a CaSi-based sealer. The 12-month data showed that both techniques had high and comparable success and survival rates ([Zavattini et al. 2020](#)). The use of CaSi-based sealer seems to reduce post-operative pain, although further studies are needed to reach a definitive conclusion ([Graunaite I et al. 2018](#)). A randomized controlled clinical trial assessed the short-term (3 months) clinical effectiveness and post-operative pain of a SC CaSi-based sealer vs SC epoxy resin-based sealer and reported no significant difference between the techniques in terms of post-operative pain and healing process ([Song M et al. 2022](#)).

Using CaSi-based sealer with a warm obturation technique potentially offers a wide range of advantages. It would allow an effective seal and the penetration of the heated sealer into the dentinal tubules. Reconsidering the use of the new generation of premixed CaSi-based sealer

with a warm technique such as the carrier-based could offer an interesting new perspective with potential new clinical advantages. Manufacturers recently developed a new category of premixed CaSi based sealers that may be used with a warm technique without any alterations. Despite their promising characteristics, due to the recent availability on the market, a limited number of clinical studies have been conducted. A recent clinical study with 24 months follow-up compared the use of carrier-based with epoxy resin and CaSi-based sealer and reported no significant difference in healing and survival outcome among the two filling groups ([Zamparini et al 2023](#)). Another clinical study with a follow-up of at least 18 months compared 4 different kinds of CaSi-based sealers used with warm gutta-percha obturation techniques. The overall success rate was 99% with 73% healed and 25.7% healing, and 0.95% not healed ([Pontoriero et al. 2023](#)). Another prospective study with 12 months follow-up reported 82% of healed teeth while 18% were healing ([Spinelli et al. 2023](#)).

A potential event to take into consideration using this technique is the increased potential of sealer extrusion, which is a common scenario in clinical practice. The extrusion of many traditional sealers can be associated with post-operative pain and neurogenic inflammation ([Ruparel NB et al. 2014](#)). However, several clinical studies have shown that the extrusion of these sealers is not associated with a higher percentage of long-term failure ([Ricucci D et al. 2016](#); [Martins JFB et al. 2023](#)). This can be justified because the resin-based and the oxide eugenol-based sealers remain bioinert after setting. On the other hand, the (controlled) extrusion of calcium silicate-based sealers can have a positive clinical rationale. As previously discussed, their unique bioactive, osteoconductive, and osteoinductive properties can be particularly suitable in the presence of large periapical lesions. Interestingly, it is noted that periapical extrusion of these materials tends to be resorbed over time. Unfortunately, only short-term follow-up studies are available now in the literature ([Chybowski et al. 2018](#); [Zamparini et al. 2023](#); [Spinelli et al. 2023](#)). Longer follow-up of at least 4 years, as suggested by ESE ([ESE guidelines 2006](#)), might show and explain a possible link between sealer resorption and the healing of a periapical bone defect.

The following papers report the outcome of two different clinical studies with a follow-up of 12 and 24 months. A new technique that involves the use of a warm carrier-based technique associated with the new generation of premixed calcium silicate-based sealers was proposed. Both studies have been approved by the ethical committee.

A paper reporting the outcome at 5 years follow-up of patients with medically compromised situations such as patients taking medication that affects bone remodeling mechanisms (Bisphosphonate Therapy) is also reported. A new approach to endodontically treat patients where extractions of teeth is not recommended have been proposed.

REFERENCES

- 1) Chybowski, E.A.; Glickman, G.N.; Patel, Y.; Fleury, A.; Solomon, E.; He, J. Clinical Outcome of Non-Surgical Root Canal Treatment Using a Single-cone Technique with Endosequence Bioceramic Sealer: A Retrospective Analysis. *J. Endod.* 2018, 44, 941–945
- 2) Donnermeyer D, Urban K, Bürklein S, Schäfer E. Physico-chemical investigation of endodontic sealers exposed to simulated intracanal heat application: epoxy resins and zinc oxide-eugenols. *Int Endod J* 2020;53:690-7.
- 3) Donnermeyer D, Schäfer E, Bürklein S. Real-time intracanal temperature measurement during different obturation techniques. *J Endod* 2018;44:1832-6.
- 4) European Society of Endodontology. Quality guidelines for endodontic treatment: consensus report of the European Society 446 of Endodontology. *Int Endod J.* 2006;39:921-30.
- 5) Gandolfi, M.G.; Shah, S.N.; Feng, R.; Prati, C.; Akintoye, S.O. Biomimetic Calcium-Silicate Cements Support Differentiation of Human Orofacial Mesenchymal Stem Cells. *J Endod.* 2011b;37:1102-1108.
- 6) Graunaite I, Skucaite N, Lodiene G, Agentiene I, Machiulskiene V. Effect of resin-based and bioceramic root canal sealers on postoperative pain: a split-mouth randomized controlled trial. *J Endod* 2018;44:689-93.
- 7) Grossman LI. *Endodontic Practice*: Lea & Febiger; 1978
- 8) Hadis M, Camilleri J. Characterization of heat resistant hydraulic sealer for warm vertical obturation. *Dent Mater.* 2020 Sep;36:1183-1189.
- 9) Heran J, Khalid S, Albaaj F, Tomson PL, Camilleri J. The single cone obturation technique with a modified warm filler. *J Dent* 2019;89:103181.
- 10) Jung S, Sielker S, Hanisch MR, Libricht V, Schäfer E, Dammachke T. Cytotoxic effects of four different root canal sealers on human osteoblasts. *PLoS One* 2018;13:e0194467.

- 11) Kooanantkul C, Shelton RM, Camilleri J. Comparison of obturation quality in natural and replica teeth root-filled using different sealers and techniques. *Clin Oral Investig.* 2023 May;27(5):2407-2417.
- 12) Leonardi R, Caltabiano M, Pagano M, Pezzuto V, Loreto C, Palestro G. Detection of vascular endothelial growth factor/ vascular permeability factor in periapical lesions. *J Endod.* 2003;29:180-183.
- 13) Martins JFB, Scheeren B, van der Waal SV. The Effect of Unintentional AH-Plus Sealer Extrusion on Resolution of Apical Periodontitis After Root Canal Treatment and Retreatment- A Retrospective Case-control Study. *J Endod.* 2023;49:1262-1268
- 14) Pirani C, Zamparini F, Peters OA, Iacono F, Gatto MR, Generali L, Gandolfi MG, Prati C. The fate of root canals obturated with Thermafil: 10-year data for patients treated in a master's program. *Clin Oral Investig.* 2019;23:3367-3377.
- 15) Pontoriero DIK, Ferrari Cagidiaco E, Maccagnola V, Manfredini D, Ferrari M. Outcomes of Endodontic-Treated Teeth Obturated with Bioceramic Sealers in Combination with Warm Gutta-Percha Obturation Techniques: A Prospective Clinical Study. *J Clin Med.* 2023;12:2867
- 16) Qu W, Bai W, Liang YH, Gao XJ. Influence of warm vertical compaction technique on physical properties of root canal sealers. *J Endod* 2016;42:1829-33.
- 17) Ruparel NB, Ruparel SB, Chen PB, Ishikawa B, Diogenes A. Direct effect of endodontic sealers on trigeminal neuronal activity. *J Endod.* 2014 May;40(5):683-7
- 18) Ricucci D, Rôças IN, Alves FR, Loghin S, Siqueira JF Jr. Apically extruded sealers: fate and influence on treatment outcome. *J Endod* 2016;42:243-9.
- 19) Schilder H. Filling root canals in three dimensions. *Dent Clin North Am.* 1967 Nov:723-44.
- 20) Song M, Park MG, Kwak SW, Kim RH, Ha JH, Kim HC. Pilot Evaluation of Sealer-Based Root Canal Obturation Using Epoxy-Resin-Based and Calcium-Silicate-Based Sealers: A Randomized Clinical Trial. *Materials (Basel).* 2022 Jul 25;15:5146
- 21) Spinelli, A, Zamparini, F, Lenzi, J, Gandolfi MG, Prati C. Clinical Evaluation of a Novel Premixed Tricalcium Silicate Containing Bioceramic Sealer Used with Warm Carrier-Based Technique: A 12-Month Prospective Pilot Study. *Appl. Sci.* 2023, 13, 11835.
- 22) Tagger M, Tagger E, Tjan AH, Bakland LK. Measurement of adhesion of endodontic sealers to dentin. *J Endod* 2002;28:351-4.
- 23) Tyagi S, Mishra P, Tyagi P. Evolution of root canal sealers: An insight story. *Eur J Gen Dent* 2013;2:199-218

- 24) Virtej A, Løes SS, Berggreen E, Bletsa A. Localization and signaling patterns of vascular endothelial growth factors and receptors in human periapical lesions. *J Endod.* 2013;39:605-11.
- 25) Zamparini F, Pelliccioni GA, Spinelli A, Gissi DB, Gandolfi MG, Prati C. Root canal treatment of compromised teeth as alternative treatment for patients receiving bisphosphonates: 60-month results of a prospective clinical study. *Int Endod J* 2021;54:156-71.
- 26) Zamparini F, Spinelli A, Cardinali F, Ausiello P, Gandolfi MG, Prati C. The Use of Premixed Calcium Silicate Bioceramic Sealer with Warm Carrier-Based Technique: A 2-Year Study for Patients Treated in a Master Program. *J Funct Biomater.* 2023;14:164.
- 27) Zavattini A, Knight A, Foschi F, Mannocci F. Outcome of root canal treatments using a new calcium silicate root canal sealer: a non-randomized clinical trial. *J Clin Med* 2020;9:782.

Article

The Use of Premixed Calcium Silicate Bioceramic Sealer with Warm Carrier-Based Technique: A 2-Year Study for Patients Treated in a Master Program

Fausto Zamparini ^{1,2}, Andrea Spinelli ¹, Filippo Cardinali ³, Pietro Ausiello ⁴, Maria Giovanna Gandolfi ² and Carlo Prati ^{1,5,*}

¹ Endodontic Clinical Section, Dental School, Department of Biomedical and Neuromotor Sciences, University of Bologna, 40125 Bologna, Italy

² Laboratory of Green Biomaterials and Oral Pathology, Dental School, Department of Biomedical and Neuromotor Sciences, University of Bologna, 40125 Bologna, Italy

³ Private Practice, 60123 Ancona, Italy

⁴ School of Dentistry, University of Naples Federico II, 80131 Naples, Italy

⁵ Dean Master in Endodontics, Dental School, University of Bologna, Via San Vitale 59, 40125 Bologna, Italy

* Correspondence: carlo.prati@unibo.it

Abstract: Background: Recently several calcium silicate flowable sealers have been introduced as endodontic materials for the root canal. This clinical study tested the use of a new premixed calcium silicate bioceramic sealer in association with the Thermafil warm carrier-based technique (TF). Epoxy-resin-based sealer with the warm carrier-based technique was the control group. Methodology: Healthy consecutive patients (n = 85) requiring 94 root canal treatments were enrolled in this study and assigned to one filling group (Ceraseal-TF n = 47, AH Plus-TF n = 47) in accordance with operator training and best clinical practice. Periapical X-rays were taken preoperatively, after root canal filling and after 6, 12 and 24 months. Two evaluators blindly assessed the periapical index (PAI) and sealer extrusion in the groups (k = 0.90). Healing rate and survival rate were also evaluated. Chi-square tests was used to analyze significant differences between the groups. Multilevel analysis was performed to evaluate the factors associated with healing status. Results: A total of 89 root canal treatments in 82 patients were analyzed at the end-line (24 months). The total drop-out was 3.6% (3 patients; 5 teeth). A total of 91.1% of healed teeth (PAI 1-2) was observed in Ceraseal-TF, with 88.6% in AH Plus-TF. No significant difference was observed on healing outcome and survival among the two filling groups ($p > 0.05$). Apical extrusion of the sealers occurred in 17 cases (19.0%). Of these, 6 occurred in Ceraseal-TF (13.3%) and 11 in AH Plus-TF (25.0%). Three Ceraseal extrusions were radiographically undetectable after 24 months. All the AH Plus extrusions did not change during the evaluation time. Conclusions: The combined use of the carrier-based technique and premixed CaSi-based bioceramic sealer showed clinical results comparable with carrier-based technique and epoxy-resin-based sealer. The radiographical disappearance of apically extruded Ceraseal is a possible event in the first 24 months.

Keywords: carrier-based obturation; bioceramic sealers; calcium-silicate-based root canal sealer; calcium silicates; calcium silicate cements; bioceramics; periapical healing; apical extrusion; premixed CaSi; flowable CaSi; gutta-percha carrier endodontic



Citation: Zamparini, F.; Spinelli, A.; Cardinali, F.; Ausiello, P.; Gandolfi, M.G.; Prati, C. The Use of Premixed Calcium Silicate Bioceramic Sealer with Warm Carrier-Based Technique: A 2-Year Study for Patients Treated in a Master Program. *J. Funct. Biomater.* **2023**, *14*, 164. <https://doi.org/10.3390/jfb14030164>

Academic Editor: Anderson de Oliveira Lobo

Received: 20 December 2022

Revised: 17 February 2023

Accepted: 10 March 2023

Published: 18 March 2023



Copyright: © 2023 by the authors. Licensee MDPI, Basel, Switzerland. This article is an open access article distributed under the terms and conditions of the Creative Commons Attribution (CC BY) license (<https://creativecommons.org/licenses/by/4.0/>).

1. Introduction

Calcium silicate cements (CaSi) were introduced in clinical use more than twenty years ago as root-end filling materials for their hydraulic properties [1,2].

Afterwards, thanks to the continuous modification of their chemical composition and mechanical properties, CaSi cements have been proposed as sealers for cold obturation techniques [3–5]. Recently, the formulation of these materials (now named “bioceramics”)

changed from powder–liquid to premixed, flowable, “ready to use materials” [6–10]. Several CaSi-based (i.e., mainly containing CaSi particles) and CaSi-containing (i.e., containing minor amounts of CaSi) sealers are now available.

Ceraseal is a premixed CaSi-based bioceramic sealer which includes tricalcium silicate (20–30%) and dicalcium silicate (1–10%) as bioactive components. Zirconium dioxide is the radiopacifier (45–50%) [11]. The chemical–physical properties have been investigated in only two studies [11,12]. These studies reported lower radiopacity, lower setting time and similar flowability when compared to AH Plus [11,12]. The ability to release calcium and to alkalize the environment was reported in one recent *in vitro* study [11]. These properties appear attractive for their clinical use in warm filling techniques, such as the warm carrier-based gutta-percha technique.

The clinical advantages of the warm carrier-based gutta-percha technique are well documented, including the easiness of the use, short learning curve, reliability in obtaining technical results [12–15] and adequate clinical results [15–18]. Traditionally, warm procedures such as carrier-based ones are associated with the use of epoxy-resin-based sealers [13]. Previous studies on carrier-based techniques reported success rates ranging from 81 to 96% after 3–5 years [15,16,18,19]. One of the drawbacks of the warm carrier-based technique is the higher risk of sealer extrusion in the periapical bone area [16,18]. In this context, the use of a CaSi-based bioceramic sealer may be clinically attractive in case of periapical extrusions. Clinical data on CaSi-based sealers used with cold filling techniques have been reported in recent short-term studies (12 months), reporting high percentages of success [20–22]. No clinical study reported the use of Ceraseal with warm carrier-based techniques.

This clinical study analyzed the use of a new premixed CaSi-based bioceramic sealer in association with the warm carrier-based technique. Epoxy-resin-based sealer with the warm carrier-based technique was the control group. The null hypothesis was that both filling techniques and sealers provide a similar outcome after 24 months.

2. Materials and Methods

2.1. Study Design and Sample

This prospective cohort study was conducted between May 2019 and March 2022. The patients were treated in the Endodontic Clinical Section, Dental School, University of Bologna. Patients were treated by a pool of postgraduate master students in accordance with standardized protocols and under the strict supervision of the experienced tutors of the master degree. The study was approved by the local ethical committee as a prospective cohort study (OUTENDOPROSP; CE 20079).

All patients were treated according to the principles established by the Declaration of Helsinki as modified in 2013 [23]. Before enrolment, written and verbal information were given by the clinical staff and each patient gave their written consent according to the above-mentioned principles. An additional signed informed consent was obtained from all patients concerning the acceptance of the treatment plan and to follow the hygiene program. This study was designed according to the STROBE checklist [24] and to the guidelines published by Dodson in 2007 [25].

2.2. Sample Size

The sample size was estimated before the recruitment of patients. The primary outcome was the survival status of teeth after root canal treatment with 2 different filling techniques. We assumed a 24-month survival rate of 0.80–0.90, according to previous studies [15,16]. Accepting a probability of a non-significant decrease in endodontic survival rate of 0.10 for patients whose teeth were filled with flowable premixed CaSi-based bioceramic sealer, we calculated that to test the null hypothesis of the equality of treatment at $\alpha = 0.05$ with 80% power, a total of 40 teeth per group was considered sufficient. This number was increased to 47 per group (94 root canal treatments) to compensate for losses during follow-up.

Table 1 summarizes the criteria for the inclusion in the clinical protocol. Exclusion criteria are reported in Table 2.

Table 1. Inclusion criteria.

<ul style="list-style-type: none"> ✓ Aged 18–75 years ✓ Healthy status (ASA 1 or 2) ✓ No use of antiresorptive or antiangiogenic drug ✓ Needing one or more root canal treatments

Table 2. Exclusion criteria.

<ul style="list-style-type: none"> ✓ ASA > 3 ✓ Lack of occlusal contacts ✓ Heavy smoking (>15 cigarettes/day) ✓ Pregnancy or breast feeding ✓ Teeth with fewer than 2 walls of structural integrity ✓ Any pathology that could compromise bone healing or the immune response ✓ Malignant disease directly involving the jaws ✓ Exposure to radiation therapy focused on the head and neck region

Patient enrolment started in May 2019 and ended in February 2020. During this period, 129 patients went in the endodontic clinical section in need of root canal treatment. Of these, 17 were excluded as unable to attend to regular follow-up examinations, 8 for geographical location (patients from other cities), 3 for presenting with multiple fixed rehabilitations, 1 for medical conditions, 15 for a tooth with insufficient structural integrity or for the tooth being considered hopeless (Figure 1).

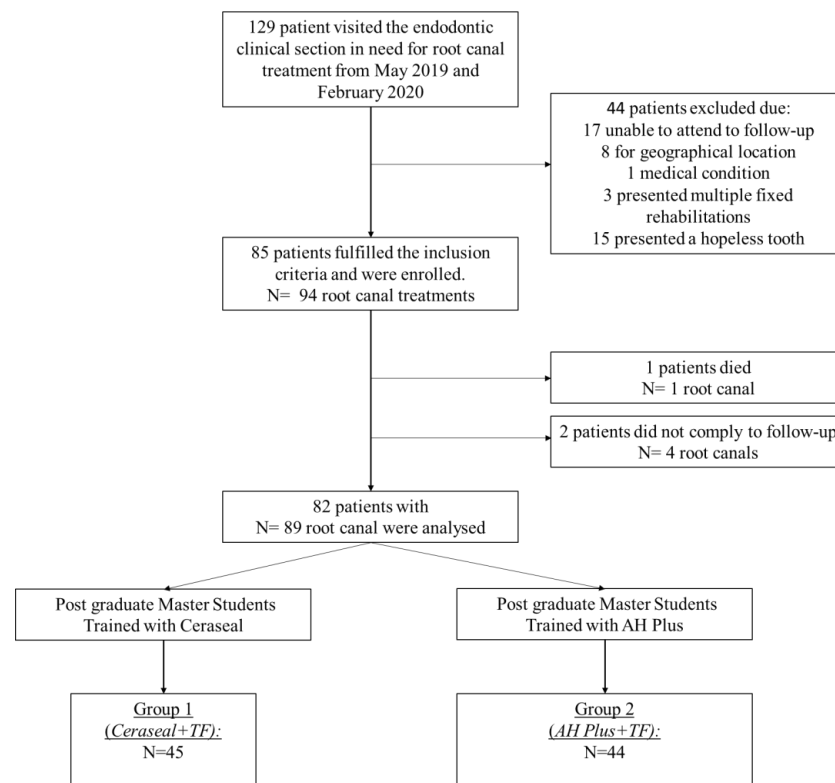


Figure 1. Flow chart of the study, patient enrolment and group constitution.

2.3. Root Canal Treatment Procedures

Root canal treatments adhered to a standardized operative protocol. The procedures were made under local anesthesia (Carboplyne 30 mg/mL Dentsply, Germany) and rubber dam isolation.

For primary root canal treatment, a straight-line access was prepared using a diamond bur mounted on high-speed water-cooled hand-pieces (Cefla, Imola, Italy). Working length (WL) was determined at 0.5 mm from the radiographic apex with periapical radiographs and an electronic apex locator (Root ZX, Morita Europe, Dietzenbach, Germany). Root canals were first pre-flared with K-file instrumentation up to #15. Then, a series of NiTi instruments were used to shape the canals (Mtwo, VDW, Germany or Rotate, VDW, Munchen, Germany). During the instrumentation, 5 mL of 5% NaOCl (Nicolor 5, OGNA, Muggiò, Italy) were used as root canal irrigant. In the presence of calcified root canals, 3.0 mL of 10% EDTA solutions was used as a calcium chelating agent. A final irrigation of 2.0 mL sterile water was made before root canal filling procedures [26–28]. No intracanal medication was placed in accordance with previous studies [26,29].

Secondary root canal treatments were performed using reciprocating NiTi instrumentation (Reciproc Blue, VDW, Munchen, Germany) and ultrasonic tips (StartX Dentsply Maillefer, Ballaigues, Switzerland).

An initial pathway was created with ultrasonic tips to approximately 4 mm in depth in the gutta-percha. Reciproc Blue #25 was activated with a Silver Reciproc Endomotor (VDW, Germany) using the “Reciproc All” program and gently inserted into the pathway and pushed to remove the coronal part of gutta-percha [30]. The instrument was then removed, and the material entrapped among the instrument threads was removed using a sterile sponge. The working length was established at the apical constriction after the removal of filling debris using periapical radiographs and an electronic apex locator (Root ZX, Morita Europe, Dietzenbach, Germany).

Then, an apical enlargement was performed using Reciproc Blue #40 that was gently forced to the apex, avoiding excessive pressure on the root canal wall.

During the instrumentation, 5 mL of 5% NaOCl (Nicolor 5, OGNA, Muggiò, Italy) were used as the root canal irrigant. In the presence of calcified root canals, 3.0 mL of 10% EDTA solutions was used as a chelating agent. A final irrigation of 2.0 mL sterile water was made before the root canal filling procedures [26,27]. When necessary, a dental surgery microscope (Pico, Zeiss, Germany) was used to detect the access to root canal orifices and to identify the presence of residual filling materials.

2.4. Root Canal Filling Techniques and Filling Group Constitution

The premixed CaSi-based bioceramic sealer (Ceraseal, MetaBiomed, Cheongju, Republic of Korea) was used in association with the warm carrier-based technique (Thermafil, Dentsply, Konstanz, Germany). The sealer contained tricalcium silicate (20–30%), dicalcium silicate (1–10%), tricalcium aluminate (1–10%), zirconium dioxide (45–50%) and thickening agents [11]. Epoxy-resin-based sealer (AH Plus, Dentsply, Konstanz, Germany) in association with the warm carrier-based technique was used as a clinical control.

The root canal filling treatments were performed by 2 different operator groups previously trained for only one technique. Before the start of the study, (February–April 2019) post-graduate operators (n = 12) of the Master Program in Endodontics were randomly assigned to receive a full training course on the clinical use of the warm carrier-based technique with Ceraseal (Ceraseal-TF) or the use of the carrier-based technique with AH Plus (AH Plus-TF).

In both filling groups, the carrier was pre-heated using a dedicated obturation oven (Thermaprep obturator oven, Dentsply, Konstanz, Germany)

Ceraseal-TF (Ceraseal with Thermafil): Ceraseal was applied with a K-file #20 inserted into the canal to reach the WL–3 mm and gently moved around the root canal walls. Pre-heated carrier was inserted in the canal at WL–0.5 mm. The carrier excess was removed with a round bur.

AH Plus-TF (AH Plus with Thermafil): AH Plus was prepared, mixed and immediately inserted into the root canal using a K-file #20 to reach the WL–3 mm and gently moved around the root canal walls. Pre-heated carrier was inserted in the canal at WL–0.5 mm. The carrier excess was removed with a round bur.

Finally, each filled root canal was sealed by a small cotton pellet and a hygroscopic radiopaque temporary restoration (Coltosol, Coltene, Switzerland).

2.5. Tooth Restoration

The post-endodontic restoration protocol was similar in the 2 groups. Two weeks after root canal filling, the temporary restoration was removed using ultrasonic tips, and crown was restored under rubber dam isolation. Self-etching dentinal bonding agent primer and bonding (Clearfil SE BOND, Kuraray, Osaka, Japan) were applied, photo-cured (Elipar 3M ESPE, St. Paul, MN, USA) for 30 s and layered by flowable (G-Aenial Flow, GC Corporation, Tokyo, Japan) and composite (G-Aenial, GC Corporation) resins. The composite was incrementally applied with 1.0 mm layers and photo-cured for 30 s. All definitive restorations were occlusally loaded. No post was applied in any cases.

When indicated, provisional and definitive prosthetic rehabilitations were performed after approx. 6 months or later from root canal fillings.

2.6. Radiological Evaluation

Periapical radiographs were taken after the root canal filling using a parallel technique. The following parameters were used: the target-film distance was approx. 30 cm, with 0.41 s exposure at 70 kV and 8 mA. The radiographs were developed in a standard developer unit at 25 °C, (Euronda s.p.a., Vicenza, Italy), with 12 s developing time and 25 s fixing time, according to the manufacturer instructions. Patients were asked to undergo a new X-ray, when these characteristics were not fulfilled.

The filling was considered “adequate” when the carrier was detected at 0–1.0 mm from the radiological apex. Overfilling and short filling were recorded.

Each patient was monitored at 6 (T6), 12 (T12) and 24 (T24) months follow-up by trained operators during a routine hygiene appointment. X-rays were digitalized using a slide scanner with a mean resolution of 1000 dpi and a magnification factor of $\times 20$.

The periapical index (PAI) [31] was used to score the preoperative diagnosis and the endpoint evaluations. PAI was evaluated in single blind by two additional operators (who did not participate in the root canal treatment) at baseline, at T6, T12 and T24 after root canal treatment. The presence of sealer extrusion was recorded and measured (in mm on the long axis diameter) on each periapical X-ray using open-source software (Image J, Bethesda, MD, USA). According to the long axis diameter, extrusions were categorized into 4 groups: 0 mm, 0.1–1.0 mm, 1.1–3.0 mm and >3 mm.

PAI calibration was performed using well-defined instructions and periapical radiographs with different periapical lesion scores (weighted kappa value, $k = 0.90$ for intra-operator assessment and $k = 0.90$ for inter-operator assessment).

2.7. Definition of Success and Survival Criteria

Teeth were defined as *healed* if they demonstrated no signs of periapical lesion (PAI 1-2) and no other clinical signs of symptoms (pain, mobility, fistula, swelling). These teeth defined the success rate [26].

The *endodontic lesion* group was defined when periapical radiolucency (PAI score ≥ 3) was detected during follow-up. A subdivision was made to discriminate between healing or stable lesions (improved or stable PAI during the follow-up) or worsened lesions (improved PAI during the follow-up)

The total of *healed* teeth and *endodontic lesion* teeth constituted the survival rate of the study [26]. The cause of extractions during the follow-up was recorded in a spreadsheet.

2.8. Statistical Analysis

Analyses were performed using Stata 17 software (StataCorp LLC, College Station, TX, USA). Chi-squared and Fisher exact tests were used to evaluate differences in the parameter distribution between the 2 filling groups. Preoperative parameters were age (<30 vs. 30–55 vs. >55 years), gender (female vs. male), tooth location (anterior vs. premolar vs. molar) and pre-operative PAI (1-2 vs. 3-5). Intraoperative parameters were endodontic treatment (primary treatment vs. secondary treatment), obturation quality (underfilled vs. adequate filling vs. overfilled), sealer extrusion (yes/no) and diameter of extrusion (0 mm vs. 0.1–1.0 mm vs. 1.1–3.0 mm vs. >3.0 mm). The post-operative parameter was definitive restoration (composite vs. crown). Multilevel mixed-effect logistic regression was performed to determine the parameters related to healed status. This outcome measure was dichotomous as healed status included all teeth that did not present a periapical lesion after 24 months (PAI score 1-2) while the *endodontic lesion group* (non-healed) included all teeth that revealed a periapical lesion after 24 months (PAI score 3-5).

The analysis was carried out at patient and tooth level. Age and gender were set as person-specific fixed effects, while clinical parameters (filling technique, tooth location, diagnosis, initial PAI, endodontic treatment, obturation quality, sealer extrusion, diameter of extrusion and definitive restoration) were set as tooth-specific random effects. The clustering effect within patients was considered and estimates of coefficient standard errors were adjusted using a robust estimator. Statistical significance was previously set at 0.050.

3. Results

3.1. Demographic Information

A total of 85 patients were initially enrolled with 94 root canal treatments. Total drop-out consisted of three patients with five root canal treatments. At the end-line, 82 patients with 89 root canal treatments were analyzed.

Information of preoperative, intraoperative and postoperative parameters between the two obturation groups is reported in Table 3. The two groups were homogeneous and did not significantly differ in almost all parameters ($p > 0.05$), with the only exception being age ($p = 0.020$, Ceraseal-TF included a higher percentage of filled teeth in patients younger than 30 years) and sealer extrusions ($p = 0.040$, Ceraseal-TF included a lower percentage of root canal teeth with sealer extrusions).

3.2. Outcome Measures

Cumulative 24-month survival rate was 97.8% as two teeth were lost (2.2%); one was filled with Ceraseal-TF and 1 with AH Plus-TF. The reasons for extraction were horizontal root fracture in both cases. No clinical manifestations, including pain, fistulae, or swelling were observed during the follow-up.

After 24 months, the percentage of healed teeth (teeth with no periapical lesion, PAI < 3) was 91.1% (Ceraseal-TF) and 88.6% (AH Plus-TF), respectively. No differences were observed between the groups (Pearson chi square = 0.9427, $p = 0.624$; Fisher exact test = 0.714) (Table 4).

Table 5 reports the comparison of healed status between the two filling groups according to the operative parameters. Some parameters showed differences in the percentages of healed teeth, such as tooth location, initial PAI, type of endodontic treatment, sealer extrusion, and diameter of extrusion (Table 5).

Table 3. Demographic characteristics of root canal treatment followed-up in the study. Data expressed as number of root canal treatments (n) and their percentage (%) of the total sample. Bold indicates statistically significant differences ($p < 0.05$).

Parameters		Ceraseal-TF	AH Plus-TF	Chi Square Test
Age	<30	15 (33.3)	7 (15.9)	Chi = 11.655 $p = 0.020$
	30–55	12 (26.6)	19 (43.8)	
	>55	18 (40.0)	18 (40.9)	
Gender	Males	18 (40.0)	20 (45.4)	Chi = 0.810 $p = 0.667$
	Females	27 (60.0)	24 (54.6)	
Tooth type	Incisors	10 (22.2)	4 (9.1)	Chi = 8.400 $p = 0.078$
	Canines	2 (4.4)	2 (4.6)	
	Premolars	11 (24.4)	10 (22.7)	
	Molars	22 (48.8)	28 (63.6)	
Tooth location	Maxilla	27 (60.0)	29 (65.9)	Chi = 5.05 $p = 0.080$
	Mandible	18 (40.0)	14 (31.8)	
Diagnosis	Prosthetic reasons	3 (6.6)	2 (4.6)	Chi = 15.672 $p = 0.109$
	Pulpitis	15 (33.3)	17 (38.6)	
	Pulp Necrosis	18 (40.0)	13 (29.5)	
	Re-exacerbated lesion	9 (20.0)	12 (27.2)	
Initial PAI	PAI ≤ 2	19 (44.2)	21 (47.7)	Chi = 0.5332 $p = 0.052$
	PAI ≥ 3	26 (55.8)	23 (42.3)	
Endodontic treatment	Primary root treatment	36 (80.0)	32 (72.2)	Chi = 1.05 $p = 0.608$
	Secondary treatment	9 (20.0)	12 (27.8)	
Obturation quality	Underfilled	2 (4.4)	4 (9.1)	Chi = 3.287 $p = 0.566$
	Adequate filling	38 (84.4)	38 (86.3)	
	Overfilled	5 (11.1)	2 (4.6)	
Sealer extrusion	No	39 (86.6)	33 (75.0)	Chi = 6.451 $p = 0.040$
	Yes	6 (13.4)	11 (25.0)	
Long axis diameter of extrusion	0	39 (84.4)	33 (75.0)	Chi = 5.53 $p = 0.477$
	0.1–1.0 mm	2 (4.4)	3 (6.8)	
	1.1–3.0 mm	1 (2.2)	6 (13.6)	
	>3.0 mm	3 (6.6)	2 (4.5)	
Definitive restoration	Composite	36 (80.0)	37 (84.1)	Chi = 1.678 $p = 0.416$
	Crown	9 (20.0)	7 (15.9)	
Total		45	44	

Table 4. Percentage of healed, healing and extracted teeth after 24 months in the two groups. Data expressed as number of root canal treatments (n) and their percentage (%) of the total samples.

	n	Healed	Healing	Extracted
Ceraseal-TF	45	41 (91.1)	3 (6.8)	1 (2.3)
AH Plus-TF	44	39 (88.6)	4 (9.2)	1 (2.2)

Table 5. Comparison of healed status in the two filling groups in terms of pre-operative and intra-operative parameters. Data expressed as number of root canal treatments (n) and their percentage (%) of the total sample.

Parameters		Ceraseal-TF			AH Plus-TF		
		n	Healed	Healing	n	Healed	Healing
Age	<30	15	15 (100)	0 (0)	7	7 (100%)	0 (0)
	30–55	12	11 (91.6)	1 (8.4)	19	16 (84.2%)	3 (15.8)
	>55	17	15 (88.2)	2 (11.8)	17	16 (94.1%)	1 (5.9)
Gender	Males	17	16 (94.1)	1 (5.9)	19	18 (94.7%)	1 (5.3)
	Females	27	25 (92.5)	2 (7.5)	24	21 (87.5%)	3 (12.5)
Tooth type	Incisors	10	7 (70)	3 (30)	4	4 (100)	0 (0)
	Canine	2	2 (100)	0 (0)	2	2 (100)	0 (0)
	Premolars	10	10 (100)	0 (0)	10	9 (90)	1 (10)
	Molars	22	22 (100)	0 (0)	27	24 (88.8)	3 (11.2)
Tooth location	Maxilla	26	23 (88.4)	3 (11.6)	29	27 (93.1)	2 (6.9)
	Mandible	18	18 (100)	0 (0)	13	11 (84.6)	2 (15.4)
Initial PAI	PAI ≤2	18	18 (100)	0 (0)	20	20 (100)	0 (0)
	PAI ≥3	26	23 (88.4)	3 (11.6)	23	19 (82.6)	4 (17.4)
Diagnosis	Prosthetic reasons	3	3 (100)	0 (0)	2	2(100)	0 (0)
	Pulpitis	14	14 (100)	0 (0)	16	16 (100)	0 (0)
	Pulp necrosis	18	18 (100)	0 (0)	13	12 (92.3)	1 (7.7)
	Re-exacerbated lesion	9	6 (66.6)	3 (33.4)	12	9 (75)	3 (25)
Endodontic treatment	Primary root treatment	35	35 (100)	0 (0)	31	30 (96.7)	1 (3.3)
	Secondary treatment	9	6 (66.6)	3 (33.4)	12	9 (75)	3 (25)
Obturation quality	Underfilled	2	1 (50)	1 (50)	4	4 (100)	0 (0)
	Adequate	37	37 (100)	0 (0)	37	34 (91.8)	3 (8.2)
	Overfilled	5	5 (100)	0 (0)	2	1 (50)	1 (50)
Extrusion	No	38	37 (97.3)	1 (6.7)	32	29 (90.6)	3 (9.4)
	Yes	6	4 (66.6)	2 (33.4)	11	10 (90.9)	1 (9.1)
Long axis diameter of extrusion	0	38	37 (97.3)	1 (2.7)	32	29 (90.6)	3 (9.4)
	0.1–1.0 mm	2	2 (100)	0 (0)	3	3 (100)	0 (0)
	1.1–3.0 mm	1	1 (100)	0 (0)	6	5 (83.3)	1 (16.7)
	>3.0 mm	3	1 (33.3)	2 (66.7)	2	2 (100)	0 (0)
Definitive restoration	Composite	35	33 (94.2)	2 (5.8)	36	32 (88.8)	4 (11.2)
	Crown	9	8 (88.8)	1 (11.2)	7	7 (100)	0 (0)

Multilevel-mixed logistic regression confirmed that only initial PAI and endodontic treatment parameters were statistically associated with a different healing outcome at 24 months ($p < 0.05$) (Table 6). A preoperative Initial PAI >3 and the presence of a previous endodontic treatment were predictors of a non-healing status at 24 months.

Table 6. Multilevel-mixed logistic regression of parameters related to healed status after 24 months. Bold indicates significant values ($p < 0.05$).

Parameters	Coefficient	Robust Standard Error	p Value	95% Confidence Interval	
				Lower Boundary	Upper Boundary
Intercept	1.488	0.201	0.000	1.0953	1.882
Age	−0.934	0.582	0.108	−2.075	0.206
Gender	−1.125	1.036	0.277	−3.156	0.905
Tooth location	0.643	0.542	0.235	−0.418	1.706
Diagnosis	0.044	0.715	0.951	−1.358	1.447
Initial PAI	−0.134	0.047	0.005	−0.228	−0.040
Endodontic treatment	−2.347	0.956	0.014	−4.216	−0.461
Filling technique	0.398	0.484	0.410	−0.551	1.348
Obturation quality	−1.60	0.917	0.081	−3.39	0.197
Sealer extrusion	0.410	0.995	0.680	−1.540	2.360
Diameter of extrusion	−0.099	0.064	0.124	−0.2271	0.027
Definitive restoration	−0.609	0.435	0.162	−1.463	0.244

3.3. Sealer Extrusion and Sealer Resorption

Table 7 reports the apically extruded sealer modifications in Ceraseal-TF and AH Plus-TF groups. Ceraseal-TF displayed 6 extrusions out of 44 root canal treatments (13.3%), while AH Plus-TF displayed 11 extrusions (25%). Three apical extrusions in the Ceraseal-TF group were resorbed after 24 months, and the other three were stable. Graphs reporting the sealer radiographical modification during follow-up are reported in Figure S1, Supplementary Materials. Representative periapical X-rays on apical extruded sealer modifications are reported in Figures 2 and 3.

Table 7. Modifications of apical extrusions at 24 months according to the two filling groups. Data expressed as number of root canal treatments (n) and their percentage (%) of the total sample.

	n	Stable	Resorbed	Total
Ceraseal-TF	45	3 (6.8)	3 (6.8)	6 (13.3)
AH Plus-TF	44	11 (25)	0 (0)	11 (25)



Figure 2. Ceraseal-TF group. (A) Tooth #25 presented a large periapical lesion (PAI 5) and a wide apical diameter (\varnothing 45). (B) Apical extrusion of the sealer occurred during the root canal filling procedures. (C) Apical extrusion was almost completely resorbed after 24 months.



Figure 3. Ceraseal-TF group. (A) Tooth #25 was treated due to deep carious lesion and irreversible pulpitis. (B) Follow-up at 12 months from root canal filling (C) Note that apically extruded sealer showed a slight resorption after 24 months.

AH Plus-TF displayed 11 extrusions out of 44 root canal treatments (25%). The size and morphology of the resulting extrusion was stable and well-detectable after 24 months (Table 7 and Table S1, Supplementary Materials). One case of root canal treatment filled with AH Plus-TF is reported in Figure 4.



Figure 4. (A) Pre-operative periapical X-ray of a root canal treatment filled with AH Plus-TF group. Tooth #15 presented a deep caries lesion (PAI = 1). (B) No sealer extrusion was observed after root canal filling. (C) Follow-up at 24 months. Periapical area appears healthy with no signs of periapical exacerbation.

4. Discussion

This clinical study innovatively tested the use of a premixed CaSi-based bioceramic sealer with the warm carrier-based gutta-percha technique and demonstrated similar results when compared to epoxy-resin-based sealer used with the warm carrier-based techniques. Both filling procedures reported a high success rate (around 90%) after 24 months.

In the present study, all the treatment procedures were conducted by post-graduate master operators after 3 months of specific training and under the strict supervision of the University Dental School tutors. The possibility of using warm carrier-based techniques in association with a premixed CaSi-based bioceramic sealer is useful and attractive for root canal obturation, as it combines the advantages of a carrier-based technique with the biological and bio-interactive properties of the sealer.

CaSi materials showed innovative properties including the ability to set in a wet environment and to release biologically active ions [32–34], to expand [35–37] and to nucleate an apatite layer in phosphate-containing solutions [32,38–41]. Several studies reported a positive bio-interaction with periapical tissues and mineralizing cells [40,42–44] and osteoinductive properties with dynamic biomineralization processes [45].

These properties represent the rationale for the design of hydrophilic bio-interactive CaSi-based sealers and justify the expected good clinical outcome.

A warm carrier-based technique was selected as it is widely considered the “gold standard” obturation technique [15,16,18,46]. Moreover, it is easier and more reproducible than other clinical techniques when proposed in a post-graduate master program, as reported in a large number of studies [15,16,18,46]. No previous studies clinically tested premixed CaSi-based bioceramic sealers with warm obturation techniques. The effect of heat application on CaSi-based sealers has been investigated in different *in vitro* studies [47–49]. Sealer dehydration and the degradation of organic components was observed on CaSi-based materials at high temperatures (100–225 °C degrees). Setting time, flowability [47–49] and film thickness [48] were critically affected. High temperatures may induce the thermal degradation of polyethyleneglycole (PEG), the water-soluble solvent included in the premixed sealer [49]. Actually, *in vivo* temperature is significantly lower than those reported in the previous studies. Donnermeier et al. demonstrated a maximum temperature rise to 58 °C when using warm-filling techniques [50]. Therefore, only limited modification of Ceraseal physical properties are expected when applied with a carrier-based technique.

In the present study, the percentage of periapical healing increased from the initial preoperative status in both groups. The percentages of healed teeth (PAI 1-2), and the survival rate was similar in both groups. It is important to underline that no new periapical lesions or apical re-exacerbation was observed during the study.

Cereseal-TF groups showed lower a percentage of periapical sealer extrusions (13.3%) when compared to the AH Plus-TF group (25%), which is likely attributable to the different chemical and physical properties of the two sealers. AH Plus used with warm techniques increase its fluidity and ability to flow out of the apex and penetrate deeper inside dentinal tubules [51]. Moreover, the radiopacity of AH Plus is markedly higher than Ceraseal (which is clinically evident from the periapical radiographs shown in Figure 3) and this may explain the high detectability and the greater diameter of the apically extruded AH Plus-TF.

It is known that the radiopacity of AH Plus is one of the highest among the current sealers, ranging from 10.00 mmAl to 11.8 mmAl [52,53]. Authors found Ceraseal radiopacity to be around 6.5 mmAl in a recent study [11]. The lower radiopacity of Ceraseal may require a greater volume of apical extrusion to be detected as a radiopaque mass in the periapical area.

In our study, three Ceraseal extrusions were resorbed and completely undetectable after 24 months. On the other hand, AH Plus extrusions proved stable results in all observational times. Our data on the stability of apically extruded AH Plus are in accordance with previous studies [54,55]. Limited information is reported regarding apical extrusion modification on CaSi-based sealers (and Ceraseal). Only two articles evaluated the frequency of apical over-extrusions of premixed CaSi-based bioceramic sealers [20,56]. Interestingly, both studies reported a higher apical over-extrusion of the premixed CaSi-based bioceramic sealers when compared to epoxy-resin-based sealer. Both studies considered cold filling techniques [20,56].

It should be underlined that the morphology and size of the extrusion is influenced by root diameter and most likely by the presence of a periapical lesion. Indeed, we found that the presence of periapical bone defects (observed in teeth with lesions PAI 3-5) were associated with sealer extrusions characterized by a circular morphology, while the (radiographic) integrity of apical bone that enveloped the apex was associated with a smaller extrusion (See Figures 2 and 3).

The effect of the periapical extrusion of the sealer on healing outcome has been debated in the literature. We would underline that the biological response to the extruded sealer strongly depends on the chemical composition of the material, on its release of biologically relevant ions or toxic components. A previous study reported that sealer extrusion lead to an unfavorable healing outcome as the sealer may act as a chronic source of inflammation in the periapical tissues [57]. More recent studies [54,55,58] found a not-significant effect of traditional extruded sealers on healing outcome.

We highlight that a different behavior in a biological environment must be supposed for Ceraseal and other premixed CaSi-based bioceramic sealers. The solubility of CaSi-based

sealers was, *in vitro*, associated with high calcium release and was related with bioactivity (the ability to nucleate apatite), and with the consequent modification of the sealer structure in the apical region [32,39,43,59–61]. Animal models confirmed the bioactivity and the sealing ability of previous CaSi-based materials [62]. On the other hand, epoxy-resin-based sealers completely set and remained chemically and dimensionally stable and inert in biological tissues, as demonstrated in a recent study [63].

The solubility of premixed CaSi-based sealers may be correlated with the (radio-graphic) disappearance of extruded sealers (Figure 2). The solubility of CaSi-based materials has been interlinked with their high calcium release [7,64,65]. The release of biologically active ions exerts a positive role in activating mineralizing stem cells [44,66]. CaSi components showed the ability to activate bone marrow cells [59], adipose-derived mesenchymal stem cells [67] and other cell types [68], in relationship with their biointeractive properties [32,43–45,59]. This could be clinically useful when the CaSi sealer is extruded into periapical bone defects or different bacteria-related bone resorptions.

Future studies are necessary to establish the long-term stability of the root canal seal, to verify if the sealer resorption also occurs along the root canal.

The use of NaOCl and EDTA as root canal irrigant solutions create a deep demineralized and deproteinized substrate [69] and increase dentin porosities and permeability, which are all conditions that may be responsible for root fracture. CaSi-based sealers can induce a new interfibrillar mineralization of demineralized dentine collagen, a mechanism described as dentin biomineralization [37,70–72]. Moreover, CaSi-based sealers showed, *in vitro*, their ability to penetrate into dentinal tubules of radicular dentine and to improve their sealing over time by filling potential interface voids [73] and by forming apatite [38] with associated dentine remineralization [38,70,71]. This is a further biological rationale in support of the use of CaSi-based sealers.

In the present study, instrumentation techniques were similar in the two groups and adhered to a standardized operative protocol. Root canal instrumentation were performed with NiTi rotating systems—having a similar final diameter (0.25), taper (0.06) and cross section (S-shape)—in presence of primary root canal treatment, whereas a NiTi reciprocating system was used for secondary root canal treatment.

A K-file #10 and 15 manual stainless system was used only for the initial preliminary scouting step and WL establishment. The technique was adopted to prevent any influence from the type of instrument.

All post-graduate master students were skilled in the use of the rotary and reciprocating instruments. All efforts were made to follow the principles of best clinical practice.

Preoperative tooth condition and a different initial diagnosis may influence root canal treatment healing (as reported in the multilevel analysis in Table 5). A long healing time increases the risks of apical reinfection in teeth affected by pulp necrosis or periapical abscesses [74–76], due to the presence of highly pathogenic Gram-negative anaerobic bacteria (as *Porphyromonas Gingivalis*, *Tannerella Forsythia*, *Prevotella Intermedia*) found in several clinical studies [76,77].

The study has some limitations including the short follow-up (24 months) and the prospective study design. A 24-month period may appear inadequate for the complete healing of teeth with a previous periapical lesion. ESE guidelines recommend a minimum period of 4 years to state the healing [78]. However, both groups showed a similar healing outcome and no periapical lesion re-exacerbation.

We highlight that primary and secondary root canal treatments were not separately analyzed, leading to a potential bias in the presentation of the tooth survival results. Another limit could be considered the randomization of the operators. We decided to randomize the operators considering the importance in obtaining experience and confidence with the clinical use of premixed CaSi-based sealers, in particular with a warm technique. Therefore, we deemed it important to create a homogeneous group of trained operators. In this way, only the randomly selected operator was able enough for the treatment with a specific material and technique. Technical skills did not influence the clinical outcome, as no root

canal perforations or iatrogenic complications occurred. Data on survival and success rate are high and in line with previously studies reporting an average success rate of 81–96% after 2–5 years [14,15,17,46]. For these reasons, the impact of the skills of post-graduate master students on the root canal treatment outcome was considered negligible.

5. Conclusions

The study supports the clinical use of premixed CaSi-based sealer with the warm carrier-based technique. The two techniques showed a comparable clinical outcome.

The study demonstrated that premixed CaSi-based sealer had less radiopacity, lower extrusion occurrence, but higher radiographic disappearance when apically extruded. This condition is likely in relationship with its solubility and calcium release. Interestingly, the sealer extrusion did not affect the healing outcome of root-canal-treated teeth.

Solid clinical scientific data may support the use of a flowable CaSi bioceramic sealer with a warm carrier-based gutta-percha technique and reduce some of the limits of epoxy-resin-based sealers. Further long-term studies may be important to validate these new filling materials.

Supplementary Materials: The following supporting information can be downloaded at: <https://www.mdpi.com/article/10.3390/jfb14030164/s1>, Figure S1: Graphs reporting the cases where sealer apical extrusion occurred. Periapical radiographs during the follow-up at 6, 12 and 24 months revealed the complete radiographical resorption of 3 extrusions in Ceraseal-TF group, one at 6 months and 2 at 12 months respectively. Differently, AH Plus-TF extrusions were stable along all the 24 months follow-up; Table S1: Quantification of radiographic apically extruded sealer in relation to PAI. Ceraseal +TF group displayed radiographic resorption of the sealer, while AH Plus+TF displayed no modification of extruded sealer.

Author Contributions: Conceptualization, C.P. and M.G.G.; methodology, C.P.; software, F.Z.; validation, F.Z.; investigation, C.P., A.S. and F.Z.; resources, C.P.; writing—original draft preparation, C.P., F.Z. and A.S.; writing—review and editing, C.P., F.C., P.A. and M.G.G.; visualization, F.Z. and A.S.; supervision, C.P.; project administration, C.P. All authors have read and agreed to the published version of the manuscript.

Funding: This research received no external funding.

Data Availability Statement: The data presented in this study are available on request from the corresponding author. The data are not publicly available due to privacy and ethical reasons.

Conflicts of Interest: The authors declare no conflict of interest.

References

1. Torabiinejad, M.; Chivian, N. Clinical applications of mineral trioxide aggregate. *J. Endod.* **1999**, *25*, 197–205. [CrossRef]
2. Pitt-Ford, T.R.; Torabiinejad, M.; McKendry, D.J.; Hong, C.U.; Kariyawasam, S.P. Use of mineral trioxide aggregate for repair of furcal perforations. *Oral Surg. Oral Med. Oral Pathol. Oral Radiol. Endod.* **1995**, *79*, 756–763. [CrossRef] [PubMed]
3. Niu, L.N.; Jiao, K.; Wang, T.D.; Zhang, W.; Camilleri, J.; Bergeron, B.E.; Feng, H.L.; Mao, J.; Chen, J.H.; Pashley, D.H.; et al. A review of the bioactivity of hydraulic calcium silicate cements. *J. Dent. Res.* **2014**, *42*, 517–533. [CrossRef]
4. Primus, C.M.; Tay, F.R.; Niu, L.N. Bioactive tri/dicalcium silicate cements for treatment of pulpal and periapical tissues. *Acta Biomater.* **2019**, *96*, 35–54. [CrossRef] [PubMed]
5. Angerame, D.; De Biasi, M.; Pecci, R.; Bedini, R. Filling ability of three variants of the single-cone technique with bioceramic sealer: A micro-computed tomography study. *J. Mater. Sci. Mater. Med.* **2020**, *31*, 91–99. [CrossRef]
6. Tanomaru-Filho, M.; Andrade, A.S.; Rodrigues, E.M.; Viola, K.S.; Faria, G.; Camilleri, J.; Guerreiro-Tanomaru, J.M. Biocompatibility and mineralized nodule formation of Neo MTA Plus and an experimental tricalcium silicate cement containing tantalum oxide. *Int. Endod. J.* **2017**, *50*, 31–39. [CrossRef]
7. Zamparini, F.; Siboni, F.; Prati, C.; Taddei, P.; Gandolfi, M.G. Properties of calcium silicate-monobasic calcium phosphate materials for endodontics containing tantalum pentoxide and zirconium oxide. *Clin. Oral Investig.* **2019**, *23*, 445–457. [CrossRef] [PubMed]
8. Giacomino, C.M.; Wealleans, J.A.; Kuhn, N.; Diogenes, A. Comparative Biocompatibility and Osteogenic Potential of Two Bioceramic Sealers. *J. Endod.* **2019**, *45*, 51–56. [CrossRef] [PubMed]
9. López-García, S.; Myong-Hyun, B.; Lozano, A.; García-Bernal, D.; Forner, L.; Llana, C.; Guerrero-Gironés, J.; Murcia, L.; Rodríguez-Lozano, F.J. Cytocompatibility, bioactivity potential, and ion release of three premixed calcium silicate-based sealers. *Clin. Oral Investig.* **2020**, *24*, 1749–1759. [CrossRef] [PubMed]

10. Hadis, M.; Camilleri, J. Characterization of heat resistant hydraulic sealer for warm vertical obturation. *Dent. Mater.* **2020**, *36*, 1183–1189. [[CrossRef](#)] [[PubMed](#)]
11. Zamparini, F.; Prati, C.; Taddei, P.; Spinelli, A.; Di Foggia, M.; Gandolfi, M.G. Chemical-Physical Properties and Bioactivity of New Premixed Calcium Silicate-Bioceramic Root Canal Sealers. *Int. J. Mol. Sci.* **2020**, *23*, 13914. [[CrossRef](#)] [[PubMed](#)]
12. Kharouf, N.; Arntz, Y.; Eid, A.; Zghal, J.; Sauro, S.; Haikel, Y.; Mancino, D. Physicochemical and Antibacterial Properties of Novel, Premixed Calcium Silicate-Based Sealer Compared to Powder-Liquid Bioceramic Sealer. *J. Clin. Med.* **2020**, *9*, 3096. [[CrossRef](#)]
13. Goldberg, F.; Artaza, L.P.; De Silvio, A. Effectiveness of different obturation techniques in the filling of simulated lateral canals. *J. Endod.* **2001**, *27*, 362–364. [[CrossRef](#)] [[PubMed](#)]
14. Mirfendereski, M.; Roth, K.; Bing, F.; Dubrowski, A.; Carnahan, H.; Azarpazhooh, A.; Basrani, B.; Torneck, C.D.; Friedman, S. Technique acquisition in the use of two thermoplasticized root filling methods by inexperienced dental students: A micro-CT analysis. *J. Endod.* **2009**, *35*, 1512–1517. [[CrossRef](#)] [[PubMed](#)]
15. Pirani, C.; Zamparini, F.; Peters, O.A.; Iacono, F.; Gatto, M.R.; Generali, L.; Gandolfi, M.G.; Prati, C. The fate of root canals obturated with Thermafil: 10-year data for patients treated in a master program. *Clin. Oral Investig.* **2019**, *23*, 3367–3377. [[CrossRef](#)] [[PubMed](#)]
16. Hale, R.; Gatti, R.; Glickman, G.N.; Opperman, L.A. Comparative analysis of carrier-based obturation and lateral compaction: A retrospective clinical outcomes study. *Int. J. Dent.* **2012**, *2012*, 954675. [[CrossRef](#)]
17. Wong, A.W.Y.; Tsang, C.S.C.; Zhang, S.; Li, S.K.Y.; Zhang, C.; Chu, C.H. Treatment outcomes of single-visit versus multiple-visit non-surgical endodontic therapy: A randomised clinical trial. *BMC Oral Health* **2015**, *15*, 162. [[CrossRef](#)]
18. Demirci, G.K.; Caliskan, M.K. A prospective randomized comparative study of cold lateral condensation versus Core/Gutta-percha in teeth with periapical lesions. *J. Endod.* **2016**, *42*, 206–210. [[CrossRef](#)]
19. Chu, C.H.; Lo, E.C.; Cheung, G.S. Outcome of root canal treatment using Thermafil and cold lateral condensation filling techniques. *Int. Endod. J.* **2005**, *38*, 179–185. [[CrossRef](#)]
20. Chybowski, E.A.; Glickman, G.N.; Patel, Y.; Fleury, A.; Solomon, E.; He, J. Clinical Outcome of Non-Surgical Root Canal Treatment Using a Single-cone Technique with Endosequence Bioceramic Sealer: A Retrospective Analysis. *J. Endod.* **2018**, *44*, 941–945. [[CrossRef](#)]
21. Zavattini, A.; Knight, A.; Foschi, F.; Mannocci, F. Outcome of root canal treatments using a new calcium silicate root canal sealer: A non-randomized clinical trial. *J. Clin. Med.* **2020**, *9*, 782. [[CrossRef](#)]
22. Bardini, G.; Casula, L.; Ambu, E.; Musu, D.; Mercadè, M.; Cotti, E. A 12-month follow-up of primary and secondary root canal treatment in teeth obturated with a hydraulic sealer. *Clin. Oral Investig.* **2021**, *25*, 2757–2764. [[CrossRef](#)] [[PubMed](#)]
23. World Medical Association. World Medical Association Declaration of Helsinki: Ethical principles for medical research involving human subjects. *J. Am. Med. Assoc.* **2013**, *310*, 2191–2194. [[CrossRef](#)] [[PubMed](#)]
24. Vandembroucke, J.P.; von Elm, E.; Altman, D.G.; Gøtzsche, P.C.; Mulrow, C.D.; Pocock, S.J.; Poole, C.; Schlesselman, J.J.; Egger, M. STROBE Initiative Strengthening the Reporting of Observational Studies in Epidemiology (STROBE): Explanation and elaboration. *Epidemiology* **2007**, *18*, 805–835. [[CrossRef](#)]
25. Dodson, T.B. A guide for preparing a patient-oriented research manuscript. *Oral Surg. Oral Med. Oral Pathol. Oral Radiol. Endod.* **2007**, *104*, 307–315. [[CrossRef](#)]
26. Prati, C.; Pirani, C.; Zamparini, F.; Gatto, M.R.; Gandolfi, M.G. A 20-year historical prospective cohort study of root canal treatments. A Multilevel analysis. *Int. Endod. J.* **2018**, *51*, 955–968. [[CrossRef](#)] [[PubMed](#)]
27. Zamparini, F.; Pelliccioni, G.A.; Spinelli, A.; Gissi, D.B.; Gandolfi, M.G.; Prati, C. Root canal treatment of compromised teeth as alternative treatment for patients receiving bisphosphonates: 60-month results of a prospective clinical study. *Int. Endod. J.* **2021**, *54*, 156–171. [[CrossRef](#)] [[PubMed](#)]
28. Pirani, C.; Cirulli, P.P.; Chersoni, S.; Micele, L.; Ruggeri, O.; Prati, C. Cyclic fatigue testing and metallographic analysis of nickel-titanium rotary instruments. *J. Endod.* **2011**, *37*, 1013–1016. [[CrossRef](#)]
29. Chong, B.S.; Ford, T.R.P. The role of intracanal medication in root canal treatment. *Int. Endod. J.* **1992**, *25*, 97–106. [[CrossRef](#)]
30. Pirani, C.; Paolucci, A.; Ruggeri, O.; Bossù, M.; Polimeni, A.; Gatto, M.R.; Gandolfi, M.G.; Prati, C. Wear and metallographic analysis of WaveOne and reciproc NiTi instruments before and after three uses in root canals. *Scanning.* **2014**, *36*, 517–525. [[CrossRef](#)]
31. Ørstavik, D.; Kerekes, K.; Eriksen, H.M. The periapical index: A scoring system for radiographic assessment of apical periodontitis. *Endod. Dent. Traumatol.* **1986**, *2*, 20–34. [[CrossRef](#)] [[PubMed](#)]
32. Gandolfi, M.G.; Taddei, P.; Modena, E.; Siboni, F.; Prati, C. Biointeractivity-related versus chemi/physisorption-related apatite precursor-forming ability of current root end filling materials. *J. Biomed. Mater. Res. Part B Appl. Biomater.* **2013**, *101*, 1107–1123. [[CrossRef](#)]
33. Rashid, F.; Shiba, H.; Mizuno, N.; Mouri, Y.; Fujita, T.; Shinohara, H.; Ogawa, T.; Kawaguchi, H.; Kurihara, H. The effect of extracellular calcium ion on gene expression of bone-related proteins in human pulp cells. *J. Endod.* **2003**, *29*, 104–107. [[CrossRef](#)]
34. Sun, J.; Wei, L.; Liu, X.; Li, J.; Li, B.; Wang, G.; Meng, F. Influences of ionic dissolution products of dicalcium silicate coating on osteoblastic proliferation, differentiation and gene expression. *Acta Biomater.* **2009**, *5*, 1284–1293. [[CrossRef](#)]
35. Gandolfi, M.G.; Iacono, F.; Agee, K.; Siboni, F.; Tay, F.; Pashley, D.H.; Prati, C. Setting time and expansion in different soaking media of experimental accelerated calcium-silicate cements and ProRoot MTA. *Oral Surg. Oral Med. Oral Pathol. Oral Radiol. Endod.* **2009**, *108*, 39–45. [[CrossRef](#)] [[PubMed](#)]

36. Iacono, F.; Gandolfi, M.G.; Huffman, B.; Sword, J.; Agee, K.; Siboni, F.; Tay, F.; Prati, C.; Pashley, D. Push-out strength of modified Portland cements and resins. *Am. J. Dent.* **2010**, *23*, 43–46.
37. Gandolfi, M.G.; Taddei, P.; Siboni, F.; Modena, E.; Ginebra, M.P.; Prati, C. Fluoride-containing nanoporous calcium-silicate MTA cements for endodontics and oral surgery: Early fluorapatite formation in a phosphate-containing solution. *Int. Endod. J.* **2011**, *44*, 938–949. [[CrossRef](#)] [[PubMed](#)]
38. Tay, F.R.; Pashley, D.H.; Rueggeberg, F.A.; Loushine, R.J.; Weller, R.N. Calcium phosphate phase transformation produced by the interaction of the portland cement component of white mineral trioxide aggregate with a phosphate-containing fluid. *J. Endod.* **2007**, *33*, 1347–1351. [[CrossRef](#)]
39. Taddei, P.; Tinti, A.; Gandolfi, M.G.; Rossi, P.L.; Prati, C. Vibrational study on the bioactivity of Portland cement-based materials for endodontic use. *J. Mol. Struct.* **2009**, *924*, 548–554. [[CrossRef](#)]
40. Gandolfi, M.G.; Taddei, P.; Tinti, A.; De Stefano Dorigo, E.; Prati, C. Alpha-TCP improves the apatite-formation ability of calcium-silicate hydraulic cement soaked in phosphate solutions. *Mater. Sci. Eng. C* **2011**, *31*, 1412–1422. [[CrossRef](#)]
41. Han, L.; Kodama, S.; Okiji, T. Evaluation of calcium-releasing and apatite-forming abilities of fast-setting calcium silicate-based endodontic materials. *Int. Endod. J.* **2015**, *48*, 124–130. [[CrossRef](#)]
42. Rodríguez-Lozano, F.J.; López-García, S.; García-Bernal, D.; Tomás-Catalá, C.J.; Santos, J.M.; Llena, C.; Lozano, A.; Murcia, L.; Forner, L. Chemical composition and bioactivity potential of the new Endosequence BC Sealer formulation HiFlow. *Int. Endod. J.* **2020**, *53*, 1216–1228. [[CrossRef](#)]
43. Hakki, S.S.; Bozkurt, B.S.; Ozcopur, B.; Gandolfi, M.G.; Prati, C.; Belli, S. The response of cementoblasts to calcium phosphate resin-based and calcium silicate-based commercial sealers. *Int. Endod. J.* **2013**, *46*, 242–252. [[CrossRef](#)] [[PubMed](#)]
44. Gandolfi, M.G.; Shah, S.N.; Feng, R.; Prati, C.; Akintoye, S.O. Biomimetic calcium-silicate cements support differentiation of human orofacial mesenchymal stem cells. *J. Endod.* **2011**, *37*, 1102–1108. [[CrossRef](#)] [[PubMed](#)]
45. Gandolfi, M.G.; Iezzi, G.; Piattelli, A.; Prati, C.; Scarano, A. Osteoinductive potential and bone-bonding ability of ProRoot MTA, MTA Plus and Biodentine in rabbit intramedullary model: Microchemical characterization and histological analysis. *Dent. Mater.* **2017**, *33*, 221–238. [[CrossRef](#)]
46. Pirani, C.; Friedman, S.; Gatto, M.R.; Iacono, F.; Tinarelli, V.; Gandolfi, M.G.; Prati, C. Survival and periapical health after root canal treatment with carrier-based root fillings: Five-year retrospective assessment. *Int. Endod. J.* **2018**, *51*, 178–188. [[CrossRef](#)]
47. Atmeh, A.R.; AlShwaimi, E. The Effect of Heating Time and Temperature on Epoxy Resin and Calcium Silicate-based Endodontic Sealers. *J. Endod.* **2017**, *43*, 2112–2118. [[CrossRef](#)]
48. Yamauchi, S.; Watanabe, S.; Okiji, T. Effects of heating on the physical properties of premixed calcium silicate-based root canal sealers. *J. Oral Sci.* **2020**, *63*, 65–69. [[CrossRef](#)] [[PubMed](#)]
49. Antunes, T.B.M.; Janini, A.C.P.; Pelepenko, L.E.; Abuna, G.F.; Paiva, E.M.; Sinhoreti, M.A.C.; Raimundo, I.M., Jr.; Gomes, B.P.F.A.; de-Jesus-Soares, A.; Marciano, M.A. Heating stability, physical and chemical analysis of calcium silicate-based endodontic sealers. *Int. Endod. J.* **2021**, *54*, 1175–1188. [[CrossRef](#)]
50. Donnermeyer, D.; Schäfer, E.; Bürklein, S. Real-time Intracanal Temperature Measurement during Different Obturation Techniques. *J. Endod.* **2018**, *44*, 1832–1836. [[CrossRef](#)] [[PubMed](#)]
51. Generali, L.; Cavani, F.; Serena, V.; Pettenati, C.; Righi, E.; Bertoldi, C. Effect of Different Irrigation Systems on Sealer Penetration into Dentinal Tubules. *J. Endod.* **2017**, *43*, 652–656. [[CrossRef](#)] [[PubMed](#)]
52. Lee, J.K.; Kwak, S.W.; Ha, J.H.; Lee, W.; Kim, H.C. Physicochemical Properties of Epoxy Resin-Based and Bioceramic-Based Root Canal Sealers. *Bioinorg. Chem. Appl.* **2017**, *2017*, 2582849. [[CrossRef](#)] [[PubMed](#)]
53. Siboni, F.; Taddei, P.; Zamparini, F.; Prati, C.; Gandolfi, M.G. Properties of BioRoot RCS, a tricalcium silicate endodontic sealer modified with povidone and polycarboxylate. *Int. Endod. J.* **2017**, *50*, 120–136. [[CrossRef](#)] [[PubMed](#)]
54. Ricucci, D.; Rôças, I.N.; Alves, F.R.; Loghin, S.; Siqueira, J.F., Jr. Apically Extruded Sealers: Fate and Influence on Treatment Outcome. *J. Endod.* **2016**, *42*, 243–249. [[CrossRef](#)]
55. Goldberg, F.; Cantarini, C.; Alfie, D.; Macchi, R.L.; Arias, A. Relationship between unintentional canal overfilling and the long-term outcome of primary root canal treatments and nonsurgical retreatments: A retrospective radiographic assessment. *Int. Endod. J.* **2020**, *53*, 19–26. [[CrossRef](#)] [[PubMed](#)]
56. Fonseca, B.; Coelho, M.S.; Bueno, C.E.D.S.; Fontana, C.E.; Martin, A.S.; Rocha, D.G.P. Assessment of Extrusion and Postoperative Pain of a Bioceramic and Resin-Based Root Canal Sealer. *Eur. J. Dent.* **2019**, *3*, 343–348. [[CrossRef](#)]
57. Schaeffer, M.A.; White, R.R.; Walton, R.E. Determining the optimal obturation length: A meta-analysis of literature. *J. Endod.* **2005**, *31*, 271–274. [[CrossRef](#)]
58. Aminoshariae, A.; Kulild, J.C. The impact of sealer extrusion on endodontic outcome: A systematic review with meta-analysis. *Aust. Endod. J.* **2020**, *46*, 123–129. [[CrossRef](#)]
59. Gandolfi, M.G.; Ciapetti, G.; Perut, F.; Taddei, P.; Modena, E.; Rossi, P.L.; Prati, C. Biomimetic calcium-silicate cements aged in simulated body solutions. Osteoblast response and analyses of apatite coating. *J. Appl. Biomater. Biomech.* **2009**, *7*, 160–170.
60. Elsayed, M.A.; Hassanien, E.E.; Elgendy, A.A.E. Ageing of TotalFill BC Sealer and MTA Fillapex in Simulated Body Fluid. *Eur. Endod. J.* **2021**, *6*, 183–188.
61. Prati, C.; Gandolfi, M.G. Calcium silicate bioactive cements: Biological perspectives and clinical applications. *Dent. Mater.* **2015**, *31*, 351–370. [[CrossRef](#)]

62. Reyes-Carmona, J.F.; Santos, A.R.; Figueiredo, C.P.; Felipe, M.S.; Felipe, W.T.; Cordeiro, M.M. In vivo host interactions with mineral trioxide aggregate and calcium hydroxide: Inflammatory molecular signaling assessment. *J. Endod.* **2011**, *37*, 1225–1235. [[CrossRef](#)]
63. Jung, S.; Sielker, S.; Hanisch, M.R.; Libricht, V.; Schäfer, E.; Dammaschke, T. Cytotoxic effects of four different root canal sealers on human osteoblasts. *PLoS ONE* **2018**, *13*, e0194467. [[CrossRef](#)]
64. Siboni, F.; Taddei, P.; Prati, C.; Gandolfi, M.G. Properties of NeoMTA Plus and MTA Plus cements for endodontics. *Int. Endod. J.* **2017**, *50*, 83–94. [[CrossRef](#)] [[PubMed](#)]
65. Razdan, A.; Benetti, A.R.; Bjørndal, L. Do in vitro solubility studies on endodontic sealers demonstrate a high level of evidence? A systematic review. *Acta Odontol. Scand.* **2019**, *77*, 253–263. [[CrossRef](#)] [[PubMed](#)]
66. Matsumoto, S.; Hayashi, M.; Suzuki, Y.; Suzuki, N.; Maeno, M.; Ogiso, B. Calcium ions released from mineral trioxide aggregate convert the differentiation pathway of C2C12 Cells into osteoblast lineage. *J. Endod.* **2013**, *39*, 68–75. [[CrossRef](#)] [[PubMed](#)]
67. Gandolfi, M.G.; Gardin, C.; Zamparini, F.; Ferroni, L.; Esposti, M.D.; Parchi, G.; Ercan, B.; Manzoli, L.; Fava, F.; Fabbri, P.; et al. Mineral-Doped Poly(L-lactide) Acid Scaffolds Enriched with Exosomes Improve Osteogenic Commitment of Human Adipose-Derived Mesenchymal Stem Cells. *Nanomaterials* **2020**, *10*, 432. [[CrossRef](#)] [[PubMed](#)]
68. Gandolfi, M.G.; Zamparini, F.; Esposti, M.D.; Chiellini, F.; Fava, F.; Fabbri, P.; Taddei, P.; Prati, C. Highly porous polycaprolactone scaffolds doped with calcium silicate and dicalcium phosphate dihydrate designed for bone regeneration. *Mater. Sci. Eng. C Mater. Biol. Appl.* **2019**, *102*, 341–361. [[CrossRef](#)]
69. Gandolfi, M.G.; Taddei, P.; Pondrelli, A.; Zamparini, F.; Prati, C.; Spagnuolo, G. Demineralization, Collagen Modification and Remineralization Degree of Human Dentine after EDTA and Citric Acid Treatments. *Materials* **2019**, *12*, 25. [[CrossRef](#)]
70. Tay, F.R.; Pashley, D.H. Guided tissue remineralisation of partially demineralised human dentine. *Biomaterials* **2008**, *29*, 1127–1137. [[CrossRef](#)]
71. Tay, F.R.; Pashley, D.H. Biomimetic remineralization of resin-bonded acid-etched dentin. *J. Dent. Res.* **2009**, *88*, 719–724. [[CrossRef](#)] [[PubMed](#)]
72. Gandolfi, M.G.; Taddei, P.; Siboni, F.; Modena, E.; De Stefano, E.D.; Prati, C. Biomimetic remineralization of human dentin using promising innovative calcium-silicate hybrid “smart” materials. *Dent. Mater.* **2011**, *27*, 1055–1069. [[CrossRef](#)] [[PubMed](#)]
73. Gandolfi, M.G.; Parrilli, A.P.; Fini, M.; Prati, C.; Dummer, P.M. 3D micro-CT analysis of the interface voids associated with Thermafil root fillings used with AH Plus or a flowable MTA sealer. *Int. Endod. J.* **2013**, *46*, 253–263. [[CrossRef](#)]
74. Love, R.M.; Jenkinson, H.F. Invasion of dentinal tubules by oral bacteria. *Crit. Rev. Oral Biol. Med.* **2002**, *13*, 171–183. [[CrossRef](#)]
75. Ricucci, D.; Siqueira, J.F., Jr. Biofilms and apical periodontitis: Study of prevalence and association with clinical and histopathologic findings. *J. Endod.* **2010**, *36*, 277–288. [[CrossRef](#)]
76. Foschi, F.; Izard, J.; Sasaki, H.; Sambri, V.; Prati, C.; Müller, R.; Stashenko, P. *Treponema denticola* in disseminating endodontic infections. *J. Dent. Res.* **2006**, *85*, 761–765. [[CrossRef](#)]
77. Buonavoglia, A.; Zamparini, F.; Lanave, G.; Pellegrini, F.; Diakoudi, G.; Spinelli, A.; Lucente, M.S.; Camero, M.; Vasinioti, V.I.; Gandolfi, M.G.; et al. Endodontic Microbial Communities in Apical Periodontitis. *J. Endod.* **2023**, *49*, 178–189. [[CrossRef](#)] [[PubMed](#)]
78. European Society of Endodontology. Quality guidelines for endodontic treatment: Consensus report of the European Society of Endodontology. *Int. Endod. J.* **2006**, *39*, 921–930. [[CrossRef](#)]

Disclaimer/Publisher’s Note: The statements, opinions and data contained in all publications are solely those of the individual author(s) and contributor(s) and not of MDPI and/or the editor(s). MDPI and/or the editor(s) disclaim responsibility for any injury to people or property resulting from any ideas, methods, instructions or products referred to in the content.

Article

Clinical Evaluation of a Novel Premixed Tricalcium Silicate Containing Bioceramic Sealer Used with Warm Carrier-Based Technique: A 12-Month Prospective Pilot Study

Andrea Spinelli ¹, Fausto Zamparini ^{1,2,*}, Jacopo Lenzi ³, Maria Giovanna Gandolfi ² and Carlo Prati ¹

¹ Endodontic Clinical Section, Dental School, Department of Biomedical and Neuromotor Sciences, University of Bologna, 40125 Bologna, Italy; andrea.spinelli4@unibo.it (A.S.); carlo.prati@unibo.it (C.P.)

² Laboratory of Green Biomaterials and Oral Pathology, Dental School, Department of Biomedical and Neuromotor Sciences, University of Bologna, 40125 Bologna, Italy; mgiovanna.gandolfi@unibo.it

³ Hygiene, Public Health and Medical Statistics Section, Department of Biomedical and Neuromotor Sciences, Alma Mater Studiorum, University of Bologna, 40125 Bologna, Italy; jacopo.lenzi2@unibo.it

* Correspondence: fausto.zamparini2@unibo.it

Abstract: Background: This pilot prospective study analysed the clinical use of a new bioceramic premixed CaSi-containing sealer in association with a warm carrier-based technique. Methodology: Healthy patients ($n = 38$) requiring 40 root canal treatments were enrolled. Periapical X-rays were taken preoperatively, after root canal filling and after 1, 6, and 12 months. Two evaluators assessed the Periapical Index (PAI) and the sealer extrusion. The healing rate and survival rate were also evaluated. Barnard test was used to assess the relationship of each potential prognostic factor with periapical index (PAI) at 12-month follow-up. The significance level was set at 0.05. Results: Root canal treatments ($n = 38$) were analysed at the end-line (12 months). The total drop-out was 5% (two patients; two teeth). A total of 31 teeth (82%) (PAI 1-2) showed complete healing, while 7 (18%) are still healing. Cumulative survival was 100%. Apical extrusion of the sealers was observed in 18 cases (47%). Of these extrusions, nine (50%) resulted radiographically undetectable after 12 months. Conclusions: The study supports the use of premixed CaSi-based bioceramic sealers in association with carrier-based techniques. Periapical extrusion of the sealer and its radiographic modification or disappearance are possible events reported in the first 12 months.

Keywords: carrier-based techniques; premixed bioceramic sealer; periapical healing; apical extrusion; post-operative pain

Citation: Spinelli, A.; Zamparini, F.; Lenzi, J.; Gandolfi, M.G.; Prati, C. Clinical Evaluation of a Novel Premixed Tricalcium Silicate Containing Bioceramic Sealer Used with Warm Carrier-Based Technique: A 12-Month Prospective Pilot Study. *Appl. Sci.* **2023**, *13*, 11835. <https://doi.org/10.3390/app132111835>

Academic Editor: Soshu Kirihara

Received: 12 September 2023

Revised: 18 October 2023

Accepted: 25 October 2023

Published: 29 October 2023



Copyright: © 2023 by the authors. Licensee MDPI, Basel, Switzerland. This article is an open access article distributed under the terms and conditions of the Creative Commons Attribution (CC BY) license (<https://creativecommons.org/licenses/by/4.0/>).

1. Introduction

Warm carrier-based techniques associated with different sealers have been shown to be effective and offer clinical advantages due to their ease of use, short learning curve, and reliable technical and clinical outcomes [1]. Warm procedures have traditionally been associated with the use of epoxy resin-based sealers, which are still considered the “gold standard” and revealing success rates from 81% to 96% after 3–5 years [2–4]. Unfortunately, epoxy-resin sealers are highly hydrophobic and require a root canal with no moisture in order to achieve a stable seal with no voids [5].

In the last few years, calcium silicate-based materials have shown increasing popularity in endodontic treatment. The introduction of calcium silicate-based materials as endodontic sealers is particularly attractive for their chemical and physical properties. These materials are able to set in the presence of moisture and blood, such as in wide apices [6,7]. Calcium silicate-based sealers are biocompatible and osteoconductive towards circulating and periapical MSC populations, as observed in recent histological and in vitro studies [8]. The use of these sealers was proposed in combination with the cold single cone

technique [9,10], thanks to their specific and innovative properties such as the ability to expand into the root canal, the capacity to produce new apatite formation and to seal the discrepancies between guttapercha and dentinal walls [11–15]. Reconsidering the application of these sealers with a warm technique, such as the carrier-based technique, could be an interesting new perspective in an attempt to simplify the technique.

A new category of premixed CaSi-based or containing sealers has been recently developed and characterised by different compositions [16–18]. AH Plus Bioceramic sealer (Dentsply, Konstanz, Germany) is a novel premixed ready-to-be-used sealer with hydraulic properties and adequate flowability. The chemical and physical properties have been investigated in some recent studies, which have reported the ability of the sealer to release calcium and alkalis the environment [19–21] and the ability to induce the formation of small apatite deposits when immersed in simulated body fluids [19]. These properties showed the sealer suitability for clinical use.

Despite their promising characteristics and considering the recent introduction on the market, a limited number of short-term clinical investigations have been conducted [9,22–24]. Further research is needed to fully understand their performance, clinical outcomes, and occurrence of post-operative pain after filling.

The aim of this clinical pilot prospective cohort study was to evaluate the 12-month outcome, survival, and periapical healing rate of endodontically affected teeth filled with AH Plus Bioceramic sealer in association with warm carrier-based technique. Post-operative pain after root canal filling was assessed after 1 day, 1 week, and 1 month.

2. Materials and Methods

2.1. Study Design and Sample

The study was designed in December 2021 as a pilot prospective clinical study. This design was chosen to provide preliminary data on the effectiveness of the new treatment in order to design a larger randomised clinical trial that was planned for January 2023. No major modifications were made to the study design after its initial conception. The patients were treated in the Endodontic Clinical Section—Dental Clinic, University of Bologna, by a pool of postgraduate master operators ($n = 8$) in accordance with standardized protocols and under the strict supervision of the experienced tutors of the master. All the operators, before the study started, were adequately instructed and trained in sealer application and obturation technique. The study was approved by the ethical committee (597-2022-SPER-AUSLBO).

The study adhered to the principles of the Declaration of Helsinki, as modified in 2013 [25]. The clinical staff provided written and verbal information to patients before enrolment.

All patients provided a signed informed consent to accept the treatment plan and to follow the hygiene program. The study was designed in compliance with the STROBE checklist [26] and the guidelines published by Dodson in 2007 [27].

2.2. Study Population

Table 1 provide the inclusion and exclusion criteria for the clinical study.

Table 1. Inclusion Criteria and Exclusion criteria.

<i>Inclusion Criteria</i>	<i>Exclusion criteria.</i>
1. Age 18–75 years 2. Healthy status (ASA 1 or 2) 3. At least one tooth affected by endodontic pathology (pulpitis, pulp necrosis, re-exacerbated lesions with a previous root canal treatment)	1. Teeth with less than 2 walls of crown structural integrity
	2. Teeth used as abutments for fixed rehabilitation
	3. Presence of active periodontal disease (PPD >4mm, general BoP >25% of the sites)
	4. Wide apices (>40 diameters) or absence of radiographic pulp chamber
	5. Any systemic pathology that could compromise bone healing or the immune response (i.e., diabetes)
	6. Pregnancy or breastfeeding
	7. Heavy smoking (>15 cigarettes/day)
	8. Exposure to radiation therapy focused on the head and neck region and malignant disease directly involving the jaws.
	9. Lack of occlusal contacts

2.3. Primary Root Canal Treatment

Nerve block anaesthesia (1.7 mL, mepivacaine chloridrate, Scandonest 3%, Septodont, St.-Maur-des-Fosses, France) and local anaesthesia (1.8 mL mepivacaine chloridrate, Scandonest 2% with 1:100,000 adrenaline, Septodont, St.-Maur-des-Fosses, France) were performed. The total duration of each endodontic session was 60 to 90 min. Dental dam isolation was positioned on the affected tooth. A straight-line access was performed with a diamond bur mounted on high-speed water-cooled handpieces (Cefla, Imola, Italy). A preoperative working length was estimated using periapical radiographs. The crown-down technique was used. Gates-Glidden burs #2 and #3 were utilised when necessary, only in the coronal third. NiTi instruments were used to shape the canals in the coronal, medium, and apical third (Rotate, VDW, Munchen, Germany). An electronic apex locator (Root ZX, Morita, Osaka, Japan) with K-file #10 was used to determine the working length during the entire clinical procedure. Intra-oral periapical X-rays were performed to confirm the working length during the root canal instrumentation. Each root canal was shaped in the apical third with an apical diameter of #25.04 at least.

Irrigation was performed after the use of each instrument with a total of 5 mL of 5% NaOCl solution (Nicolor 5, OGNA, Muggiò, Italy).

2.4. Secondary Root Canal Treatment

An initial pathway was created with Gates-Glidden burs #3 and #4 (Dentsply Maillefer, Ballaigues, Switzerland) to approximately 3–4 mm depth in the gutta-percha.

Reciprocating NiTi instruments (Reciproc Blue, VDW, Munchen, Germany) were then used with Silver Reciproc Endomotor in the “Reciproc All” setting. After each step, the material entrapped among the instrument threads was removed using a sterile sponge. The working length was established after the removal of root canal remnants using periapical X-ray and an electronic apex locator. An apical enlargement was performed with Reciproc Blue #40 and #50 when needed. Irrigation was performed using a total amount of 5.0 mL of 5% NaOCl. When necessary, a dental surgery microscope (OMS3200 Dental Microscope, Zumax Medical Co., Suzhou, China) was used to detect the access to root canal orifices and to identify the presence of remnants.

2.5. Root Canal Filling Procedures

A premixed CaSi-containing bioceramic sealer (Ah Plus Bioceramic, Dentsply, Konstanz, Germany) was used in association with a warm carrier-based technique (Thermafil, Dentsply, Konstanz, Germany). AH Plus Bioceramic is mostly composed of zirconium dioxide (50–70%) as a radiopacifier and tricalcium silicate (10–15%) as a bioactive component. Dimethyl sulfoxide and traces of lithium carbonate and thickening agents are also reported by the manufacturer.

The sealer was applied with a sterile K-file inserted into the canal to reach the WL–3 mm and gently moved around the root canal walls. The carrier was heated using a dedicated obturation oven (Thermaprep obturation, Dentsply, Konstanz, Germany) and slowly inserted into the canal at WL–0.5 mm. The excess of the carrier was cut with a round bur. An X-ray was performed to verify the quality of the root canal obturation. Finally, a small cotton pellet and a temporary restoration (Coltosol, Coltene, Altstaetten, Switzerland) were positioned in the access cavity and maintained until definitive restoration. In case of severe pain, a medical prescription to take NSAID medications (such as ibuprofen or ketoprofen) was prepared by the university staff. In this case, the event was recorded, and the patient was excluded from the study.

2.6. Tooth Restoration

Teeth were definitely restored within 2 weeks under rubber dam isolation. Temporary restoration was removed using ultrasonic tips, and a crown was restored under rubber dam isolation. Self-etching dentinal bonding agent primer and bonding (Clearfil SE BOND, Kuraray, Osaka, Japan) were applied, photo-cured (Elipar, 3M ESPE, St. Paul, MN, USA) for 30 s and layered by flowable (G_Aenial Flow, GC Corporation, Tokyo, Japan) and composite (G-Aenial, GC Corporation, Tokyo, Japan) resins applied incrementally with 1.5 mm layers.

2.7. Radiological Evaluation

X-rays were taken after the root canal filling using a parallel technique. The following parameters were used: the target–film distance was approx. 30 cm, 0.41 s exposure at 70 Kw and 8 mA. The radiographs were developed in a standard developer unit at 20 °C (Euronda s.p.a., Vicenza, Italy), 12 s developing time, and 25 s fixing time according to the manufacturer instructions.

Intra-oral periapical X-rays and clinical criteria were used to classify the final outcome, with each patient monitored at 1, 6, and 12 months of follow-up. The root canal obturation was considered “adequate” when the filling material was detected at 0–1.0 mm from the radiological apex. Overfilling, short filling, and sealer extrusion were recorded. X-rays were digitalised using a slide scanner with a mean resolution of 1.000 dpi and a magnification factor of 20×.

Periapical Index (PAI) [28] was used to score the preoperative diagnosis and endpoint evaluations, which were evaluated in a double-blind manner by two operators (university researchers trained in this analysis) who did not perform the root canal treatment. PAI calibration was performed using well-defined instructions and periapical radiographs

with different periapical lesion scores. To ensure their reliability, the evaluators independently assessed the X-rays. In the event of any discrepancies between their assessments, these were extensively discussed until a mutual consensus was achieved. Sealer extrusion was recorded and measured on each periapical X-ray using open-source software (Image J, Bethesda, MD, USA).

2.8. Post-Operative Pain Assessment

Post-operative pain was assessed as Patient Reported Outcome (PRO) using a 10 cm Visual Analogical Scale, divided into 0–100 steps, with 0 indicating no pain and 100 indicating the most intense pain [29]. Post-operative pain was evaluated after root canal filling (T0), after 1 day (T1), after 7 days (T7), after 1 month (T28), and after 12 months (T365).

When a tooth presented a PAI 1 or 2, the tooth was considered “radiographically healed”.

When a tooth presented an improvement in PAI, the tooth was considered as “radiographically healing”.

2.9. Statistical Methods

Variables were summarised as counts and percentages. Barnard CSM (Convexity, Symmetry, and Minimization) test was used to assess the relationship of each potential prognostic factor with PAI at 12-month follow-up (1–2 [healed] vs. ≥3 [still healing]). Barnard test is an exact unconditional test recommended for association in 2 × 2 tables due to its power and preservation of test size [30,31]. Operationally, it starts with the most extreme table and sequentially adds more extreme ones based on the smallest *p*-value calculated by iteratively maximising the probability of a 2 × 2 table. Effect sizes were expressed as differences in percentages with 95% confidence intervals (CIs) derived by matching Barnard CSM *p*-values.

The 95% CIs for healing and survival rates were obtained with the Bayesian-derived Jeffreys method [32]. The significance level was set at 0.05, and all tests were two-sided. Data analysis was performed with the “Exact” R package [33].

3. Results

Demographic Information

A total of 38 patients requiring 40 root canal treatments were accepted to be included in the study (Figure 1). Two patients contributing with two root canal treatments (5%) were unable to complete the follow-up and were excluded. A total of 38 teeth were analysed at the end-line. Information on patient and tooth-related parameters is reported in Table 2, while obturation-related parameters are reported in Table 3a,b.

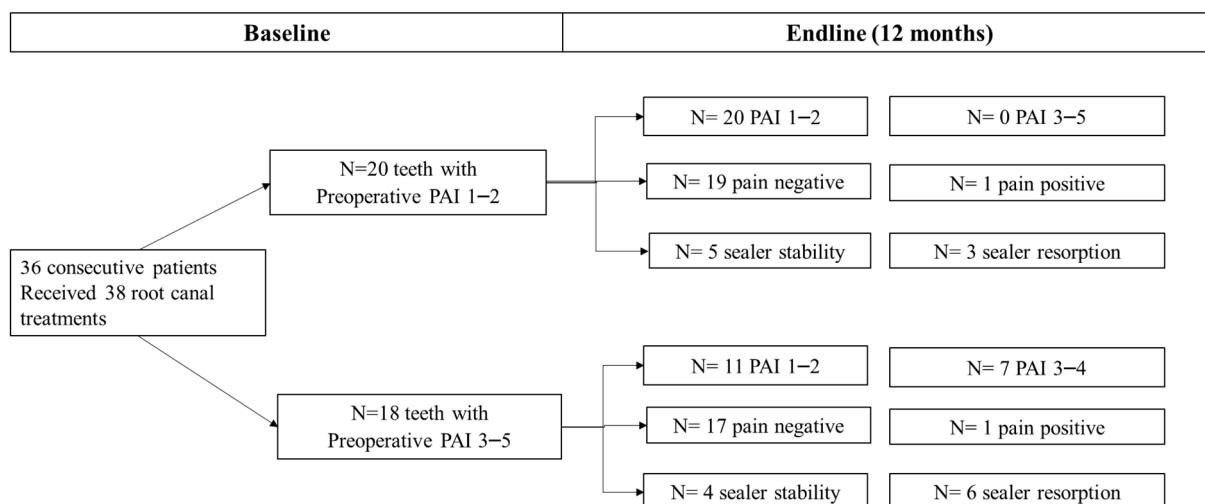


Figure 1. Endline PAI, frequency of post-operative Pain and sealer stability between teeth with pre-operative PAI 1–2 versus teeth with a preoperative PAI 3–5. No differences in post-operative pain distribution were observed at 12 months between the two groups. Two root canal treatments still presented a slight tenderness to percussion at 1-year follow-up. Teeth with preoperative PAI > 2 had a higher percentage of healing lesions and a higher percentage of sealer resorption.

Table 2. Patient and tooth-related characteristics of the study at baseline.

Characteristic	All (n = 38)
Sex	
Male	16 (42%)
Female	22 (58%)
Age group	
<30	6 (16%)
30–54	17 (45%)
≥55	15 (39%)
Tooth type	
Anterior	6 (16%)
Premolar	14 (37%)
Molar	18 (47%)
Tooth location	
Maxilla	26 (68%)
Mandible	12 (32%)
Diagnosis	
Pulpitis	20 (53%)
Pulp necrosis	8 (21%)
Re-exacerbated lesion	10 (26%)
Baseline PAI	
1–2	20 (53%)
≥3	18 (47%)
Endodontic treatment	
Root canal treatment	28 (74%)
Re-treatment	10 (26%)
Obturation	
Underfilled	4 (11%)
Adequate filling	30 (79%)
Overfilled	4 (11%)
Extrusion	
No	20 (53%)
Yes	18 (47%)
Extrusion, mm	
No extrusion	20 (53%)
0.1–2.0	9 (24%)
2.1–5.0	6 (16%)
>5.0	3 (8%)
Sealer Resorption *	
No	9 (50%)
Yes	9 (50%)

* Among extrusions (n = 18).

Table 3. (a) Patient-related characteristics of the study sample at 12-month follow-up (1–2 [healed] vs. ≥ 3 [still healing]). (b) Obturation-related parameters of the study sample at 12-month follow-up (1–2 [healed] vs. ≥ 3 [still healing]).

(a)				
Characteristic	Healed (n = 31)	Healing (n = 7)	Diff. in % s (95% CI)	p-Value
Sex				
Male	13 (42%)	3 (43%)		
Female	18 (58%)	4 (57%)	+1 (−31, +38)	0.840
Age group				
<30	5 (16%)	1 (14%)	+2 (−36, +24)	0.923
30–54	13 (42%)	4 (57%)	−15 (−47, +22)	0.550
≥ 55	13 (42%)	2 (29%)	+13 (−28, +41)	0.497
Tooth type				
Anterior	3 (10%)	3 (43%)	−33 (−65, −3)	0.029 *
Premolar	13 (42%)	1 (14%)	+28 (−13, +50)	0.202
Molar	15 (48%)	3 (43%)	+5 (−32, +37)	1.000
Tooth location				
Maxilla	22 (71%)	4 (57%)		
Mandible	9 (29%)	3 (43%)	−14 (−18, +48)	0.529
Diagnosis				
Pulpitis	18 (58%)	2 (29%)	+29 (−12, +57)	0.185
Pulp necrosis	4 (13%)	4 (57%)	−44 (−73, −9)	0.012 *
Re-exacerbated lesion	9 (29%)	1 (14%)	+15 (−25, +36)	0.472
Baseline PAI				
1–2	20 (65%)	0 (0.0%)		
≥ 3	11 (35%)	7 (100%)	−65 (−79, −25)	0.001 *
Endodontic treatment				
Root canal treatment	22 (71%)	6 (86%)		
Re-treatment	9 (29%)	1 (14%)	+15 (−25, +36)	0.472
(b)				
Characteristic	Healed (n = 31)	Healing (n = 7)	Diff. in % s (95% CI)	p-Value
Obturation				
Underfilled	4 (13%)	0 (0%)	+13 (−22, +27)	0.604
Adequate	24 (77%)	6 (86%)	−9 (−30, +31)	0.757
Overfilled	3 (10%)	1 (14%)	−4 (−41, +15)	0.439
Sealer Extrusion				
No	17 (55%)	3 (43%)		
Yes	14 (45%)	4 (57%)	−12 (−44, +25)	0.623
Sealer Extrusion, mm				
No extrusion	17 (55%)	3 (43%)	+12 (−25, +44)	0.623
0.1–2.0	8 (26%)	1 (14%)	+12 (−28, +33)	0.630
2.1–5.0	4 (13%)	2 (29%)	−16 (−53, +10)	0.221
>5.0	2 (6%)	1 (14%)	−8 (−44, +11)	0.285
Sealer Resorption †				
No	8 (57%)	1 (25%)		
Yes	6 (43%)	3 (75%)	−32 (−67, +19)	0.333

* p -value ≤ 0.05 . † Among extrusions ($n = 18$).

The pilot cohort included a high number of teeth with a periapical lesion (PAI ≥ 3) (47%), pulp necrosis (21%), and re-exacerbated periapical lesion (26%). The majority of root canal obturation length was considered adequate (79%), while 10% resulted in over-filled and 13% were underfilled. Sealer periapical extrusion was observed in a high percentage of cases (47%). Most of the radiographic extrusion resulted in smaller than 5 mm.

The cumulative percentage of healed teeth at 12 months was 82% (95% CI 67–91%). Seven out of thirty-eight teeth presented a periapical radiolucency after 12 months (18%). Cumulative survival rate was 100% (95% CI = 94–100%).

Patient-related characteristics (age, sex, tooth location, and type) did not influence the healing percentage. Interestingly, at the tooth level, the type of treatment (root canal treatment vs. retreatment) did not influence the healing percentage (p -value = 0.472). Initial PAI was significantly related to periapical healing; that is, teeth with a preoperative PAI > 2 had lower healing rates at 12 months (p -value = 0.001) (Table 3a).

As shown in Table 3b, obturation length, sealer extrusion and extrusion size did not influence the outcome (all p -values > 0.05). Interestingly, healed teeth exhibited a lower periapical sealer resorption as compared with healing teeth (43% vs. 75%), but the difference was not statistically significant due to small sample sizes (p -value = 0.333).

Tables 4 and 5 report the post-operative pain intensity according to VAS during the follow-up. No pain was observed in 84% of the cases 1 day after treatment. This percentage increased, reaching 95% at 1 year after root canal filling. No severe pain after filling was recorded in any case. A total of two root canal treatments still presented slight tenderness to percussion at 1-year follow-up. The percentage of healing was significantly influenced by post-operative pain detected at one day (p -value = 0.029), one week (p -value = 0.007), one month (p -value = 0.007), and 12 months (p -value = 0.011) after obturation; that is, patients with no pain had higher healing percentages (Table 4).

Table 4. Pain-related parameters of the study sample, overall and by periapical index (PAI) at 12-month follow-up (1–2 [healed] vs. ≥ 3 [still healing]).

Characteristics	All (<i>n</i> = 38)	Healed (<i>n</i> = 31)	Healing (<i>n</i> = 7)	Diff. in %s (95% CI)	<i>p</i> -Value
One-day pain					
No	32 (84%)	28 (90%)	4 (57%)		
Yes †	6 (16%)	3 (10%)	3 (43%)	−33 (−65, −3)	0.029 *
One-week pain					
No	34 (89%)	30 (97%)	4 (57%)		
Yes †	4 (11%)	1 (3%)	3 (43%)	−40 (−72, −11)	0.007 *
One-month pain					
No	34 (89%)	30 (97%)	4 (57%)		
Yes †	4 (11%)	1 (3%)	3 (43%)	−40 (−72, −11)	0.007 *
Twelve-month pain					
No	36 (95%)	31 (100%)	5 (71%)		
Yes †	2 (5%)	0 (0%)	2 (29%)	−29 (−66, −5)	0.011 *

* p -value ≤ 0.05 . † Visual analogue scale (VAS) ≥ 1 .

Table 5. Post-operative pain intensity according to VAS at 1 day, 7 days, 28 days and 1 year after root canal obturation.

	No Pain (0)	Mild (1–2)	Moderate (3–7)	Severe (8–10)
One day	32 (84%)	3 (8%)	3 (8%)	0 (0%)
One week	34 (89%)	4 (11%)	0 (0%)	0 (0%)
One month	34 (89%)	4 (11%)	0 (0%)	0 (0%)
Twelve months	36 (95%)	2 (5%)	0 (0%)	0 (0%)

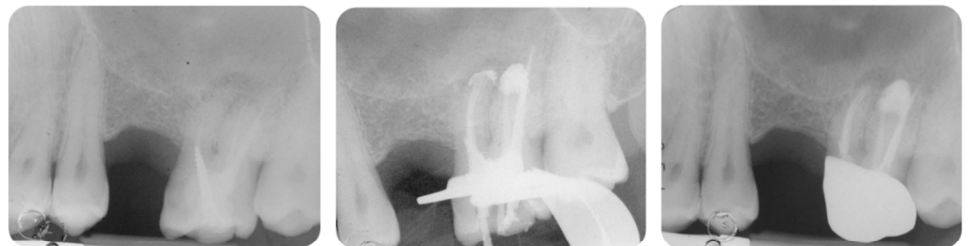
Figure 1 depicts endline PAI, frequency of post-operative pain and sealer stability between teeth with no preoperative periapical lesion (PAI 1–2) versus teeth with a preoperative periapical lesion (PAI 3–5). No differences in post-operative pain distribution were observed at 12 months between the two groups. Differently, teeth with preoperative PAI > 2 had a higher percentage of healing lesions and a higher percentage of sealer resorption. When comparing the extrusion frequencies in upper or lower jaws, we found a higher percentage of extrusions in maxillary locations, namely 12/18 teeth, when compared to the mandibular sites (6/18 teeth). Sealer resorption occurred in 6/9 maxillary teeth and 3/9 mandibular teeth.

Four representative cases included in the study are reported in Figure 2A–D.

A



B



C



D



Figure 2. (A) Upper incisor with a periapical lesion (PAI = 5). The periapical X-ray at 12 months showed resolution of the periapical pathology (PAI = 2). Note the disappearance of sealer extrusion. (B) Upper molar with previous failed root canal treatment (PAI = 4). The mesio-buccal root revealed a periapical lesion, a metal post, and an incomplete filling of the apical third. It is interesting to observe the sealer morphology after root canal obturation and after 12 months of follow-up. The extrusion around the mesio-buccal root seems to have disappeared, while the one in the palatal root is still present. No post-operative pain was reported (VAS = 0 throughout the entire treatment and follow-up). (C) Lower first molar with a deep carious lesion. Slight periapical extrusion was observed in the mesial and distal canals. Uneventful healing was observed at the 12-month follow-up. (D) Upper second premolar with a deep carious lesion and no periapical radiolucencies (PAI = 2). Slight modification of the sealer extrusion was observed at the 12-month recall.

4. Discussion

This pilot study analysed the outcome of root canal treatments filled with a recently introduced premixed CaSi-containing bioceramic sealer and warm carrier-based technique. The cumulative percentage of healed teeth was approx. 81.6%, with no extractions. The cumulative survival rate was 100%. These data are in line with previously published studies on carrier-based techniques used with an epoxy resin sealer [2–4]. A total of 8 teeth still presented a radiographically detectable periapical radiolucency at 12 months, which was stable or improved compared to the preoperative periapical lesion. Approximately half of the endodontically treated teeth had a diagnosis of necrotic pulp (21%) or a re-exacerbated periapical lesion (26%) at baseline. This condition critically affected the 12-month healing outcome, as demonstrated by the statistical analysis in Table 3a,b. Other obturation-related parameters were analysed to assess the potential effect of the sealer and technique on the healing rate of the root canal performed.

Interestingly, a high percentage of periapical sealer extrusion (47% of the total) was observed. The analysis of periapical X-rays demonstrated some modification of their morphology or partially complete disappearance over time. The extrusion, at least in the present study, is mainly composed only of sealers. Recent studies confirmed that warm-carrier-based systems may induce a great percentage of extrusion, ranging from approx. 25% to 58% of the cases [23,29]. A conventional gold-standard sealer (AH Plus), mainly composed of epoxy-resin components, offered a high percentage of radiographic extrusion (30%) [23], likely attributable to the higher flow when heating is applied [34]. In the present study, teeth that showed partial or complete resorption (and radiographic disappearance) of apical extrusion were associated with lower percentages of healing at 12 months but were not statistically significant ($p > 0.05$). Longer follow-up (4 years, according to the European Society of Endodontology) may reveal a more significant association with the effect of sealer resorption on healing outcome [35].

Only a small number of studies evaluated the presence and the role of periapical extrusion on healing and their effect on clinical results [36,37]. Previous studies found the non-significant effect of sealer extrusions on periapical healing (such as in the case of epoxy resin-based sealers and calcium hydroxide-based sealers) [36,37] as also indicated by a recent meta-analysis [38]. The sealer composition, the ability to release bioactive ions, and the bioactivity properties could influence the periapical bone healing and formation of new bone tissue detectable by radiographic inspection [39]. The biological consequences of extrusion are probably modest if the sealer is mainly composed of biocompatible components [40] that induce fast bone regeneration during their degradation and release of bioactive ions [21,23,39].

The non-complete healing observed in this study may be explained by the fact that biological phases of periapical bone remodelling need time to remove the sealer radiopacifiers and to complete the bone regeneration. Moreover, the potential bioactivity (apatite nucleation ability) of the sealer could induce the formation of hard tissue in the periapical lesion, which may appear less radio opaque than healthy periapical bone. This aspect needs to be elucidated at longer follow-up to assess if the complete resolution of the periapical healing proceeds or remains stable.

In previous times, the use of mineral trioxide aggregate (MTA) and other CaSi-based cement were tested as an approach to achieve effective sealing of wide apices [7] while simultaneously facilitating the development of a durable and biologically active barrier in proximity to the periapical bone and into the internal surface of the canal. The formation of a biocompatible, osteoconductive cement barrier can stabilise the sealing, potentially stimulating the generation of new bone tissue [41,42]. Hence, CaSi-based cements create the so-called “biomimetic remineralisation” of demineralised dentin [43,44]. Tay et al. first proposed the use of CaSi Portland-derived cements to induce the solid interfibrillar remineralisation of root demineralised dentin [43,44].

The percentage of tri Calcium Silicate component in the total sealer composition is probably lower than in the traditional powder/liquid cement. It is important to remark that the CaSi component is the bioactive ingredient of the material [43,44].

The present study analysed post-operative pain at the different end points. Post-operative pain was assessed as a patient-related outcome. A recent meta-analysis reported that root canal filling procedures are some of the most associated factors that affect post-operative pain [45]. During the obturation steps, the endodontic sealer establishes direct contact with periapical tissues. Consequently, the physical and chemical properties of the sealer could influence the magnitude of post-operative endodontic pain.

Interestingly, the persistence of (mild) pain in the first month after root canal filling was significantly associated with slower periapical healing. Two teeth presented only slight tenderness after occlusal load but no periapical recrudescence at 12 months follow-up. A previous study on a bioceramic CaSi-based sealer showed a similar trend, with an overall reduction in pain intensity during the first 1–2 weeks [29]. In another study, the authors reported that unintentional apical extrusion of calcium silicate-based root canal sealers leads to post-operative pain results that are comparable to resin-based sealers [46]. Pontoriero et al. compared four different types of bioceramic sealer and reported that the presence of post-operative pain was not affected by the extrusion of the sealer [24]. Other conditions may affect the persistence of pain after endodontic therapy, and the presence of specific microbiota (and an elevated number of pathogens) may alter the healing steps [47].

5. Conclusions

This pilot preliminary study opens new questions for the next clinical studies on bioceramic sealers. When an extrusion of sealer occurs in a periapical area with bone deficit, how will the periapical area heal? Will it form mineralised tissue, fibrous tissue, or an inert deposit of biocompatible sealer?

In theory, the extrusion of a bioactive sealer such as AH Plus Bioceramic could potentially enhance the formation of new mineralised tissue at the apex area and promote the creation of new bone and bone-like tissue at periapical levels. However, the question remains whether extrusion should be considered an index of perfect healing or merely a modest defect of therapy. It is also unclear whether extruded AH Plus Bioceramic used with the carrier-based technique will induce dentin remineralisation of the root canal. Further studies are needed to investigate the optimal amount of sealer extrusion for promoting healing and apical bone regeneration. In conclusion, it is important to note that this is an early study; a more detailed analysis of non-linear relationships across variables will be performed in the upcoming randomised clinical study. Despite the need for further research, this study supports the routine clinical use of flowable premixed sealers in combination with the warm carrier-based technique.

Author Contributions: Conceptualization, C.P. and M.G.G.; methodology, C.P.; software, A.S. and F.Z.; validation, A.S.; formal analysis, A.S., F.Z., and J.L.; investigation, C.P., A.S. and F.Z.; resources, C.P.; data curation, A.S., F.Z. and J.L.; writing—original draft preparation, C.P. and A.S.; writing—review and editing, C.P., M.G.G. and A.S.; visualisation, A.S. and F.Z.; supervision, C.P.; project administration, C.P. All authors have read and agreed to the published version of the manuscript.

Funding: This research received no external funding.

Institutional Review Board Statement: The study was approved by the ethical committee (597-2022-SPER-AUSLBO).

Informed Consent Statement: Informed consent was obtained from all subjects.

Data Availability Statement: Data available upon reasonable request.

Conflicts of Interest: The authors deny any conflicts of interest.






References

1. Mirfendereski, M.; Roth, K.; Bing, F.; Dubrowski, A.; Carnahan, H.; Azarpazhooh, A.; Basrani, B.; Torneck, C.D.; Friedman, S. Technique acquisition in the use of two thermoplasticized root filling methods by inexperienced dental students: A micro-CT analysis. *J. Endod.* **2009**, *35*, 1512–1517.
2. Pirani, C.; Zamparini, F.; Peters, O.A.; Iacono, F.; Gatto, M.R.; Generali, L.; Gandolfi, M.G.; Prati, C. The fate of root canals obturated with Thermafil: 10-year data for patients treated in a master program. *Clin. Oral Investig.* **2019**, *23*, 3367–3377.
3. Hale, R.; Gatti, R.; Glickman, G.N.; Opperman, L.A. Comparative analysis of carrier-based obturation and lateral compaction: A retrospective clinical outcomes study. *Int. J. Dent.* **2012**, *2012*, 954675.
4. Demirci, G.K.; Caliskan, M.K. A prospective randomized comparative study of cold lateral condensation versus Core/Gutta-percha in teeth with periapical lesions. *J. Endod.* **2016**, *42*, 206–210.
5. Zhou, H.M.; Shen, Y.; Zheng, W.; Li, L.; Zheng, Y.F.; Haapasalo, M. Physical properties of 5 root canal sealers. *J. Endod.* **2013**, *39*, 1281–1286.
6. Prati, C.; Siboni, F.; Polimeni, A.; Bossu, M.; Gandolfi, M.G. Use of calcium-containing endodontic sealers as apical barrier in fluid-contaminated wide-open apices. *J. Appl. Biomater. Funct. Mater.* **2014**, *12*, 263–270.
7. Pace, R.; Giuliani, V.; Nieri, M.; Di Nasso, L.; Pagavino, G. Mineral trioxide aggregate as apical plug in teeth with necrotic pulp and immature apices: A 10-year case series. *J. Endod.* **2014**, *40*, 1250–1254.
8. Sanz, J.L.; López-García, S.; Rodríguez-Lozano, F.J.; Melo, M.; Lozano, A.; Llana, C.; Forner, L. Cytocompatibility and bioactive potential of AH Plus Bioceramic Sealer: An in vitro study. *Int. Endod. J.* **2022**, *55*, 1066–1080.
9. Chybowski, E.A.; Glickman, G.N.; Patel, Y.; Fleury, A.; Solomon, E.; He, J. Clinical Outcome of Non-Surgical Root Canal Treatment Using a Single-cone Technique with Endosequence Bioceramic Sealer: A Retrospective Analysis. *J. Endod.* **2018**, *44*, 941–945.
10. Angerame, D.; De Biasi, M.; Pecci, R.; Bedini, R. Filling ability of three variants of the single-cone technique with bioceramic sealer: A micro-computed tomography study. *J. Mater. Sci. Mater. Med.* **2020**, *31*, 91.
11. Prati, C.; Gandolfi, M.G. Calcium silicate bioactive cements: Biological perspectives and clinical applications. *Dent. Mater.* **2015**, *31*, 351–370.
12. Gandolfi, M.G.; Perut, F.; Ciapetti, G.; Mongiorgi, R.; Prati, C. New Portland cement-based materials for endodontics mixed with artocaine solution: A study of cellular response. *J. Endod.* **2008**, *34*, 39–44.
13. Gandolfi, M.G.; Siboni, F.; Botero, T.; Bossù, M.; Riccitiello, F.; Prati, C. Calcium silicate and calcium hydroxide materials for pulp capping: Biointeractivity, porosity, solubility and bioactivity of current formulations. *J. Appl. Biomater. Funct. Mater.* **2015**, *13*, 43–60.
14. Gandolfi, M.G.; Van Landuyt, K.; Taddei, P.; Modena, E.; Van Meerbeek, B.; Prati, C. Environmental scanning electron microscopy connected with energy dispersive x-ray analysis and Raman techniques to study ProRoot mineral trioxide aggregate and calcium silicate cements in wet conditions and in real time. *J. Endod.* **2010**, *36*, 851–857.
15. Gandolfi, M.G.; Siboni, F.; Primus, C.M.; Prati, C. Ion release, porosity, solubility, and bioactivity of MTA Plus tricalcium silicate. *J. Endod.* **2014**, *40*, 1632–1637.
16. Primus, C.M.; Tay, F.R.; Niu, L.N. Bioactive tri/dicalcium silicate cements for treatment of pulpal and periapical tissues. *Acta Biomater.* **2019**, *96*, 35–54.
17. Primus, C.; Gutmann, J.L.; Tay, F.R.; Fuks, A.B. Calcium silicate and calcium aluminate cements for dentistry reviewed. *J. Am. Ceram. Soc.* **2022**, *105*, 1841–1863.
18. Camilleri, J.; Atmeh, A.; Li, X.; Meschi, N. Present status and future directions: Hydraulic materials for endodontic use. *Int. Endod. J.* **2022**, *55*, 710–777.
19. Zamparini, F.; Prati, C.; Taddei, P.; Spinelli, A.; Di Foggia, M.; Gandolfi, M.G. Chemical-Physical Properties and Bioactivity of New Premixed Calcium Silicate-Bioceramic Root Canal Sealers. *Int. J. Mol. Sci.* **2022**, *23*, 13914.
20. Souza, L.C.; Neves, G.S.T.; Kirkpatrick, T.; Letra, A.; Silva, R. Physicochemical and Biological Properties of AH Plus Bioceramic. *J. Endod.* **2023**, *49*, 69–76.
21. Donnermeyer, D.; Schemkämper, P.; Bürklein, S.; Schäfer, E. Short and Long-Term Solubility, Alkalizing Effect, and Thermal Persistence of Premixed Calcium Silicate-Based Sealers: AH Plus Bioceramic Sealer vs. Total Fill BC Sealer. *Materials* **2022**, *15*, 7320.
22. Zavattini, A.; Knight, A.; Foschi, F.; Mannocci, F. Outcome of root canal treatments using a new calcium silicate root canal sealer: A non-randomized clinical trial. *J. Clin. Med.* **2020**, *9*, 782.

23. Zamparini, F.; Spinelli, A.; Cardinali, F.; Ausiello, P.; Gandolfi, M.G.; Prati, C. The Use of Premixed Calcium Silicate Bioceramic Sealer with Warm Carrier-Based Technique: A 2-Year Study for Patients Treated in a Master Program. *J. Funct. Biomater.* **2023**, *14*, 164.
24. Pontoriero, D.I.K.; Ferrari Cagidiaco, E.; Maccagnola, V.; Manfredini, D.; Ferrari, M. Outcomes of Endodontic-Treated Teeth Obturated with Bioceramic Sealers in Combination with Warm Gutta-Percha Obturation Techniques: A Prospective Clinical Study. *J. Clin. Med.* **2023**, *12*, 2867.
25. World Medical Association. World Medical Association Declaration of Helsinki: Ethical principles for medical research involving human subjects. *J. Am. Med. Assoc.* **2013**, *310*, 2191–2194. <https://doi.org/10.1001/jama.2013.281053>.
26. Vandembroucke, J.P.; von Elm, E.; Altman, D.G.; Gøtzsche, P.C.; Mulrow, C.D.; Pocock, S.J.; Poole, C.; Schlesselman, J.J.; Egger, M. STROBE Initiative Strengthening the Reporting of Observational Studies in Epidemiology (STROBE): Explanation and elaboration. *Epidemiology* **2007**, *18*, 805–835.
27. Dodson, T.B. A guide for preparing a patient-oriented research manuscript. *Oral Surg. Oral Med. Oral Pathol. Oral Radiol. Endod.* **2007**, *104*, 307–315.
28. Ørstavik, D.; Kerekes, K.; Eriksen, H.M. The periapical index: A scoring system for radiographic assessment of apical periodontitis. *Endod. Dent. Traumatol.* **1986**, *2*, 20–34.
29. Fonseca, B.; Coelho, M.S.; Bueno, C.E.D.S.; Fontana, C.E.; Martin, A.S.; Rocha, D.G.P. Assessment of Extrusion and Postoperative Pain of a Bioceramic and Resin-Based Root Canal Sealer. *Eur. J. Dent.* **2019**, *13*, 343–348.
30. Barnard, G.A. A new test for 2x2 tables. *Nature* **1945**, *156*, 177.
31. Lydersen, S.; Fagerland, M.W.; Laake, P. Recommended tests for association in 2 x 2 tables. *Stat. Med.* **2009**, *28*, 1159–1175.
32. Brown, L.D.; Cai, T.T.; Das Gupta, A. Interval estimation for a binomial proportion. *Stat. Sci.* **2001**, *16*, 101–133.
33. Calhoun, P. Exact: Unconditional Exact Test. R Package Version 3.2, 2022. Available online: <https://CRAN.R-project.org/package=Exact> (accessed on 18th October 2023).
34. Donnermeyer, D.; Schäfer, E.; Bürklein, S. Real-time Intracanal Temperature Measurement during Different Obturation Techniques. *J. Endod.* **2018**, *44*, 1832–1836.
35. European Society of Endodontology. Quality guidelines for endodontic treatment: Consensus report of the European Society of Endodontology. *Int. Endod. J.* **2006**, *39*, 921–930.
36. Ricucci, D.; Rôças, I.N.; Alves, F.R.; Loghin, S.; Siqueira, J.F., Jr. Apically Extruded Sealers: Fate and Influence on Treatment Outcome. *J. Endod.* **2016**, *42*, 243–249.
37. Martins, J.F.B.; Scheeren, B.; van der Waal, S.V. The Effect of Unintentional AH-Plus Sealer Extrusion on Resolution of Apical Periodontitis After Root Canal Treatment and Retreatment-A Retrospective Case-control Study. *J. Endod.* **2023**, *49*, 1262–1268. <https://doi.org/10.1016/j.joen.2023.07.021>.
38. Aminoshariae, A.; Kulild, J.C. The impact of sealer extrusion on endodontic outcome: A systematic review with meta-analysis. *Aust. Endod. J.* **2020**, *46*, 123–129.
39. Gandolfi, M.G.; Iezzi, G.; Piattelli, A.; Prati, C.; Scarano, A. Osteoinductive potential and bone-bonding ability of ProRoot MTA, MTA Plus and Biodentine in rabbit intramedullary model: Microchemical characterization and histological analysis. *Dent. Mater.* **2017**, *33*, 221–238.
40. Geurtsen, W.; Leyhausen, G. Biological aspects of root canal filling materials—histocompatibility, cytotoxicity, and mutagenicity. *Clin. Oral. Investig.* **1997**, *1*, 5–11.
41. Von Arx, T. Mineral Trioxide Aggregate (MTA) a success story in apical surgery. *Swiss. Dent. J.* **2016**, *126*, 573–595.
42. Giacomino, C.M.; Wealleans, J.A.; Kuhn, N.; Diogenes, A. Comparative Biocompatibility and Osteogenic Potential of Two Bioceramic Sealers. *J. Endod.* **2019**, *45*, 51–56.
43. Tay, F.R.; Pashley, D.H.; Rueggeberg, F.A.; Loushine, R.J.; Weller, R.N. Calcium phosphate phase transformation produced by the interaction of the portland cement component of white mineral trioxide aggregate with a phosphate-containing fluid. *J. Endod.* **2007**, *33*, 1347–1351.
44. Tay, F.R.; Pashley, D.H. Guided tissue remineralisation of partially demineralised human dentine. *Biomaterials* **2008**, *29*, 1127–1137.
45. Mekhdieva, E.; Del Fabbro, M.; Alovisi, M.; Comba, A.; Scotti, N.; Tumedei, M.; Carossa, M.; Berutti, E.; Pasqualini, D. Postoperative Pain following Root Canal Filling with Bioceramic vs. Traditional Filling Techniques: A Systematic Review and Meta-Analysis of Randomized Controlled Trials. *J. Clin. Med.* **2021**, *10*, 4509.
46. Drumond, J.P.S.C.; Maeda, W.; Nascimento, W.M.; Campos, D.L.; Prado, M.C.; de-Jesus-Soares, A.; Frozoni, M. Comparison of Postobturation Pain Experience after Apical Extrusion of Calcium Silicate- and Resin-Based Root Canal Sealers. *J. Endod.* **2021**, *47*, 1278–1284.
47. Buonavoglia, A.; Zamparini, F.; Lanave, G.; Pellegrini, F.; Diakoudi, G.; Spinelli, A.; Lucente, M.S.; Camero, M.; Vasinioti, V.I.; Gandolfi, M.G.; Martella, V.; Prati, C. Endodontic Microbial Communities in Apical Periodontitis. *J. Endod.* **2023**, *49*, 178–189.

Disclaimer/Publisher’s Note: The statements, opinions and data contained in all publications are solely those of the individual author(s) and contributor(s) and not of MDPI and/or the editor(s). MDPI and/or the editor(s) disclaim responsibility for any injury to people or property resulting from any ideas, methods, instructions or products referred to in the content.

Root canal treatment of compromised teeth as alternative treatment for patients receiving bisphosphonates: 60-month results of a prospective clinical study

F. Zamparini^{1,2} , G. A. Pelliccioni¹ , A. Spinelli¹ , D. B. Gissi¹ , M. G. Gandolfi² 
& C. Prati¹ 

¹Endodontic Clinical Section; and ²Laboratory of Green Biomaterials and Oral Pathology, School of Dentistry, Department of Biomedical and Neuromotor Sciences (DIBINEM), University of Bologna, Bologna, Italy

Abstract

Zamparini F, Pelliccioni GA, Spinelli A, Gissi DB, Gandolfi MG, Prati C. Root canal treatment of compromised teeth as alternative treatment for patients receiving bisphosphonates: 60-month results of a prospective clinical study. *International Endodontic Journal*, **54**, 156–171, 2021.

Aim This 60-month prospective study aimed to evaluate tooth survival and healing rates after root canal treatment in patients taking bisphosphonates (BPs). Secondary outcomes were complications and clinical variables observed during and after treatment.

Methods Root canal treatment was performed using manual K-file canal instrumentation and a carrier-based filling technique with an epoxy resin-based sealer. Teeth without adequate root/crown integrity were restored by trained operators at the tissue level (TL group) to prevent occlusal/mechanical stress and to enable periapical lesion healing without the risk of root fracture. Other teeth were restored with normal occlusal contacts (OC group). Healthy patients who had undergone one or more root canal treatments of the same type constituted the control group. The relationships of the following variables to survival and health status were examined (chi-squared test and multivariate analysis, $P = 0.05$): age, gender, smoking habit, tooth location, treatment type, BPs treatment, BPs exposure, initial periapical index (PAI) and occlusal restoration. Survival curves were constructed using Kaplan–Meier analysis, with extraction serving as the end-point.

Results In total, 65 patients with 109 root canal-treated teeth who were taking BPs were included. At 60 months, data from 57 patients (52F, 5M; median age 65.7 ± 8.6 years) who had undergone 96 root canal treatments were analysed (drop-out rate = 16.9%). The survival rate was 85%, and the success rate was 76%. The control group consisted of 46 patients (21F, 25M; median age 60.3 ± 7.2 years) who had undergone 102 root canal treatments. The survival rate was 88%, with 12 teeth lost during follow-up. The success rate was 73%. In the BP group, 55 teeth were restored normally (OC group) and 41 teeth were restored at the tissue level (TL group). No difference in the success or survival rate was observed between the BP and control groups ($P > 0.05$). Univariate Kaplan–Meier analysis revealed that only tooth type significantly affected survival status in the BP group. The analysis revealed the clinical relevance of smoking, tooth location and initial PAI on patients' health status ($P < 0.05$).

Conclusion Root canal treatments and post-endodontic restoration with tissue-level filling procedures represent a safe approach for severely damaged teeth in patients receiving BPs having comparable results to root filled teeth restored with occlusal contacts and to the control group.

Keywords: Bisphosphonates, root canal treatment, prospective cohort study, MRONJ, PAI.

Received 28 May 2020; accepted 2 September 2020

Correspondence: Carlo Prati, Endodontic Clinical Section, School of Dentistry, Department of Biomedical and Neuromotor Sciences (DIBINEM), University of Bologna, Via San Vitale 59, 40125 Bologna, Italy (e-mail: carlo.prati@unibo.it).

Introduction

Bisphosphonates (BPs) comprise the major class of antiresorptive drugs for the treatment of pathosis characterized by increased bone resorption. The main uses of BPs are to manage severe bone resorption in patients with cancer-related conditions, such as bone metastases induced by the systemic dissemination of solid malignant breast, prostate and lung cancer and bone lesions caused by multiple myeloma and malignant hypercalcaemia (Fantasia 2009, Ruggiero *et al.* 2009). Oral BPs are used primarily for the treatment of osteoporosis and osteopenia. Less common uses are for Paget's disease and osteogenesis imperfecta (Marx 2003, Ruggiero *et al.* 2004, Aljohani *et al.* 2017).

Poor oral health, periodontal disease, tooth extraction and other surgical procedures, chronic dental prosthetic trauma and endodontic abscesses are the most common factors responsible for the development of medication-related osteonecrosis of the jaw (MRONJ; Hoff *et al.* 2008, Kyrgidis *et al.* 2010, Ruggiero *et al.* 2014).

MRONJ has been described as 'an avascular area of necrotic bone in the maxillofacial area, with or without exposed bone, that has been evolving for longer than 8 weeks in patients without a history of irradiation in the head and neck region' (Ruggiero *et al.* 2014). The pathophysiology of MRONJ is not well defined and is likely multifactorial (Landesberg *et al.* 2011). Osteoclastic inhibition of bone remodelling induced by BPs (Reid *et al.* 2007), the anatomic vascularization of the oral region, angiogenesis process alteration, oral microbiome dysbiosis and sustained chronic inflammation may lead to this condition (Reid *et al.* 2007, Hokugo *et al.* 2010, Allen & Burr 2011). In addition, a potential genetic marker for this association has been considered (Marozik *et al.* 2019).

Amongst the most common triggers for the development of MRONJ are tooth extraction leading to oral infections and their complications (Ficarra *et al.* 2005, Ruggiero *et al.* 2014, McGowan *et al.* 2018).

Several clinical studies have suggested that the extraction of compromised teeth must be limited, and when possible avoided, in patients receiving BP therapy to prevent the development of MRONJ (Fehm *et al.* 2009, Vahntsevanos *et al.* 2009, Saad *et al.* 2012). Similarly, patients receiving antiresorptive therapy for osteoporosis may develop the same pathosis to a lesser degree after tooth extraction or minor trauma (Lo *et al.* 2010).

For these two categories of patients, the recommendation of less-invasive alternatives to extraction, such

as root canal treatment, seems prudent (Moinzadeh *et al.* 2013).

Few data are available regarding the risk of MRONJ development in patients exposed to antiresorptive medications and undergoing less-invasive dentoalveolar procedures (Edwards *et al.* 2008, Ruggiero *et al.* 2014). Some studies have involved the consideration of root canal treatments as valid alternatives to tooth extraction, but their main aims were to analyse clinical implications and ways to avoid the onset of MRONJ or protocols to limit progression of the disease (Moretti *et al.* 2011, Moinzadeh *et al.* 2013).

No prospective study has been performed to analyse root canal treatment procedures for patients taking BPs in the medium to long term, and only a few retrospective studies are reported in the literature, with follow-up periods of 12–15 months (Hsiao *et al.* 2009, Dereci *et al.* 2016, Di Fede *et al.* 2018).

For patients affected by or at risk of developing MRONJ, a more conservative approach is to attempt to preserve all compromised teeth, thereby reducing the number of extractions and minimizing the risk of MRONJ. The concepts behind this approach are to try to avoid extraction (and related complications), to remove infected tissue from the root canal, to prevent bacterial dissemination (Foschi *et al.* 2006, Nair 2006, Ricucci & Siqueira 2011) and to preserve hopelessly compromised teeth with or without occlusal function. The removal of endodontically treated teeth from the occlusal load could prevent subsequent root fracture and extraction. Root canal-treated teeth may be more susceptible to fracture in the medium to long term due to inadequate coronal restoration or insufficient coronal structure (Ng *et al.* 2011a,b, Fransson *et al.* 2016, Prati *et al.* 2018).

This prospective cohort clinical study was performed to evaluate the tooth survival and healing rates after root canal treatment in patients receiving BPs. The secondary outcomes were complications and other clinical parameters observed during and after root canal treatment.

Materials and methods

Study design

This single-blind longitudinal prospective human cohort study was approved in 2008 by the institutional university board of the Odontostomatological Sciences Department Council.

It was conducted in the endodontic clinical department of the university's dental school between January 2009 and December 2017 by the same clinical staff. All included patients were treated according to the principles established by the Declaration of Helsinki, as modified in 2013 (World Medical Association Declaration of Helsinki 2013). Before enrolment, each patient provided written informed consent, including indication that they accepted the treatment plan and agreed to cover its costs and follow the maintenance hygiene programme. This report was written according to the Consolidated Standards of Reporting Trials guidelines for the reporting of clinical trials (STROBE statement; Vandembroucke *et al.* 2007) and following Dodson guidelines (Dodson 2007). The protocol of this study was submitted and registered to ClinicalTrials.gov (ClinicalTrials.gov Identifier: NCT04399720).

Sample size

Based on the primary outcome of tooth survival status after root canal treatment in patients taking BPs and controls, the sample size was estimated as follows. A 60-month survival rate of 0.88–0.90% was assumed in the control group of patients who had undergone root canal treatment (Chevigny *et al.* 2008a,b, Morris *et al.* 2009, Pirani *et al.* 2018, Prati *et al.* 2018). Accepting the probability of a non-significant decrease in the endodontic survival rate of 0.1% for patients taking BPs, it was calculated that the inclusion of 85–97 teeth would be sufficient to test the null hypothesis of treatment equality at $\alpha = 0.05$ with 80% power for each group. This number was increased slightly to compensate for losses during follow-up.

Patients who fulfilled the following inclusion criteria were enrolled:

1. age 40–85 years;
2. BPs treatment for ≥ 24 months;
3. at least one compromised tooth requiring endodontic treatment/retreatment.

Exclusion criteria were:

1. tooth extraction performed ≥ 3 months before patient enrolment;
2. any disease that could compromise bone healing and immune response, including hepatitis, diabetes and AIDS;
3. heavy smoking (>15 cigarettes day⁻¹; Tverdal & Bjartveit 2006);
4. pregnancy or breast feeding;

5. exposure to radiation therapy focussed on the head and neck region;
6. malignant disease directly involving the jaws.

As a control group, a cohort of healthy patients was included retrospectively according to the following strict criteria:

1. age 40–85 years;
2. no BPs treatment or use of any antiresorptive or antiangiogenic drug;
3. healthy status (ASA 1 or 2).

Exclusion criteria for the control group were:

1. ASA > 3 ;
2. diabetes;
3. any condition that could compromise bone healing or the immune response;
4. corticosteroid treatment;
5. pregnancy or breast feeding;
6. heavy smoking (>15 cigarettes day⁻¹; Tverdal & Bjartveit 2006);
7. exposure to radiation therapy focussed on the head and neck region;
8. malignant disease directly involving the jaws.

Eighty patients taking BPs (BP group) visited the endodontic clinic. In total, 15 of these patients were excluded from the study due to geographical location (patients from other cities unable to attend regular follow-up appointments; $n = 8$) and inability to attend/refusal of participation ($n = 7$).

At their first visits, patients' data (including information on age, gender, primary disease necessitating treatment with BPs and drug use) were recorded in computerized clinical files. Two trained operators performed intraoral X-ray examinations and determined initial periapical indices (PAIs; Ørstavik *et al.* 1986).

The choice of occlusal restoration type was based on the best treatment criteria (Taxel *et al.* 2014).

After careful radiographic and intraoral examination, teeth in the BP group with endodontic lesions or deep caries were allocated to the occlusal (OC) loaded restoration group (sufficient crown/root and periodontal tissues for functional occlusal restoration) or to tissue-level (TL) unloaded restoration group (highly compromised, with insufficient structure for functional restoration). In the TL group, roots were restored with gingival tissue-level restoration after root canal treatment to prevent occlusal stress and to permanently seal the root canals.

Trained operators performed the root canal treatments and restorative procedures. All teeth in the control group were restored with functional occlusal restoration (as in the OC group).

Root canal treatment

Root canal treatment procedures were similar in the BP and control groups. All procedures were conducted under local anaesthesia (Carboline, 30 mg mL⁻¹; Dentsply DeTrey, Konstanz, Germany). Briefly, rubber dam isolation was performed with careful attention to avoid damaging the soft tissues with the clamp. Straight-line access was prepared using a diamond bur mounted on a high-speed, water-cooled handpiece (W&H Dentalwerk, Bürmoos, Austria). A modified step-back instrumentation technique was used as a routine procedure; the coronal third was enlarged with No. 3 or 4 Gates Glidden burs at low speed. The working length (WL) was first determined 0.5 mm from the radiographic apex with periapical radiographs. Then, through the use of an electronic apex locator (Root ZX; Morita, Tokyo, Japan), WL was established going through 0.0 point and going back to 0.5 mm.

For each root, 5 mL 5% NaOCl (NiClor 5; OGNA, Muggiò, Italy) and 3.0 mL 10% EDTA solutions were used as canal irrigants. Intraoral radiographs were used to evaluate the WL during root canal instrumentation. For teeth with vital pulps, instrumentation and definitive restoration (OC or TL restoration) were usually performed in one session; otherwise, teeth were restored temporarily with a provisional non-eugenol dressing (Coltosol; Coltene AG, Altstätten, Switzerland).

In teeth with pulp necrosis, instrumentation and tooth restoration were performed in two separate sessions. No intracanal medication was applied to avoid and prevent any risk of tissue irritation in case of apical extrusion. A limited effectiveness of intracanal medication against bacterial biofilm was reported in a previous review (Estrela *et al.* 2009).

Root canal retreatment procedures (NSRCTs) were performed using a manual K-file only, with the addition of ultrasonic tips (StartX; Dentsply Sirona, Ballaigues, Switzerland). When necessary, an operating microscope (Zeiss Pico; Zeiss, Oberkochen, Germany) was used to detect the access to root canal orifices and to identify the presence of residual filling materials/posts.

Compacted warm gutta-percha points (Hygienic/Whaledent Inc., Cuyahoga Falls, OH, USA) or a carrier-based technique (Thermafil; Dentsply DeTrey) with AH Plus sealer (Dentsply DeTrey) were used to complete the root canal filling, which was considered to be satisfactory at 0–2 mm from the radiological apex. Filling was repeated immediately when short

filling (<2 mm from the radiological apex) or the presence of voids or unfilled canals was identified on periapical X-rays.

Tooth restoration

TL restoration in the BP group

Teeth with inadequate root/crown integrity were restored with the aim of preventing occlusal and mechanical stress and to allow healing of the periapical lesion without the risk of root fracture. Briefly, the teeth were restored (immediately or within 2 weeks) under rubber dam isolation when possible or with careful control of moisture and saliva. After removal of the Coltosol and cotton pellet with a high-speed diamond bur, remaining enamel/dentine were eliminated and a flat surface was created at or just above the approximate level of the cemento-enamel junction. Gutta-percha was removed to obtain a cavity with a depth of 2.0 mm.

Self-etching dentinal bonding agent primer and bonding (Clearfil SE BOND; Kuraray, Osaka, Japan) were applied to the cavity and on the dentine (enamel) surface and photocured for 30 s (Elipar; 3M ESPE, St. Paul, MN, USA; Prati *et al.* 2005). A resin-reinforced glass-ionomer cement was then applied to fill the cavity (Vitrebond LC; 3M), and a second layer of bonding was applied and photocured. A flowable composite resin (and, when possible, a high-filled composite resin) was applied incrementally in 1.0-mm layers (Gradia Flow; GC Corporation, Tokyo, Japan; Prati *et al.* 1992). Each layer was photocured for 30 s.

OC restoration in the BP and control groups

Teeth with adequate root/crown integrity were restored with the aim of completely functional (and aesthetic) restoration. Briefly, the teeth were restored (immediately or within 2 weeks) under rubber dam isolation. When indicated, posts were placed in roots with adequate morphology (i.e. distal roots of mandibular first molars). The post space was prepared with sizes 4, 3 and 2 Gates Glidden drills, etched with 35% phosphoric acid for 15 s, rinsed with water for 10 s and dried with paper points. Carbon posts (Tech 2000 XOP; Isasan, Rovello Porro, Italy) were cemented with Scotchbond 1/RelyX ARC (3M).

Self-etching dentinal bonding agent primer and bonding (Clearfil SE BOND; Kuraray) were applied and photocured (Elipar; 3M ESPE) for 30 s followed by incremental application of flowable (Gradia Flow;

GC Corporation) and high-filled composite resins (Gradia; GC Corporation) in 1mm layers, each photocured for 30 s. All definitive restorations were occlusally loaded.

Outcome evaluation and disease staging

Intraoral periapical radiographs and clinical criteria were used to classify final outcomes. At an annual routine hygiene appointment, one of the two operators who had performed root canal treatment assessed each patient's coronal/crown and radiographic periapical status. The periapical index (PAI; Ørstavik *et al.* 1986), determined by two trained single-blind operators, was used for baseline (pre-operative) diagnosis and end-point evaluation (at 60 months). Calibration was performed using well-defined instructions and periapical radiographs with different periapical lesion scores.

Teeth were defined as healthy when they showed no sign of a periapical lesion (PAI 1 or 2) and no other clinical sign or symptom requiring an additional intervention during follow-up. These teeth were used to define the success rate (Prati *et al.* 2018).

Endodontic lesions were diagnosed based on radiological signs of endodontic disease (PAI ≥ 3) during follow-up. In the presence of acute symptomatology, such as periapical re-exacerbation or endodontic abscess with pus, swelling and pain, root canal retreatment was performed. Retreatment was also performed in all cases of loss of coronal restoration integrity.

The survival rate was determined by calculating the total numbers of healthy teeth and those with endodontic lesions (Prati *et al.* 2018).

Irrespective of the number of treated roots, the tooth was always the unit of evaluation, with classification performed according to the worst/highest value amongst roots.

Causes of extraction during follow-up were recorded in a spreadsheet.

Statistical analyses

Descriptive analyses were performed at the patient and tooth levels; means (standard deviations) or proportions and were computed and bivariate tables were constructed according to the parameter type (quantitative or qualitative), the clustering effect within patients was considered.

Non-parametric (chi-squared and Fisher's exact) tests were used to evaluate differences in demographic

characteristics between the BP and control groups. Patients were summarized as follows: age (≤ 65 vs. >65 years), sex (female vs. male), smoking status (smoker vs. non-smoker) and number of teeth receiving root canal treatment (1 vs. 2 vs. ≥ 3). Tooth characteristics were summarized as follows: location (anterior vs. premolar vs. molar), treatment type (RCT vs. NSRCT) and pre-operative PAI (1 or 2 vs. 3–5).

Kaplan–Meier survival analysis was performed to examine the times to tooth survival and healthy status. The loss of survival status was defined as the time from root canal treatment to extraction or ONJ appearance in the BP group. Loss of healthy status was defined as the time from root canal treatment to the appearance of a periapical lesion (symptomatic or asymptomatic) and/or endodontic need for reintervention. Patients were followed from the date of root canal treatment (or pre-operative diagnosis) to the occurrence of an event or censored at the last follow-up visit.

Survival rates were estimated using the Kaplan–Meier method. Statistical significance was evaluated using the log-rank test. In the BP group, the relationships of the following variables to tooth survival and healthy status were analysed: length of BP exposure (≤ 3 vs. ≥ 2 years), primary indication for BP treatment (prevention of bone metastasis in oncological patients vs. osteometabolic diseases), type of BP treatment, root canal treatment (primary vs. secondary) and restoration (loaded vs. non-loaded). The relationships of group allocation (BP vs. control) to survival and healthy status were evaluated, and a multivariable analysis of patient (age, sex, smoking status) and tooth (location, treatment type, baseline PAI) variables was performed. Variables found to be significant in univariate analysis were evaluated further in a Cox proportional-hazards model with stepwise bidirectional selection (significance level for entry/removal = 0.05). Hazard ratio and 95% confidence intervals were estimated using robust standard error to allow for clustering within patients. *P* values < 0.05 were considered to be significant in all analyses.

Results

Study population

BP group

In total, 65 patients (59 females, six males; median age 64.6 ± 8 years) with 109 root canal-treated teeth were included in the study (Fig. 1). Of them, 29 patients reported BP treatment for oncological reasons

and 36 patients were prescribed BPs for osteometabolic reasons.

The length of BP treatment ranged from 22 to 140 months; the types of BP treatment are summarized in Table 1. Eight patients (13 teeth) failed to attend 60-month follow-up appointments; four patients had severe oncological complications, two patients were unable to attend these appointments, and two patients had died. The overall drop-out rate was 16.9%. At 60 months, data from 57 patients (52 females, five males; median age 65.7 ± 8.6 years) with 96 root canal-treated teeth were analysed. Most (41/96) of the treated teeth were molars, followed by premolars (31/96) and anterior teeth (24/96).

Control group

The control group consisted of 46 patients (21 females, 25 males; median age 60.3 ± 7.2 years) who underwent a total of 102 root canal treatments performed in the same department by the same clinical team.

Demographic characteristics and root canal treatments for the two groups are summarized in Table 2. The two groups do not differ significantly in mean age, smoking status, tooth location, tooth type, root

canal treatment type or baseline PAI ($P = 0.95$). The sex distribution differed significantly between groups ($\chi^2 = 25.6$, $P < 0.05$).

Coronal restoration

Root canal-treated teeth in the two groups were divided based on coronal restoration. In the BP group, 55 teeth were rehabilitated normally (OC group) and 41 teeth were restored at the tissue level (TL group). In the control group, all 102 teeth were rehabilitated normally (Table 2).

Most (41/96) treated teeth in the BP group were molars, followed by premolars (31/96) and anterior teeth (24/96; Table 2). Periapical radiolucency (PAI ≥ 3) was identified in 39% of root canal-treated teeth in the BP group.

In the control group, 42/102 teeth were molars, and 40/102 teeth showed periapical radiolucency before treatment (Table 2).

Tooth survival

BP group

The tooth survival rate was 85%, as 82 root canal-treated teeth were still present at the end of the study

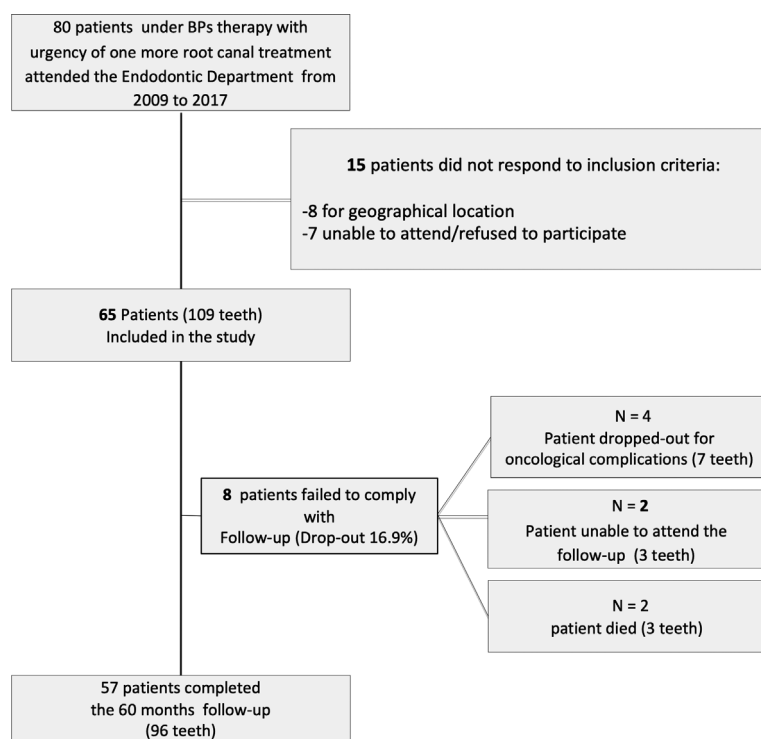


Figure 1 Study flowchart of patients receiving BPs enrolment and drop-out.

Table 1 List of BPs assumption of patients included in the study

	Type BPs	Primary indication	Relative potency ^a	Patients (n)
Alendronate	NBPs	Osteoporosis	1000	21
Clodronate	BPs	Osteoporosis	10	8
Risedronate	NBPs	Osteoporosis	5000	1
Zoledronate	NBPs	Bone metastases	10 000+	27
Neridronate	NBPs	Breast cancer	100	2
Ibandronate	NBPs	Osteoporosis	10 000	6

BPs, Bisphosphonate; NBPs, nitrogen-containing Bisphosphonate.

^aRelative to etidronate (1).

period. Of these teeth, 73 were healthy (PAI ≤ 2) and nine showed periapical radiolucency (PAI ≥ 3), which remained stable or improved slightly. No periapical re-exacerbation or abscess was observed in these cases.

The cumulative success rate was 76%. In total, 14 teeth were lost during follow-up for reasons indicated in Fig. 2. Six of the 14 failures were attributable to periodontal disease. Two (2.1%) adjacent mandibular incisors were lost due to MRONJ after root canal treatment.

Representative periapical radiographs are provided in Fig. 3.

Univariate Kaplan–Meier analysis revealed that only tooth type was related to survival status in the BP group; the survival rate was significantly higher for posterior than for anterior teeth (90.3% vs. 70.8%; $\chi^2 = 6.12$, $P < 0.05$). This analysis also revealed that smoking status, tooth location and baseline PAI were related to healthy tooth status at 60 months (Table 3). Stepwise model selection showed that smoking was the only variable related independently to a worse tooth health status (Table 4).

BP group versus control group

The tooth survival rate in the control group was 88%, as 12 teeth were lost during follow-up. Causes of extraction were tooth fracture (58%) and periodontal disease (42%). The success rate was 73%, as 74 teeth had no sign of periapical radiolucencies and 16 teeth had asymptomatic periapical radiolucencies (16%). Non-surgical retreatments were performed on three of these 16 teeth due to periapical re-exacerbation.

Figure 4 shows tooth outcomes and complications occurring during the 60-month follow-up period. The survival status did not differ significantly between the BP and control groups, as evidenced by Kaplan–Meier survival curves reported in Fig. 5.

Multivariate analyses revealed a higher survival rate of treated teeth amongst non-smokers

Table 2 Demographic characteristics of the group BPs and control group included in the study and followed for 60 months

	BPs Group	Control group	Test (P value)
No. of patients	57	46	
Median age	65.7 ± 8.6	60.3 ± 7.2	$P = 0.35$
Sex	5 males	25 males	$P < 0.05^*$
	52 females	21 females	
Smoking status	6 Yes	10 Yes	$P = 0.12$
	51 No	36 No	
Number of teeth with root canal treatment per patient	41 Single teeth	25 Single teeth	$P = 0.85$
	10 Two teeth	9 Two teeth	
	6 Three or multiple teeth	12 Three or multiple teeth	
No. of teeth	96	102	
Tooth type	24 anterior	20 anterior	Chi 1.3
	31 premolars	40 premolars	$P = 0.51$
	41 molars	42 molars	
Maxilla-mandible location	54 maxilla	57 maxilla	Chi 0.03
	42 mandible	45 mandible	$P = 0.95$
Endodontic treatment	80 RCT	81 RCT	Chi 0.5
	16 NSRCT	21 NSRCT	$P = 0.47$
Initial PAI	58 < 3	62 < 3	Chi 0.003
	38 ≥ 3	40 ≥ 3	$P = 0.95$
Restoration	55 Loaded (OC)	102 Loaded (Ctrl)	
	41 Unloaded (TL)	0 Unloaded (TL)	

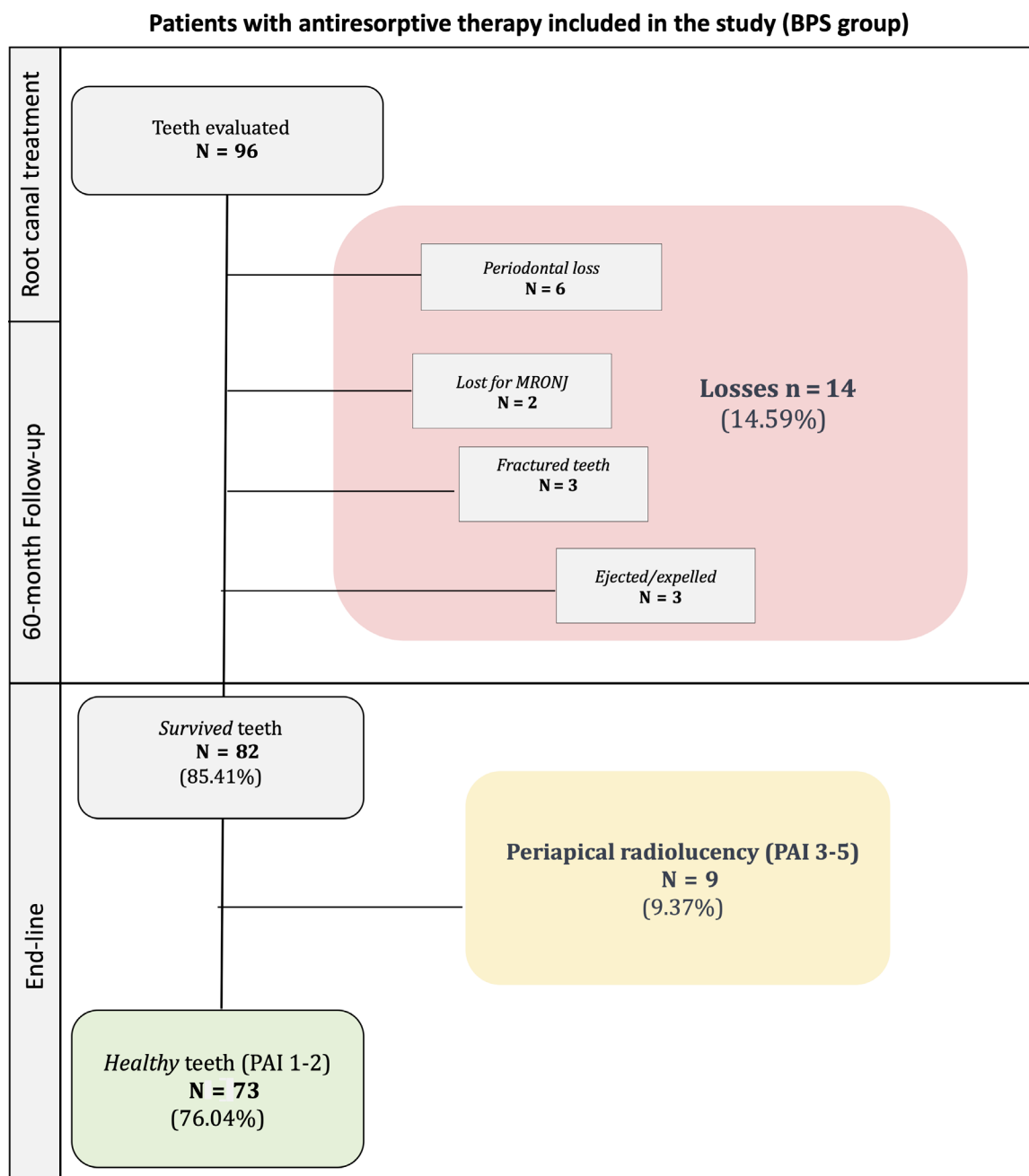


Figure 2 Flowchart of root canal treatments performed in the BPs group and final outcome at the endline (after 60 months).

in the control group than of those amongst non-smokers in the BP group ($\chi^2 = 6.6$, $P < 0.05$). They also revealed a higher healthy status rate for treated maxillary teeth in the BP group than in the control group ($\chi^2 = 4.1$, $P < 0.05$; Table 5).

Relationship of definitive restoration to tooth survival and healthy status

Table 6 shows the outcomes of root canal-treated teeth in relation to occlusal restoration in the BP and control groups at 60 months. Survival curves for the BP group according to definitive restoration are provided as Fig. 5.

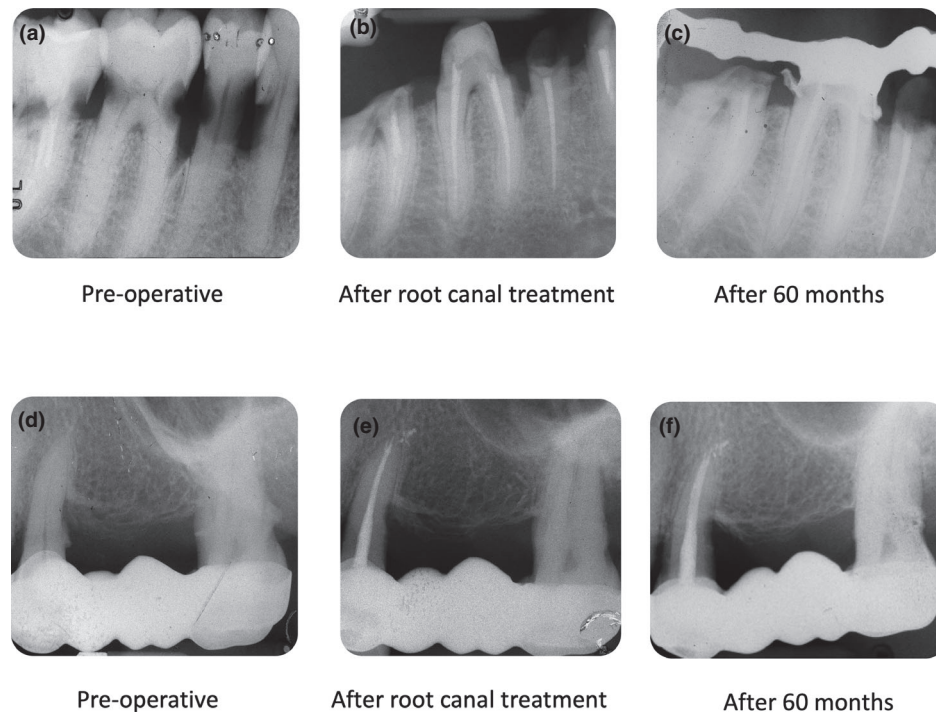


Figure 3 Series of periapical radiographs of patients under BPs therapy enrolled in the study and followed for 60 months. (a) 68-year patient with zoledronate-endovenous therapy started for multiple myeloma. Root canal treatment was performed on teeth 4.7, 4.6, 4.5 and 4.4 due to multiple deep caries lesion with no periapical radiolucency (Initial PAI was 1 in all cases). (b) roots were shaped with manual step-back instrumentation and filled with carrier-based technique and epoxy resin based sealer. Due to the large coronal destruction of tooth 4.7 and 4.5, these two teeth were restored at tissue level (TL group), the other teeth were rehabilitated with occlusal contact restorations (OC group). (c) At the end-line all teeth demonstrated no periapical radiolucency (PAI \leq 2). (d) 84-year patient assuming neridronate for metastatic breast cancer with acute symptomatology on 2.4 and tenderness to percussion. Initial PAI was 1 in all cases. (e) Single session root canal treatment was performed using a manual step-back instrumentation and a carrier-based filling technique with epoxy resin based sealer. (f) No sign of periapical radiolucency was observed at 60-month follow-up (PAI = 1).

The survival rate tended to be higher for teeth in the TL group than for those in the OC and control groups, although this difference was not significant ($P = 0.093$). The timing of extractions differed amongst these three groups. In the control group, most extractions were performed several years (≥ 36 months) after initial treatment; in the OC group, most extractions were performed in the first 2 years after root canal treatment.

Discussion

The clinical practice concept underlying this study was to prevent the onset of MRONJ in patients taking BPs. The number of tooth extractions was reduced, and every tooth was endodontically treated with at least minimal periodontal stability and root structure. Information on rates of tooth survival and root canal

treatment success in this group of patients is limited due to the patients' medical conditions and disease progression. To prevent the fracture (and extraction) of root canal-treated teeth, several roots were kept free from occlusal and mechanical stress by limiting their restoration to the gingival tissue level, similar to the concept of tissue-level implant placement. Results were similar in the TL and OC groups relative to the control group.

The few recorded endodontic complications (i.e. abscess) and the low prevalence of secondary caries and root fractures in the TL group support the concept that hopelessly compromised teeth can be preserved with root canal treatment and occlusion-free restorations.

A survival rate of approximately 85% and a success rate of 75% were observed in the BP group, similar to the rates in the control group and in line with data

Table 3 Pre-operative, intra-operative and post-operative variables in the BPs group in terms of survival status and healthy status

	Survived teeth					Healthy teeth				
	<i>N</i>	%	<i>P</i>	Adjusted HR (95% CI) ^a	Robust SE ^a	<i>N</i>	%	<i>P</i>	Adjusted HR (95% CI) ^a	Robust SE ^a
Pre-operative parameters										
Sex										
Male <i>N</i> = 19	16	84.2	0.9	0.92 (0.13–6.4)	0.91	14	73.7	0.8	0.89 (0.19–4.1)	0.68
Female <i>N</i> = 77	66	85.7				59	76.7			
Age										
<65 <i>N</i> = 28	25	89.3	0.47	1.58 (0.38–6.6)	1.03	21	75	0.9	0.99 (0.35–2.77)	0.52
≥65 <i>N</i> = 68	57	83.8				52	76.5			
Smoking habits										
Smoker <i>N</i> = 6	4	66.7	0.18	2.64 (0.59–11.8)	2.02	2	33.4	0.01*	3.61 (1.37–9.46)	1.77
No smoker <i>N</i> = 90	78	86.7				71	78.9			
Tooth location										
Maxilla <i>N</i> = 54	48	88.9	0.26	1.79 (0.61–5.31)	0.99	46	85.2	0.02*	2.57 (1.07–6.16)	1.15
Mandible <i>N</i> = 42	34	80.9				27	64.3			
Tooth type										
Anterior <i>N</i> = 24	17	70.8	0.013*	0.57 (0.27–1.18)	0.21	16	66.7	0.14	0.86 (0.464–1.59)	0.27
Premolar <i>N</i> = 41	29	93.5				27	87.1			
Molar <i>N</i> = 31	36	87.8				30	73.2			
Initial PAI score										
PAI ≤ 2 <i>N</i> = 58	49	84.5	0.71	0.89 (0.58–1.34)	0.19	49	84.5	0.04*	1.24 (0.89–1.71)	0.2
PAI ≥ 3 <i>N</i> = 38	33	86.8				24	63.2			
Length of BPs exposure										
<3 years <i>N</i> = 34	30	88.2	0.61	1.34 (0.27–6.48)	1.08	26	76.5	0.93	1.03 (0.37–2.87)	0.54
≥3 years <i>N</i> = 62	52	83.9				47	75.8			
Indication for BPs assumption										
Oncological <i>N</i> = 36	34	94.4	0.056	3.82 (0.45–32.3)	4.16	30	83.3	0.16	1.88 (0.59–6.02)	1.12
Osteometabolic <i>N</i> = 60	48	80				43	71.7			
Type BPs										
Zoledronate <i>N</i> = 38	34	89.5	0.4	0.62 (0.12–3.25)	0.52	30	78.9	0.58	0.79 (0.25–2.53)	0.47
Others BPs <i>N</i> = 58	48	82.8				43	74.4			
Intra-operative parameters										
Endodontic treatment										
RCT <i>N</i> = 80	70	87.5	0.21	2.04 (0.59–7.01)	1.29	63	78.7	0.16	1.89 (0.74–4.87)	0.91
NSRCT <i>N</i> = 16	12	75				10	62.5			
Post-operative parameters										
Restoration										
Unloaded (TL) <i>N</i> = 41	38	92.7	0.08	2.91 (0.69–12.3)	2.15	34	82.9	0.15	1.87 (0.75–4.65)	0.87
Loaded (OC) <i>N</i> = 55	44	80				39	70.9			

Entries in bold and with asterisk(*) indicate significant *P* values ($P < 0.05$) of variables related to survival status and healthy status during follow-up period.

^aConfidence interval (CI) for hazard ratio (HR) and Standard Error (SE) estimated using robust standard error to allow for clustering within patients.

from healthy patients in several medium–long-term studies (Hsiao *et al.* 2009, Ng *et al.* 2011, Pirani *et al.* 2015).

Tooth survival rates were similarly high in the TL and OC group, suggesting that tissue-level retention is useful to avoid the performance of surgical procedures on hopeless/unrestorable teeth, which potentially triggers osteonecrosis in patients with oncological or osteometabolic pathologies.

Table 4 Statistically significant variables by multivariate analysis related to healthy status

Parameters	Hazard ratio	95% confidence interval	df	<i>P</i>
Smoking habits	3.26	1.103–9.650	1	0.03*
PAI score	1.74	0.734–4.148	1	0.208
Tooth location	2.19	0.904–5.302	1	0.08

Entries in bold and with asterisk(*) indicate significant *P* values ($P < 0.05$).

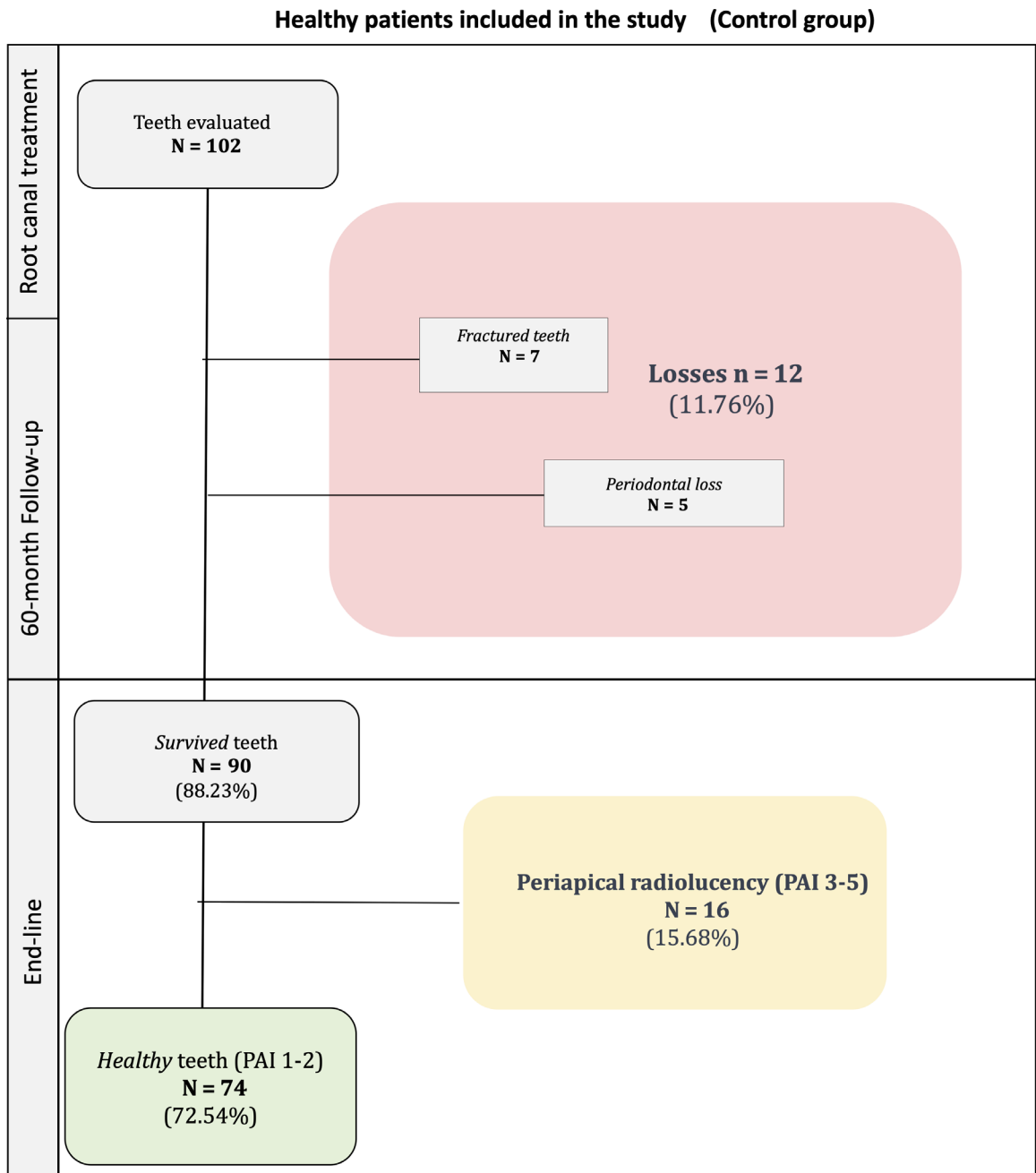


Figure 4 Flowchart of root canal treatments performed in the control group and final outcome at the endline (after 60 months).

Few authors have reported the outcomes of root canal treatment in BP-treated patients (Hsiao *et al.* 2009, Dereci *et al.* 2016). In a retrospective study, Hsiao *et al.* (2009) observed a 12-month healing rate of approximately 75% after root canal treatment in patients taking oral BPs for osteometabolic reasons.

Dereci *et al.* (2016) evaluated the root canal treatment success rate in patients taking zoledronate and observed a larger percentage of incomplete healing at 12 months amongst patients on longer-term therapy.

In this study, the absence of a previous periapical lesion and non-smoking status improved the 60-

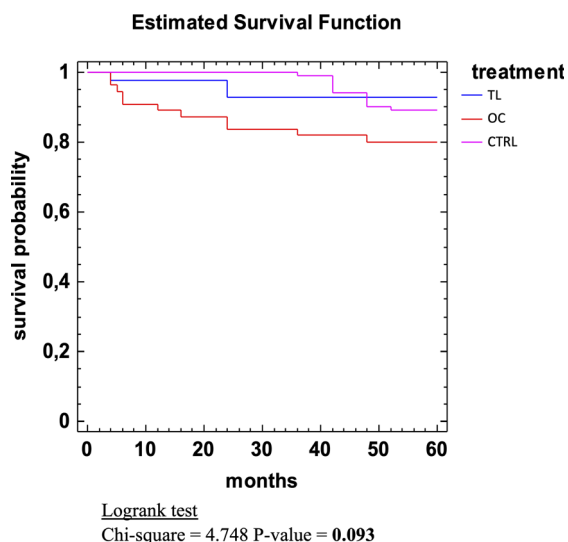


Figure 5 Kaplan–Meier survival curve of TL, OC and CTRL group. Chi-square test = 4.74. TL = tissue level unloaded. OC = occlusal loaded. CTRL = control.

month healing outcome in the BP group significantly ($P < 0.05$).

Interestingly, the reason for BP treatment (oncological vs. osteometabolic disease) and duration of treatment did not significantly affect the outcomes, possibly due to the tissue-level restoration of a large number of teeth to avoid extraction.

These results support the concept that root canal treatment performed according to specific recommendations is safe for patients taking BPs for oncological and osteometabolic pathosis and that it represents a valid alternative to tooth extraction. These findings are in agreement with those of Di Fede *et al.* (2018), where the extraction rate was approximately 15%. These root canal-treated teeth were at high risk of failure, and doomed to extraction; they were not extracted during the patients' first appointments because of BP use. No patient who had a tooth extracted (vs. spontaneous loss) developed MRONJ.

Table 5 Comparison of survival status and healthy status in BPs group and control group in terms of pre-operative and intra-operative variables

	Survival status					Healthy status				
	BPs Group n (%)	Control group n (%)	P value	Adjusted HR (95% CI) ^a	Robust SE ^a	BPs Group n (%)	Control group n (%)	P value	Adjusted HR (95% CI) ^a	Robust SE ^a
Sex										
Males	16 (84.2)	57 (85.1)	0.8	0.85 (0.79–9.28)	1.04	14 (73.7)	48 (71.6)	0.97	1.02 (0.18–5.6)	0.89
Females	66 (85.7)	34 (97.1)	0.07	0.19 (0.02–1.53)	0.2	59 (76.6)	26 (74.3)	0.99	0.99 (0.42–2.37)	0.44
Age										
<65	25 (89.3)	68 (87.2)	0.8	1.12 (0.17–7.25)	1.07	21 (75)	53 (67.9)	0.55	1.27 (0.44–3.62)	0.68
>65	57 (83.8)	23 (95.8)	0.13	0.24 (0.03–1.87)	0.25	52 (76.5)	21 (87.5)	0.22	0.48 (0.13–1.75)	0.32
Smoking habits										
No	78 (86.7)	78 (97.5)	0.009*	0.18 (0.04–0.81)	0.14	71(78.9)	63 (78.7)	0.7	0.91 (0.43–1.94)	0.35
Yes	4 (66.7)	13 (59.1)	0.97	0.98 (0.15–6.32)	0.93	2 (33.4)	11 (50)	0.44	0.66 (0.18–2.4)	0.43
Tooth type										
Anterior	17 (70.8)	18 (90%)	0.09	0.29 (0.38–2.21)	0.3	16 (66.7)	16 (80)	0.23	0.5 (1.22–2.02)	0.36
Premolar	29 (93.5)	36 (87.9)	0.45	1.85 (0.85–12.31)	1.77	27 (87.1)	25 (61)	0.06	3.13 (0.95–10.3)	1.91
Molar	36 (87.9)	37 (90.2)	0.69	0.76 (0.14–4.07)	0.65	30 (73.2)	33 (80.5)	0.43	0.7 (0.24–2.03)	0.38
Tooth location										
Maxilla	48 (88.9)	49 (85.9)	0.73	1.2 (0.2–7.3)	1.1	46 (85.2)	35 (66.7)	0.04*	2.23 (0.77–6.42)	1.2
Mandible	34 (80.9)	42 (93.3)	0.07	0.32 (0.09–1.19)	0.21	27 (64.3)	36 (80)	0.07	0.5 (0.21–1.2)	0.22
Initial PAI										
PAI < 3	49 (84.5)	54 (87.1)	0.5	0.76 (0.11–4.99)	0.73	49 (84.5)	51 (82.3)	0.9	1.05 (0.21–5.34)	0.87
PAI ≥ 3	33 (86.8)	37 (92.5)	0.38	0.54 (0.14–2.07)	0.37	24 (63.2)	23 (57.5)	0.79	1.08 (0.59–1.98)	0.33
Endodontic treatment										
RCT	70 (87.5)	74 (91.4)	0.36	0.64 (0.17–2.48)	0.44	63 (78.7)	62 (76.5)	0.89	1.04 (0.48–2.28)	0.42
NSRCT	12 (75)	17 (80.9)	0.57	0.67 (0.9–5.09)	0.7	10 (62.5)	12 (57.1)	0.94	1.04 (0.28–3.8)	0.69
Total	82 (85.4)	91 (89.2)	0.33	0.68 (0.16–2.94)	0.51	73 (76)	74 (72.5)	0.78	1.07 (0.49–2.38)	0.44

Entries in bold and with asterisk (*) indicate significant P values ($P < 0.05$).

^aConfidence interval (CI) for hazard ratio (HR) and standard error (SE) estimated using robust standard error to allow for clustering within patients.

Table 6 Outcome of root treated teeth in relation to occlusal restoration after 60-month follow-up ($n = 198$)

Groups	BPs group		Control group	
	Loaded (OC) n (%)	Unloaded (TL) n (%)	Loaded n (%)	Total n (%)
PAI 1–2 (healthy)	39 (70.9)	34 (82.9)	74 (72.5)	145 (73.2)
PAI 3–4 (periapical radiolucency)	5 (9.1)	4 (9.7)	16(15.7)	25 (12.6)
Extracted for perio	6 (10.9)	0	5 (4.9)	10 (5.1)
Lost for MRONJ	0	2 (4.8)	0	2 (1.0)
Extracted for fracture and large secondary caries	3 (5.4)	0	7 (6.8)	13 (8.1)
Ejected (expelled)	2 (3.6)	1(2.4)	0	3 (1.5)
Total	55	41	102	198

Smoking was found to significantly affect the 60 months healing status in the BPs group; non-smoker patients had a higher healthy status compared to smoker patients (as shown in Table 3, $P = 0.01$). A higher prevalence of periapical radiolucencies in smoking patients has been described with moderate evidence in a recent systematic review (Pinto *et al.* 2020a). Smoking was also significantly associated with a negative tooth survival status when comparing root canal treatment performed in BPs patients and treatment performed in healthy patients (as shown in Table 5).

It is known that smoking induces delayed bone repair (Kubota *et al.* 2016) and impaired inflammatory response, due to vasoconstriction and reduction of local oxygenation, restricting the inflow of nutrients and oxygenation in the local tissue (Segura-Egea *et al.* 2015). A immunohistological study suggested a more intense inflammatory infiltrate, extensive areas of bone resorption and higher immunoreaction against RANKL antibodies in animals exposed to nicotine compared to not exposed specimens (Pinto *et al.* 2020b). It may be expected that this effect may be increased in patients with low-immune response such as in patients taking antiresorptive medications (i.e. BPs).

A useful strategy to reduce the MRONJ incidence in patients receiving BPs could be the implementation of preventive measures in this class of patients.

In a clinical study (Dimopoulos *et al.* 2009), the use of a mouthwash, antibiotic therapy and the performance of less-invasive surgery yielded a significant (almost three-fold) decrease in zolendronate-related osteonecrosis. In endodontics, the use of a chlorhexidine rinse before root canal treatment, antibiotic administration, taking care not to harm gingival tissues with the rubber dam clamp (Kyrgidis *et al.* 2011) and lack of vasoconstrictor use during anaesthesia may account for the low incidence of MRONJ in the present study.

Hasegawa *et al.* (2017) demonstrated that MRONJ was associated significantly with traumatic surgical procedures, such as root amputation and single-tooth extraction, and wound non-closure. Other authors have recommended the use of surgery with the primary intention of closure or atraumatic avulsion with the secondary intention of closure in the presence of unrestorable or compromised teeth (Migliorati *et al.* 2013).

MRONJ develops after treatment with nitrogen-containing BPs (ibandronate and zoledronate), as described in numerous review articles (Russell *et al.* 2008, Ruggiero *et al.* 2014). Nitrogen-containing BPs are more potent than classical BPs.

Instrumentation into the apical area should be avoided, as it may be a potential risks of infected debris being extruded apically. It should be clarified that in the present protocol, WL was established at 0.5 mm from the radiological apex, to avoid over instrumentation. The Root ZX was used in the present study as demonstrated a satisfactorily establishment of the WL in accordance with a previous study (Bernardes *et al.* 2007), reaching a WL within 1 mm from the anatomical apex in 97.4% of the cases and 81.6% within 0.5 mm. At the same time, overfilling during root canal treatment is not recommended in patients on antiresorptive therapy because of irritation and cytotoxicity (Moinzadeh *et al.* 2013).

The cytotoxicity of AH Plus, an epoxy-based root canal sealer, decreases significantly after complete setting, which occurs after 3 days (Siboni *et al.* 2017, Jung *et al.* 2018).

Overall, the BPs group had similar survival and healing outcomes when compared to the control group. Only smoking habits negatively influenced tooth survival in the BPs group compared to the control group, whilst other critical parameters, such as initial PAI and type of endodontic treatment (RCT/NSRCT), did not reveal differences in terms of survival

and healthy status ($P > 0.05$; Table 5). The reason of these data may be that in all cases, a similar instrumentation and filling protocol was performed.

This study has several limitations. First, a second control group with hopeless teeth that were extracted was not included for the evaluation of clinical complications of the surgical technique. Second, the control group was enrolled retrospectively. This group consisted of healthy patients treated by the same clinical staff using a similar root canal treatment and restoration protocol. A limitation of the clinical procedure was the relative operative difficulty of rubber dam positioning and root canal shaping. In addition, the aesthetic and functional results of TL treatment are largely inadequate.

Conclusion

Root canal treatment and post-endodontic restoration with tissue-level restoration represent a safe approach for hopeless, severely damaged teeth in patients on bisphosphonate therapy. Tissue-level treatment was able to maintain hopeless teeth with comparable results to teeth restored with occlusal contacts and the control group.

Acknowledgements

The protocol of this study was submitted and registered to ClinicalTrials.gov (ClinicalTrials.gov Identifier: NCT04399720).

Conflict of interest

The authors have stated explicitly that there are no conflicts of interest in connection with this article.

References

- Aljohani S, Fliefel R, Ihbe J, Kühnisch J, Ehrenfeld M, Otto S (2017) What is the effect of anti-resorptive drugs (ARDs) on the development of medication-related osteonecrosis of the jaw (MRONJ) in osteoporosis patients: a systematic review. *Journal of Cranio-Maxillofacial Surgery* **45**, 1493–502.
- Allen MR, Burr DB (2011) The pathogenesis of bisphosphonate related osteonecrosis of the jaw: so many hypotheses, so few data. *Journal of Oral and Maxillofacial Surgery* **67**, 61–70.
- Bernardes RA, Duarte MA, Vasconcelos BC et al. (2007) Evaluation of precision of length determination with 3 electronic apex locators: root ZX, Elements Diagnostic Unit and Apex Locator, and RomiAPEX D-30. *Oral Surgery, Oral Medicine, Oral Pathology, Oral Radiology, and Endodontology* **104**, 91–4.
- De Chevigny C, Dao TT, Basrani BR et al. (2008a) Treatment outcome in endodontics: the Toronto study—phases 3 and 4: orthograde retreatment. *Journal of Endodontics* **34**, 131–7.
- De Chevigny C, Dao TT, Basrani BR et al. (2008b) Treatment outcome in endodontics: the Toronto study—phase 4: initial treatment. *Journal of Endodontics* **34**, 258–63.
- Dereci Ö, Orhan EO, Irmak Ö, Ay S (2016) The effect of the duration of intravenous zoledronate medication on the success of non-surgical endodontic therapy: a retrospective study. *BMC Oral Health* **16**, 1–6. <https://doi.org/10.1186/s12903-016-0163-6>
- Di Fede O, Panzarella V, Mauceri R et al. (2018) The dental management of patients at risk of medication-related osteonecrosis of the jaw: new paradigm of primary prevention. *Biomed Res Int* **16**, 2684924.
- Dimopoulos MA, Kastritis E, Bamia C et al. (2009) Reduction of osteonecrosis of the jaw (ONJ) after implementation of preventive measures in patients with multiple myeloma treated with zoledronic acid. *Annals of Oncology* **20**, 117–20.
- Dodson TB (2007) A guide for preparing a patient-oriented research manuscript. *Oral Surgery, Oral Medicine, Oral Pathology, Oral Radiology, and Endodontology* **104**, 307–15.
- Edwards BJ, Gounder M, McKoy JM et al. (2008) Pharmacovigilance and reporting oversight in US FDA fast-track process: bisphosphonates and osteonecrosis of the jaw. *The Lancet. Oncology* **9**, 1166–72.
- Estrela C, Sydney GB, Figueiredo JA, Estrela CR (2009) Antibacterial efficacy of intracanal medicaments on bacterial biofilm: a critical review. *Journal of Applied Oral Science* **17**, 1–7.
- Fantasia JE (2009) Bisphosphonates-what the dentist needs to know: practical considerations. *Journal of Oral and Maxillofacial Surgery* **67**, 53–60.
- Fehm T, Beck V, Banys M et al. (2009) Bisphosphonate-induced osteonecrosis of the jaw (ONJ): Incidence and risk factors in patients with breast cancer and gynecological malignancies. *Gynecologic Oncology* **112**, 605–9.
- Ficarra G, Beninati F, Rubino I et al. (2005) Osteonecrosis of the jaws in periodontal patients with a history of bisphosphonates treatment. *Journal of Clinical Periodontology* **32**, 1123–8.
- Foschi F, Izard J, Sasaki H et al. (2006) Treponema denticola in disseminating endodontic infections. *Journal of Dental Research* **85**, 761–5.
- Fransson H, Dawson VS, Frisk F, Bjørndal L, EndoReCo KT (2016) Survival of root-filled teeth in the Swedish adult population. *Journal of Endodontics* **42**, 216–20.
- Hasegawa T, Kawakita A, Ueda N et al. (2017) A multicenter retrospective study of the risk factors associated with medication-related osteonecrosis of the jaw after tooth

- extraction in patients receiving oral bisphosphonate therapy: can primary wound closure and a drug holiday really prevent MRONJ? *Osteoporosis International* **28**, 2465–73.
- Hsiao A, Glickman G, He J (2009) A retrospective clinical radiographic study on healing of periradicular lesions in patients taking oral bisphosphonates. *Journal of Endodontics* **35**, 1525–8.
- Hoff AO, Toth BB, Altundag K, Johnson MM, Warneke CL, Hu M et al. (2008) Frequency and risk factors associated with osteonecrosis of the jaw in cancer patients treated with intravenous bisphosphonates. *Journal of Bone and Mineralization Research*, **23**, 826–36.
- Hokugo A, Christensen R, Chung E et al. (2010) Increased prevalence of bisphosphonate related osteonecrosis of the jaw with vitamin D deficiency in rats. *Journal of Bone and Mineral Research* **25**, 1237–49.
- Jung S, Sielker S, Hanisch MR, Libricht V, Schäfer E, Dammerschke T (2018) Cytotoxic effects of four different root canal sealers on human osteoblasts. *PLoS One* **13**, e0194467.
- Kubota M, Yanagita M, Mori K (2016) The effects of cigarette smoke condensate and nicotine on periodontal tissue in a periodontitis model mouse. *PLoS One* **11**, e0155594.
- Kyrgidis A, Arora A, Lyroudia K, Antoniadis K (2010) Root canal therapy for the prevention of osteonecrosis of the jaws: an evidence-based clinical update. *Australian Endodontic Journal* **36**, 130–3.
- Kyrgidis A, Arora A, Antoniadis K (2011) Rubber dam clamp trauma, root canal therapy, and osteonecrosis of the jaw. *Journal of Oral and Maxillofacial Surgery* **69**, 1854–5.
- Landesberg R, Woo V, Cremers S et al. (2011) Potential pathophysiological mechanisms in osteonecrosis of the jaw. *Annals of the New York Academy of Sciences* **1218**, 62–79.
- Lo J, O’Ryan F, Gordon N et al. (2010) Prevalence of osteonecrosis of the jaw in patients with oral bisphosphonate exposure. *Journal of Oral and Maxillofacial Surgery* **68**, 243–6.
- Marx RE (2003) Pamidronate (Aredia) and zoledronate (Zometa) induced avascular necrosis of the jaws: a growing epidemic. *Journal of Oral and Maxillofacial Surgery* **61**, 1115–7.
- Moizadeh AT, Shemesh H, Neiryneck NAM, Aubert C, Weselink PR (2013) Bisphosphonates and their clinical implications in endodontic therapy. *International Endodontic Journal* **46**, 391–8.
- Marozik P, Alekna V, Rudenko E et al. (2019) Bone metabolism genes variation and response to bisphosphonate treatment in women with postmenopausal osteoporosis. *PLoS One* **14**, e0221511.
- McGowan K, McGowan T, Ivanovski S (2018) Risk factors for medication-related osteonecrosis of the jaws: a systematic review. *Oral Diseases* **24**, 527–36.
- Migliorati C, Saunders D, Conlon M et al. (2013) Assessing the association between bisphosphonate exposure and delayed mucosal healing after tooth extraction. *The Journal of the American Dental Association* **144**, 406–14.
- Moretti F, Pelliccioni GA, Montebugnoli L, Marchetti C (2011) A prospective clinical trial for assessing the efficacy of a minimally invasive protocol in patients with bisphosphonate-associated osteonecrosis of the jaws. *Oral Surgery, Oral Medicine, Oral Pathology, Oral Radiology, and Endodontology* **112**, 777–82.
- Morris MF, Kirkpatrick TC, Rutledge RE, Schindler WG (2009) Comparison of nonsurgical root canal treatment and single-tooth implants. *Journal of Endodontics* **35**, 1325–30.
- Nair PNR (2006) On the causes of persistent apical periodontitis: a review. *International Endodontic Journal* **39**, 249–81.
- Ng YL, Mann V, Gulabivala K (2011a) Tooth survival following non-surgical root canal treatment: a systematic review of the literature. *International Endodontic Journal* **43**, 171–89.
- Ng YL, Mann V, Gulabivala K (2011b) prospective study of the factors affecting outcomes of nonsurgical root canal treatment: part 1: Periapical health. *International Endodontic Journal* **44**, 583–609.
- Ørstavik D, Kerekes K, Eriksen HM (1986) The periapical index: a scoring system for radiographic assessment of apical periodontitis. *Endodontics & Dental Traumatology* **2**, 20–34.
- Pinto KP, Ferreira CM, Maia LC, Sassone LM, Fidalgo TKS, Silva EJNL (2020a) Does tobacco smoking predispose to apical periodontitis and endodontic treatment need? A systematic review and meta-analysis. *International Endodontic Journal* **53**, 1068–83.
- Pinto KP, Ferreira CMA, Guimarães AFC et al. (2020b) Effects of alcohol and nicotine consumption on the development of apical periodontitis in rats: a correlative micro-computed tomographic, histological and immunohistochemical study. *International Endodontic Journal* **52**, 1238–52.
- Pirani C, Chersoni S, Montebugnoli L, Prati C (2015) Long-term outcome of non-surgical root canal treatment: a retrospective analysis. *Odontology* **103**, 185–93.
- Pirani C, Friedman S, Gatto MR et al. (2018) Survival and periapical health after root canal treatment with carrier-based root fillings: five-year retrospective assessment. *International Endodontic Journal* **51**, 178–88.
- Prati C, Simpson M, Mitchem J, Tao L, Pashley DH (1992) Relationship between bond strength and microleakage measured in the same Class I restorations. *Dental Materials* **8**, 37–41.
- Prati C, Chersoni S, Pashley DH (2005) Permeability of marginal hybrid layers in composite restorations. *Clinical Oral Investigations* **9**, 1–7.

- Prati C, Pirani C, Zamparini F, Gatto MR, Gandolfi MG (2018) A 20-year historical prospective cohort study of root canal treatments. A multilevel analysis. *International Endodontic Journal* **51**, 955–68.
- Reid IR, Bolland MJ, Grey AB (2007) Is bisphosphonate-associated osteonecrosis of the jaw caused by soft tissue? *Bone* **41**, 318–20.
- Ricucci D, Siqueira JF Jr (2011) Recurrent apical periodontitis and late endodontic treatment failure related to coronal leakage: a case report. *Journal of Endodontics* **37**, 1171–5.
- Ruggiero SL, Merhotra B, Rosemberg TJ, Engroff LE (2004) Osteonecrosis of the jaws associated with the use of bisphosphonates: a review of 63 cases. *Journal of Oral and Maxillofacial Surgery* **62**, 527–34.
- Ruggiero SL, Dodson TB, Assael LA, Landesberg R, Marx RE, Mehrotra B (2009) American Association of Oral and Maxillofacial Surgeons position paper on bisphosphonate-related osteonecrosis of the jaws—2009 update. *Journal of Oral and Maxillofacial Surgery* **67**, 2–12.
- Ruggiero SL, Dodson TB, Fantasia J et al. (2014) American Association of oral and maxillofacial surgeons position paper on medication-related osteonecrosis of the jaw update. *Journal of Oral and Maxillofacial Surgery* **72**, 1938–56.
- Russell RGG, Watts NB, Ebetino FH, Roger JM (2008) Mechanisms of action of bisphosphonates: similarities and differences and their potential influence on clinical efficacy. *Osteoporosis International* **19**, 733–59.
- Saad F, Brown J, Van Poznak C et al. (2012) Incidence, risk factors, and outcomes of osteonecrosis of the jaw: integrated analysis from three blinded active-controlled phase III trials in cancer patients with bone metastases. *Annals of Oncology* **23**, 1341–7.
- Siboni F, Taddei P, Zamparini F, Prati C, Gandolfi MG (2017) Properties of BioRoot RCS, a tricalcium silicate endodontic sealer modified with povidone and polycarboxylate. *International Endodontic Journal* **50**, 120–36.
- Segura-Egea JJ, Martin-Gonzalez J, Castellanos-Cosano L (2015) Endodontic medicine: connections between apical periodontitis and systemic diseases. *International Endodontic Journal* **48**, 933–51.
- Taxel P, Ortiz D, Shafer D et al. (2014) The relationship between implant stability and bone health markers in postmenopausal women with bisphosphonate exposure. *Clinical Oral Investigations* **18**, 49–57.
- Tverdal A, Bjartveit K (2006) Health consequences of reduced daily cigarette consumption. *Tobacco Control* **15**, 472–80.
- Vahtsevanos K, Kyrgidis A, Verrou E, Katodritou E, Triaridis S, Andreadis CG et al. (2009) Longitudinal cohort study of risk factors in cancer patients of bisphosphonate-related osteonecrosis of the jaw. *Journal of Clinical Oncology* **27**, 53–56.
- Vandenbroucke J, von Elm E, Altman D et al. (2007) Strengthening the reporting of observational studies in epidemiology (STROBE): explanation and elaboration. *Epidemiology* **18**, 805–35.
- World Medical Association Declaration of Helsinki (2013) Ethical principles for medical research involving human subjects. *Journal of the American Medical Association* **310**, 2191–4.

5. *Novel Endodontic Biomaterials and Advanced Implant Surface Technologies: Their Impact on the Decision-making Between Endodontic Retreatment and Implant Rehabilitation*

The advancements in instrumentation techniques and canal obturation have allowed endodontics to expand the range of applications, making treatments technically easier and more predictable.

Recently, new implant designs, surface treatments, and implant placement protocols have been developed ([Albrektsson et al. 2017](#)). The placement of a post-endodontic implant now presents an interesting therapeutic choice. Understanding the limits of endodontics, is now more than ever a complex and challenging clinical decision.

The survival rate of endodontic retreatments varies widely, with percentages ranging from 65% to 85% in the first 10 years. This variation considers the type and difficulty of cases, as well as the experience of the operators ([Zitzmann et al. 2009](#), [Ng et al. 2010](#), [Pirani et al. 2019](#), [Gorni & Gagliani 2002](#), [Signor B et al. 2019](#), [Pettersson et al. 2016](#), [De Chevigny et al. 2008](#)). The outcome of a secondary root canal treatment can present early or late complications or complications that are not strictly endodontic.

Early complication could be perforations, ledges, intracanal contamination, inflammation at the periapical level, and not a good management of the apical enlargement / instrumentation can lead to flare-ups post-instrumentation. Root fractures also can occur and need to be evaluated, especially when a post has been removed.

Late complications, sometimes indicated as “failures”, are generally manifested as partial healing with lasting a periapical radiolucency or a new endodontic pathology once healing has occurred.

Complications that are not strictly endodontic (sometimes unexpected), are often cited in the literature as the primary causes of tooth loss ([Prati et al. 2018](#); [Fonzar et al. 2021](#)). These include root fractures, internal and external root resorptions, periodontal diseases, bone resorption at the furcation in molars, and periodontal diseases.

An alternative to the retreatment and even to the extraction can be the apical surgery, which is, of course, only possible in suitable anatomical situations and in the hands of experienced operators ([Kim S & Kratchman S 2006](#); [Prati et al. 2018](#)).

The literature on the clinical outcome and survival rate of implants over time is vast and reflects the evolution of techniques and implants. Upon initial assessment, it is evident that the

use of implants is associated with a higher success rate (90–95% at 10 years) than what is reported for endodontic retreatment ([Chércoles-Ruiz et al. 2017](#), [Corbella et al. 2015](#), [Covani et al. 2012](#), [Lai et al. 2013](#), [Roccuzzo et al. 2010](#), [Rossi et al. 2018](#)). However, this data isn't directly comparable since the clinical conditions (for instance, patient inclusion criteria and pathologies) of studies conducted in the endodontic or implant fields are different.

The implant surface characteristics can play an important role during the osseointegration processes and influence the long-term success rate ([Wennerberg & Albrektsson 2009](#)). Recent advancements in surface engineering have led to the development of implants specifically designed to promote osseointegration. These innovations include the use of micro and nano-scale texturing, surface coatings with bioactive molecules, and modifications aimed at increasing the hydrophilicity of implant surfaces ([Zamparini et al. 2021](#)). These treatments are designed to improve the biological response at the bone-implant interface, facilitating the recruitment and differentiation of osteogenic cells ([Nikkhah et al. 2012](#)). Also the shape and design of the implant neck play an important role in maintaining the marginal bone level around the implant during the healing stages. The Laser-Lok technique, for example involves a computer-guided laser process which create a highly precise implant neck microchannels that are specifically sized for cells (8 µm in diameter). Research has shown that this method promotes the growth of fibroblasts, leading to the formation of a stable connective tissue. This bond acts as an epithelial seal in the early stages of healing. Histological examinations have verified the ability to form a direct connective tissue attachment to the microchannel surface on the dental implant's neck, enhancing the implant's integration and stability ([Nevins et al. 2008, 2012](#)).

Interesting investigations from Italian researchers have examined the success rate of implants placed after the extraction of teeth with chronic periapical endodontic lesions. The studies report excellent success rates while noting the technical challenges, the necessity of complete removal of the periapical lesion, and the need to have a definitive diagnosis of chronic periapical pathology not in an active phase ([Crespi et al. 2008](#); [Corbella et al. 2014](#); [Covani et al. 2014](#); [Barone et al. 2014](#); [Prati et al. 2017](#)). Patient management proves to be important, from the choice of antibiotics to the handling of tissues post-implantation.

The clinical procedures for implant placement will differ based on the initial endodontic pathology, for instance, an asymptomatic periapical lesion of modest radiographic dimensions (2-4 mm) or a large endodontic abscess with clinical symptoms and loss of the cortical buccal bone. Only a few studies report the survival rate of implants placed immediately after the

extraction of teeth with active endodontic lesions ([Lincoln-Bell C et al. 2011](#); [Montoya-Salazar V et al. 2014](#)).

Also Implant therapies can present complications, which can be classified as early or late.

Early complications can occur during the surgical procedure or during the initial phases of bone remodeling. Intraoperative complications (such as improper implant placement, damage to important anatomical structures, and lack of primary stability) can be attributed to a wrong surgical planning. Biological complications can arise due to infection at the implant site and the lack of implant osseointegration, reported in the literature with a frequency of about 2-3% of implant treatments ([Berglundh T et al. 2002](#)). These rapid-onset events often prevent the deposition of bone tissue in contact with the implant threads, leading to the formation a fibro-integration, mobility, and implant loss ([Manzano G et al.2016](#)).

Late complications can be divided based on their cause into biological (bacterial colonization on the exposed portion of the implant) or mechanical (occlusal overload). In both cases, these events lead to the gradual loss of peri-implant bone, which can be detected radiographically.

Few studies have analyzed the success rate of both treatments when dealing with cases where there is doubt about the most appropriate therapeutic approach (whether to extract the tooth or retreat it). Vozza ([Vozza I et al. 2013](#)) compared endodontically treated and implant-therapy populations in a retrospective analysis. Over an eight-year follow-up, both groups exhibited comparable success rates. Notably, endodontic treatments presented a higher complication incidence relative to implant rehabilitations, particularly in patients maintaining optimal oral hygiene. Several reviews in high ranked international journals have assessed the optimal treatment decisions ([Setzer FC & Kim S 2014](#); [Morris MF et al. 2009](#); [Zitzmann NU et al. 2009](#)). A consistent finding across these investigations is the imperative role of operators experience and a multidisciplinary approach in determining appropriate decision making.

Various parameters must be considered when deciding whether to retreatment (orthograde or retrograde) or extraction followed by implant rehabilitation. Literature indicates that teeth with PAI 4 and 5, especially on a second treatment, have a prognosis less favorable ([Prati et al. 2018](#)). Root anomalies, iatrogenic perforations, the presence of posts, and the type of filling material are primary endodontic variables to consider before starting a retreatment. The presence of 2 or more of these factors often lead to an extraction-implant option. The integrity of the crown structure of the treated element is a critical evaluation parameter, including assessing the number of intact tooth walls and the height of the remaining walls. Teeth with less

than 30% of the original structure have a high post-treatment failure risk (Al-Nuaimi N et al. 2017). Acute symptoms like the emergence of fistula, masticatory pain, or periodontal probing often indicate a possible vertical root fracture, justifying a CBCT examination and a potential extraction-implant therapy. A previous canal perforation in a tooth with periapical lesion is relatively common. In cases of canal retreatment, a perforation can result in an unfavorable outcome for the long-term maintenance of the tooth. A 3-year retrospective study on iatrogenically perforated teeth reported a 73% success rate (Krupp C et al. 2013). Retreatment challenges include risks of canal perforation, instrument fracture, and anatomical complexities, with perforation risks ranging from 0.6% to 17.6% (Sarao SK et al. 2021).

The use of bioceramic sealers, due to their bioactivity and biocompatibility, allows for a more conservative approach to the perforated element, avoiding or delaying tooth extraction (Gandolfi MG et al. 2011; Zamparini et al. 2019). The presence of intracanal posts doesn't result in an unfavorable prognosis during canal retreatment, as demonstrated in a recent study (Riis A et al. 2018). Recent findings indicate that general dentists without an endodontic specialty background tend to favor the extraction option more frequently (Lee J et al. 2020). Identifying untreated canals (missed canal) using CBCT provides the chance to retreat and maintain the tooth. The presence of a broken instrument can be a significant contraindication for canal retreatment, leading to the extraction-implant route. A broken instrument often indicates a previous error (ledge, canal calcification) at the more apical portion of the canal (McGuigan MB et al. 2013). Clearly, if a periapical lesion is also present, the prognosis is generally worse. The operator wouldn't have been able to remove the bacterial load at the apical level responsible for the pathology (Panitvisai P et al. 2010). In such cases, retrograde surgical retreatment, if anatomically possible, is recommended before planning the extraction. Surgical endodontics has demonstrated good success rates in recent studies, especially considering the new techniques and bioceramic materials introduced (von Arx T et al. 2019; Del Fabbro M et al. 2007). Accessing the endodontic system while retaining the prosthetic crown has notable disadvantages, including the inability to identify and remove secondary carious lesions often hidden by the prosthetic artifact (Patel S & Rhodes J 2007). The prosthetic crown may also lead to inaccurate length measurements by the apex locator. Radiographic examination is essential in such cases to confirm the working length (Alley BS et al. 2004). Overall, removing the prosthetic device is sometimes even impossible. In these cases, after radiological/CBCT assessment, retrograde surgery of the element might be recommended (Del Fabbro M et al. 2007).

Post-endodontic implantology provides a significant opportunity for endodontics, addressing critical "point of no return" situations by offering therapeutic alternatives in increasingly common scenarios anticipated during retreatments.

The following papers investigate both in vivo and in vitro different types of implants. Two clinical studies performed with 2 different types of implants and with a follow-up of 4 and 10 years was conducted. The marginal bone level and periodontal parameters were evaluated. Another laboratory investigation aims to evaluate the surface micro-nanomorphology and bioactivity of a new implant. An environmental scanning electronic microscopy, energy dispersive X-ray spectroscopy, field emission gun SEM-EDX and micro-Raman spectroscopy and X-ray photoelectron spectroscopy was performed before and after immersion in simulated body fluids.

REFERENCES

- 1) Al-Nuaimi N, Patel S, Austin RS, Mannocci F. A prospective study assessing the effect of coronal tooth structure loss on the outcome of root canal retreatment. *Int Endod J* 2017;50:1143-57.
- 2) Albrektsson T, Chrcanovic B, Östman PO, Sennerby L. Initial and long- term crestal bone responses to modern dental implants. *Periodontol 2000* 2017;73:41-50.
- 3) Alley BS, Kitchens GG, Alley LW, Eleazer PD. A comparison of survival of teeth following endodontic treatment performed by general dentists or by specialists. *Oral Surg Oral Med Oral Pathol Oral Radiol Endod* 2004;98:115-8.
- 4) Barone A, Toti P, Quaranta A et al. The clinical outcomes of immediate versus delayed restoration procedures on immediate implants: a comparative cohort study for single-tooth replacement. *Clin Implant Dent Relat Res* 2014;17:1114-26.
- 5) Berglundh T, Persson L, Klinge B. A systematic review of the incidence of biological and technical complications in implant dentistry reported in prospective longitudinal studies of at least 5 years. *J Clin Periodontol* 2002;29:197-212.
- 6) Chércoles-Ruiz A, Sánchez-Torres A, Gay-Escoda C. Endodontics, Endodontic Retreatment, and Apical Surgery Versus Tooth Extraction and Implant Placement: A Systematic Review. *J Endod.* 2017;43:679-686.

- 7) Corbella S, Taschieri S, Tsesis I, Del Fabbro M. Postextraction implant in sites with endodontic infection as an alternative to endodontic retreatment: a review of literature. *J Oral Implantol*. 2013 Jun;39:399-405.
- 8) Corbella S, Taschieri S, Samaranayake L et al. Implant treatment choice after extraction of a vertically fractured tooth. A proposal for a clinical classification of bony defects based on a systematic review of literature. *Clin Oral Implants Res* 2014;25:946-56.
- 9) Covani U, Chiappe G, Bosco M, Orlando B, Quaranta A, Barone A. A 10-year evaluation of implants placed in fresh extraction sockets: a prospective cohort study. *J Periodontol*. 2012;83:1226-34.
- 10) Covani U, Canullo L, Toti P et al. Tissue stability of implants placed in fresh extraction sockets: a 5-year prospective single-cohort study. *J Periodontol* 2014;85:323-32.
- 11) Crespi R, Capparé P, Gherlone E, Romanos GE. Immediate versus delayed loading of dental implants placed in fresh extraction sockets in the maxillary esthetic zone: a clinical comparative study. *Int J Oral Maxillofac Implants* 2008;23:753-8.
- 12) De Chevigny C, Dao TT, Basrani BR, Marquis V, Farzaneh M, Abitbol S, Friedman S. Treatment outcome in endodontics: the Toronto study--phases 3 and 4: orthograde retreatment. *J Endod*. 2008;34:131-7.
- 13) Del Fabbro M, Taschieri S, Testori T, Francetti L, Weinstein RL. Surgical versus non-surgical endodontic re-treatment for periradicular lesions. *Cochrane Database Syst Rev* 2007;18:CD005511.
- 14) Fonzar F, Kalemai Z, Fonzar RF, Buti J, Buttolo P et al. The prognosis of root canal therapy: a 20-year follow-up ambispective cohort study on 411 patients with 1169 endodontically treated teeth. *Clinical Trial Dentistry* 2021;3:5-17.
- 15) Gandolfi MG, Taddei P, Siboni F, Modena E, Ginebra MP, Prati C. Fluoride-containing nanoporous calcium-silicate MTA cements for endodontics and oral surgery: early fluorapatite formation in a phosphate-containing solution. *Int Endod J* 2011;44:938-49.
- 16) Gorni FGM, Gagliani MM. The outcome of endodontic retreatment: A 2-yr follow-up. *J Endod* 2004;30:1-4.
- 17) Kim S, Kratchman S. Modern endodontic surgery concepts and practice: a review. *J Endod* 2006;32:601-23.


- 18) Krupp C, Bargholz C, Brüsehaber M, Hülsmann M. Treatment outcome after repair of root perforations with mineral trioxide aggregate: a retrospective evaluation of 90 teeth. *J Endod* 2013;39:1364-8.
- 19) Lai HC, Si MS, Zhuang LF, Shen H, Liu YL, Wismeijer D. Long-term outcomes of short dental implants supporting single crowns in posterior region: a clinical retrospective study of 5-10 years. *Clin Oral Implants Res.* 2013;24:230-7.
- 20) Lee J, Kang S, Jung HI, Kim S, Karabucak B, Kim E. Dentists' clinical decision-making about teeth with apical periodontitis using a variable-controlled survey model in South Korea. *BMC Oral Health* 2020;20.
- 21) Lincoln-Bell C, Diehl D, Bell BM et al. The immediate placement of dental implant into extraction site with periapical lesions: a retrospective chart review. *J Oral Maxillofac Surg* 2011;69:1623-7.
- 22) Manzano G, Montero J, Martín-Vallejo J, Del Fabbro M, Bravo M, Testori T. Risk factors in early implant failure: a meta-analysis. *Implant Dent* 2016;25:272-80.
- 23) McGuigan MB, Louca C, Duncan HF. The impact of fractured endodontic instruments on treatment outcome. *Br Dent J* 2013;214:285-9.
- 24) Montoya-Salazar V, Castillo-Oyagüe R, Torres-Sánchez C, Lynch CD, Gutiérrez-Pérez JL, Torres-Lagares D. Outcome of single immediate implants placed in post-extraction infected and non-infected sites, restored with cemented crowns: a 3-year prospective study. *J Dent* 2014;42:645-52.
- 25) Morris MF, Kirkpatrick TC, Rutledge RE, Schindler WG. Comparison of nonsurgical root canal treatment and single-tooth implants. *J Endod* 2009;35:1325-30.
- 26) Nevins, M.; Nevins, M.L.; Camelo, M.; Boyesen, J.L.; Kim, D.M. Human histologic evidence of a connective tissue attachment to a dental implant. *Int. J. Periodontics Restor. Dent.* 2008, 28, 111–121.
- 27) Nevins, M.; Camelo, M.; Nevins, M.L.; Schuepbach, P.; Kim, D.M. Connective tissue attachment to laser-microgrooved abutments: A human histologic case report. *Int. J. Periodontics Restor. Dent.* 2012, 32, 385–392.
- 28) Nikkhah, M.; Edalat, F.; Manoucheri, S.; Khademhosseini, A. Engineering microscale topographies to control the cell-substrate interface. *Biomaterials* 2012, 33, 5230-5246
- 29) Ng YL, Mann V, Gulabivala K. Tooth survival following non-surgical root canal treatment: a systematic review of the literature. *Int Endod J.* 2010;43:171-89

- 30) Panitvisai P, Parunnit P, Sathorn C, Messer HH. Impact of a retained instrument on treatment outcome: a systematic review and meta-analysis. *J Endod* 2010;36:775-80.
- 31) Patel S, Rhodes J. A practical guide to endodontic access cavity preparation in molar teeth. *Br Dent J* 2007;11;203:133-40.
- 32) Petersson K, Fransson H, Wolf E, Håkansson J. Twenty-year follow-up of root filled teeth in a Swedish population receiving high-cost dental care. *International Endodontic Journal* 2016;49, 636–45.
- 33) Pirani C, Zamparini F, Peters OA, Iacono F, Gatto MR, Generali L, Gandolfi MG, Prati C. The fate of root canals obturated with Thermafil: 10-year data for patients treated in a master's program. *Clin Oral Investig.* 2019;23:3367-3377.
- 34) Prati C, Pirani C, Zamparini F, Gatto MR, Gandolfi MG. A 20-year historical prospective cohort study of root canal treatments. A Multilevel analysis. *Int Endod J* 2018;51:955-68.
- 35) Prati C, Azizi A, Pirani C, Zamparini F, Iacono F, Montebugnoli L et al. Apical surgery vs apical surgery with simultaneous orthograde retreatment: a prospective cohort clinical study of teeth affected by persistent periapical lesion. *G Ital Endod* 2018;32:2-8.
- 36) Prati C, Zamparini F, Pirani C, Gatto MR, Piattelli A, Gandolfi MG. Immediate early and delayed implants: a 2-year prospective cohort study of 131 transmucosal flapless implants placed in sites with different pre-extractive endodontic infections. *Implant Dent* 2017;26:654-63.
- 37) Riis A, Taschieri S, Del Fabbro M, Kvist T. Tooth survival after surgical or nonsurgical endodontic retreatment: long-term follow-up of a randomized clinical trial. *J Endod* 2018;44:1480-6.
- 38) Rocuzzo M, De Angelis N, Bonino L, Aglietta M. Ten-year results of a three-arm prospective cohort study on implants in periodontally compromised patients. Part 1: implant loss and radiographic bone loss. *Clin Oral Implants Res.* 2010;21:490-6.
- 39) Rossi F, Lang NP, Ricci E, Ferraioli L, Baldi N, Botticelli D. Long-term follow-up of single crowns supported by short, moderately rough implants-A prospective 10-year cohort study. *Clin Oral Implants Res.* 2018;29:1212-1219.
- 40) Sarao SK, Berlin-Broner Y, Levin L. Occurrence and risk factors of dental root perforations: a systematic review. *Int Dent J* 2021;71:96-105.
- 41) Setzer FC, Kim S. Comparison of long-term survival of implants and endodontically treated teeth. *J Dent Res* 2014;93:19-26.

- 42) Signor B, Blomberg LC, Kopper PMP, Augustin PAN, Rauber MV et al. Root canal retreatment: a retrospective investigation using regression and data mining methods for the prediction of technical quality and periapical healing. *J Appl Oral Sci.* 2021;19:29.
- 43) von Arx T, Jensen SS, Janner SFM, Hänni S, Bornstein MM. A 10-year follow-up study of 119 teeth treated with apical surgery and root-end filling with mineral trioxide aggregate. *J Endod* 2019;45:394-401.
- 44) Vozza I, Barone A, Quaranta M, De Paolis G, Covani U, Quaranta A. A comparison between endodontics and implantology: an 8-year retrospective study. *Clin Implant Dent Relat Res* 2013;15:29-36.
- 45) Wennerberg, A.; Albrektsson, T. Effects of titanium surface topography on bone integration: A systematic review. *Clin. Oral Implant. Res.* 2009, 20, 172–184.
- 46) Zamparini F, Siboni F, Prati C, Taddei P, Gandolfi MG. Properties of calcium silicate-monobasic calcium phosphate materials for endodontics containing tantalum pentoxide and zirconium oxide. *Clin Oral Investig* 2019;23:445-7.
- 47) Zamparini,F.;Prati,C.; Generali, L.; Spinelli, A.; Taddei, P.; Gandolfi, M.G. Micro-Nano Surface Characterization and Bioactivity of a Calcium Phosphate-Incorporated Titanium Implant Surface. *J. Funct. Biomater.* 2021, 12, 3.
- 48) Zitzmann NU, Krastl G, Hecker H, Walter C, Weiger R. Endodontics or implants? A review of decisive criteria and guidelines for single tooth restorations and full arch reconstructions. *Int Endod J.* 2009;42:757-74.

Article

Tissue-Level Laser-Lok Implants Placed with a Flapless Technique: A 4-Year Clinical Study

Andrea Spinelli ¹, Fausto Zamparini ^{1,2} , Georgios Romanos ³ , Maria Giovanna Gandolfi ²  and Carlo Prati ^{1,*}

¹ Endodontic Clinical Section, Department of Biomedical and Neuromotor Sciences, School of Dentistry, University of Bologna, 40125 Bologna, Italy

² Laboratory of Biomaterials and Oral Pathology, Department of Biomedical and Neuromotor Sciences, School of Dentistry, University of Bologna, 40125 Bologna, Italy

³ Department of Periodontics and Endodontics, School of Dental Medicine, Stony Brook, NY 11794, USA

* Correspondence: carlo.prati@unibo.it

Abstract: Background: The present study aims to analyze the use of Laser-Lok microtextured neck implants placed with a transmucosal surgical approach. The marginal bone level (MBL) and periodontal parameters were evaluated in a cohort prospective 4-year clinical study. Methods: A total of 41 implants were placed in 36 healthy consecutive patients (16 males, 20 females, mean age 60 ± 9 years). Tapered tissue level implants, characterized by a 2.0 mm laser-microtextured neck, were used with a flapless approach. Customized abutments and provisional resin crowns were positioned. Definitive metal–ceramic crowns were cemented approximately 4 months after insertion. Periapical radiographs were taken after 1, 3, 6, 12, 36 and 48 months from implant placement to evaluate MBL. Gingival thickness (thin/thick), plaque score (PS) and bleeding on probing (BoP) were evaluated. Results: After 48 months, all implants were safe from complications. No complications, peri-implantitis, early implant failures or mucositis occurred. The survival rate was 100%. Mean MBL during the follow-up was -0.15 ± 0.18 at T1, -0.29 ± 0.29 at T3, -0.45 ± 0.37 at T6, -0.53 ± 0.45 at T12, -1.06 ± 1.13 at T 36 and -1.10 ± 0.89 at T 48. Implants placed 2–3 months after tooth extraction revealed lower MBL variation when compared to those placed immediately (in fresh extraction sockets) or in completely healed ridges (delayed group). Narrower diameter implants (3.8 mm) showed significantly higher MBL variation when compared to 4.6 diameter implants. Multilevel analysis at T48 revealed that among all the evaluated variables, implant diameter was the factor mostly associated with MBL modifications ($p = 0.027$). Conclusion: This 4-year clinical study supports the use of Laser-Lok implants placed at tissue level with a flapless approach. A limited bone loss during the 48-month follow-up was observed. Periodontal parameters were stable with no sign of inflammation or soft tissue alteration. The use of Laser-Lok implants with transmucosal surgery represents a suitable technique with a minimally invasive approach.



Citation: Spinelli, A.; Zamparini, F.; Romanos, G.; Gandolfi, M.G.; Prati, C. Tissue-Level Laser-Lok Implants Placed with a Flapless Technique: A 4-Year Clinical Study. *Materials* **2023**, *16*, 1293. <https://doi.org/10.3390/ma16031293>

Academic Editor: Eugenio

Velasco-Ortega

Received: 12 October 2022

Revised: 29 December 2022

Accepted: 27 January 2023

Published: 2 February 2023



Copyright: © 2023 by the authors. Licensee MDPI, Basel, Switzerland. This article is an open access article distributed under the terms and conditions of the Creative Commons Attribution (CC BY) license (<https://creativecommons.org/licenses/by/4.0/>).

Keywords: dental implants; flapless surgery; laser-lok; marginal bone level; tapered tissue level implant

1. Introduction

Recent dental implant protocols show substantial variations from those initially designed 20–30 years ago. Those protocols required the submerged positioning of the implant, a 4–6-month healing time and a second surgery to expose the neck before the prosthetic phases [1,2].

According to recent studies, bone-level and submerged implant insertion may present a similar outcome in terms of peri-implant bone preservation [3], in particular in non-molar areas [4]. However, some disadvantages must be highlighted, including the need to re-expose the implant emergence before the prosthetic phases, the presence of an implant abutment connection relocated deep in bone tissues and the transmucosal soft tissue tunnel. The presence of a deep transmucosal tunnel was demonstrated to induce a higher risk of

peri-implant diseases in the long term, in accordance with a previous study [5]. Similarly, histological studies reported that a deeper implant insertion would result in a greater bone loss during the first months after insertion [6]. Both clinicians and patients are now demanding simplified, less invasive surgical protocols with predictable results [7–9] to reduce discomfort and post-operative pain caused by flap elevation and surgery connected with implant placement and exposure.

Transmucosal implant placement may represent a minimally invasive approach to reduce the number of surgeries after implant placement and does not require a second surgical exposition of the implants [8].

New surface treatments (coating techniques, blasting with bioactive fillers) [10] and modifications of implant macro- and microgeometry [11–13] lead to the design of minimally invasive surgeries for transmucosal implant placement [8].

The flapless approach may lead to important advantages in hard and soft tissue stability in single edentulous areas. This approach requires only a single low-invasive surgery, minimizes soft tissue trauma and contributes to avoiding a second surgery to expose the implant neck [9,14–16].

The implant neck morphology plays an important role in the preservation of marginal bone level (MBL) during the healing phases [8]. Laser-Lok is a computer-controlled laser ablation technique, which creates an implant neck with precision-engineered cell-sized microchannels (size 8 μm). It has been demonstrated that this treatment induces a fibroblast growth that leads to a stable connective tissue attachment, providing an epithelial barrier during initial healing phases [17–19]. Histological studies confirmed the possibility of achieving a physical connective tissue attachment to the cell-sized microchannel collar of a dental implant [20].

A recent study evidenced that the laser-ablated cell-sized microchannels of the collar surface may have a positive effect on peri-implant trabecular bone remodeling [21]. The use of an implant neck with this design and morphology may be of great interest concerning tissue-level implants placed with minimal invasive surgery (i.e., the flapless approach). To date, no clinical data are reported regarding this protocol.

This study aimed to investigate clinical and radiographic outcomes of tissue-level implants with a Laser-Lok neck placed tissue-level with a flapless technique. The primary outcome was the analysis of implant survival rates and MBL. The secondary outcome was the analysis of soft tissue inflammation by using bleeding on probing (BoP) and plaque score (PS) indexes. All the implants were followed up at 1, 3, 6, 12, 36 and 48 months.

2. Materials and Methods

2.1. Study Setting and Patient Selection

The present investigation was designed in the Endodontic Clinical Section of the Dental School of Bologna University. All patients were recruited in one private dental office.

Patient enrollment started in September 2017 and ended in November 2018 [22]. Patients follow-up had a minimum duration of 48 months. A flowchart of the study protocol is reported in Figure 1.

The patients were considered eligible or non-eligible for inclusion in the clinical protocol based on the following criteria:

Inclusion criteria:

- 18–75 years of age;
- Requiring a single implant rehabilitation;
- Being able to be included in a hygiene recall program and implant control for at least 4 years;
- Smoking less than 10 cigarettes per day.

Exclusion criteria:

- Medical and/or general contraindications for the surgical procedures (ASA score ≥ 3);
- Poor oral hygiene and lack of motivation (presence of visible plaque on more than 75% of teeth);

- Active clinical periodontal disease in the dentition (probing pocket depth > 4 mm, bleeding on probing in 25% of sites);
- Uncontrolled diabetes mellitus, oncological patients receiving bisphosphonate therapy;
- Alcohol and/or drug abuse as specified in the patient medical anamnesis;
- Pregnancy or lactation period;
- Malocclusion and other occlusal disorder (bruxism, open- and closed bite);
- Lack of minimum crestal bone levels to place a 3.8 × 10 mm implant;
- Post extraction sites requiring guided bone regeneration, biomaterials and membrane insertion.

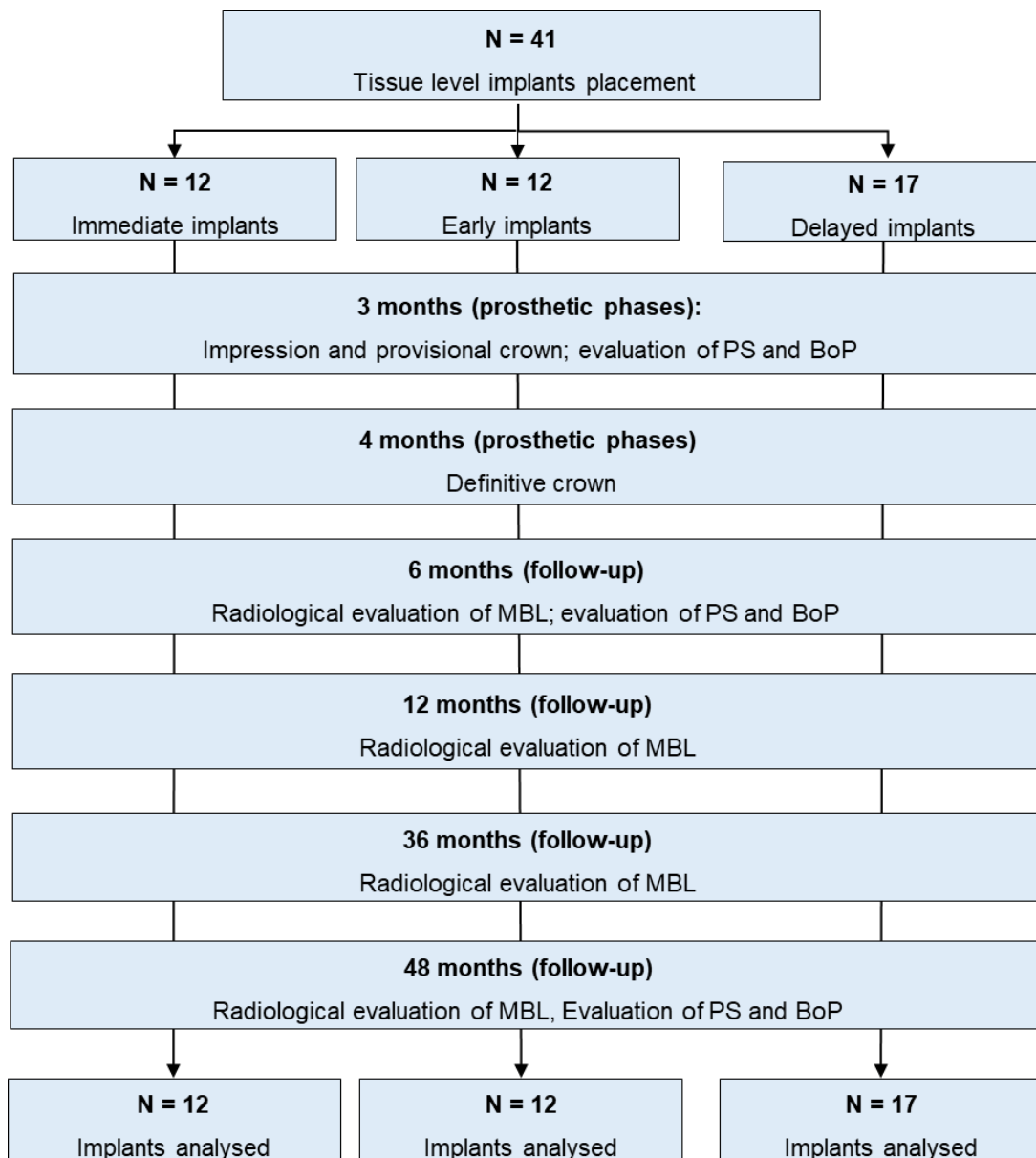


Figure 1. Scheme of the study, research phases and methods.

All patients were treated according to the principles established by the Declaration of Helsinki as modified in 2013.

Before enrollment, written and verbal information was given by the clinical staff, and each patient gave written consent according to the above-mentioned principles. This report was written according to the Consolidated Standards of Reporting Trials guidelines for reporting clinical trials (STROBE) [23]. Hopeless teeth were radiographically examined

to assess the presence/absence of any periapical radiolucency by the clinical team of the Endodontic Clinical Section.

Choice of the surgical approach and timing of implant placement (immediate, early or delayed according to the timing classification proposed by the Third ITI Consensus Conference) [24] were determined following the principles of “best clinical practice”. Thus, three surgical implant placement timings were defined as follows:

- Immediate post-extraction implant [24]: when the implant was placed into fresh extraction socket immediately after extraction of a root affected by chronic periapical disease and/or seriously damaged hopeless (or fractured) teeth were assigned to this group. Only chronic periapical lesions were present and identified by periapical radiolucency.
- Early implant [24]: when the implant was placed in a healed alveolar bone 8–12 weeks after extraction of the root affected by acute periapical lesion and/or abscess, suppuration and clinical symptoms.
- Delayed implant [24]: when the implant was placed in edentulous mature alveolar bone 10–12 months after the tooth extraction for different reasons (Figure 1).

2.2. Surgical Procedures

An implant, characterized by a 2 mm transmucosal part (1.8 mm laser-microtextured surface and 0.2 mm smooth surface in the most coronal part of the implant) was used (Tapered Tissue-level Laser-Lok, Biohorizons, Birmingham, AL, USA).

One single experienced surgeon performed all surgeries. Before surgery, a careful occlusal and periodontal examination was performed on each patient, including presence of plaque (PS), gingivitis, pocket depth, BoP and radiographic bone loss of all remaining teeth.

Periodontal therapy and oral hygiene training were carried out as needed and as indicated.

All patients were required to follow a pharmacological regimen that included taking an amoxicillin/clavulanic acid 1 g tablet and applying chlorhexidine di-gluconate 0.2% gel (Corsodyl Gel, GlaxoSmithKline UK, Brantford, UK) twice a day for two days prior to the intervention. All surgical procedures were conducted under local anesthesia with mepivacaine chloral hydrate 30 mg/mL (Carboplyina, Dentsply, Germany).

A flapless approach was performed for early and delayed timings. The initial drill used to indicate the position, angulation, and depth had a 1.2 mm diameter. The drill passed through the mucosa, cortical bone and cancellous bone under extensive saline irrigation. A twist and calibrated drill at 225 rpm was used and a site of the adequate depth and diameter was created whilst irrigating with a sterile saline solution. The entire rough surface was in the cortical bone, and the divergent surface of the resulting implant was immersed in gingival thickness tissue.

In case of immediate (in the fresh extraction sockets) implant insertion, an atraumatic flapless root extraction was performed. Inspection of the socket site was carried out and the granulation tissue debrided from the apical portion of the socket. The intra-socket site was prepared with a 1.2 mm drill under generous irrigation following oral bony wall as a guide, followed by a twist and calibrated drill at 225 rpm. The primary implant stability was obtained by anchoring the implant in the remaining apical portion of the socket at least 3 mm beyond the root apex area. No computer-aided guide was used.

2.3. Post-Operative Recommendation

All patients had a surgical periodontal dressing (Coe-Pak[®], GC, Tokyo, Japan) applied to the wound for one week. Patients were told to follow a soft diet program for one week, rinse three times per day with 0.12% chlorhexidine mouthwash for three weeks and clean their teeth around the Coe-Pak[®] during the first week and for two weeks after the surgical pack was removed. After that, regular brushing and flossing were allowed.

2.4. Prosthetic Rehabilitation

The prosthetic procedures were made four months after insertions in all cases. Polyether impressions (Permadyne and Garant[®], 3M ESPE, Seefeld, Germany) were obtained using

the pick-up plastic customized trays for analogues technique. After 7 days, customized abutments were screwed onto the implants and acrylic temporary single crowns cemented with zinc-oxide temporary cement (Temp Bond[®], Kerr, Scafati, Italy). After 15 days, a definitive metal–ceramic crown, made by two equally experienced prosthodontists, was positioned on the customized abutment and fixed using a radiopaque polycarboxylate powder/liquid cement (Heraeus Kulzer, Hanau, Germany) with careful attention to prevent any cement overflowing or excess.

2.5. Follow-Up Implant Evaluation

2.5.1. Radiographic Assessment of MBL

A paralleling technique with Rinn-holders and analog films (Kodak Ektaspeed Plus, Eastman Kodak Co., Rochester, NY, USA) was used to take intraoral periapical radiographs of all implants at the baseline, 1 month, 3 months, 6 months, 12 months, 36 months and 48 months after implant placement (T48).

The target–film distance was roughly 30 cm, the exposure period was 0.41 s, the voltage was 70 kV and the intensity was 8 mA. Following the manufacturers recommendations, radiographic development was carried out in a developer unit (Euronda s.p.a., Vicenza, Italy) at standard room temperature (25 °C) with 12 s developing and 25 s fixing times. When not fulfilling the parameters, patients were asked to get a new radiograph. All periapical radiographs were then scanned with a scanner with the following acquisition parameters: resolution 968 dpi and $\times 20$ magnification factor.

A slide scanner with a resolution of 968 dpi and a magnification of $\times 20$ was used to scan all radiographs. The measurement was calibrated using implants with known lengths and diameters [16,25]. Calibration of brightness and contrast was performed in order to standardize the acquisition of the images.

To assess the MBL change, the crestal marginal bone and the bone–implant contact were examined. Using a scale with 0.1 mm increments, the distance from the reference point (the implant shoulder) to the level of coronal bone-to-implant contact was measured in order to evaluate MBL at the mesial and distal implant surfaces. The implants length and diameter were used to calibrate the measurements of the MBL.

One operator conducted the single-blind radiographic evaluation. A reference set of radiographs with various MBL values and clear instructions was used to calibrate the operator prior to the radiographic evaluation.

2.5.2. Analyzed Variables Related to MBL

MBL was measured and evaluated according to the following variables:

- Pre-operative parameters: gender, implant location, time of implant placement;
- Intraoperative parameters: implant diameter;
- Post-operative parameters: gingival thickness.

2.6. Clinical Periodontal Parameters

PS and BoP [7] were monitored around the implant restoration and in correspondence with adjacent teeth at 3 months (T3), 6 months (T6), 12 months (T12) and 48 months (T48).

Around the implant restorations and on adjacent teeth, four sites (mesial, distal, buccal, and oral) were evaluated for PS. The results were expressed as a dichotomous score (0 = no visible plaque at the soft margin; 1 = visible plaque at the soft margin).

BoP was assessed at four sites (mesial, distal, buccal, and oral) [7] around the implant restorations and on adjacent teeth, and a dichotomous score (0 = no bleeding; 1 = bleeding) was given.

During the surgical operations, the gingival thickness around the implants and their corresponding mesial neighboring teeth was identified. An endodontic file was used to penetrate the soft tissue three millimeters apical to the gingival edge (K-file Nr. 20; Dentsply-Maillefer, Tulsa, OK, USA). According to the mean registered value, the gingival

phenotype was classified as thick (soft tissue thickness > 2 mm) or thin (soft tissue thickness 2 mm) [26].

2.7. Statistical Analysis

Stata 17.1 (StataCorp, College Station, TX, USA) was used to perform all statistical analysis.

The skewness and kurtosis indexes were used to measure the distribution of the samples. Due to the normal distribution of data, linear regression models were fitted to evaluate the existence of any significant difference regarding the evaluated parameters, times (T1, T3, T6, T12, T36, T48) and the interactions between parameters and time. The aforementioned regression models were calculated using a generalized estimating equation approach in consideration of the correlation of the data caused by the presence of many implants per subject. Using a reliable variance–covariance estimator, we modified the estimates of the standard errors of the coefficients and the confidence intervals.

The connection between MBL at 48 months and the analyzed variables was assessed using a multiple linear regression with stepwise selection.

3. Results

A total of 41 implants were placed in 36 consecutive patients (16 males, 20 females, mean age 60 ± 9 years). No complications, peri-implantitis, peri-implant bone necrosis, early implant failures or mucositis occurred, and the survival rate was 100%. No drop-out has been reported. After 48 months, all implants were safe from complications.

MBL according to operative parameters is reported in Table 1.

Table 1. MBL (Mean \pm SD) of the placed implants evaluated at 1 and 3 months (pre-loading) and at 6,12,36 and 48 months (post-loading) from implant insertion. Different superscript letters represent statistically significant differences in the same horizontal row (capital letters among times) or in the same column (small letters for each parameter). p -value was set at 0.05.

Parameters	n	Pre-Loading			Post-Loading			
		T ₁	T ₃	T ₆	T ₁₂	T ₃₆	T ₄₈	
Gender	Males	17	+0.12 \pm 0.22 ^{aA}	−0.27 \pm 0.45 ^{aA}	−0.42 \pm 0.39 ^{aB}	−0.52 \pm 0.39 ^{aC}	−0.90 \pm 0.48 ^{aB}	−1.03 \pm 0.49 ^{aB}
	Females	24	−0.18 \pm 0.20 ^{bA}	−0.31 \pm 0.33 ^{aB}	−0.47 \pm 0.50 ^{aC}	−0.54 \pm 0.38 ^{aC}	−1.20 \pm 1.13 ^{bC}	−1.16 \pm 1.10 ^{aC}
Implant location	Maxilla	18	−0.12 \pm 0.20 ^{aA}	−0.28 \pm 0.32 ^{aA}	−0.47 \pm 0.40 ^{aB}	−0.61 \pm 0.78 ^{aB}	−0.92 \pm 1.13 ^{aC}	−1.08 \pm 1.01 ^{aC}
	Mandible	23	−0.19 \pm 0.21 ^{aA}	−0.31 \pm 0.35 ^{aB}	−0.43 \pm 0.41 ^{aB}	−0.47 \pm 0.39 ^{aB}	−1.16 \pm 1.19 ^{aC}	−1.12 \pm 1.16 ^{aC}
Implant placement timing	Immediate	12	−0.20 \pm 0.22 ^{aA}	−0.37 \pm 0.35 ^{aA}	−0.47 \pm 0.45 ^{aB}	−0.53 \pm 0.12 ^{aB}	−1.06 \pm 1.11 ^{aC}	−1.01 \pm 1.01 ^{aC}
	Early	12	+0.13 \pm 0.24 ^{bA}	−0.31 \pm 0.38 ^{aB}	−0.31 \pm 0.43 ^{aB}	−0.42 \pm 0.41 ^{aB}	−0.69 \pm 1.18 ^{bB}	−0.63 \pm 0.89 ^{bB}
	Delayed	17	−0.19 \pm 0.22 ^{aA}	−0.45 \pm 0.35 ^{aB}	−0.54 \pm 0.40 ^{aC}	−0.68 \pm 0.41 ^{aC}	−1.29 \pm 1.13 ^{aC}	−1.45 \pm 1.10 ^{aC}
Implant diameter	3.8 mm	14	−0.23 \pm 0.10 ^{aA}	−0.49 \pm 0.33 ^{aB}	−0.73 \pm 0.40 ^{aB}	−0.89 \pm 0.38 ^{aB}	−1.39 \pm 1.13 ^{aC}	−1.43 \pm 1.01 ^{aC}
	4.6 mm	27	−0.12 \pm 0.21 ^{aA}	−0.19 \pm 0.34 ^{aA}	−0.29 \pm 0.41 ^{bB}	−0.35 \pm 0.38 ^{bB}	−0.64 \pm 1.16 ^{bC}	−0.64 \pm 1.12 ^{bC}
Gingival thickness	Thin	23	−0.18 \pm 0.20 ^{aA}	−0.36 \pm 0.33 ^{aA}	−0.45 \pm 0.38 ^{aAB}	−0.57 \pm 0.38 ^{aB}	−1.09 \pm 1.13 ^{aC}	−1.27 \pm 1.11 ^{aC}
	Thick	18	−0.10 \pm 0.21 ^{aA}	−0.14 \pm 0.35 ^{aA}	−0.44 \pm 0.45 ^{aB}	−0.45 \pm 0.47 ^{aB}	−1.01 \pm 1.15 ^{aC}	−1.01 \pm 1.02 ^{aC}
Total	41	−0.15 \pm 0.18 ^A	−0.29 \pm 0.29 ^A	−0.45 \pm 0.37 ^B	−0.53 \pm 0.45 ^B	−1.06 \pm 1.13 ^C	−1.10 \pm 0.89 ^C	

MBL according to gender and location did not reveal statistically significant differences up to 48 months ($p > 0.05$).

Differently, some statistically significant differences were observed when considering implant placement timing, implant diameter and gingival thickness.

Implants placed 2–3 months after tooth extraction revealed lower MBL variation when compared to those placed immediately (immediate implants placed in fresh extraction sockets) or in completely healed ridges (delayed group), with a mean bone gain at T1. These values were lower at all evaluation times, but only from T36 were the differences statistically significant.

Implant diameter was found to significantly affect MBL. Narrower diameter implants (3.8 mm) showed significantly higher MBL variation from T3 to T48 when compared to 4.6 diameter implants. At T48, the greatest MBL variations were observed for 3.8 mm implants (mean MBL was 1.43 ± 1.01).

Gingival thickness significantly affects MBL during pre-load. Implants surrounded by a thick biotype showed lower MBL variations when compared to thin tissues. In the post-loading period, the differences decreased, with non-statistical differences at T12 and T48.

Multilevel analysis at T48 revealed that among all the evaluated variables, implant diameter was the factor mostly associated with MBL modifications ($p = 0.027$) (Table 2).

Table 2. Multilevel mixed-effects logistic regression exploring factors associated with MBL at 48 months.

Parameters	Coefficient	Robust Std. Err.	p	[95% Conf. Interval]	
Gender	0.2609	0.2775	0.347	−0.282	0.804
Implant location	−0.1749	0.3525	0.62	−0.865	0.516
Implant placement timing	0.2711	0.2018	0.179	−0.124	0.666
Implant diameter	−0.7855	0.3552	0.027	−1.481	−0.089
Gingival thickness	0.2611	0.4551	0.567	−0.632	1.154

BoP and PS around implants is reported in Table 3.

Table 3. Peri-implant parameters around implant restorations after provisional and definitive load. Values are expressed as percentages.

	Plaque Score (%)						Bleeding on Probing (%)					
	T ₃		T ₆		T ₄₈		T ₃		T ₆		T ₄₈	
	0	1	0	1	0	1	0	1	0	1	0	1
Mesial	87.1	12.9	90.3	9.7	87.1	12.9	90.3	9.7	90.3	9.7	93.5	6.5
Distal	93.5	6.5	94.4	5.6	93.5	6.5	93.5	6.5	100	0	94.4	5.6
Buccal	87.1	12.9	94.4	5.6	94.4	5.6	90.3	9.7	93.5	6.5	94.4	5.6
Oral	100	0	100	0	100	0	100	0	100	0	100	0

Low BoP values were observed at T3, percentages of bleeding sites were 4.7 ± 4.0 (range 0–9.7%) and 4.05% (range 0–9.7%). These percentages were similar at T48 and the mean value was 4.42% (0–6.5%). The mesial site was the most affected.

PS showed a similar trend: sites with plaque accumulation were 8.1% (range 0–12.9%) and 5.2% (range 0–9.7%) at T3 and T6. The most affected areas were the mesial and the buccal sites, while in the oral site no difference was observed. Similar results were observed at T48.

Periapical radiographs reporting two treated cases are shown in Figures 2 and 3.

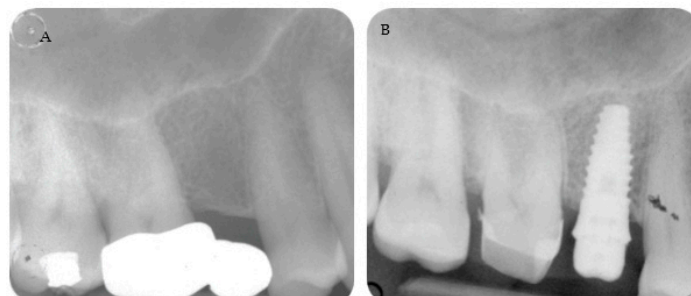


Figure 2. Cont.

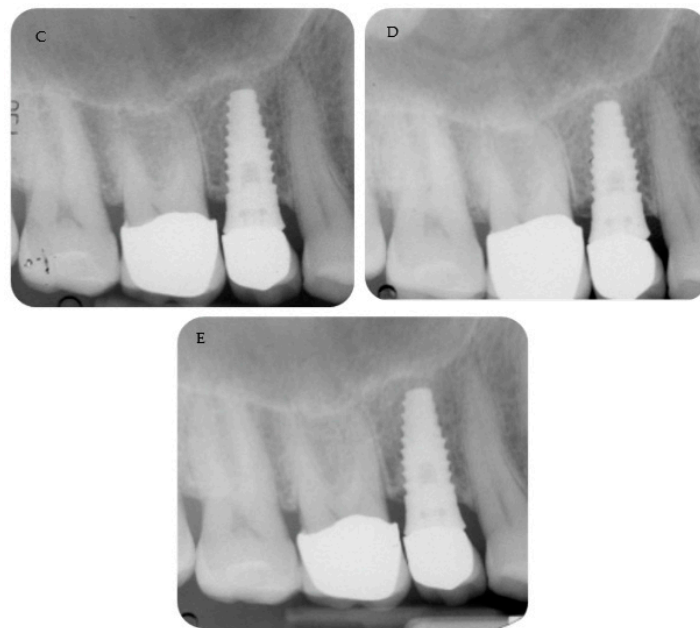


Figure 2. A 4.6 mm tissue-level implant was placed with a flapless approach. (A) Pre-operative radiograph. (B) Periapical radiograph shows the abutment screwed and the cemented provisional crown. Follow-up at 3 months. (C) Follow-up at 12 months with the metal ceramic crown cemented on the abutment. MBLs were stable at (D) 36 months and (E) 48 months, with limited bone loss.

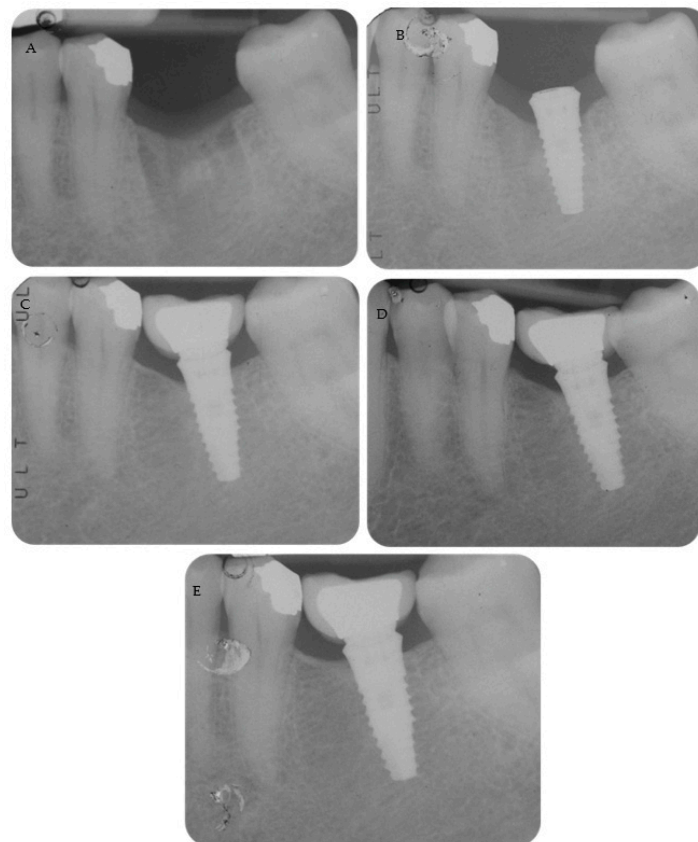


Figure 3. (A) Early timing placement to rehabilitate a single edentulous ridge. Tooth was extracted 2 months before for a root fracture. (B) Implant placement with a flapless approach. Please note that the neck was positioned at tissue level. (C) Periapical radiograph after abutment and definitive crown cementation. (D) Follow-up at 36 months and (E) 48 months showed MBL stability around the implant.

4. Discussion

In the present study, tissue-level implants with a laser-microtextured neck were placed with a flapless technique with the cover screw exposed. Our findings revealed hard tissue stability and limited MBL during the 4-year period.

The valid periodontal parameters and MBL observed during the early phase after placement and during the 4-year evaluations support the use of a Laser-Lok surface for an implant placed at tissue-level. Soft tissue morphology and mucosa integrity proved sufficient to avoid bacteria penetration and to induce fibroblast attachment and a correct vascular environment for bone formation and a stable MBL.

The result of our investigation is supported by a recent clinical study that compared the expression of pro-inflammatory cytokines in peri-implant crevicular fluid of implants placed at bone level versus tissue level [27]. Bone-level implants demonstrated, after 5 years, a higher level of inflammatory cytokines than tissue-level implants [27].

A recent review reported that the fibro-collagenous attachment around the microgrooved neck might stabilize the bone and reduce crestal bone resorption [28]. Previous *in vitro* investigations revealed osteoblast attachment on the laser-microtextured neck and cell alignment along the microgroove directions [29]. An animal model also demonstrated a direct connective tissue attachment to the microgrooved surface where the fibers were mostly disposed perpendicular to the implant surface [30].

Clinically, these aspects may also induce less incidence of peri-implant inflammation around the transmucosal portion. A recent 5-year retrospective multicenter study reported a lower incidence of peri-implant mucositis on laser-microtextured neck implants, suggesting lower pathological bacteria concentration compared to non-laser implants with the implant design [19].

In this study, different clinical operative parameters were analyzed, including implant placement timing, soft tissue thickness and implant diameters.

Interestingly and unexpectedly, neither timing nor soft tissue thickness parameters showed any significant differences at 48 months from insertions. Other studies that consider implants characterized with a transmucosal neck [31] or platform-switch implants [16] found different results. In this context, the neck morphology and the laser-microtextured design could have influenced the clinical outcomes.

Interestingly, implant diameter was the factor mostly associated with MBL variation. A wider implant diameter (4.6 mm in this case) better preserved bone marginal morphology and crestal level, while a narrower diameter implant (3.6 mm) revealed greater marginal bone loss. Implant diameter was selected before placement in accordance with the bone crest morphology in healed crest (early and delayed implants) or in accordance with the residual bone in the post-extractive sites (immediate implants).

As observed in Table 2, 3.6 mm diameter implants showed the greatest bone loss at T48. Stress values affecting the crestal cortical bone can influence peri-implant crestal bone resorption. Wider implant diameters may reduce mechanical stress on crestal bone, directly influencing MBL. Some studies reported a higher risk of prosthetic complications for narrow diameter implants, including abutment and implant fracture, screw loosening or fracture and ceramic fracture, which may occur in the long term [32,33]. In the present study, none of these complications occurred.

The proposed protocol allowed the management of dental implant insertion, impression techniques and prosthetic restorations with limited surgical trauma, limited bone loss and no complications.

A relatively high mean age of patients was observed in this study (mean age 60 ± 9 years). Patients with older age often require minimally invasive protocols including flapless surgeries, one-stage surgery, immediate placement/immediate loading and the use of short and narrow diameter implants [34,35].

All provisional and definitive crowns were cement-retained. Temporary zinc-oxide eugenol-based cement was selected for provisional restorations, as enough retention on the neck has been observed (with no presence of de-cemented crowns). Definitive

rehabilitations were cemented with a polycarboxylate-based cement, which made them easier to remove during setting time and less irritating than methacrylate-based definitive cements [36]. According to a review, no significant differences were observed when comparing single implant restorations between cement-retained and screw-retained crowns [37]. Moreover, in the tissue-level technique, the risk for excess cement retention under soft tissue levels was reduced, as the implant abutment connection is located more coronally than in conventional bone-level implants [37].

The limitation of this study may be represented by the relatively low number of patients. In the future, impression techniques must be obtained via a 3D scanner, and the preparation of abutment design may be affected by the new digital technique and workflow. Further studies with a larger sample size and at a longer follow-up should validate the flapless technique with tissue-level implant placement that is proposed here [38,39]. The lack of complications may be influenced by patient selections and by strict compliance with the protocol.

5. Conclusions

The use of Laser-Lok implants placed at tissue level using a flapless technique is supported by this four-year clinical research. During the 48-month follow-up, minimal bone loss and stable marginal bone levels were seen. These values were in line with those reported in the literature. This transmucosal flapless technique allows a soft tissue healing as demonstrated by periodontal parameters that were stable during the 4 years of follow-up. No signs of inflammation or soft tissue alteration around the laser-microtextured neck were observed. The wider diameter implant seems to preserve bone levels.

Author Contributions: Conceptualization, C.P.; methodology, C.P.; software, A.S. and F.Z.; validation, A.S. and F.Z.; investigation, C.P., A.S. and F.Z.; resources, C.P. and M.G.G.; data curation, A.S. and F.Z.; writing—original draft preparation, C.P., A.S., F.Z. and M.G.G.; writing—review and editing, G.R. and M.G.G.; visualization, A.S.; supervision, C.P. All authors have read and agreed to the published version of the manuscript.

Funding: This research received no external funding.

Institutional Review Board Statement: Not applicable.

Informed Consent Statement: Informed consent was obtained from all subjects involved in the study.

Data Availability Statement: Not applicable.

Conflicts of Interest: The authors declare no conflict of interest.

References

1. Albrektsson, T.; Brånemark, P.I.; Hansson, H.A.; Lindström, J. Osseointegrated titanium implants. Requirements for ensuring a long-lasting, direct bone-to-implant anchorage in man. *Acta Orthop. Scand.* **1981**, *52*, 155–170. [[PubMed](#)]
2. Albrektsson, T.; Zarb, G.; Worthington, P.; Eriksson, A.R. The long-term efficacy of currently used dental implants: A review and proposed criteria of success. *Int. J. Oral Maxillofac. Implant.* **1986**, *1*, 11–25.
3. Cruz, R.S.; Lemos, C.A.A.; de Luna Gomes, J.M.; Fernandes E Oliveira, H.F.; Pellizzer, E.P.; Verri, F.R. Clinical comparison between crestal and subcrestal dental implants: A systematic review and meta-analysis. *J. Prosthet. Dent.* **2022**, *127*, 408–417. [[PubMed](#)]
4. Flores-Guillen, J.; Álvarez-Novoa, C.; Barbieri, G.; Martín, C.; Sanz, M. Five-year outcomes of a randomized clinical trial comparing bone-level implants with either submerged or transmucosal healing. *J. Clin. Periodontol.* **2018**, *45*, 125–135. [[CrossRef](#)]
5. Obreja, A.K.; Ramanauskaitė, A.; Begić, A.; Galarraga-Vinueza, M.E.; Parvini, P.; Sader, R.; Schwarz, F. The prevalence of peri-implant diseases around subcrestally placed implants: A cross-sectional study. *Clin. Oral Implant. Res.* **2021**, *32*, 702–710.
6. Hermann, J.S.; Buser, D.; Schenk, R.K.; Schoolfield, J.D.; Cochran, D.L. Biologic Width around one- and two-piece titanium implants. *Clin. Oral Implant. Res.* **2001**, *12*, 559–571. [[CrossRef](#)] [[PubMed](#)]
7. Cosyn, J.; Eghbali, A.; Hermans, A.; Vervaeke, S.; De Bruyn, H.; Cleymaet, R. A 5-year prospective study on single immediate implants in the aesthetic zone. *J. Clin. Periodontol.* **2016**, *43*, 702–709.
8. Paul, S.; Petsch, M.; Held, U. Modeling of crestal bone after submerged vs. transmucosal implant placement: A Systematic Review with Meta-Analysis. *Int. J. Oral Maxillofac. Implant.* **2017**, *32*, 1039–1050. [[CrossRef](#)]

9. Sanz, M.; Ivanoff, C.J.; Weingart, D.; Wiltfang, J.; Gahlert, M.; Cordaro, L.; Ganeles, J.; Bragger, U.; Jackowski, J.; Martin, W.C.; et al. Clinical and radiologic outcomes after submerged and transmucosal implant placement with two-piece implants in the anterior maxilla and mandible: 3-year results of a randomized controlled clinical trial. *Clin. Implant. Dent. Relat. Res.* **2015**, *17*, 234–246. [[CrossRef](#)]
10. Bucci-Sabattini, V.; Cassinelli, C.; Coelho, P.G.; Minnici, A.; Trani, A.; Dohan Ehrenfest, D.M. Effect of titanium implant surface nanoroughness and calcium phosphate low impregnation on bone cell activity in vitro. *Oral Surg. Oral Med. Oral Pathol. Oral Radiol.* **2010**, *109*, 217–224.
11. Lazzara, R.J.; Porter, S.S. Platform switching: A new concept in implant dentistry for controlling postrestorative crestal bone levels. *Int. J. Periodontics Restor. Dent.* **2006**, *26*, 9–17.
12. Dank, A.; Aartman, I.H.A.; Wismeijer, D.; Tahmaseb, A. Effect of dental implant surface roughness in patients with a history of periodontal disease: A systematic review and meta-analysis. *Int. J. Implant Dent.* **2019**, *5*, 12. [[CrossRef](#)] [[PubMed](#)]
13. Uraz, A.; Isler, S.C.; Cula, S.; Tunc, S.; Yalim, M.; Cetiner, D. Platform-switched implants vs. platform-matched implants placed in different implant-abutment interface positions: A prospective randomized clinical and microbiological study. *Clin. Implant. Dent. Relat. Res.* **2020**, *22*, 59–68. [[CrossRef](#)] [[PubMed](#)]
14. Jeong, S.M.; Choi, B.H.; Li, J.; Kim, H.S.; Ko, C.Y.; Jung, J.H.; Lee, H.J.; Lee, S.H.; Engelke, W. Flapless implant surgery: An experimental study. *Oral Surg. Oral Med. Oral Pathol. Oral Radiol.* **2007**, *104*, 24–28. [[CrossRef](#)]
15. Chrcanovic, B.R.; Albrektsson, T.; Wennerberg, A. Flapless versus conventional flapped dental implant surgery: A meta-analysis. *PLoS ONE* **2014**, *9*, 100624.
16. Prati, C.; Zamparini, F.; Pirani, C.; Montebugnoli, L.; Canullo, L.; Gandolfi, M.G. A Multilevel Analysis of Platform-Switching Flapless Implants Placed at Tissue Level: 4-year Prospective Cohort Study. *Int. J. Oral Maxillofac. Implant.* **2020**, *35*, 330–341. [[CrossRef](#)]
17. Nevins, M.; Camelo, M.; Nevins, M.L.; Schuepbach, P.; Kim, D.M. Connective tissue attachment to laser-microgrooved abutments: A human histologic case report. *Int. J. Periodontics Restor. Dent.* **2012**, *32*, 385–392.
18. Nevins, M.; Leziy, S.; Kerr, E.; Janke, U.; Rasperini, G.; Hanratty, J.; Pasquinelli, K.; Testori, T.; Shapoff, C.A.; Kim, D.M. A Prospective Clinical and Radiographic Assessment of Platform-Switched Laser-Microchannel Implants Placed in Limited Interimplant Spaces. *Int. J. Periodontics Restor. Dent.* **2017**, *37*, 33–38.
19. Guarneri, R.; Grande, M.; Zuffetti, F.; Testori, T. Incidence of peri-implant diseases on implants with and without laser-microgrooved collar: A 5-Year retrospective study carried out in private practice patients. *Int. J. Oral Maxillofac. Implant.* **2018**, *33*, 457–465.
20. Nevins, M.; Nevins, M.L.; Camelo, M.; Boyesen, J.L.; Kim, D.M. Human histologic evidence of a connective tissue attachment to a dental implant. *Int. J. Periodontics Restor. Dent.* **2008**, *28*, 111–121.
21. Guarneri, R.; Miccoli, G.; Di Nardo, D.; D'Angelo, M.; Morese, A.; Seracchiani, M.; Testarelli, L. Effect of a laser-ablated micron-scale modification of dental implant collar surface on changes in the vertical and fractal dimensions of peri-implant trabecular bone. *Clin. Ter.* **2020**, *171*, 385–392.
22. Zamparini, F.; Spinelli, A.; Montebugnoli, L.; Pelliccioni, G.A.; Gandolfi, M.G.; Prati, C. Soft and hard tissues analysis around tissue level implants with laser microtextured neck: A 12-month pilot study. *Dent. Cadmos* **2022**, *90*, 532–541. [[CrossRef](#)]
23. Vandembroucke, J.P.; von Elm, E.; Altman, D.G.; Gøtzsche, P.C.; Mulrow, C.D.; Pocock, S.J.; Poole, C.; Schlesselman, J.J.; Egger, M.; STROBE Initiative. Strengthening the reporting of observational studies in epidemiology (STROBE): Explanation and elaboration. *Int. J. Surg.* **2014**, *12*, 1500–1524. [[CrossRef](#)] [[PubMed](#)]
24. Hämmerle, C.H.; Chen, S.T.; Wilson, T.G., Jr. Consensus statements and recommended clinical procedures regarding the placement of implants in extraction sockets. *Int. J. Oral Maxillofac. Implant.* **2004**, *19*, 26–28.
25. Prati, C.; Zamparini, F.; Scialabba, V.S.; Gatto, M.R.; Piattelli, A.; Montebugnoli, L.; Gandolfi, M.G. A 3-year prospective cohort study on 132 calcium phosphate-blasted implants: Flap vs. flapless technique. *Int. J. Oral Maxillofac. Implant.* **2016**, *31*, 413–423.
26. Cosgarea, R.; Gasparik, C.; Ducea, D.; Culic, B.; Dannewitz, B.; Sculean, A. Peri-implant soft tissue colour around titanium and zirconia abutments: A prospective randomized controlled clinical study. *Clin. Oral. Implants Res.* **2015**, *26*, 537–544.
27. Guarneri, R.; Reda, R.; Di Nardo, D.; Miccoli, G.; Zanza, A.; Testarelli, L. Clinical, radiographic, and biochemical evaluation of two-piece versus one-piece single implants with a laser-microgrooved collar surface after 5 years of functional loading. *Clin. Implant. Dent. Relat. Res.* **2022**, *24*, 676–682. [[PubMed](#)]
28. Koodaryan, R.; Hafezeqoran, A. Effect of laser-microtexturing on bone and soft tissue attachments to dental implants: A systematic review and meta-analysis. *J. Dent. Res. Dent. Clin. Dent. Prospect.* **2021**, *15*, 290–296. [[CrossRef](#)]
29. Chen, J.; Ulerich, J.P.; Abelev, E.; Fasasi, A.; Arnold, C.B.; Soboyejo, W.O. An investigation of the initial attachment and orientation of osteoblast-like cells on laser grooved Ti-6Al-4V surfaces. *Mater. Sci. Eng. C* **2009**, *29*, 1442–1452.
30. Nevins, M.; Kim, D.M.; Jun, S.-H.; Guze, K.; Schuepbach, P.; Nevins, M.L. Histologic evidence of a connective tissue attachment to laser microgrooved abutments: A canine study. *Int. J. Periodontics Restor. Dent.* **2010**, *30*, 245–255.
31. Ceruso, F.M.; Ieria, I.; Tallarico, M.; Meloni, S.M.; Lumbau, A.I.; Mastroianni, A.; Zotti, A.; Gargari, M. Comparison between Early Loaded Single Implants with Internal Conical Connection or Implants with Transmucosal Neck Design: A Non-Randomized Controlled Trial with 1-Year Clinical, Aesthetics, and Radiographic Evaluation. *Materials* **2022**, *15*, 511. [[PubMed](#)]
32. Allum, S.R.; Tomlinson, R.A.; Joshi, R. The impact of loads on standard diameter, small diameter and mini implants: A comparative laboratory study. *Clin. Oral Implant. Res.* **2008**, *19*, 553–559.
33. Assaf, A.; Saad, M.; Daas, M.; Abdallah, J.; Abdallah, R. Use of narrow-diameter implants in the posterior jaw: A systematic review. *Implant Dent.* **2015**, *24*, 294–306. [[PubMed](#)]

34. Sato, Y.; Kitagawa, N.; Isobe, A. Implant treatment in ultra-aged society. *Jpn. Dent. Sci. Rev.* **2018**, *54*, 45–51. [[PubMed](#)]
35. Schimmel, M.; Müller, F.; Suter, V.; Buser, D. Implants for elderly patients. *Periodontology* **2000**, *73*, 228–240. [[CrossRef](#)] [[PubMed](#)]
36. Al Amri, M.D.; Al-Rasheed, A.S.; Al-Kheraif, A.A.; Alfadda, S.A. Comparison of clinical, radiographic, and immunologic inflammatory parameters around dental implants with cement-Retained and Screw-Retained Restorations: A 5-Year Prospective Cohort Study in Men. *Int. J. Prosthodont.* **2017**, *30*, 384–389. [[CrossRef](#)]
37. Sailer, I.; Mühlemann, S.; Zwahlen, M.; Hämmerle, C.H.F.; Schneider, D. Cemented and screw-retained implant reconstructions: A systematic review of the survival and complication rates. *Clin. Oral Implant. Res.* **2012**, *23*, 163–201.
38. Prati, C.; Zamparini, F.; Canullo, L.; Pirani, C.; Botticelli, D.; Gandolfi, M.G. Factors Affecting Soft and Hard Tissues Around Two-Pies Transmucosal Implants: A 3-Year Prospective Cohort Study. *Int. J. Oral Maxillofac. Implant.* **2020**, *35*, 1022–1036. [[CrossRef](#)]
39. Zamparini, F.; Pirani, C.; Chavarría-Bolanos, D.; Gandolfi, M.G.; Prati, C. Rehabilitation of anterior maxilla with a novel hyperbolic profile transmucosal implant in elderly patients. *Minerva Stomatol.* **2019**, *68*, 249–258. [[CrossRef](#)]

Disclaimer/Publisher’s Note: The statements, opinions and data contained in all publications are solely those of the individual author(s) and contributor(s) and not of MDPI and/or the editor(s). MDPI and/or the editor(s) disclaim responsibility for any injury to people or property resulting from any ideas, methods, instructions or products referred to in the content.



Article

Micro-Nano Surface Characterization and Bioactivity of a Calcium Phosphate-Incorporated Titanium Implant Surface

Fausto Zamparini ^{1,2}, Carlo Prati ², Luigi Generali ³, Andrea Spinelli ^{1,2}, Paola Taddei ⁴
and Maria Giovanna Gandolfi ^{1,*}

- ¹ Laboratory of Biomaterials and Oral Pathology, School of Dentistry, Department of Biomedical and Neuromotor Sciences, University of Bologna, 40126 Bologna, Italy; fausto.zamparini2@unibo.it (F.Z.); andrea.spinelli4@unibo.it (A.S.)
 - ² Endodontic Clinical Section, School of Dentistry, Department of Biomedical and Neuromotor Sciences, University of Bologna, 40126 Bologna, Italy; carlo.prati@unibo.it
 - ³ Department of Surgery, Medicine, Dentistry and Morphological Sciences with Transplant Surgery, Oncology and Regenerative Medicine Relevance, University of Modena and Reggio Emilia, 41121 Modena, Italy; luigi.generali@unimore.it
 - ⁴ Biochemistry Unit, Department of Biomedical and Neuromotor Sciences, University of Bologna, 40126 Bologna, Italy; paola.taddei@unibo.it
- * Correspondence: mgiovanna.gandolfi@unibo.it

Abstract: The surface topography of dental implants and micro-nano surface characterization have gained particular interest for the improvement of the osseointegration phases. The aim of this study was to evaluate the surface micro-nanomorphology and bioactivity (apatite forming ability) of Ossean[®] surface, a resorbable blast medium (RBM) blasted surface further processed through the incorporation of a low amount of calcium phosphate. The implants were analyzed using environmental scanning electronic microscopy (ESEM), connected to Energy dispersive X-ray spectroscopy (EDX), field emission gun SEM-EDX (SEM-FEG) micro-Raman spectroscopy and X-ray photoelectron spectroscopy (XPS) before and after immersion in weekly refreshed Hank's balanced salt solution (HBSS) for 28 days. The analysis of the samples before immersion showed a moderately rough surface, with micropits and microgrooves distributed on all of the surface; EDX microanalysis revealed the constitutional elements of the implant surface, namely titanium (Ti), aluminum (Al) and vanadium (V). Limited traces of calcium (Ca) and phosphorous (P) were detected, attributable to the incorporated calcium phosphate. No traces of calcium phosphate phases were detected by micro-Raman spectroscopy. ESEM analysis of the implant aged in HBSS for 28 days revealed a significantly different surface, compared to the implant before immersion. At original magnifications <2000×, a homogeneous mineral layer was present on all the surface, covering all the pits and microgrooves. At original magnifications ≥10,000×, the mineral layer revealed the presence of small microspherulites. The structure of these spherulites (approx. 2 μm diameter) was observed in nanoimmersion mode revealing a regular shape with a hairy-like contour. Micro-Raman analysis showed the presence of B-type carbonated apatite on the implant surface, which was further confirmed by XPS analysis. This implant showed a micro-nano-textured surface supporting the formation of a biocompatible apatite when immersed in HBSS. These properties may likely favor bone anchorage and healing by stimulation of mineralizing cells.

Keywords: dental implant surfaces; ESEM-EDX; SEM-FEG; bioactivity; micro-Raman spectroscopy



Citation: Zamparini, F.; Prati, C.; Generali, L.; Spinelli, A.; Taddei, P.; Gandolfi, M.G. Micro-Nano Surface Characterization and Bioactivity of a Calcium Phosphate-Incorporated Titanium Implant Surface. *J. Funct. Biomater.* **2021**, *12*, 3. <https://doi.org/10.3390/jfb12010003>

Received: 28 November 2020

Accepted: 4 January 2021

Published: 7 January 2021

Publisher's Note: MDPI stays neutral with regard to jurisdictional claims in published maps and institutional affiliations.



Copyright: © 2021 by the authors. Licensee MDPI, Basel, Switzerland. This article is an open access article distributed under the terms and conditions of the Creative Commons Attribution (CC BY) license (<https://creativecommons.org/licenses/by/4.0/>).

1. Introduction

A direct bone apposition onto the surface of titanium is critical for the successful integration of the implant, and the long-term success of the rehabilitation. Indeed, several biological processes start immediately after implant insertion [1], which follows the traditional intrabony wound healing phases: hemostasis (minutes to first hours), inflammatory

phase (first hours to days), proliferative days (days to three weeks) and remodeling phase (from three weeks to years) [2].

An essential role in osseointegration processes during this period is played by the surface topography of the dental implants [3]. The micro and nano structures of the implants in contact with the bone tissues significantly enhance bone apposition, through a higher bone-to-implant contact [4], osteoblast cells attachment proliferation, and differentiation [5].

Topographically modified titanium surfaces such as sandblasted, large-grit, acid-etched implants are already implemented clinically, showing successful performances [6]. Calcium phosphates (CaPs) such as hydroxyapatite, beta-tricalcium phosphate and mixtures have been considered attractive blasting materials, being resorbable, biocompatible, osteoconductive and bioactive [7,8].

When considering implants surface modifications, these could be achieved through addition or subtraction methods [9]. Additive methods imply the addition of another material/compound, which is added onto the surface (implant coating) or integrated within the titanium oxide layer (incorporation process) [10].

However, the addition of a CaP coating revealed several drawbacks in the past years, including its dissolution after surgical procedures, failed interfacial adhesion between implant and CaP layer and subsequently higher early implant failure [11,12].

Ossean[®] is a moderately rough Ti-Al-V surface obtained through the resorbable blasted medium (RBM) process and followed by the incorporation of a low amount of CaP.

The surface roughness was conceived to obtain micro and nano irregularities, which should enhance implant biocompatibility compared to traditional surfaces, increasing the available contact surface and potentially improving the mineralizing cells attachment and expansion [13].

The incorporation of a low amount of CaP may improve the surface biointeractivity during the initial osseointegration processes through the apatite nucleation on its surface without the abovementioned detrimental effects; however, no information on the apatite nucleation ability of the implant has been reported.

The evaluation of the apatite-forming ability of implant materials in simulated body fluids (SBF) is useful for the assessment of their biointeractivity (ability to exchange information with a biological system) and bioactivity (ability to cause a positive reaction in the host tissues), as well as to predict their *in vivo* bone-bonding ability [14,15].

The aim of this study was to analyze the surface micro and nano/morphology of Ossean[®] surface and its modifications after immersion in SBF. The null-hypothesis of the present study was that there is no difference in the superficial elemental composition of a Ti-Al-V implant treated with a resorbable blasted medium process before and after immersion in Hank's balanced salt solution.

2. Materials and Methods

2.1. Implants

Two implants were received in the commercial packaged and sterilized form (Intralock, Boca Raton, FL, USA) (lot: ak980, exp. Date 2018-10; lot: ak991, exp. Date 2018-10).

2.2. Surface Micro and Nano Characterization and CaPs Nucleation in Simulated Body Fluids (SBF)

The International Standard ISO 23317 method (BS ISO 23317, 2007) was used to evaluate the formation of a layer rich in Ca and P on the surface of the implants soaked in Hank's balanced salt solution (HBSS), which was used as SBF according to several studies [16–20]. The HBSS (Cambrex Bio Science Verviers, Belgium) composition was: Ca²⁺ 1.27 mM, Cl⁻ 144.7 mM, K⁺ 5.8 mM, Na⁺ 141.6 mM, Mg²⁺ 0.81 mM, HCO₃⁻ 4.17 mM, SO₄²⁻ 0.81 mM, H₂PO₄⁻ 0.44 mM and HPO₄²⁻ 0.336 mM.

One sample was analyzed before immersion. The other sample was placed vertically (BS ISO 23317, 2007) in 20 mL of HBSS at 37 °C. The medium was weekly refreshed for

28 days. At this endpoint, the surface was non-invasively examined by ESEM-EDX and micro-Raman spectroscopy to assess the formation of CaP.

2.2.1. ESEM-EDX Microanalysis

Microanalyses were performed using an environmental scanning electron microscope (ESEM-Quanta 200, Fei Company-Oxford Instruments, Eindhoven, NL, USA) connected to a secondary electron detector for energy dispersive X-ray spectroscopy (EDS; INCA, Oxford Instruments, Oxford, UK) using computer-controlled software [16–21]. The whole samples were examined without sputtering at low vacuum (100 Pascal), accelerating voltage of 20 kV, working distance 8.5 mm, 0.5 wt% detection level, 133 eV resolution, amplification time 100 μ s, measuring time: 60 s for spectra. Standard acquisition resolution was 1536×1024 .

Then, EDX microanalyses were carried out at $2000\times$ original magnification at random areas of $\sim 50 \times 50 \mu\text{m}$ to evaluate the relative element content. The elemental microanalysis (weight % and atomic %) with ZAF correction method, a procedure in which corrections for atomic number effect (Z), absorption (A), and fluorescence (F) are calculated separately, was performed in full frame and spot mode to analyze entire areas or specific points, respectively [19–21].

2.2.2. FEG-SEM-EDX

Surface characterization of the implant surface on the implant before immersion and after 28 days immersion in HBSS solution was performed by using a field emission gun scanning electron microscope (FEG-SEM: Nova NanoSEM 450; FEI Company-Oxford Instruments, Eindhoven, NL, USA). Samples were observed without sputtering with the following parameters: accelerating voltage of 12 kV, working distance 6.0–6.5 mm, 133 eV resolution, amplification time 100 μ s, measuring time: 60 s for spectra. Standard acquisition resolution was 1536×1024 .

EDX (Quantax-200 system with XFlash 6/10 Si-drift detector: Bruker Corp., Billerica, MA, USA) spot microanalyses were performed at $500\text{--}2000\times$ and $10,000\text{--}200,000\times$ original magnifications. Areas of $\sim 30 \times 30 \mu\text{m}$ were selected for images at $2000\times$ original magnifications, while areas of $\sim 2 \times 2 \mu\text{m}$ at original magnifications $\geq 10,000\times$ were investigated.

2.2.3. Raman Spectroscopy and XPS Analysis

Micro-Raman spectra were obtained by using an NRS-2000C (Jasco International Co. Ltd., Tokyo, Japan) instrument with a microscope of $100\times$ original magnification. All the spectra were recorded in back-scattering conditions with 5 cm^{-1} spectral resolution by using the 532 nm green diode-pumped solid-state laser driver (RgBLase LLC, Fremont, CA, USA). A 160 K cooled digital charge coupled device (Spec-10: 100B, Roper Scientific Inc., Sarasota, FL, USA) was used as a detector. Laser power on the sample was about 10 mW for the implant before immersion and about 20 mW for the HBSS-aged sample. To obtain a good representation of the analyzed implants, 8–10 micro-Raman spectra were collected in different points of each sample.

XPS was performed on the implant before and after immersion for 28 days in HBSS to investigate the surface modification and apatite nucleation ability. A hemispherical energy analyzer (9 channeltron Phoibos HSA3500 150, SPECS GmbH, Berlin, Germany) was used. X-ray source was $\text{MgK}\alpha$ emission line (1253.6 eV) with an incidence of 45° . Samples were analyzed without any treatment at 7×10^{-10} mbar pressure. Data were acquired with LabSpecs and analyzed with Igor Pro 6.37 software.

3. Results

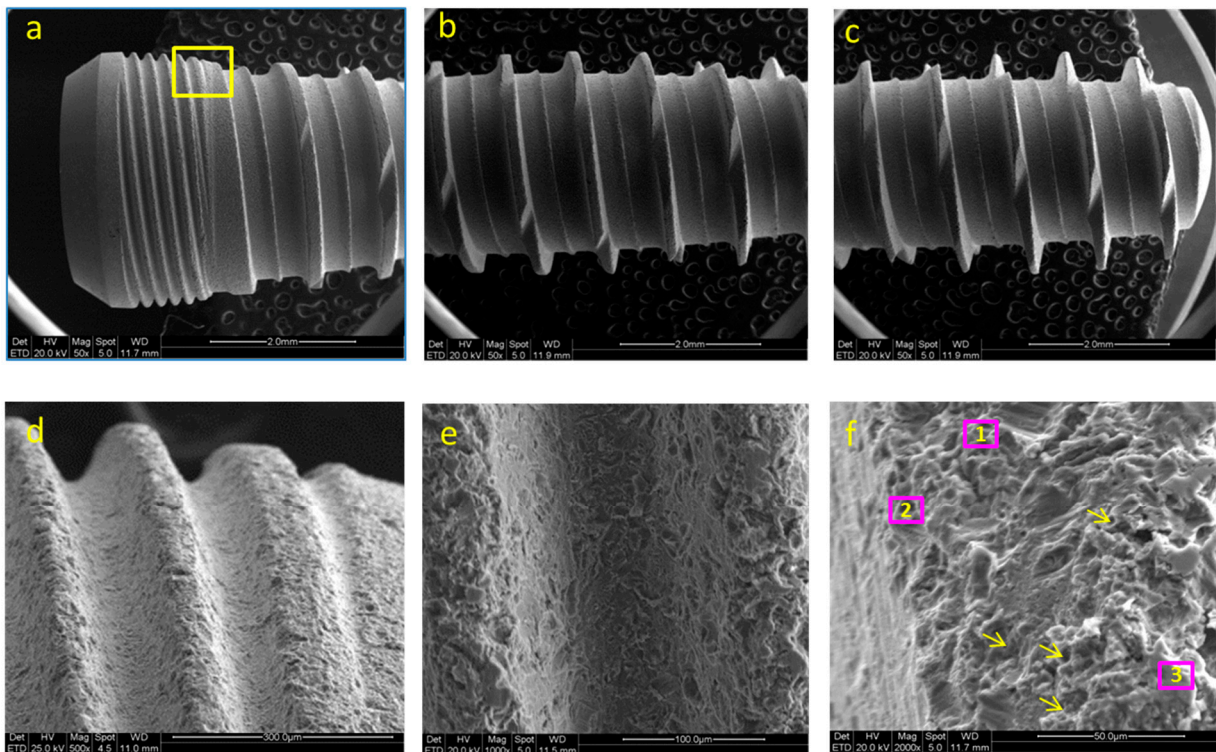
3.1. Implant before Immersion

3.1.1. ESEM-EDX Analysis

ESEM images of the coronal, medium and apical portion of the implant before immersion are reported in Figure 1a–c. A tapered configuration with regular threads is revealed.

Tapping segments, designed to reduce the stress during the implant insertion procedures, are present along all the threads. The images of one thread at the collar portion at 500×, 1000× and 2000× original magnifications are reported in Figure 1d–f. The analysis revealed a moderately rough surface, with irregular pits and craters. The structures identified were comprised between 2 and 10 microns and were uniformly distributed on all of the implant surface.

EDX microanalysis revealed the elements constituting the implant surface, namely titanium (Ti), aluminum (Al) and vanadium (V). Very low traces of calcium (Ca) (detected on all the spectra) and phosphorous (P) (detected only in one spectrum) were detected (Figure 1).



EDX analysis of implant surface before immersion in HBSS (results in atomic %)											
	C	O	Na	Mg	Al	Si	P	Cl	Ca	Ti	V
1					19.93				0.23	72.52	9.32
2					22.90				0.03	72.36	4.71
3	4.96				8.57		0.41		0.13	82.23	3.71

Figure 1. ESEM images of the coronal (a), medium (b) and apical (c) portion of the implant before immersion. EDX analyses (f) performed in five regions of interest; the pink square mark represents the area observed at progressively higher magnification. Thread at the collar portion at 500× (d), 1000× (e) and 2000× (f) original magnifications. EDX microanalysis is of on one thread located on the medium portion of the implant before immersion. Pink numbered squares represent the random areas analyzed through EDX. In addition to the constitutional elements of the Ti-Al-V dental implant surface, very low traces of Ca and P were detected. Arrows indicate the presence of pits and craters on the implant surface.

3.1.2. FEG-SEM-EDX Analysis

FEG-SEM images of the as-received implant are reported in Figure 2a–f. The surface appeared similar on all of the implant body, with no differences between the coronal,

medium and apical portions. One thread located in the same region as the previous ESEM analysis was selected and observed at progressively higher magnifications. At $10,000\times$ original magnifications, some crystal rods may be observed. The presence of these crystals may likely be attributed to the CaP incorporation. One area with a well-identifiable rod (measuring approx. 600 nm in length and 200 nm in width) was observed by using nanoimmersion mode at $25,000\times$, $50,000\times$, $100,000\times$ and $200,000\times$ original magnifications.

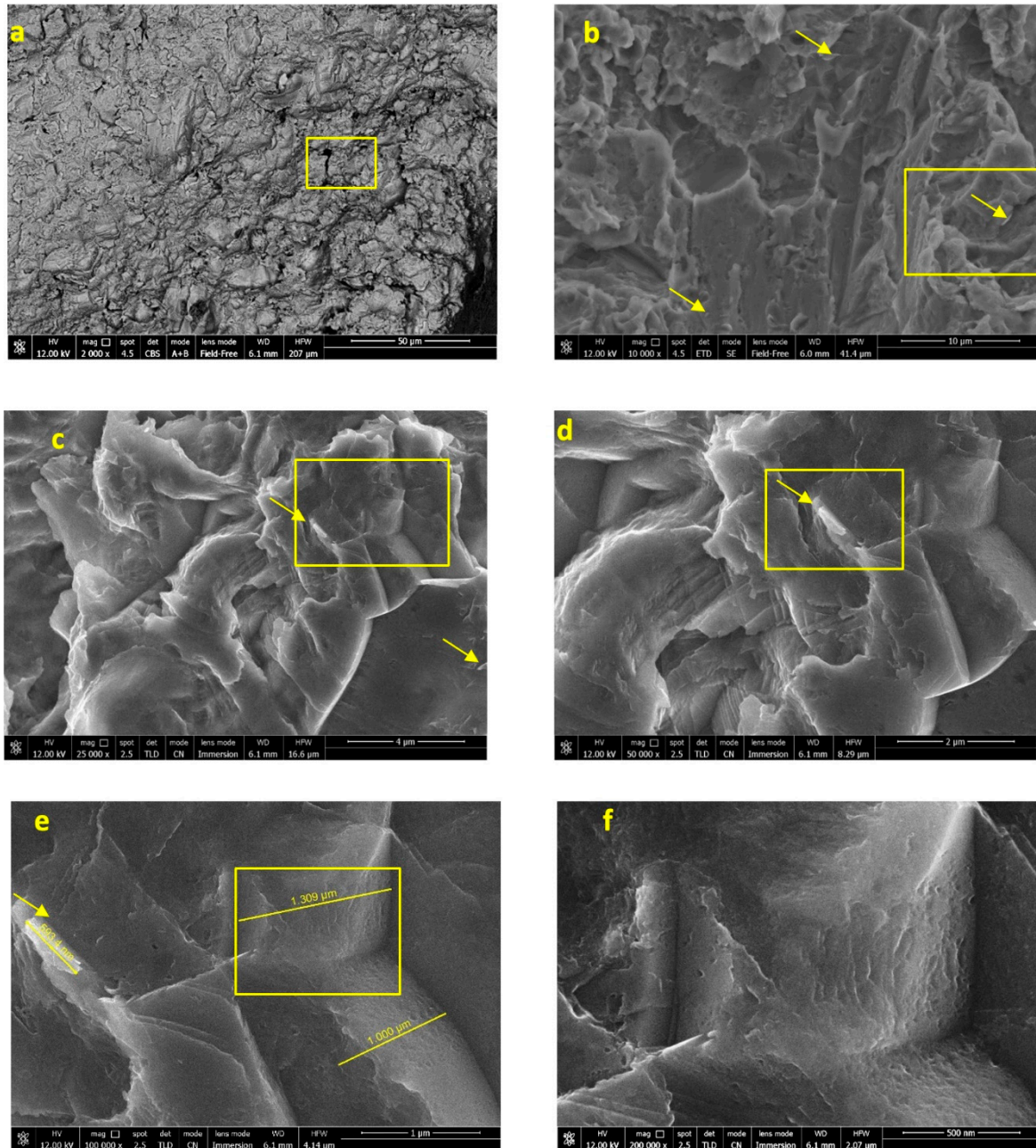
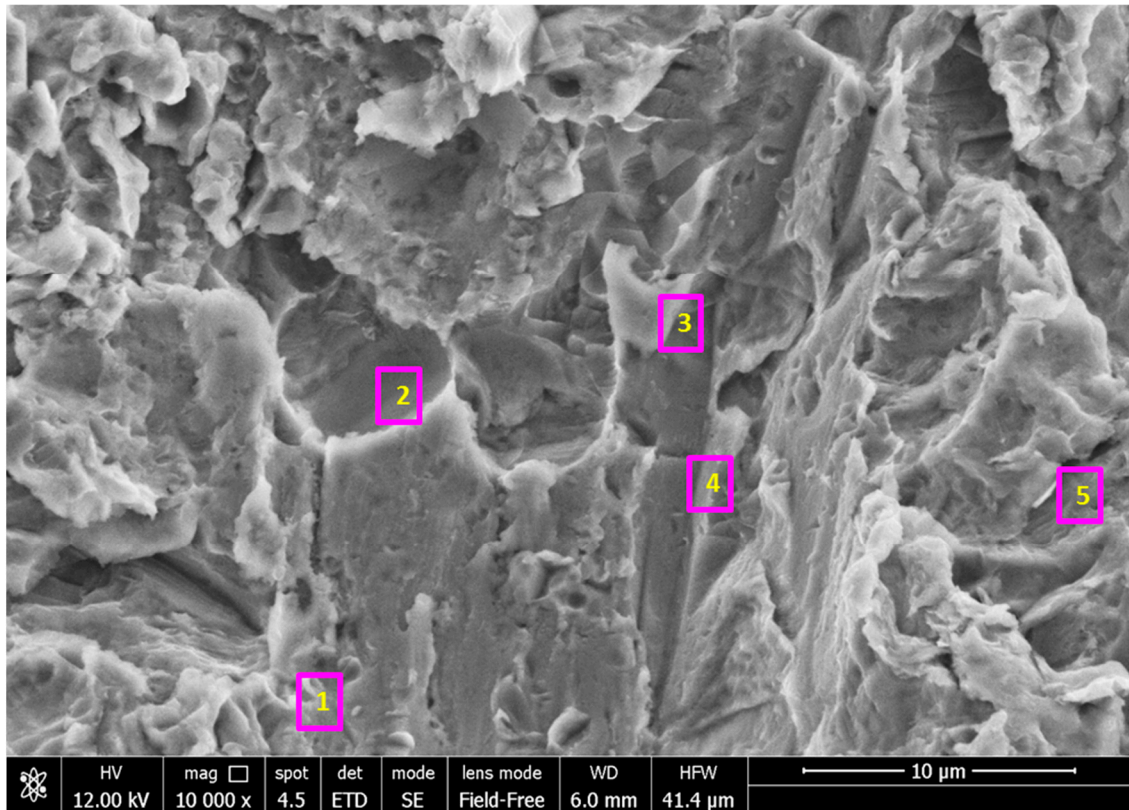


Figure 2. FEG-SEM images of the implant before immersion taken of one random thread located on the implant collar. Yellow square marks represent the areas observed at progressively higher magnifications (a) In backscattering mode, the pits and micro-irregularities of the moderately rough surface are well evident ($2000\times$ original magnification). (b) At $10,000\times$ original magnification, some crystal rods may be observed (arrows). One area was observed in nanoimmersion mode at $25,000\times$ (c), $50,000\times$ (d) and $100,000\times$ (e) original magnifications. Frame at original $200,000\times$: (f) the pits and microgrooves were not smooth.

The pits, observed at high magnifications, were not smooth, but revealed homogeneous nanorough structures, such as nanopits and nanogrooves uniformly distributed along all of the surface; the range of these structures was between 30 and 100 nm.

EDX spectra (Figure 3) taken in five regions of interest at 10,000× original magnification revealed the presence of Ca and P only on the areas with the crystal rods previously identified. Interestingly, these sites also revealed the presence of Si. Spectra taken on the implant surface revealed the presence of Ti, Al, V (attributable to the dental implant alloy), O (attributable to the titanium oxide layer on the surface), and C.



EDX microanalyses of the implant surface before immersion in HBSS. Results are expressed in atomic %.

	C	O	Na	Mg	Al	Si	P	Cl	Ca	Ti	V
1	1.50	19.49			7.60	0.50	0.71		0.86	68.35	0.98
2	3.14	15.12			7.88					72.32	1.53
3	2.13	14.53			6.60					74.11	2.62
4	2.94	8.26			8.8					78.27	1.71
5	2.06	19.71			7.71	0.34	0.62		0.55	67.72	1.29

Figure 3. EDX microanalyses taken at 10,000× original magnification in five regions of interest (shown by numbered pink squares) of one randomly chosen area of the implant before immersion. The analyses revealed the constitutional elements of the tested implant (Ti, Al, V), O from the TiO₂ layer. Presence of C and Si was also detected in low concentration.

3.1.3. Raman Spectroscopy and XPS Analysis

Figure 4 (spectrum a) shows the average micro-Raman spectrum recorded on the implant before immersion at 100× magnification and laser power at the sample of 10 mW. No bands were observed under these spectral conditions, according to the prevalently metallic composition of the sample (metals have no active vibrational Raman bands); at higher laser powers (i.e., 20 mW), the bands typical of Ti oxide as rutile polymorphic form were

observed, due to sample degradation under laser exposure (Figure 4, inset). No CaP component was detected, due to its low concentration.

These data were further confirmed by the XPS analysis, which revealed the presence of Ti oxide peaks with limited and no traces of Ca and P (Figure 5).

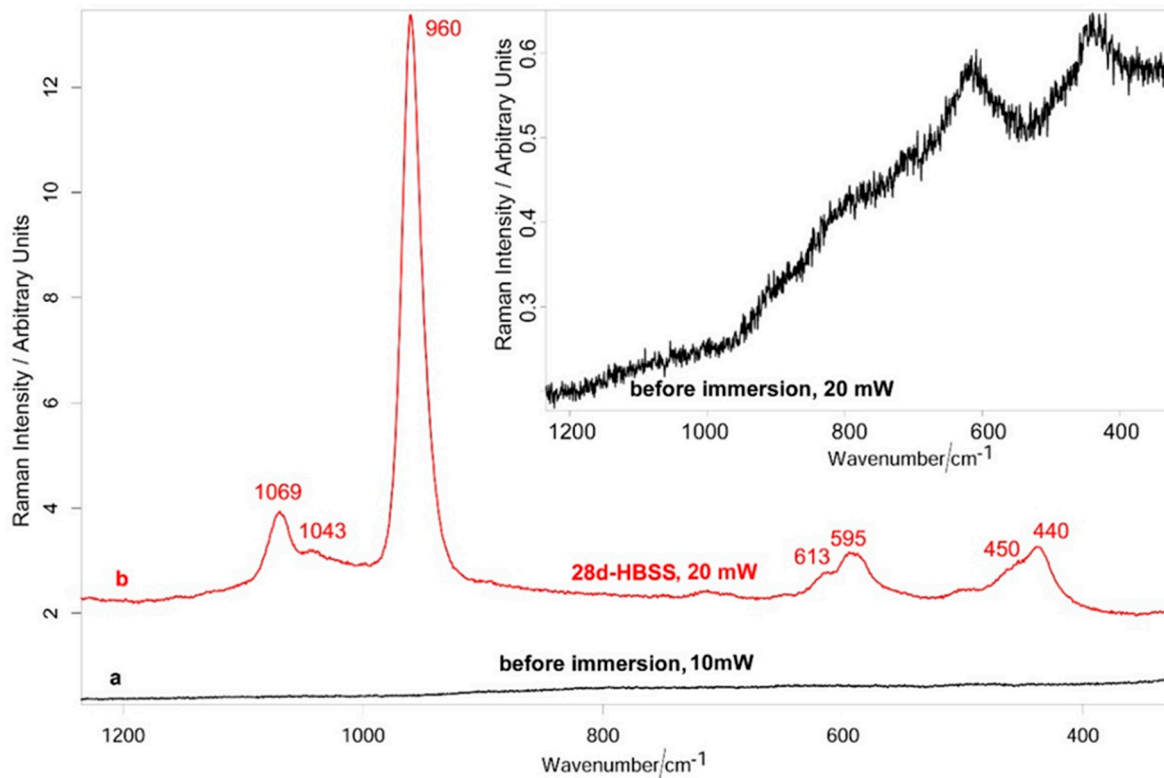


Figure 4. Average micro-Raman spectra: (a) recorded on the implant before immersion ($100\times$ magnification and laser power at the sample of 10 mW), and (b) after ageing in HBSS for 28 days ($100\times$ magnification and laser power at the sample of 20 mW). The spectrum in the inset was recorded on the implant before immersion at $100\times$ magnification and laser power at the sample of 20 mW (i.e., under the same conditions as the aged implant). All the spectra are reported with their original intensity (no scaling-up was performed).

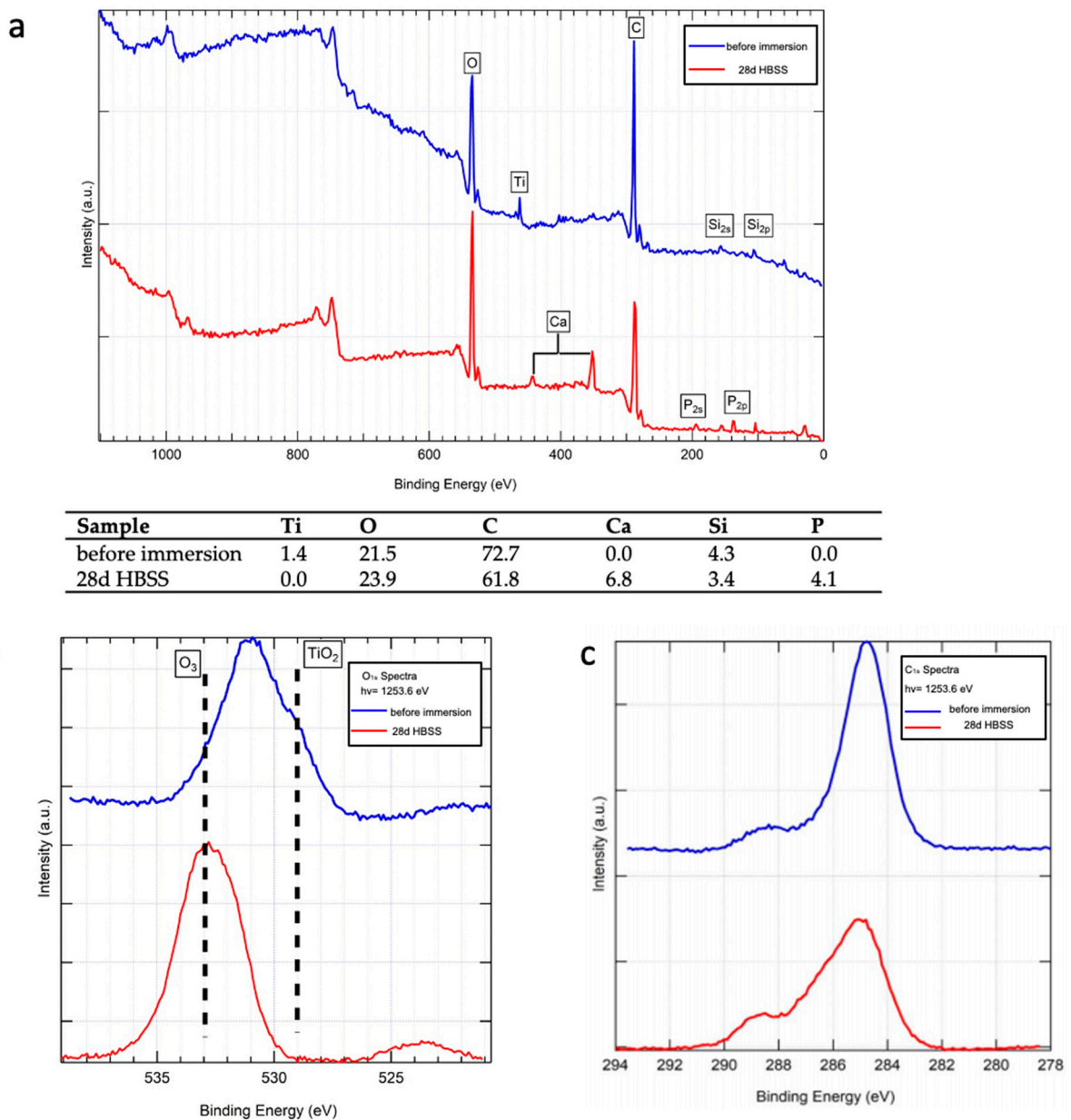


Figure 5. XPS analysis of the implant surface before immersion (blue trace) and after 28 days immersion in HBSS (red trace). The table reports the quantitative atomic percentage of elements on the implant surface of the sample before immersion and after immersion in HBSS. (a) Spectra acquisition using 2.0 eV step; (b) focused spectra using the same pass energy but 0.1 eV step at the oxygen site; (c) focused spectra using same pass energy but 0.1 eV step at the carbon site.

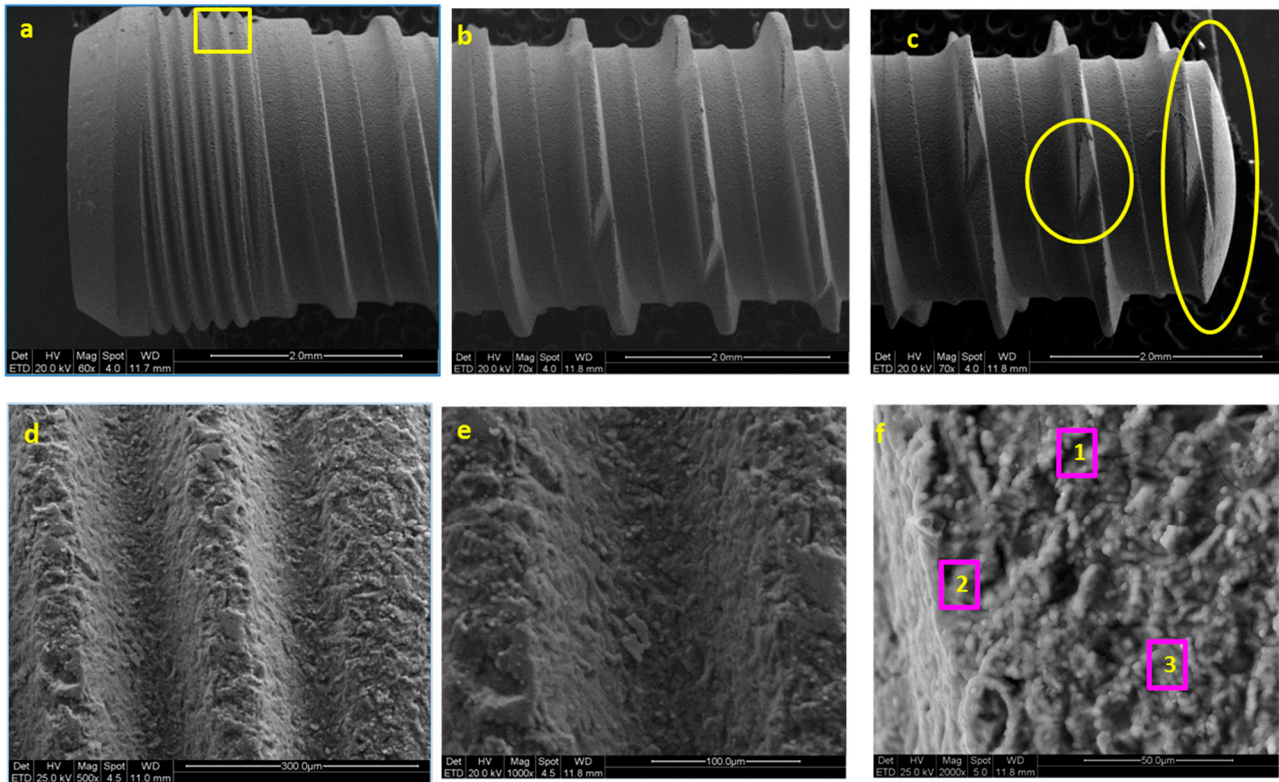
3.2. Implants Soaked in HBSS (Time 28 Days)

3.2.1. ESEM-EDX Analysis

ESEM microanalysis of the implant soaked for 28 days in HBSS was carried out on all of the implant surface. Figure 6a–c reports the images taken at the coronal, medium and apical portion after 28 days immersion in HBSS. The surface appeared significantly different compared to the implant before immersion. A homogeneous mineral layer was present on all of the surface, covering all the pits and the microgrooves. Images of one coronal thread, which was in the same location as the implant before immersion, were analyzed at progressively higher magnifications. The micromorphology of the mineral layer revealed numerous regular spherical structures (Figure 6d–f).

As the mineral deposit was present on all of the surface, EDX microanalysis was performed on three randomly chosen regions of one thread located in the medium portion

at 2000× original magnification (Figure 6). The analysis revealed similar results: the presence of Na, Mg, Cl, C, O (attributable to the HBSS medium), a general decrease of Ti, Al, V, (attributable to the presence of the mineral layer that covered the implant surface), an increase of Ca and P (attributable to the CaP layer). Ca/P atomic ratios calculated on sites 1–3 ranged from 1.01 to 1.05 (i.e., were 1.05, 1.01 and 1.05, respectively).



EDX microanalyses of implant after 28 days immersion in HBSS. Results are expressed in atomic %

	C	O	Na	Mg	Al	Si	P	Cl	Ca	Ti	V	Ca/P
1	12.64	65.23	1.15	0.58	1.27	0.19	3.64	0.38	3.83	10.64	0.46	1.05
2	10.40	65.71	1.14	0.53	1.57		3.32	0.33	3.34	13.08	0.57	1.01
3	10.27	65.28	1.21	0.58	1.43		3.56	0.34	3.75	13.00	0.56	1.05

Figure 6. ESEM images taken at the coronal (a), medium (b) and apical (c) portion after 28 days immersion in HBSS. A homogeneous mineral layer was present on all of the implant surface. One random area taken at the implant collar was progressively observed at 500× (d), 1000× (e) and 2000× (f) original magnifications. EDX microanalysis was performed in three randomly chosen regions of one implant thread located in the coronal portion (2000× original magnification).

3.2.2. FEG-SEM-EDX Analysis

FEG-SEM analysis carried out at the top of the previously observed coronal thread after 28 days immersion in HBSS was focused on one random area in the coronal portion (Figure 7). At low magnification (Figure 7a,b), a homogeneous mineral layer is displayed on all of the surface, markedly different from the implant before immersion. At high magnifications, the microspherulites were more deeply investigated. Some microcracks, attributable to the SEM high vacuum, were also identified. The structure of these spherulites (approx. 2 µm diameter) was observed in nanoimmersion mode (Figure 7c–f) revealing a regular shape with a hairy-like contour. These needle-like crystals (width approx. 30 nm) were better observed at 100,000× and 200,000× original magnifications.

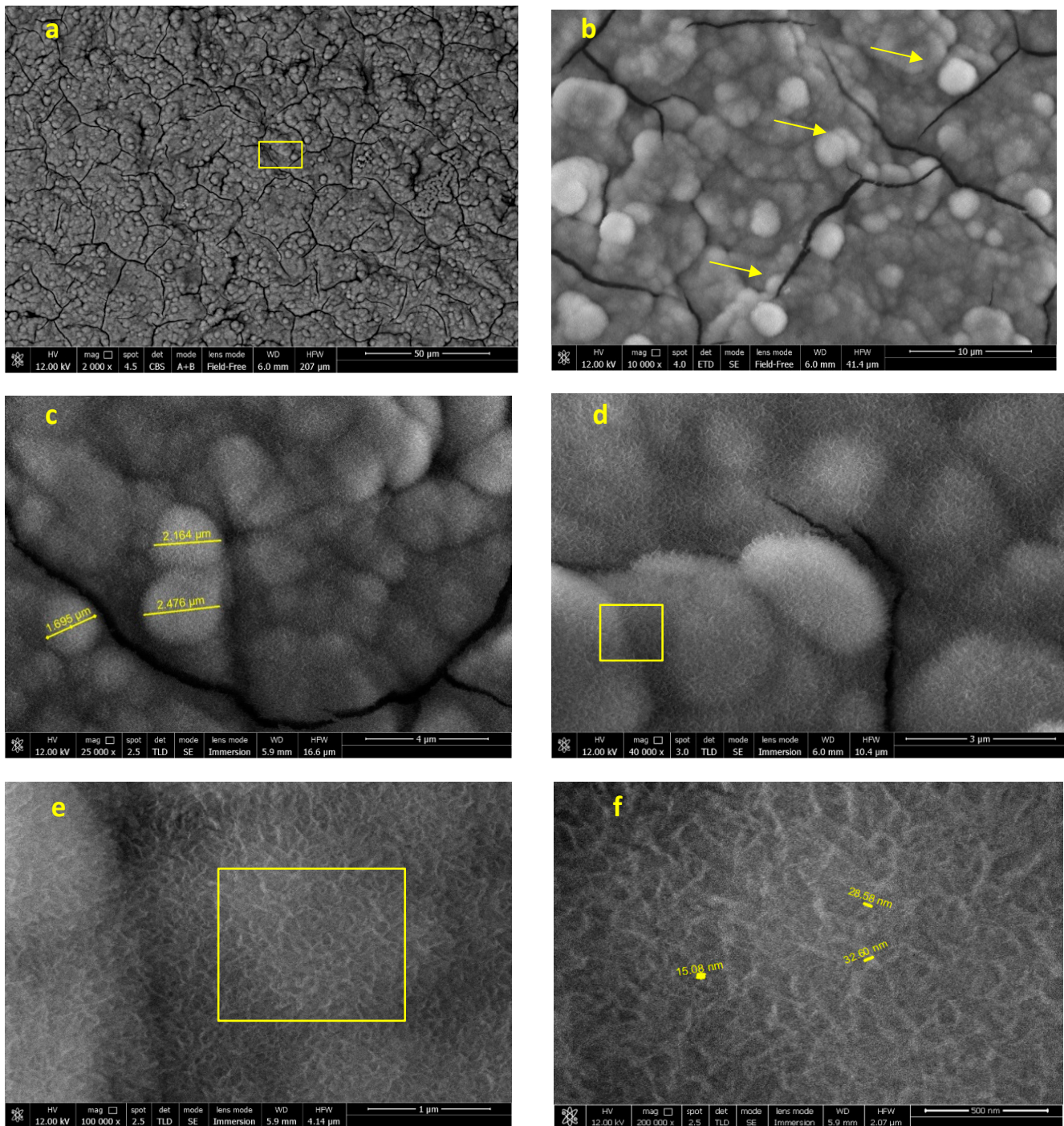
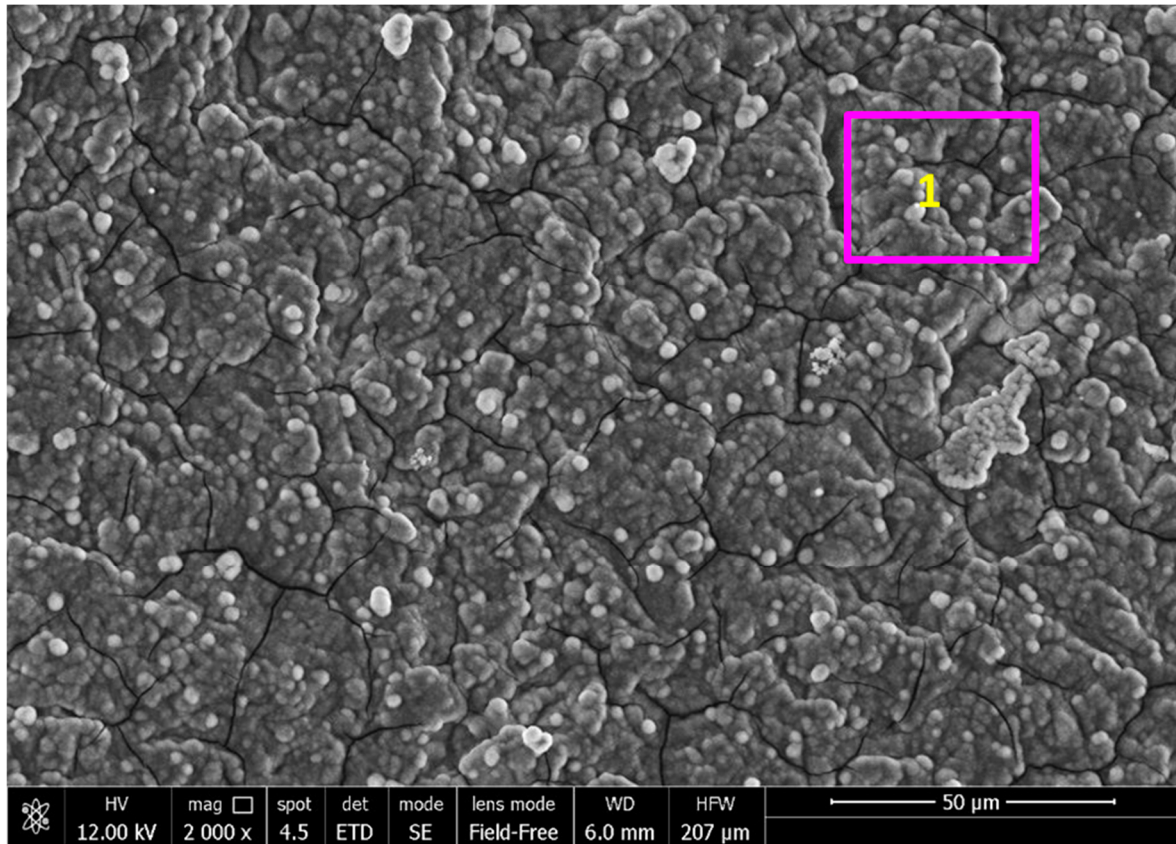


Figure 7. FEG-SEM images of the implant after 28 days of immersion in HBSS. One area in the coronal portion as investigated. Yellow square marks represent the areas observed at progressively higher magnifications: (a) Images at 2000× original magnification revealed that the mineral layer is uniform in all the investigated area. The pits and microgrooves are now covered and undetectable; the surface appears markedly different when compared to the implant before immersion. (b) The mineral layer revealed the presence of small circular structures (microspherulites, evidenced by arrows). (c,d) The morphology of these spherulites was observed at 25,000× and 40,000× original magnification. Needle-like crystals (width approx. 30 nm) can be identified at 100,000× (e) and 200,000× (f) original magnification.

EDX microanalysis (Figure 8) at 2000× original magnification revealed that the elements attributable to the implant surface, such as Ti and V, markedly decreased, while Al became undetectable. A notable increase of Ca and P and the appearance of Na, Cl, K,

C and O (attributable to HBSS) were also detected, confirming the presence of a uniform mineral thin layer on the area. Ca/P atomic ratio was 1.28.

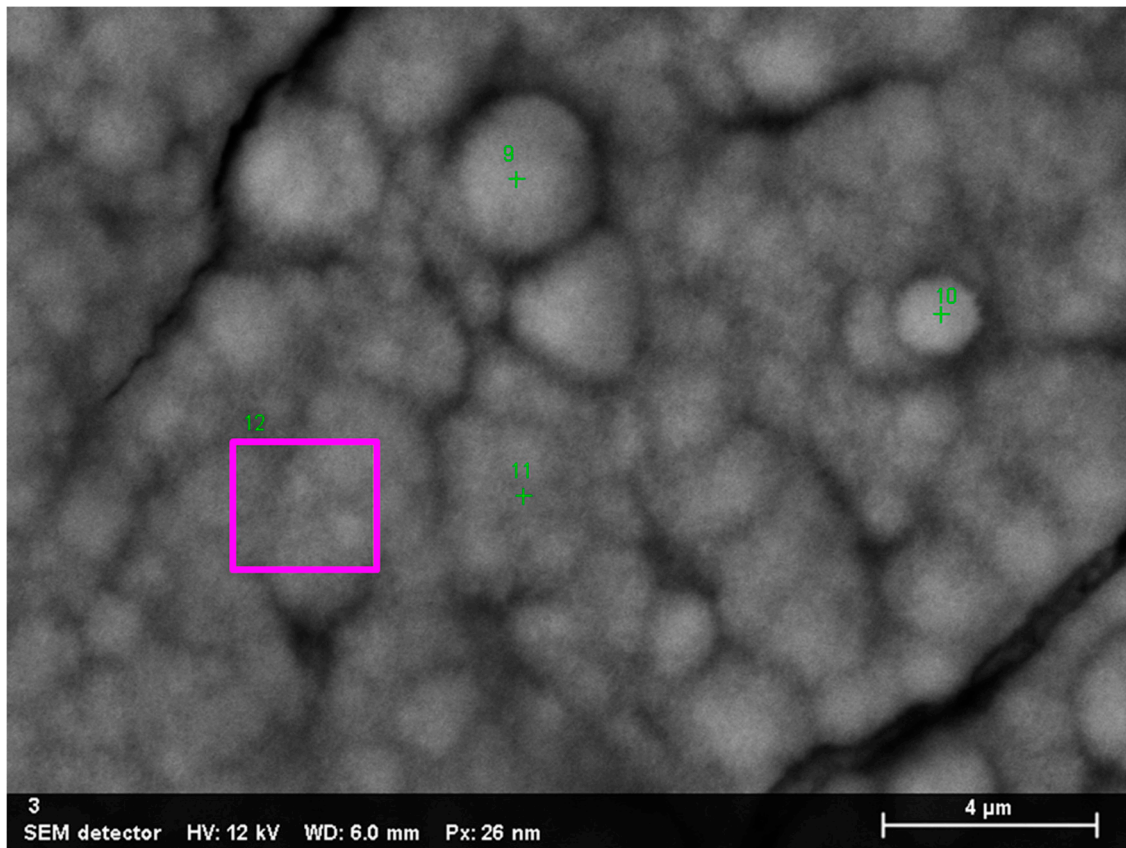


EDX microanalyses of implant after 28 days immersion in HBSS. Results are expressed in atomic %

	C	O	Na	Mg	Al	Si	P	Cl	Ca	Ti	V	Ca/P
1	7.85	63.25	3.41	1.62			9.3	0.11	11.93	1.17	1.32	1.28

Figure 8. EDX microanalysis performed at 2000× original magnification on a randomly chosen area of the implant immersed in HBSS for 28 days.

EDX microanalysis was performed at 25,000× original magnification on a randomly chosen layer of microspherulites (Figure 9). The analysis revealed the marked decrease of the elements attributable to the Ti-Al-V surface (Al and V were not detected, while Ti was observed only in 2 of 4 sites), and the presence of Na, Cl, Mg, C and O (attributable to HBSS solution). Ca/P atomic ratios were calculated on sites 9–12 and ranged from 1.27 to 1.28 (1.27,1.28, 1.28 and 1.28).



EDX microanalyses after 28 days immersion in HBSS. Results are expressed in atomic %

	C	O	Na	Mg	Al	Si	P	Cl	Ca	Ti	V	Ca/P
9	8.78	61.64	3.44	2.03			10.61		13.49			1.27
10	10.68	68.26	2.51	0.58			7.85		10.09			1.28
11	7.87	64.55	3.26	1.66			9.15		11.73	1.78		1.28
12		69.47	3.88	1.87			10.48	0.05	13.45	0.79		1.28

Figure 9. EDX microanalysis (at 25,000× original magnification) of a randomly chosen layer of microspherulites on the implant surface after 28 days of immersion in HBSS.

3.2.3. Raman Spectroscopy and XPS Analysis

Figure 4 (spectrum b) shows the average micro-Raman spectrum recorded on the implant aged in HBSS. All the ten recorded spectra were analogous to those reported in the figure, confirming the homogeneous nature of the deposit. Bands at 1069, 1043, 960, 613–595, 450–440 cm^{-1} , assignable to B-type carbonated apatite [18], were observed. To obtain a higher signal-to-noise ratio, the spectra were recorded under a laser power at the sample of 20 mW (i.e., higher than for the sample before immersion, analyzed at 10 mW); no bands of the rutile phase were detected under these conditions. XPS (Figure 5) confirmed the micro-Raman findings. The spectrum of the 28 d aged sample (Figure 5a) showed the presence of Ca and P peaks on the implant surface; at the same time, the Ti peak disappeared (see also the Table reported in Figure 5) together with the TiO_2 O_{1s} peak (Figure 5b). The positions of the O_{1s} (Figure 5b) and C_{1s} (Figure 5c) peaks are consistent with those reported in the literature for carbonated apatites [22,23].

4. Discussion

In the present study, an implant surface characterization was performed by using repeatable, non-destructive methodologies (except desiccation artifacts due to vacuum), as samples did not require any manipulation, preparation or paraffin embedment. ESEM allowed visualization of the changes in the surface micro-topography, while SEM-FEG allowed us to assess the changes and nanotopography of the surface. The latter technique allows achievement of higher resolutions with lowered accelerating voltages.

HBSS solution was chosen, being a commercially available standardized soaking medium; it contains a lower calcium amount than human plasma, but the same phosphate concentration (mimicking human blood plasma). A 28-day immersion period was selected—in agreement with numerous studies investigating the biomaterials apatite nucleation ability—as this time represents the endpoint of a series of chemical reactions that lead to the formation of apatite or apatite precursors [14–17,19,20,24,25]. Indeed, a series of *in vitro* studies followed this protocol to analyze several experimental biomaterials, dental implant surfaces and bone tissue engineering scaffolds [14–17,19,20,24–26].

Surface reactivity and apatite nucleating ability of the present implant surface have been never investigated, and may provide useful information regarding the most suitable clinical use of this implant; a particularly bioactive surface stimulates cell attachment, differentiation and bone matrix synthesis [27], leading to an increased bone-implant contact in a shorter time, accelerating the process of bone-implant contact formation, and providing the implant with increasing secondary stability at the earliest stages of healing [18]. Thus, a highly reactive surface may be useful when complex cases are approached, namely when the implant is placed in endodontic post-extractive sites [28], where the implant is anchored only at the apical sites (such is the case of immediate post-extractive implants) [29,30], or when low density bone is present [11].

To obtain a reactive and osteoconductive surface, addition of a CaP coating has been studied and marketed in the past. However, these efforts were undermined by several complications, including peri-implantitis susceptibility, hydroxyapatite dissolution after surgery, and failed interfacial adhesion between implant and hydroxyapatite [11,12]. For these reasons, the current trend is to prefer to actively blast implant surface with bioactive compounds, modifying the surface micro and nano-topography, rather than provide a uniform bioactive layer *a priori* [6,11].

In the present study, the implant displayed a moderately rough surface with pits and grooves well identifiable at ESEM observation, the range was approx. 2–5 μm . Few CaP crystals from resorbable blasting procedures were detected using ESEM and semiquantitative EDX analysis (evidenced by limited traces of Ca and P), while they were not revealed by micro-Raman analyses [31].

SEM-FEG investigation allowed analysis of surface topography at higher magnifications. Interestingly, images at 200,000 \times original magnifications of the implant before immersion revealed a uniform nanorough surface, with well-identifiable irregular nanopits and nanogrooves, ranging from 30–100 nm. SEM-FEG also revealed the presence of limited crystal rods, identified as CaP crystals from EDX microanalysis. These data indicate that the surface showed a regular micro- and nanorough surface, in agreement with a previous investigation, which suggested a fractal architecture [13].

The surface nano topography of a biomaterial may strongly affect the cellular response [32–36].

Nanorough structures (1–100 nm) play an important role in the first moments after implant insertion, with regards to osteoblasts adhesion and protein adsorption [32,34,35].

Microrough structures (within 1–10 μm) were found to improve the interlocking between mineralized bone and implant surface and play a key role in mineralizing cells maturation and activity [36]. A previous study compared different titanium surfaces and showed a significantly higher osteoblast cell attachment and activity in presence of moderately rough surfaces when compared to a smooth untreated surface [37].

ESEM and SEM-FEG analyses revealed that the surface was markedly different after 28 days immersion in HBSS. A uniform mineral layer composed of microspherulites with 2–4 μm diameter that filled and covered the implant rough surface was detected. These data suggest a high reactivity of the surface upon exposure to biological fluids. EDX proved a fast, mainly superficial method able to semiquantitatively analyze precipitates in terms of atomic percentages (revealing a marked increase of Ca and P) [31].

Micro-Raman spectroscopy revealed that the microspherulites were mainly composed of B-type carbonated apatite. It may be observed that the spectra of the implant after immersion in HBSS were recorded at a higher laser power at the sample (i.e., 20 mW, Figure 4 spectrum b) than the implant before immersion (i.e., 10 mW, Figure 4 spectrum a); this choice was made to obtain stronger spectra, with higher signal-to-noise ratios, to obtain a more reliable characterization of the CaP phase. On the other hand, the spectra recorded on the implant at the same laser power at the sample (i.e., 20 mW, Figure 4, inset) showed sample degradation with formation of rutile, due to laser exposure. It is interesting to note that the latter phase was never detected in the spectra of the implant after immersion in HBSS obtained under the same conditions (Figure 4, spectrum b). This result suggests that the B-type carbonated apatite had a thickness sufficient to protect the titanium underneath from laser-induced degradation.

The micro-Raman results were further confirmed by XPS analysis. The XPS spectrum of the implant after immersion in HBSS is consistent with the formation of a B-type carbonated apatite and was free from Ti and TiO_2 peaks. It must be recalled that XPS is a surface method (with ~ 10 nm penetration depth), so the latter behavior may be explained by considering that the nucleated CaP phase covered the implant surface completely, masking the signals from beneath.

Spectroscopic analyses showed that a highly biocompatible CaP (i.e., B-type carbonated apatite) formed on the implant surface. Actually, the mineral component of bone is primarily a carbonate substituted calcium apatite, where carbonate content is typically 2–8% by weight [38]. Carbonate may substitute into two anionic sites of the $\text{Ca}_{10}(\text{PO}_4)_6(\text{OH})_2$ hydroxyapatite structure: at PO_4^{3-} sites (B-type carbonated apatite) and OH^- sites (A-type carbonated apatite) [17,19,39]. Carbonate in bone mineral is primarily B-type; the fraction of A-type carbonate in biological apatites is very low. Actually, the carbonate in the A-sites has been reported to exert a greater predominant effect than B-type carbonate on the long-range order of apatite [40].

The result obtained in our study appears encouraging; actually, B-type carbonate apatite has been reported as an ideal artificial bone substitute because it is closer in chemical composition to bone mineral [41]. The biocompatibility of carbonated apatite may be related to the crystallinity decrease induced by the carbonate substitution, which increases solubility and, in turn, bone reformation or turnover [42].

The nucleation of a regular, homogeneous osteoconductive and biointeractive apatite layer provides a particularly suitable surface for osteoblasts, in terms of cell attachment and for new bone apposition, in particular for the presence of biologically active ions (such as Ca^{++}) [17,24–26,39,43].

The transformation processes at the early phases from amorphous calcium phosphate to bone-like apatite has been recently observed at the nanoscale in an in-vitro model, describing amorphous calcium phosphate crystals that subsequently arrange in size very close to the needle-like crystals detected in our investigation (size 30–50 nm) [44]. These crystals will gradually transform to apatite crystals with elongated and platelet-like morphology [45]. The presence of a bioactive B-type carbonated apatite layer may well explain the histological finding and the gene expression recently reported for similar implant surfaces in animal and in laboratories studies [46–50].

5. Conclusions

The null-hypothesis was rejected, as in the present study we could find differences in superficial elemental composition in terms of higher amounts of Ca and P after HBSS immersion using EDX, XPS and micro-Raman spectroscopy.

This implant showed a micro-nano-textured surface supporting the formation of B-type carbonated apatite when immersed in HBSS. These properties may likely favor bone anchorage and healing by stimulation of mineralizing cells, revealing attractive characteristics to approach post-extractive implant placements and low-bone density area.

Author Contributions: Conceptualization: C.P. and M.G.G.; methodology: M.G.G. validation: P.T., investigation: P.T., F.Z. and L.G.; data curation: F.Z., P.T., A.S.; writing—original draft preparation: C.P., M.G.G., F.Z., P.T.; writing—review and editing: C.P., M.G.G., F.Z. and P.T.; supervision, C.P., M.G.G. All authors have read and agreed to the published version of the manuscript.

Funding: This research received no external funding.

Institutional Review Board Statement: Not applicable.

Informed Consent Statement: Not applicable.

Data Availability Statement: Data sharing not applicable.

Acknowledgments: The research was financed by the academic funds from RFO of MG Gandolfi, RFO of C. Prati.

Conflicts of Interest: The authors declare no conflict of interest.

References

1. Albrektsson, T.; Johansson, C. Osteoinduction, osteoconduction and osseointegration. *Eur. Spine J.* **2001**, *10*, 96–101.
2. Terheyden, H.; Lang, N.P.; Bierbaum, S.; Stadlinger, B. Osseointegration—Communication of cells. *Clin. Oral Implant. Res.* **2012**, *23*, 1127–1135. [[CrossRef](#)] [[PubMed](#)]
3. Wennerberg, A.; Albrektsson, T. Effects of titanium surface topography on bone integration: A systematic review. *Clin. Oral Implant. Res.* **2009**, *20*, 172–184.
4. Padial-Molina, M.; Galindo-Moreno, P.; Fernández-Barbero, J.E.; O’Valle, F.; Jódar-Reyes, A.B.; Ortega-Vinuesa, J.L.; Ramón-Torregrosa, P.J. Role of wettability and nanoroughness on interactions between osteoblast and modified silicon surfaces. *Acta Biomater.* **2011**, *7*, 771–778. [[CrossRef](#)] [[PubMed](#)]
5. Nikkhah, M.; Edalat, F.; Manoucheri, S.; Khademhosseini, A. Engineering microscale topographies to control the cell-substrate interface. *Biomaterials* **2012**, *33*, 5230–5246. [[CrossRef](#)]
6. Zhao, G.; Schwartz, Z.; Wieland, M.; Rupp, F.; Geis-Gerstorfer, J.; Cochran, D.L.; Boyan, B.D. High surface energy enhances cell response to titanium substrate microstructure. *J. Biomed. Mater. Res. Part A* **2005**, *74*, 49–58. [[CrossRef](#)]
7. Yip, I.; Ma, L.; Mattheos, N.; Dard, M.; Lang, N.P. Defect healing with various bone substitutes. *Clin. Oral Implant. Res.* **2014**, *26*, 606–614. [[CrossRef](#)]
8. LeGeros, R.Z.; Lin, S.; Rohanizadeh, R.; Mijares, D.; LeGeros, J.P. Biphasic calcium phosphate bioceramics: Preparation, properties and applications. *J. Mater. Sci. Mater. Med.* **2003**, *14*, 201–209. [[CrossRef](#)]
9. Jemat, A.; Ghazali, M.J.; Razali, M.; Otsuka, Y. Surface Modifications and Their Effects on Titanium Dental Implants. *BioMed Res. Int.* **2015**, *2015*, 1–11. [[CrossRef](#)]
10. Ong, J.L.; Chan, D.C.N. Hydroxyapatite and Their Use as Coatings in Dental Implants: A Review. *Crit. Rev. Biomed. Eng.* **2000**, *28*, 667–707. [[CrossRef](#)]
11. Jung, J.; Kim, S.-Y.; Yi, Y.-J.; Lee, B.-K.; Kim, Y.-K. Hydroxyapatite-coated implant: Clinical prognosis assessment via a retrospective follow-up study for the average of 3 years. *J. Adv. Prosthodont.* **2018**, *10*, 85–92. [[CrossRef](#)]
12. Zablotsky, M.H. Hydroxyapatite coatings in implant dentistry. *Implant. Dent.* **1992**, *1*, 253–257. [[CrossRef](#)] [[PubMed](#)]
13. Bucci-Sabattini, V.; Cassinelli, C.; Coelho, P.G.; Minnici, A.; Trani, A.; Dohan Ehrenfest, D.M. Effect of titanium implant surface nano-roughness and calcium phosphate low impregnation on bone cell activity in vitro. *Oral Surg. Oral Med. Oral Pathol. Oral Radiol.* **2010**, *109*, 217–224. [[CrossRef](#)] [[PubMed](#)]
14. Kokubo, T.; Takadama, H. How useful is SBF in predicting in vivo bone bioactivity? *Biomaterials* **2006**, *27*, 2907–2915. [[CrossRef](#)] [[PubMed](#)]
15. Zadpoor, A.A. Relationship between in vitro apatite-forming ability measured using simulated body fluid and in vivo bioactivity of biomaterials. *Mater. Sci. Eng. C* **2014**, *35*, 134–143. [[CrossRef](#)]
16. Gandolfi, M.G.; Ciapetti, G.; Taddei, P.; Perut, F.; Tinti, A.; Cardoso, M.V.; Van Meerbeek, B.; Prati, C. Apatite formation on bioactive calcium-silicate cements for dentistry affects surface topography and human marrow stromal cells proliferation. *Dent. Mater.* **2010**, *26*, 974–992. [[CrossRef](#)]

17. Gandolfi, M.G.; Taddei, P.; Modena, E.; Siboni, F.; Prati, C. Biointeractivity-related versus chemi/physisorption related apatite precursor-forming ability of current root end filling materials. *J. Biomed. Mater. Res. B* **2013**, *101*, 1107–1123. [[CrossRef](#)]
18. Nelson, D.G.; Featherstone, J.D. Preparation, analysis, and characterization of carbonated apatites. *Tissue* **1982**, *34*, 69–81.
19. Gandolfi, M.G.; Iezzi, G.; Piattelli, A.; Prati, C.; Scarano, A. Osteoinductive potential and bone-bonding ability of ProRoot MTA, MTA Plus and Biodentine in rabbit intramedullary model: Microchemical characterization and histological analysis. *Dent. Mater.* **2017**, *33*, 221–238. [[CrossRef](#)]
20. Gandolfi, M.G.; Taddei, P.; Siboni, F.; Perrotti, V.; Iezzi, G.; Piattelli, A.; Prati, C. Micro-Topography and Reactivity of Implant Surfaces: An In Vitro Study in Simulated Body Fluid (SBF). *Microsc. Microanal.* **2015**, *21*, 190–203. [[CrossRef](#)]
21. Prati, C.; Zamparini, F.; Scialabba, V.S.; Gatto, M.R.A.; Piattelli, A.; Montebugnoli, L.; Gandolfi, M.G. A 3-Year Prospective Cohort Study on 132 Calcium Phosphate-Blasted Implants: Flap vs Flapless Technique. *Int. J. Oral Maxillofac. Implant.* **2016**, *31*, 413–423. [[CrossRef](#)] [[PubMed](#)]
22. Leonor, I.B.; Kim, H.-M.; Carmona, D.; Kawashita, M.; Reis, R.L.; Kokubo, T.; Nakamura, T. Surface potential change in bioactive polymer during the process of biomimetic apatite formation in a simulated body fluid. *J. Mater. Chem.* **2007**, *17*, 4057–4063. [[CrossRef](#)]
23. Núñez, J.D.; Benito, A.M.; González, R.; Aragón, J.; Arenal, R.; Maser, W.K. Integration and bioactivity of hydroxyapatite grown on carbon nanotubes and graphene oxide. *Carbon* **2014**, *79*, 590–604. [[CrossRef](#)]
24. Gandolfi, M.G.; Zamparini, F.; Degli Esposti, M.; Chiellini, F.; Aparicio, C.; Fava, F.; Fabbri, P.; Taddei, P.; Prati, C. Polylactic acid-based porous scaffolds doped with calcium silicate and dicalcium phosphate dihydrate designed for biomedical application. *Mater. Sci. Eng. C* **2018**, *82*, 163–181. [[CrossRef](#)]
25. Gandolfi, M.G.; Zamparini, F.; Degli Esposti, M.; Chiellini, F.; Fava, F.; Fabbri, P.; Taddei, P.; Prati, C. Highly porous polycaprolactone scaffolds doped with calcium silicate and dicalcium phosphate dihydrate designed for bone regeneration. *Mater. Sci. Eng. C* **2019**, *102*, 341–361. [[CrossRef](#)]
26. Vitti, R.P.; Prati, C.; Sinhoretto, M.A.C.; Zanchi, C.H.; Souza E Silva, M.G.; Oglari, F.A.; Piva, E.; Gandolfi, M.G. Chemical-physical properties of experimental root canal sealers based on butyl ethylene glycol disalicylate and MTA. *Dent. Mater.* **2013**, *29*, 1287–1294. [[CrossRef](#)]
27. Muzzarelli, R.A.A.; Biagini, G.; Belmonte, M.M.; Talassi, O.; Gandolfi, M.G.; Solmi, R.; Carraro, S.; Giardino, R.; Fini, M.; Nicoli-Aldini, N. Osteoinduction by Chitosan-Complexed BMP: Morpho-Structural Responses in an Osteoporotic Model. *J. Bioact. Compat. Polym.* **1997**, *12*, 321–329. [[CrossRef](#)]
28. López-Martínez, F.; Moreno, G.G.; Olivares-Ponce, P.; Jaramillo, D.E.; De-Val, J.-E.M.-S.; Calvo-Guirado, J.L. Implants failures related to endodontic treatment. An observational retrospective study. *Clin. Oral Implant. Res.* **2014**, *26*, 992–995. [[CrossRef](#)]
29. Prati, C.; Zamparini, F.; Pirani, C.; Gatto, M.R.; Piattelli, A.; Gandolfi, M.G. Immediate early and delayed implants: A 2-year prospective cohort study of 131 transmucosal flapless implants placed in sites with different pre-extractive endodontic infections. *Implant. Dent.* **2017**, *26*, 654–663. [[CrossRef](#)]
30. Mangano, F.; Iezzi, G.; Shibli, J.A.; Pires, J.T.; Luongo, G.; Piattelli, A.; Mangano, C. Early bone formation around immediately loaded implants with nanostructured calcium-incorporated and machined surface: A randomized, controlled histologic and histomorphometric study in the human posterior maxilla. *Clin. Oral Investig.* **2017**, *21*, 2603–2611. [[CrossRef](#)]
31. Scholz, K.J.; Federlin, M.; Hiller, K.-A.; Ebersberger, H.; Ferstl, G.; Buchalla, W. EDX-analysis of fluoride precipitation on human enamel. *Sci. Rep.* **2019**, *9*, 1–11. [[CrossRef](#)]
32. Boyan, B.D.; Bonewald, L.; Paschalis, E.; Lohmann, C.; Rosser, J.; Cochran, D.; Dean, D.; Schwartz, Z.; Boskey, A. Osteoblast-Mediated Mineral Deposition in Culture is Dependent on Surface Microtopography. *Calcif. Tissue Int.* **2002**, *71*, 519–529. [[CrossRef](#)]
33. Dalby, M.J.; Riehle, M.; Johnstone, H.; Affrossman, S.; Curtis, A. Investigating the limits of filopodial sensing: A brief report using SEM to image the interaction between 10 nm high nano-topography and fibroblast filopodia. *Cell Biol. Int.* **2004**, *28*, 229–236. [[CrossRef](#)]
34. Dalby, M.J.; McCloy, D.; Robertson, M.; Agheli, H.; Sutherland, D.; Affrossman, S.; Oreffo, R.O. Osteoprogenitor response to semi-ordered and random nanotopographies. *Biomaterials* **2006**, *27*, 2980–2987. [[CrossRef](#)]
35. Souza, J.C.M.; Sordi, M.B.; Kanazawa, M.; Ravindran, S.; Henriques, B.; Silva, F.S.; Aparicio, C.; Cooper, L.F. Nano-scale modification of titanium implant surfaces to enhance osseointegration. *Acta Biomater.* **2019**, *94*, 112–131. [[CrossRef](#)]
36. Shalabi, M.; Gortemaker, A.; Hof, M.V.; Jansen, J.; Creugers, N. Implant Surface Roughness and Bone Healing: A Systematic Review. *J. Dent. Res.* **2006**, *85*, 496–500. [[CrossRef](#)]
37. Le Guehennec, L.; Lopez-Heredia, M.A.; Enkel, B.; Weiss, P.; Amouriq, Y.; Layrolle, P. Osteoblastic cell behaviour on different titanium implant surfaces. *Acta Biomater.* **2008**, *4*, 535–543. [[CrossRef](#)]
38. Boskey, A.L.; Coleman, R. Aging and Bone. *J. Dent. Res.* **2010**, *89*, 1333–1348. [[CrossRef](#)]
39. Gandolfi, M.G.; Taddei, P.; Tinti, A.; De Stefano Dorigo, E.; Prati, C. Alpha-TCP improves the apatite-formation ability of calcium-silicate hydraulic cement soaked in phosphate solutions. *Mat. Sci. Eng. C* **2011**, *31*, 1412–1422.
40. Madupalli, H.; Pavan, B.; Tecklenburg, M.M.J. Carbonate substitution in the mineral component of bone: Discriminating the structural changes, simultaneously imposed by carbonate in A and B sites of apatite. *J. Solid State Chem.* **2017**, *255*, 27–35. [[CrossRef](#)]

41. Zaman, C.T.; Takeuchi, A.; Matsuya, S.; Zaman, Q.H.; Ishikawa, K. Fabrication of B-type carbonate apatite blocks by the phosphorization of free-molding gypsum-calcite composite. *Dent. Mater. J.* **2008**, *27*, 710–715. [[CrossRef](#)] [[PubMed](#)]
42. Ison, I.C.; Fulmer, M.T.; Barr, B.M.; Constantz, B.R. Synthesis of Dahllite: The Mineral Phase of Bone. In *Hydroxyapatite and Related Materials*; Informa UK Limited: Colchester, UK, 2017; pp. 215–224.
43. Prati, C.; Gandolfi, M.G. Calcium silicate bioactive cements: Biological perspectives and clinical applications. *Dent. Mater.* **2015**, *31*, 351–370. [[CrossRef](#)] [[PubMed](#)]
44. Blair, H.C.; Larrouture, Q.C.; Li, Y.; Lin, H.; Beer-Stoltz, D.; Liu, L.; Tuan, R.S.; Robinson, L.J.; Schlesinger, P.H.; Nelson, D.J. Osteoblast Differentiation and Bone Matrix Formation In Vivo and In Vitro. *Tissue Eng. Part B Rev.* **2017**, *23*, 268–280. [[CrossRef](#)] [[PubMed](#)]
45. Lotsari, A.; Rajasekharan, A.K.; Halvarsson, M.; Andersson, M. Transformation of amorphous calcium phosphate to bone-like apatite. *Nat. Commun.* **2018**, *9*, 1–11. [[CrossRef](#)]
46. Nitiputri, K.; Ramasse, Q.M.; Autefage, H.; McGilvery, C.M.; Boonrungsiman, S.; Evans, N.D.; Stevens, M.M.; Porter, A.E. Nanoanalytical Electron Microscopy Reveals a Sequential Mineralization Process Involving Carbonate-Containing Amorphous Precursors. *ACS Nano* **2016**, *10*, 6826–6835. [[CrossRef](#)]
47. Jimbo, R.; Xue, Y.; Hayashi, M.; Schwartz-Filho, H.; Andersson, M.; Mustafa, K.; Wennerberg, A. Genetic Responses to Nanostructured Calcium-phosphate-coated Implants. *J. Dent. Res.* **2011**, *90*, 1422–1427. [[CrossRef](#)]
48. Coelho, P.; Granato, R.; Marin, C.; Jimbo, R.; Lin, S.; Witek, L.; Suzuki, M.; Bonfante, E.A. Effect of Si addition on Ca- and P-impregnated implant surfaces with nanometer-scale roughness: An experimental study in dogs. *Clin. Oral Implant. Res.* **2011**, *23*, 373–378. [[CrossRef](#)]
49. Coelho, P.G.; Takayama, T.; Yoo, D.; Jimbo, R.; Karunakaran, S.; Tovar, N.; Janal, M.N.; Yamano, S. Nanometer-scale features on micrometer-scale surface texturing: A bone histological, gene expression, and nanomechanical study. *Bone* **2014**, *65*, 25–32. [[CrossRef](#)]
50. Favero, R.; Botticelli, D.; Antunes, A.A.; Martinez Sanchez, R.; Caroprese, M.; Salata, L.A. Sequential Healing at Calcium-versus Calcium Phosphate-Modified Titanium Implant Surfaces: An Experimental Study in Dogs. *Clin. Implant. Dent. Relat. Res.* **2016**, *18*, 369–378. [[CrossRef](#)]

6. Conclusion

The present PhD thesis aimed to investigate innovative biomaterials and develop new clinical techniques for endodontics therapy.

The investigation focused on two central themes: a significant attention was dedicated to the chemical-physical characterization and bioactivity of the new generation of premixed calcium-silicate sealers compared to traditional ones. Our investigation validated their use in clinical practice.

Two clinical studies (approved by the ethical committee) with a follow-up of 12 and 24 months were conducted and were able to assess the efficacy and biocompatibility of these CaSi-based obturation techniques. Our findings open new consideration on the encouraging use of premixed calcium-silicate bioceramic sealers combined with warm techniques. These findings highlight the potential to improve current therapies, offering new solutions and application in the endodontic field.

The bioactive and bio-interactive properties of the new generation of CaSa-based sealers sign a new era in dental research and clinical practice opening future research and potentially changing clinical outcomes.